

Temperature and light entrainment of the
Drosophila circadian clock

Thesis submitted for the degree of
Doctor of Philosophy
at the University of Leicester

Carlo Breda
Department of Genetics
University of Leicester

March 2010

Temperature and light entrainment of the *Drosophila* circadian clock

Carlo Breda

Abstract

Drosophila melanogaster locomotor activity responds to seasonal conditions by modulating the “evening” activity component. During simulated winters of cold temperature and short days an advanced evening locomotor peak occurs with more daytime locomotor activity; on the other hand long photoperiods and warm temperatures give a delay in the evening peak, thereby avoiding a possible desiccation during the hottest times of the day. This pattern of activity is related to a thermosensitive splicing event that occurs in a 3' intron in the *period* gene, with a higher level of splicing and earlier accumulation of PERIOD in short days and low temperatures. A mutation in *norpA* which encodes a phospholipase C, generates a high level of spliced *per* at warmer temperature, so mutants behave as if it is colder than it actually is. The relation between *norpA*, *per* splicing and the circadian neurons has been analysed. Initially, *norpA* expression has been investigated *via in situ* hybridisation and immunocytochemistry. *norpA* transcript has been localised among the clock pacemakers but not NORPA. Subsequently, *norpA* expression has been knocked-down by RNAi in specific subset of neurons. The resulting locomotor behaviour shows seasonally related effects implicating the photoreceptors, lateral and dorsal clock neurons as structures involved in timing the locomotor behaviour. In parallel, the thermal role of a second PLC β , *plc21C*, has been investigated *via* RNAi among circadian pacemakers. It has been possible to show that *plc21C* expression in the photoreceptors, lateral and dorsal neurons is required to set different locomotor behaviours at different temperatures, but not *via per* and *tim* splicing.

Finally, in contrast to reports that the double photoreceptor mutants involving *glass* and *cryptochrome* are “circadian blind”, these flies have been observed to entrain to light-dark cycles at moderate temperatures. Candidate orphan G protein coupled receptors have been screened in order to identify a further set of putative circadian-relevant photoreceptors contributing to this residual entrainment in *glass*^{60j}*cry*^b mutants. In constant light conditions, the RNAi of *CG7497* and *CG16958* generates rhythmic or arrhythmic flies depending on the genetic background tested.

Acknowledgments

There are several people that I would like to thank very much for their help and encouragement. They have enabled me to finish this work. Each of them has given me something which helped me to mature and grow up.

Firstly, I am grateful to Prof. Bambos Kyriacou, for supporting and encouraging me in all the occasions. With his “super” relaxed manner, he made me enjoy these past years without stressing me and giving all the freedom that I wanted. At the same time, his precious and helpful advices have increased my passion for my research.

I would like to acknowledge EUCLOCK for funding this research and for all the German trips to the “Island”.

I would also like to thank all the people who I worked or shared time with during these years. The list would be infinitely long, so whoever is reading this thesis and contributed also with a simple smile, is thanked. I need to spend some particular words for Valeria who has been always close to me, in particular during my first year when I had my English hospital experience. For having been the “Sister” that I never had, I’m immensely grateful.

A sincere thank goes to my family who supports and trusts me. To my mom who, although she does not understand circadian clocks, had always asked me about my experiments. A thank to dad for keeping mom quiet and calm in all situations. To grandma who is still asking herself/others where I am and what I am doing.

Last but not least, a huge, deep and amorous thank to Eva. Despite of the distance, she is always been close to me like if she was here. We spent a lot of money on phone bills, but I believe that allowed us to survive to a long distance relationship.

My dear children: I rejoice to see you before me today, happy youth of a sunny and fortunate land. Bear in mind that the wonderful things that you learn in your schools are the work of many generations, produced by enthusiastic effort and infinite labour in every country of the world. All this is put into your hands as your inheritance in order that you may receive it, honour it, and add to it, and one day faithfully hand it on to your children. Thus do we mortals achieve immortality in the permanent things which we create in common. If you always keep that in mind you will find meaning in life and work and acquire the right attitude towards other nations and ages.

Albert Einstein, talking to a group of school children, 1934.

Abbreviations

aME = accessory medulla
CNS = central nervous system
d.f. = degrees of freedom
DAG = diacylglycerol
DBT = double-time
DD = dark/dark regime
dp= dorsal projection of the s-LN_v
E OFF = Evening Offset
E ON = Evening Onset
EAG=electroantennogram
fra = *frazzled*
ICC = immunocytochemistry
IP3 = inositol trisphosphate
IPNa = IPNamide
KD = Knock down
LD = light/dark regime (usually 12 hours of light followed by 12 hours of dark)
LL = light/light regime
M OFF = Morning Offset
M ON = Morning Onset
MB = Mushroom Bodies
MT = Malpighian tubules
nocte = no circadian temperature entrainment mutant, gene or mRNA
norpA = no receptor potential A mutant, gene or mRNA
PACAP = Pituitary adenylate cyclase activating polypeptide
PDF = Pigment Dispersing Factor
PDP1ε = Par Domain Protein 1ε
per = *period* mutant, gene or mRNA
PER = *period* protein
PKC = Protein Kinase C
PLC = phospholipase C
plc21C = phospholipase C at 21C
POT = posterial optic tract
RNAi = RNA interference
SCN = suprachiasmatic nucleus or nuclei
SEM = Standard error of the mean
sgg = shaggy mutant, gene or mRNA
tim = *timeless* mutant, gene or mRNA
TIM = *timeless* protein
VIP = Vasoactive intestinal peptide
VRI = VRILLE

Table of contents

Title	Page
1. Introduction	
1.1. Biological clocks and their natural function	1
1.2. Common features of clocks	2
1.3. <i>Drosophila</i> clock: molecules at work	3
1.3.1. First negative feedback loop: <i>period</i> and <i>timeless</i>	4
1.3.2. Second feedback loop: <i>Clock</i> and <i>cycle</i>	9
1.4. Stimuli to the clock: the input pathway	11
1.4.1. Light entrainment	11
1.4.1.1. Cryptochrome	12
1.4.1.2. Visual system	13
1.4.2. Temperature entrainment	16
1.4.3. Social entrainment and feeding	20
1.5. Outputs	21
1.6. Where are the “ticking cells” located?	24
1.6.1. Central clock	24
1.6.2. Ventral lateral neurons	26
1.6.3. Dorsal lateral neurons (LN _d)	26
1.6.4. Dorsal neurons 1 (DN1s)	27
1.6.5. Dorsal neurons 2 (DN2s)	27
1.6.6. Dorsal neurons 3 (DN3s)	27
1.6.7. Lateral posterior neurons (LPNs)	28
1.6.8. Networking between circadian neurons	28
1.6.9. Peripheral clocks	30
1.7. Clocks in other organisms	32
1.7.1. The circadian clock in <i>Neurospora crassa</i>	32
1.7.2. The circadian clock in mammals	33
1.8. Aim of the project	36
2. Materials and methods	
2.1. Genomic DNA extraction from <i>Drosophila</i> individuals	38
2.2. RNA extraction from <i>Drosophila</i> individuals	38
2.3. cDNA synthesis	39
2.4. PCR (Polymerase Chain Reaction)	40
2.5. Agarose Gel Electrophoresis	42
2.6. Recovery of DNA from an agarose gel	42
2.7. Sequencing	42
2.8. Vectors	42
2.8.1. pBluescript II KS (pBS)	42
2.8.2. pUAST	43
2.9. Bacteria transformation by electroporation	44
2.10. Transformation	45

2.11.	Speed preparation of the plasmid DNA (“Mini-prep”)	45
2.12.	Restriction digest of DNA	46
2.13.	Western Blotting	46
2.13.1.	Protein extraction from <i>Drosophila</i> heads	46
2.13.2.	SDS-Polyacrylamide Gel Electrophoresis (SDS-PAGE)	47
2.13.3.	Transfer onto Nitrocellulose Membrane	47
2.13.4.	Immunostaining with Antibodies	48
2.13.5.	Protein Detection	48
2.14.	<i>in situ</i> hybridisation	48
2.14.1.	Synthesis of RNA probes	48
2.14.2.	Brain dissection	49
2.14.3.	<i>in situ</i> protocol	50
2.15.	Immunocytochemistry in <i>Drosophila</i> brain (ICC)	51
2.16.	Fly Stocks	52
2.17.	Locomotor activity	54
2.18.	Data collection and Analysis	55

3. NORPA as a component of temperature entrainment

3.1.	Introduction	57
3.2.	Materials and methods	59
3.2.1.	Synthesis of <i>norpA</i> RNA probes	59
3.3.	Results	59
3.3.1.	Spatial localisation of NORPA in fly adult brains <i>via</i> ICC	59
3.3.2.	Spatial localisation of NORPA in fly larval brains <i>via</i> ICC	65
3.3.3.	Spatial localisation of <i>norpA</i> in fly brain <i>via in situ</i> hybridisation	68
3.4.	Discussion	74
3.5.	Conclusions	76

4. RNA interference of *norpA*

4.1.	Introduction	77
4.2.	Materials and Methods	80
4.2.1.	<i>norpA</i> RNAi VDRC lines	80
4.2.2.	Cloning strategy to generate “our” <i>norpA</i> silencing lines	80
4.3.	Results	81
4.3.1.	Testing the silencing level in <i>norpA</i> RNAi flies	81
4.3.2.	Behaviour analysis	84
4.3.2.1.	<i>actin</i> GAL4 driver: <i>norpA</i> downregulation in whole <i>Drosophila</i>	84
4.3.2.2.	<i>norpA</i> off-targeting: <i>frazzled</i> gene	86
4.3.2.3.	<i>nina</i> EGMRGAL4 driver: <i>norpA</i> silencing in photoreceptor cells	86
4.3.2.4.	Pan-neuronal <i>elav</i> GAL4 driver	89
4.3.2.5.	<i>tim</i> GAL4 driver: <i>norpA</i> silencing in circadian cells	91
4.3.2.6.	<i>pdf</i> GAL4 driver: <i>norpA</i> silencing in morning cells	95
4.3.2.7.	<i>cry</i> GAL4 driver: <i>norpA</i> silencing in CRY cells	97
4.3.2.8.	Implementation of GAL80 element	99

4.3.2.9. FGAL4: <i>norpA</i> downregulation in chordotonal organs	101
4.4. Discussion	102
4.5. Conclusions	106
5. Temperature synchronisation of the <i>Drosophila</i> circadian clock	
5.1. Introduction	108
5.2. Materials and Methods	109
5.2.1. Stock flies	109
5.2.2. Locomotor activity	109
5.3. Results	110
5.3.1. Temperature synchronisation of wild-type and <i>norpA^{p41}</i> mutant	110
5.3.2. Temperature resynchronisation in photoreceptor mutants	113
5.3.3. Temperature resynchronisation in <i>norpA;;cry</i> mutants	115
5.3.4. Temperature resynchronisation of <i>norpA</i> interference flies	116
5.3.5. Temperature resynchronisation: <i>norpA</i> KD in chordotonal organs	118
5.4. Discussion	119
5.5. Conclusions	121
6. <i>plc21C</i>: is the phospholipase C located at 21C involved in the same pathway as <i>norpA</i>?	
6.1. Introduction	122
6.2. Materials and Methods	123
6.2.1. Fly strains	123
6.2.2. Locomotor analysis	123
6.2.3. RNA extraction from <i>Drosophila</i> individuals and cDNA synthesis	124
6.2.4. RT-PCR	124
6.3. Results	125
6.3.1. <i>plc21C</i> mRNA level in wild-type flies and <i>norpA</i> mutants	125
6.3.2. Analysis of locomotor activity	127
6.3.2.1. Silencing <i>plc21C</i> in all <i>Drosophila</i> tissues via the <i>actinGAL4</i> driver	127
6.3.2.2. <i>ninaEGMRGAL4</i> driver: silencing PLC21C in photoreceptor cells	137
6.3.2.3. <i>timGAL4</i> : <i>plc21C</i> silencing in circadian cells	139
6.3.2.4. <i>pdfGAL4</i> : <i>plc21C</i> silencing in morning cells	140
6.3.2.5. <i>cryGAL4</i> driver: <i>plc21C</i> silencing in CRY cells	143
6.4. Discussion	144
6.5. Conclusions	148
7. Are <i>glass^{60j}cry^b</i> flies really circadian blind?	
7.1. Introduction	149
7.2. Material and Methods	150

7.2.1. <i>glass</i> ^{60j} and <i>cry</i> ^b mutations	150
7.3. Results: Locomotor activity of <i>glass</i> ^{60j} <i>cry</i> ^b mutants	152
7.3.1. <i>glass</i> ^{60j} <i>cry</i> ^b locomotor activity in LD regime	152
7.3.2. <i>glass</i> ^{60j} <i>cry</i> ^b locomotor activity in DD regime	153
7.3.3. <i>glass</i> ^{60j} <i>cry</i> ^b locomotor activity in LL regime	155
7.3.4. Are temperature fluctuations influencing <i>glass</i> ^{60j} <i>cry</i> ^b locomotor activity?	156
7.3.5. <i>glass</i> ^{60j} <i>cry</i> ^b locomotor activity under different LD regimes	158
7.3.6. <i>glass</i> ^{60j} <i>cry</i> ^b locomotor activity under temperature cycles	161
7.4. Discussion	165
7.5. Conclusions	168
8. Orphan GPCRs	
8.1. Introduction	169
8.2. Materials and Methods	172
8.2.1. Fly Stocks	172
8.2.2. Crosses	172
8.2.3. Locomotor activity	173
8.3. Results	173
8.3.1. Behavioural analysis of flies downregulating <i>CG12290</i>	173
8.3.2. Behavioural analysis of flies downregulating <i>CG7497</i>	175
8.3.3. Behavioural analysis of flies downregulating <i>CG13995</i>	178
8.3.4. Behavioural analysis of flies downregulating <i>CG13579</i>	180
8.3.5. Behavioural analysis of flies downregulating <i>CG16958</i>	181
8.4. Discussion	184
8.5. Conclusions	187
9. Final discussion	
9.1. Temperature entrainment: <i>norpA</i> and <i>plc21C</i>	188
9.2. Light signalling: <i>glass</i> ^{60j} <i>cry</i> ^b and putative photoreceptor candidates	193
Appendix 1 NORPA overexpression	195
Appendix 2 Behaviour of <i>norpA</i> and <i>plc21C</i> knocked-down flies	200
2.1. <i>norpA</i> RNAi in LD 12:12	200
2.2. <i>fra</i> KD in PDF cells	205
2.3. Temperature synchronisation of the <i>Drosophila</i> circadian clock	205
2.4. <i>plc21C</i> RNAi in LD 12:12	207
Appendix 3 GPCRs	214
3.1. GPCRs in <i>glass</i> ^{60j} <i>cry</i> ^b genetic background	214
3.2. <i>CG12290</i>	214
3.3. <i>CG7497</i>	218

3.4.	<i>CG13995</i>	223
3.5.	<i>CG13579</i>	228
3.6.	<i>CG16958</i>	231

References	234
-------------------	-----

Chapter 1: Introduction

1.1. Biological clocks and their natural function

Today, we are living in a world in which “time” means everything: appointments, deadlines and timetables. We spend most of our time looking at different watches barely aware that we possess an internal one that starts to tick from before we are born. Most lay people (not scientists) are not familiar with biological clocks, and only become aware of their existence when they suffer “shift work blues” or “jet lag”. This latter phenomenon occurs as a consequence of rapid long-distance transmeridian (east-west or west-east) travel. It has been shown that the effect of this event is more severe when travelling from west to east, and increases with distance (Recht *et al.*, 1995). Thus internal clocks appear to be just another aspect of life that makes it more difficult and stressful. However, this allows us to raise a scientific question: “why is it important to have them?”. The answer is simple: biological clocks are advantageous for organisms, because they enhance biological fitness in a wide range of organisms from unicellular to complex.

Internal timekeeping systems can be classified depending on the length of their period: *ultradian* when their period is less than 24 hours (for example the love song of fruit flies which has a ~60 s cycle [Ashburner, 1987]), *infradian* when the rhythmicity is repeated within an interval longer than a day (for example the menstrual cycle in women) and *circadian* when the repeating interval is close to 24 h. One of the first recorded observations of the existence of circadian clocks was made by Androstenes, a soldier-philosopher serving with Alexander’s army in the fourth century B.C. During long marches, he noted that leaves of the tamarind tree changed position throughout the day. In 1729, Jean Jacques d’Ortous de Marain wrote formally about his observations on the circadian clock of the leaves of heliotropic plants, which open in the morning and close in the evening, and continue to open and close even in the absence of a daily light/dark cycle (Hall, 1995). de Marain thus observed one of the key characteristics of circadian clocks, namely, they are endogenous and self-sustained in constant conditions. Caroluos Linnaeus also noticed that different flowers opened and closed their blossoms at different times of

the day. He grew a garden that told the time by planting flowers that opened or closed their blossoms an hour apart around the clock (Hall, 1995).

Clocks are thus an adaptation to a rotating planet. For the fitness of an organism, it is more advantageous to predict changes of environment than simply respond to them, so, for example, an early induction of a metabolic pathway has the advantage that the final product is available when needed. A functional circadian clock in constant darkness and temperature does not necessarily provide any competitive advantages, reinforcing the idea that circadian rhythms are adaptive in LD conditions (Woelfle *et al.*, 2004). Thus, photosynthesis, nitrogen fixation and cell division in prokaryotic bacteria; leaf movement, photosynthesis and flowering in plants; locomotor activity and eclosion (the emergence of adult flies from their pupal case) in insect; body temperature and sleep/wake cycle in mice and humans, are under circadian control.

1.2. Common features of clocks

Circadian clock are highly conserved within a wide range of organisms and they share common characteristics:

- the capability to be synchronised to environmental stimuli (called *Zeitgebers*). One of the major external stimuli is light (the alternation of day and night), but also temperature plays an important role;
- the capability to keep ticking in the absence of a *Zeitgeber*. This endogenous *free-running* period can be different in length from that observed in the presence of *Zeitgebers*.
- the capability to be temperature compensated. Usually, in a biochemical process, an increase in temperature leads to an increase in the rate of the process itself (for example increasing the turnover of proteins). Circadian clocks are largely temperature insensitive.
- the molecular mechanism that generates the circadian rhythm. Although the single elements of the process can be different, they belong to a circuit in which negative elements are able to inhibit the transcription of their own genes (negative feedback loop).

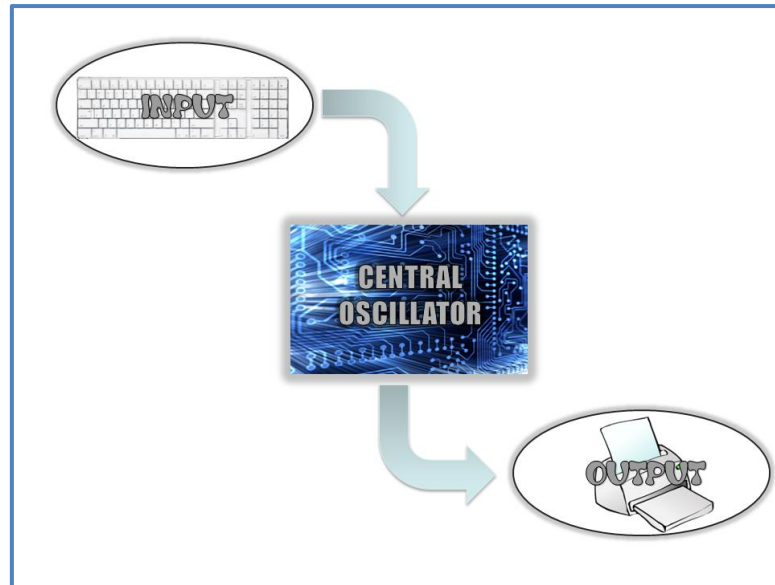


Figure 1.1: General structure of biological clocks. The oscillator (represented by the electrical circuit) manifests its rhythm in the output pathway (printer) after having been synchronised by the input pathway (keyboard).

As mentioned above circadian clocks are not isolated from the external environment but they are influenced by it, so it is possible to define a system which is based on three elements (Figure 1.1):

- ✓ INPUT which represents all the ways that connect the clock to the external conditions.
- ✓ CORE or CENTRAL OSCILLATOR based on molecular processes that oscillate between a minimum and maximum level with a certain period. Transcription, translation and post-translation events collaborate to maintain a constant rhythmicity.
- ✓ OUTPUTs which are all the phenotypes regarding metabolism or cell processes regulated by the circadian core. Genes which are controlled by the clock, are called *clock controlled genes* or *ccgs*.

1.3. *Drosophila* clock: molecules at work

Drosophila melanogaster has played a central role in the identification of components and mechanisms that lie behind the circadian clock. The *period* gene was the first to be identified (Konopka and Benzer, 1971), and since then, the use of *Drosophila* as a model organism has greatly contributed to novel insights into the mechanism of the clock. A number of genetic and molecular tools are available in *D.*

melanogaster which allow the dissection of the molecular and cellular components of circadian phenotypes (Venken and Bellen, 2005). Studies of tissue-specific expression patterns are performed using the GAL4/UAS system (Brand and Perrimon, 1993). Mutagenesis and transgenesis in fly are achieved relatively easily using transposons or chemical methods. Numerous behavioural processes can be genetically dissected using *Drosophila* and extrapolated to other organisms, including humans, since there is considerable conservation of clock genes across species.

1.3.1 First negative feedback loop: *period* and *timeless*

Chemical mutagenesis by Konopka and Benzer (1971) identified three sex-linked mutants with altered circadian rhythms in constant conditions (DD). One mutant showed a shorter rhythm of approximately 19 hours, another had a longer rhythmicity of about 28 hours and the last was arrhythmic. The mutations that caused these altered circadian rhythms were located in a locus subsequently called *period* (*per*) and the mutants were named *per^S*, *per^L* and *per⁰*, respectively. *per* encodes a protein of 1218 amino acids (Citri *et al.*, 1987) which has been shown to rescue the arrhythmicity of *per⁰* transformants (Zehring *et al.*, 1984). In *per^S* an asparagine replaces a serine at amino acid 589, in *per^L* an aspartate substitutes a valine in position 243 and a stop codon is introduced at position 464 in the *per⁰¹* mutant (Baylies *et al.*, 1987; Figure 1.3).

Furthermore, *per* obtained from *D. pseudoobscura* and transformed into *per⁰* *D. melanogaster* flies generates flies which display locomotor activity resembling that of *D. pseudoobscura* (Petersen *et al.*, 1988). This is a demonstration of how species-specific differences in behaviour are due to *per*, giving an example of a complex pattern of behaviour being controlled by a single gene. *per*, not only controls locomotor activity but also male courtship song cycle. Wild-type flies display an ultradian rhythm of 60 seconds but mutant flies show 40 seconds rhythm in *per^S* males, 75 seconds in *per^L* mutants and no rhythms in *per⁰* (Kyriacou and Hall, 1980).

The discovery that the level of PER and its mRNA oscillates out of phase with each other suggested that PER is a negative regulator of its own transcription (Hardin

et al., 1990). The increase of PER levels during the night phase is also associated with a changing in molecular mass indicating post-translation regulation such as phosphorylation (Edery *et al.*, 1994; Figure 1.2).

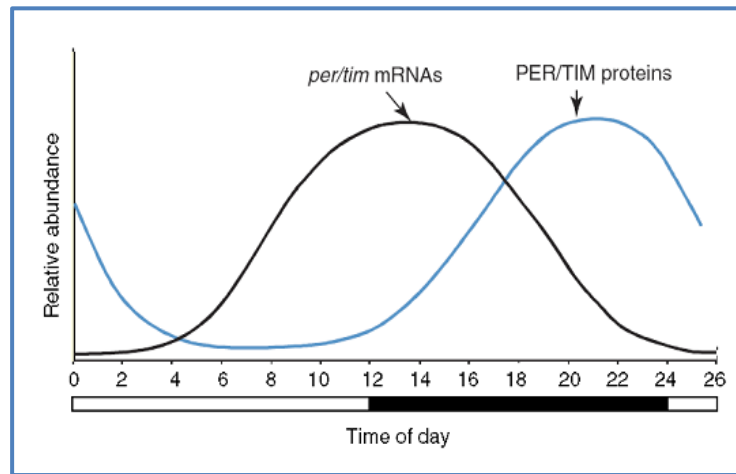


Figure 1.2: Rhythmic expression of PER and its mRNA (from Nitabach and Taghert, 2008). The expression profile for *per* mRNA and its protein were studied in 12 hours of light (open bar; ZT 0-12) and 12 hours of dark (black bar; ZT 12-24).

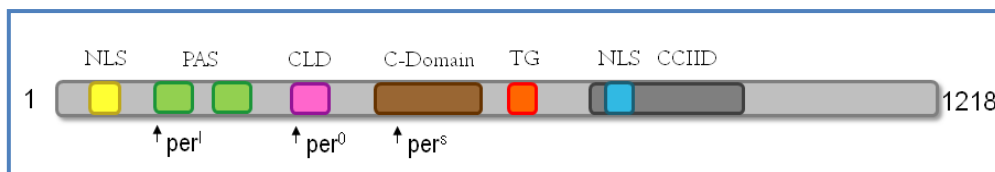


Figure 1.3: PER domains in *D. melanogaster*.

Referring to Figure 1.3, PER protein contains 5 domains:

- NLS (Nuclear Localisation Signal): this domain allows the nuclear translocation of PER for downregulating its own transcription;
- PAS: this domain is divided in two regions and both have important role in protein-protein interactions. Since PER does not have any DNA binding domains, PAS domains guarantee interaction with other proteins/transcription factors that are essential to regulate PER expression (Huang *et al.*, 1993);
- CLD (Cytoplasmatic Localisation Domain): this domain maintains PER in the cytoplasm as long as the NLS is activated.
- TG domain: this domain contains a motif of alternative threonine and glycine amino acids. The Thr-Gly region is polymorphic in the number of repeats with natural variants between 14 to 24 pairs (Costa and Kyriacou, 1998).

Furthermore this variation provides an example of balancing selection (Sawyer *et al.*, 1997) and provides *per* with an important role in geographic adaptations in temperature compensation. This evidence emerges from the distribution of 17 and 20 TG repeats (generating 90% of natural alleles) in Europe and their temperature compensation properties: TG_{17} is mostly distributed in southern Europe and shows a period of about 24 hours at warmer temperatures; on the other hand TG_{20} is predominant in the north of Europe and presents a period close to 24 hours over a wide range of temperatures. Additionally, Thr-Gly region has also been shown to be important in the species-specific ultradian courtship song rhythm (Wheeler *et al.*, 1991).

- CCID: this region is called the "CLK and CYC inhibition domain" since it is essential for the regulation of PER through the disruption of the circadian transcription factors CLK and CYC (see paragraph 1.3.2). Moreover, recently in this region a second NLS domain has been described which seems to be more important than the one mentioned earlier (Chang and Reppert, 2003).

A second clock gene that belongs to the first negative feedback loop is *timeless*. It was identified by forward genetics in 1994 and located on the second chromosome (Sehgal *et al.*, 1994). *timeless* encodes a protein of 1389 amino acids (Myers *et al.*, 1995) that is characterised by different essential domains: a NLS, a CLD (Saez and Young, 1996) and a central acidic region followed by a basic region which has been shown to interact with the PAS domain of PERIOD (Myers *et al.*, 1995). *timeless* shows a natural single nucleotide polymorphism in the 5' region which results in the existence of a truncated TIM protein lacking 23 amino acids at the N-terminus, with respect to the full length product (Rosato *et al.*, 1997). The distribution of this polymorphism follows a latitudinal cline across Europe: *ls-tim*, which is the allele that allows the formation of long and short TIM isoforms from two ATG's, is prevalent in the south of Europe, whereas the other allele that encodes the short form of TIM is predominantly present in northern Europe (Tauber *et al.*, 2007). It has been shown that these alleles give differences in diapause responses (i.e. a neurohormonally mediated, dynamic state of low metabolic activity): *ls-tim* homozygous flies show

elevated diapause compared to *s-tim* strains (Tauber *et al.*, 2007). Molecularly, a possible explanation can be found in the strength S-TIM and L-TIM interaction with CRY (see description below): S-TIM interacts more strongly with CRY than L-TIM (Sandrelli *et al.*, 2007).

tim-null mutants show an arrhythmic phenotype in DD conditions (Sehgal *et al.*, 1994) and have arrhythmic *tim* and *per* mRNA expression (Sehgal *et al.*, 1994). These data together suggest that *tim*, as well as *per*, are negative regulators of their own transcription. Furthermore *tim*⁰ mutants revealed that TIM is necessary for the translocation of PER from the cytoplasm to the nucleus. PER is restricted to the cytoplasm in *tim*⁰ mutants (Sehgal *et al.*, 1995), whereas in wild-type individuals, it is known that PER can move between the nucleus and the cytoplasm (Shafer *et al.*, 2002). In the same mutants PER does not accumulate in the cytoplasm implying that TIM has a role in the stabilisation of PER (Vosshall *et al.*, 1994). These data were supported by the finding that TIM is light sensitive (Zeng *et al.*, 1996) and in the presence of light the level of TIM is low. Since PER is not stable in the absence of TIM, its level during the day is low. Only when TIM starts to accumulate, the concentration of PER also increases (Price *et al.*, 1995).

CLK and CYC (described in paragraph 1.3.2), two basic helix-loop-helix (bHLH) transcription factors, dimerise and bind to E-box elements in *per* and *tim* promoters to initiate their transcription (Darlington *et al.*, 1998). *per* and *tim* mRNAs are translocated to the cytoplasm where their translation starts. However, from the appearance of *per* and *tim* mRNAs in the cytoplasm (early in the evening) to their proteins, there is a time gap of 4-6 hours controlled by the casein kinase I homologue *doubletime* (*dbt*) which phosphorylates PER and directs it to degradation (Price *et al.*, 1998). This kinase was identified in a screen for circadian rhythm mutants allowing the discovery of two mutants with long and short periods: *dbt*^l and *dbt*^s respectively (Price *et al.*, 1998). These mutations gave a change in the level of phosphorylation of PER, implying a role for DBT in the PER stability (Kloss *et al.*, 1998). *dbt*^s mutants show a faster transition between hypophosphorylated and hyperphosphorylated PER than in wild-type and cause a short period of 18 hours in

DD. On the other hand, *dbt^l* results in a longer period of 28 hours and a longer delay between hypophosphorylated and hyperphosphorylated PER (Price *et al.*, 1998). A null mutant for *dbt* (*dbt⁰*) reinforces the importance of this kinase in monomeric PER phosphorylation, since in this mutant the level of PER is high no matter if it is kept in LL which is a condition that would normally degrade TIM. Thus, DBT is essential and necessary to maintain PER at low levels until TIM levels increase and stabilise PER (Price *et al.*, 1998).

The clock can be reset by light *via* CRYPTOCHROME (CRY) which is a circadian photoreceptor. In the presence of light, CRY is active and interacts with PER and TIM eventually leading to their degradation *via* the proteasome which is also mediated by JETLAG (JET, Ceriani *et al.*, 1999; Koh *et al.*, 2006). Thus, during the day PER and TIM are not able to translocate back to the nucleus to repress their own transcription.

In the evening, PP2A dephosphorylates PER which can translocate to the nucleus since it is more stable (Sathyanarayanan *et al.*, 2004). Experiments in which PP2A activity is increased generated short circadian periods, and an opposite effect is obtained if the PP2A activity is decreased (Sathyanarayanan *et al.*, 2004). Thus the effects of PP2A are opposite to DBT with respect to the PER stability. At the same time, TIM concentration increases since CRY is not longer active (Ceriani *et al.*, 1999). SHAGGY, a serine-threonine kinase (SSG) phosphorylates TIM promoting its nuclear localisation and the formation of a heterodimer with PER (Martinek *et al.*, 2001). This has been demonstrated using transgenic flies that allow the overexpression or downregulation of *sgg*: increasing SGG activity generates a short circadian period due to the premature nuclear localisation of TIM; a decreased level of SGG delays TIM translocation resulting in a long period (Martinek *et al.*, 2001). The complex formed by PER/TIM/DBT and CRY is able to enter the nucleus (Ceriani *et al.*, 1999) and the PER/TIM dimer or PER alone can bind to the CLK/CYC heterodimer preventing further transcription of *per* and *tim* (Darlington *et al.*, 1998). Once the PER/TIM/DBT trimer has exhausted its inhibitory role, PER is degraded by DBT kinase and so the negative effect gradually decays. Consequently, this allows CLK/CYC to activate *tim* and *per* promoters again and a new cycle starts (Bae *et al.*, 1998).

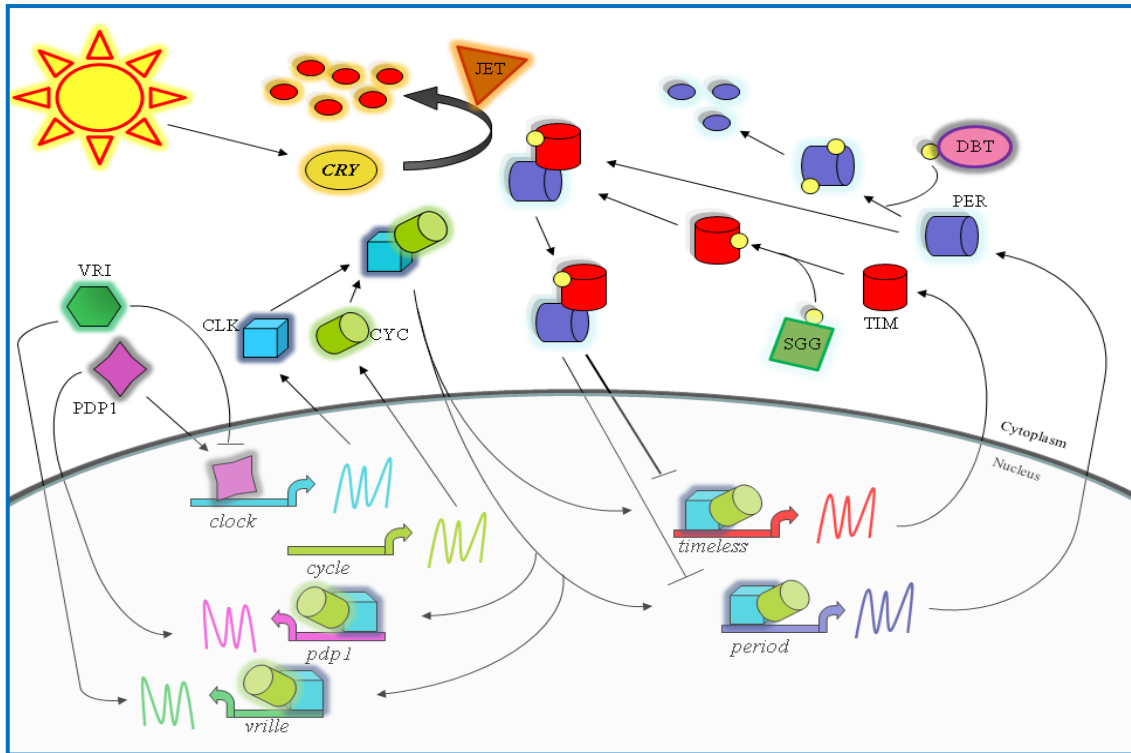


Figure 1.4: *Drosophila melanogaster* circadian clock. Transcription of *tim* and *per* is regulated by the positive elements CLK and CYC. TIM and PER proteins inhibit their own synthesis, generating a feedback loop. *vri* and *Pdp1* regulate, negatively and positively respectively, the expression of *Clk*. CRY acts on TIM and PER in a light-dependent manner, so the photoreceptor entrains the clock to the environmental cues.

1.3.2. Second feedback loop: *Clock* and *cycle*

PER and TIM have been shown to be sufficient and necessary to regulate their own transcription, but the fact that they do not possess any DNA binding domain suggests that they cannot interact directly with their own DNA (Huang *et al.*, 1993). The discovery of *Drosophila* CLOCK was prefaced by the identification of the mouse *Clock* mutant (Vitaterna *et al.*, 1994) and by the finding that it encodes for a bHLH transcription factor that is able to drive the rhythmic expression of mouse *per* (King *et al.*, 1997). Later, a *Drosophila* homologue was identified by mutagenesis and flies carrying a mutation on this gene (i.e. *Clk^{irk}*) were shown to be arrhythmic and characterised by low levels of *per* and *tim* transcription (Allada *et al.*, 1998).

A second bHLH-PAS transcription factor, CYCLE (CYC) homologous to mouse BMAL1, was identified and also found to be essential for the activation of *per* and *tim* transcription (Rutila *et al.*, 1998). Mutant flies for CYC are arrhythmic whereas heterozygous mutants are rhythmic but with a longer period (Rutila *et al.*, 1998).

Most of the information about CLK and BMAL1 (CYC in *Drosophila*) has been provided by studies in the mouse, in which these two transcription factors form a heterodimer (Hogenesch *et al.*, 1998) suggesting a similar interaction between the homologues in *Drosophila* (Darlington *et al.*, 1998). The heterodimer is able to activate *per* and *tim* transcription by binding to the E-boxes present in their promoters (Darlington *et al.*, 1998).

As in the case of *per* and *tim*, *Clk* is also expressed in a rhythmic manner through an autoregulatory feedback loop (Lee *et al.*, 1999). The levels of *dClk* RNA and protein rise as PER and TIM enter the nucleus, and the peak level of CLK and its mRNA occur simultaneously between ZT 23 and ZT 4 (Rutila *et al.*, 1998). How is the expression of *Clk* sustained in a circadian manner? Two transcription factors were described to influence negatively and positively *Clk* expression: VRILLE and PDP1 ϵ (Blau and Young, 1999; Cyran *et al.*, 2003).

vri mRNA cycles in a similar phase to *tim* suggesting a possible regulation by the CLK/CYC heterodimer. Indeed, the *vri* promoter has potential E-box CLK/CYC binding sites. In *Clk* and *cyc* mutants, the level of *vri* mRNA is low (Blau and Young, 1999). Homozygous *vri* mutants are not viable since this gene is involved in the developmental *decapentaplegic* signaling pathway, however heterozygous mutants show a short locomotor activity period (Blau and Young, 1999). Moreover in the *Clk* promoter a *vri* binding site was found (Glossop *et al.*, 2003). Finally, the overexpression of VRI reduces *Clk* mRNA level, enforcing the idea that VRI binds to *Clk* promoter and inhibits its transcription (Glossop *et al.*, 2003).

The second gene that positively influences the expression of *Clk* is *Pdp1 ϵ* , which is activated by the CLK/CYC dimer, and encodes a bZIP transcription factor, which oscillates with a different phase to VRI (mRNA and protein). PDP1 ϵ presents its maximal level at ZT 18 whereas VRI peaks at ZT 15 (Cyran *et al.*, 2003). Furthermore, mutants for *Pdp1 ϵ* have a longer period compared to *vri* mutants, suggesting an opposite role for them in clock regulation (Cyran *et al.*, 2003). In *Pdp1 ϵ* mutants the level of *Clk* is reduced demonstrating that PDP1 ϵ activates the expression of CLK (Cyran *et al.*, 2003). Recently a role for PDP1 ϵ (or one of its isoforms) has been also proposed in the appropriate formation of neural connections between the small

lateral ventral neurons (s-LN_vs) and their target neurons (described below in paragraph 1.6). In fact, these neural circuits are abolished by the inhibition of PDP1ε activity, thereby resulting in the arrhythmic behaviour of *Pdp1ε* mutant flies (Lim *et al.*, 2007). On the other hand, CYC is constitutively expressed (Rutila *et al.*, 1998) and has been found to only interact with PER or TIM when in a complex with CLK (Bae *et al.*, 2000).

In summary, the heterodimer formed by CLK/CYC activates the expression of *per* and *tim*. PER and TIM once in the cytoplasm, start to accumulate and translocate to the nucleus to repress their own transcription by disrupting CLK/CYC. This latter complex activates the expression of *vri* and *Pdp1ε*. VRI peaks before PDP1ε and represses *Clk* transcription. However when the level of PDP1ε starts to increase, the expression of *Clk* starts to increase since VRI and PDP1ε compete for the same promoter in *Clk*. Once the level of CLK increases, the dimer CLK and CYC starts to form, but it is not able to activate the expression of *per*, *tim*, *vri* and *Pdp1ε* due to the residual presence of PER that is present until early morning, when it is degraded by DBT (Cyran *et al.*, 2003).

1.4. Stimuli to the clock: the input pathway

In the previous paragraphs, the mechanisms behind the *D. melanogaster* circadian clockwork have been described. Although this process is self-sustained and “ticks” by itself, the external environment can entrain the clock. This allows a finer regulation and a constant resetting in relation to the external conditions. In general, different cues can synchronise the clock, but light and temperature are considered the most important.

1.4.1. Light entrainment

Light is considered the most essential and strongest environmental *Zeitgeber* that synchronises the clock. *Drosophila* perceives light information by different pathways: the visual system and through cryptochrome, a dedicated blue-light photoreceptor (Ashmore and Sehgal, 2003).

1.4.1.1. Cryptochrome

Cryptochromes (CRY) were first discovered in *Arabidopsis*. CRYs are flavin containing blue light photoreceptors related to bacterial photolyases (Ahmad and Cashmore, 1993). The photolyases are flavoproteins, which repair the DNA damage caused by UV-B irradiation (Sancar, 2003). Cryptochromes are found in algae, ferns, plants and animals but they have lost their capability to repair DNA (Lin, 2002). They possess two domains situated on the opposite termini. The N-terminal photolyase-related (PHR) domain contains two chromophore binding sites: one for the binding of FAD (flavin adeno-nucleotide) and the other for a pterin. In particular this domain is the one that is highly conserved between photolyases and cryptochromes, suggesting a similar structure and mechanism of reaction. The second difference between these categories of proteins (photolyases and cryptochromes) is the C-terminal: a region of 20-200 amino acids that allows protein-protein interactions and signal transduction and which is present in cryptochromes.

In *D. melanogaster* the *cry* gene (Emery *et al.*, 1998; Stanewsky *et al.*, 1998) is expressed in most of the clock pacemaker cells (Emery *et al.*, 2000). CRY is a crucial component of the circadian input pathway used for the photic entrainment of the *Drosophila* circadian clock. The *cry^b* mutation blocks CRY mediated circadian photoreception and affects the photic entrainment of molecular oscillations while temperature entrainment is retained (Stanewsky *et al.*, 1998). *cry^b* flies are rhythmic in 12:12 LD, DD, but in LL they remain rhythmic (Emery *et al.*, 1998). Also a light pulse early or late in the night does not modify their behaviour, whereas a normal fly would delay or advance its locomotor activity (Emery *et al.*, 2000).

As in other clock gene transcripts, *cry* has a cyclic expression with a peak at ZT 1-5. However, this oscillation is disrupted in circadian clock mutants of *per*, *tim*, *Clk* and *cyc*. Furthermore flies kept in free-running conditions (DD and constant temperature) show continuous accumulation of CRY (Emery *et al.*, 1998) indicating that it is normally degraded by light. Regulation comes directly from its expression (transcriptional) plus a light mediated post-translational event via *Jetlag* (*Jet*), which leads to a degradation of CRY by the proteasome (Peschel *et al.*, 2009).

As described above, CRY is responsible for the degradation of TIM, thereby providing a delay in the translocation of PER/DBT/TIM into the nucleus (Ceriani *et al.*, 1999). The mechanism by which CRY can be activated and trigger TIM degradation in a light dependent manner seems to involve inter or intra-molecular changes of the flavin domain at the N-terminal (Lin *et al.*, 2001). This might generate conformational modifications that expose the C-terminal of CRY, allowing the interaction with TIM. In darkness, a putative repressor might inhibit the C-terminal domain of CRY not allowing its interaction with TIM (Rosato *et al.*, 2001). This has been demonstrated in CRY Δ in which 20 amino acids in the C-terminal domain were eliminated. Yeast and flies carrying this deletion behave as a constitutively active form of CRY (Dissel *et al.*, 2004).

1.4.1.2. Visual system

Despite the fact that flies carrying *cry^b* are not able to respond to a light pulse, they can still entrain to a light-dark regime and the molecular clock in the LN_v cells is still entrainable (paragraph 1.6; Stanewsky *et al.*, 1998). This indicates that another light pathway is available and the obvious candidates are the photoreceptors. In *Drosophila* two externally visible photoreceptor structures are present, a pair of compound eyes and the ocelli (Figure 1.7). *Drosophila* also has a further photoreceptor structure called the Hofbauer-Buchner (H-B) eyelet (Helfrich-Förster, 2002, Figure 1.7). All these photoreceptors express the retinal based photopigment rhodopsin. In *D. melanogaster* there are 6 different rhodopsin (Rh) molecules (Montell, 1999) and their maximum sensitivity varies from a minimum of 345 nm of Rh3 (absorbing in the UV) to a maximum of 508 nm of Rh6 that absorbs in the green (Figure 1.6). Most of them are expressed in the photoreceptor cells (R1-R8) of the compound eyes. Rhodopsins are G protein coupled receptors (GPCR) and their phototransduction involves factors encoded by many genes (Montell, 1999) since the elimination of any of these gene products provokes a block in the phototransduction cascade. In this process, rhodopsins are activated by light absorption, determining their activation by a change in their conformation, which ends in an activation of a G α subunit. The latter binds and activates the effector enzyme, phosphoinositide-specific phospholipase C (PLC β), encoded by the *norpA* gene in *Drosophila* (Figure

1.5). It hydrolyses the membrane phospholipid phosphatidylinositol 4,5-bisphosphate (PIP₂) to produce soluble inositol 1,4,5-triphosphate (IP₃) and diacylglycerol (DAG, Hardie, 2001). It results in the activation of cation-permeable channels and membrane depolarisation (Hardie, 2001). *norpA*^{P41} is a null mutation for phospholipase C, and hence *norpA*^{P41} flies cannot perform this catalytic reaction (Pearn *et al.*, 1996) so the rhodopsin based phototransduction *via* PLCβ is not functional. The phosphoinositide cascade is of central importance in controlling cellular Ca²⁺ levels, by releasing Ca²⁺ from IP₃-sensitive stores and also by activating Ca²⁺ influx through specific channels in the plasma membrane. The central role of PLC in invertebrate photoreceptors is not disputed, but how activation of PLC is linked to the opening of the light sensitive channels remains unresolved (Hardie, 2001). In *D. melanogaster* the light sensitive conductance is highly Ca²⁺ permeable and mediated by at least two channels encoded by the *trp* (transient receptor potential) gene and a homologue with approximately 40% sequence identity, *trpl* (*trp*-like; Hardie, 2001).

All the known rhodopsin expressing photoreceptors can be removed by the double mutant *sine oculis*¹; *glass*^{60j}. *sine oculis* (*so*¹) flies lack the compound eyes and ocelli because the homeobox gene required for visual system development is affected in this mutant (Cheyette *et al.*, 1994). Mutations in the *glass* gene, which encodes a transcription factor necessary for the general development of photoreceptor cells (Moses *et al.*, 1989), impair development of all known external and internal visual structures. Flies carrying the loss of function allele *glass*^{60j} lack all ommatidial photoreceptors and the ocelli, as well as the primary and secondary pigment cells in the compound eyes. Recently it was found that they also lack the H-B eyelet and the DN1s (Helfrich-Förster *et al.*, 2001; described in paragraph 1.6). However, *so*¹; *gl*^{60j} flies are still capable of LD synchronisation and phase-shifting circadian locomotor rhythms (Helfrich-Förster *et al.*, 2001) indicating that a non-rhodopsin photopigment plays a role in circadian photoreception, and this of course is CRY.

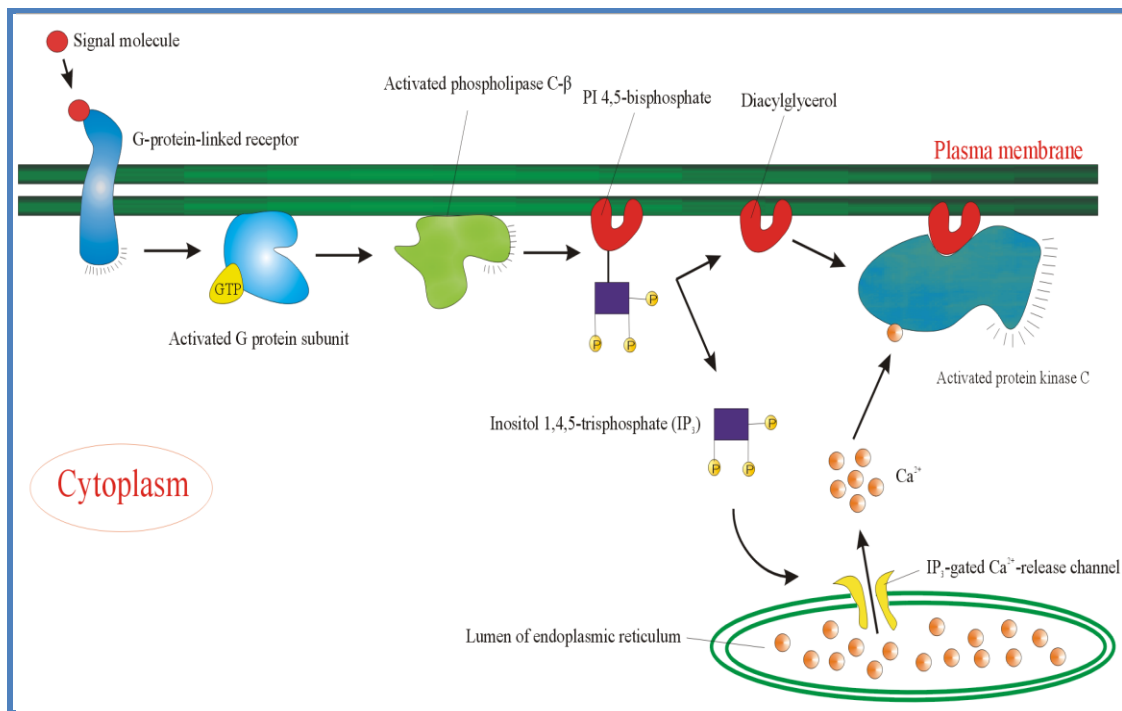


Figure 1.5 General functioning of phospholipase C (PLC). The activated receptor stimulates the plasma-membrane-bound enzyme phospholipase C- β *via* a G protein. Two intracellular messenger molecules are produced when PI(4,5)P₂ is hydrolysed by the activated phospholipase C- β . Inositol 1,4,5-trisphosphate (IP₃) diffuses through the cytosol and releases Ca²⁺ from the endoplasmic reticulum by binding to and opening IP₃-gated Ca²⁺-release channels in the endoplasmic reticulum membrane. The large electrochemical gradient for Ca²⁺ across this membrane causes Ca²⁺ to escape into the cytosol. Diacylglycerol remains in the plasma membrane and, together with Ca²⁺, helps to activate the enzyme protein kinase C, which is recruited from the cytosol to the cytosolic face of the plasma membrane.

In *norpA^{P41};cry^b* double mutant flies, both rhodopsin and cryptochrome mediated phototransduction into the circadian clock is blocked (Stanewsky *et al.*, 1998; Helfrich-Förster *et al.*, 2001). However, these double mutant flies are still able to entrain to LD, although it takes them much longer time to synchronise their behaviour to shifted LD (Stanewsky *et al.*, 1998). Therefore, in *norpA^{P41};cry^b* double mutant flies the circadian clock is not absolutely blind. This indicates that the circadian clock receives light input through additional, extra-retinal photoreceptors/photopigments independent of *norpA* and *cry*. Moreover, in *norpA^{P41};cry^b* flies the molecular synchronisation of PER and TIM expression in the s-LN_vs and in the DN1s by light is still possible (see paragraph 1.6; Helfrich-Förster *et al.*, 2001), again pointing to an alternative pathway for the light-dependent TIM degradation in addition to the known CRY-dependent mechanism.

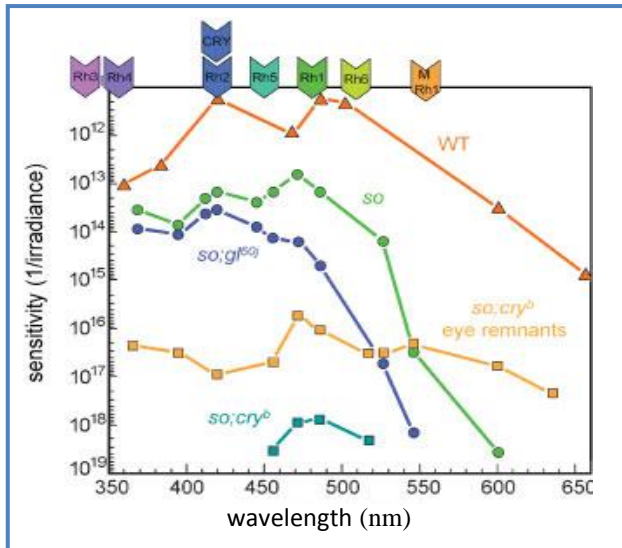


Figure 1.6: Action spectra for entrainment of the activity rhythm of wild-type flies and mutant for the input pathway. *so* mutants lack eyes and ocelli, *so;gl^{60j}* possesses only cry as the photoreceptor, *so;cry^b* only the H-B eyelets and rudiments of compound eyes. The absorption maxima of CRY and the different fly rhodopsins is reported above (Helfrich-Förster, 2002).

The residual behavioural and molecular synchronisation retained in the *norpA^{P41};cry^b* flies is eliminated by combining *glass^{60j}* with *cry^b*, thus the *gl^{60j} cry^b* double mutants are reported to be absolutely circadian blind (Helfrich-Förster *et al.*, 2001). What additional photoreceptive structures were affected by the *gl^{60j}* mutation? As mentioned above, the H-B eyelet and the DN1s are additionally removed in *gl^{60j}* flies. Therefore, these structures *per se* can be the possible candidates that mediate residual light signalling into the circadian clock in the *norpA^{P41};cry^b* flies.

1.4.2. Temperature entrainment

In addition to variation of light exposure, organisms are subjected to daily changes in temperature. While much is understood about how a fly uses light to align its behaviour to the 24 h environmental cycle, less is known about how flies use temperature as a *Zeitgeber*. From a molecular point of view PER and TIM have been shown to be rapidly downregulated by a short high temperature pulse which results in a phase delay in behavioural activity if administered in the early night (Sidote *et al.*, 1998). On the other hand, a temperature pulse administered in the late night does not give any response, as would be the case with a light pulse given at the same time (Sidote *et al.*, 1998).

Behaviourally, locomotor activity of *D. melanogaster* can be entrained to temperature cycles as little as 3°C (Wheeler *et al.*, 1993) with most activity during

the thermophase and a peak of activity at the end of this phase. In addition temperature cycles can drive locomotor activity in arrhythmic clock mutants such as *per⁰*, *tim⁰*, *Clk^{irk}* and *cyc⁰* (Yoshii *et al.*, 2002). However, as in the case of LD cycles, these mutants do not completely entrain since there is no anticipation of the temperature transition, and their rhythmicity is lost when they are released in constant conditions. Wild-type flies can be entrained to temperature cycles in the presence of constant light (LL regime), a condition that would normally generate arrhythmicity. In this case, there is anticipation of temperature transitions, but when the temperature cycle is removed flies become arrhythmic (Yoshii *et al.*, 2005).

The oscillation of PER and TIM is maintained during temperature entrainment in DD and it is also maintained during constant conditions following temperature entrainment (Stanewsky *et al.*, 1998). This indicates that temperature acts on one of the same molecular components of the circadian clock as light. Furthermore, temperature cycles can drive PER and TIM oscillation during constant light, implying that temperature can somehow override the light induced degradation of TIM by CRY (Glaser and Stanewsky, 2005).

Most of the recent molecular work on temperature and circadian clock rhythm has focused on an alternative splicing event of an 89 bp intron in the 3' UTR in *per* mRNA. This event has been associated to a seasonal adaptation: at low temperature, more of the spliced *per* form is produced than the unspliced (Majercak *et al.*, 1999). This results in an earlier increase in PER protein abundance and an advanced locomotor activity phase. The presumed adaptive and ecological advantage of this event is that a fly would move its behaviour toward the middle part of the day which is characterised by brighter and warmer conditions. However at low temperature, long photoperiods counteract this advanced behaviour by delaying TIM accumulation and rendering any prematurely produced PER unstable (Majercak *et al.*, 1999). Thus, temperature and light information collaborate to align fly behaviour to the environmental day. At warmer temperatures, the splicing event in *per* is inhibited (Collins *et al.*, 2004; Majercak *et al.*, 2004). This is a clock dependent effect that results in the fly moving its behaviour to the later part of the day, which would be cooler, and thus avoid possible desiccation caused by the high temperature in the middle of the day. Thus *per* splicing allows the fly to adapt to changes in both

temperature and photoperiod by regulating the amount of available PER, while TIM appears to be responsible for relaying environmental light/dark information to the clock by regulating the rate of PER accumulation (Collins *et al.*, 2004; Majercak *et al.*, 2004). Moreover, by using transgenic flies which encoded for the spliced or the unspliced *per* isoform, it has been demonstrated that the splicing *per se* is important in generating biochemical high steady state levels of *per* RNA during cold days (Majercak *et al.*, 1999).

A screening aimed to understand the relation between visual system mutants and *per* splicing, revealed that the phospholipase C (PLC) encoded by *norpA* (Bloomquist *et al.*, 1988) plays a nonphotic role in this *per* splicing event, relaying information about temperature to the clock (Collins *et al.*, 2004). The *norpA*^{P41} mutant presents a high level of *period* spliced form, with the consequent early accumulation of PER at low and high temperatures. Indeed, these flies exhibit the cold behavioural phenotype regardless of the temperature and the time of the day. Furthermore, this appears to be a light independent effect since the downregulation of *per* splicing due to a light pulse is still maintained in this mutant strain (Majercak *et al.*, 2004; Collins *et al.*, 2004). However, *norpA* does not seem to be just involved in the regulation of the splicing event, but also in temperature entrainment, since *norpA* mutants show an impaired molecular and behavioural synchronisation to temperature cycles in LL (Glaser and Stanewsky, 2005).

Recently another gene, *nocte* (*no-circadian temperature entrainment*), has been implicated in temperature entrainment (Glaser and Stanewsky, 2005). This gene was identified in a PER-LUC reporter assay. *nocte* mutant flies cannot be entrained by temperature cycles, but possess a normal rhythm in LD or DD conditions over a range of constant temperatures. Moreover, this mutant presents an immediate behavioural shift in response to an advance in temperature cycle whereas wild-type flies take about 4-5 day to adjust to the new condition. Molecularly, PER and TIM oscillations are completely abolished in the heads of these mutants when they are entrained to temperature cycle in LL. Thus, *nocte* represents a mirror phenocopy of *cry*^b regarding temperature, underlining the possibility that *nocte* encodes for a thermoreceptor or a molecule involved in the transduction of thermal signal to the clock (Glaser and Stanewsky, 2005). However it has to be mentioned that the

thermal behavioural synchronisation observed in *norpA* mutant appears to be less severe than the one in *nocte* mutants, probably as a result of the existence of genes that encode for different PLCs (Shortridge *et al.*, 1991).

per mRNA is not the only one regulated by temperature: *timeless* presents a similar process. *tim* mRNA generates two transcripts: *tim^{normal}* and *tim^{cold}*. In this latter variant, the last intron of 858 bases is not removed *via* splicing. As a consequence, translation is affected by a premature stop codon inside the unspliced intron which generates a protein truncated by about 3.5kDa (33 amino acids) compared to TIM^{NORMAL}. The effects of splicing or the TIM^{COLD} protein are still not known, but it has been shown that *tim^{cold}* proportion increases in response to a decrease in temperature (Boothroyd *et al.*, 2007).

What are the tissues and structures that are important and necessary to perceive and then transfer the thermal information to the circadian clockwork?. The outer segments of the *Drosophila* antenna have been described to act as thermosensors. Flies lacking of these structures present an impaired thermotactic behaviour: they fail to orient themselves in a temperature gradient (Zars, 2001). However, genetical or manual removals of antenna structures do not impair PER and TIM oscillation in temperature cycles, indicating that traditional thermoreceptive pathways are not necessary for circadian thermoreception (Glaser and Stanewsky, 2005). Furthermore, isolated *Drosophila* body parts and tissues (such as heads, legs, wings, abdomens and proboscises) are able to synchronise to temperature cycle regimes showing robust PER and TIM oscillations. This indicates that circadian thermoreception is tissue autonomous in all clock-gene-expressing tissues (Glaser and Stanewsky, 2005). However, at the neuronal level in *Drosophila* brain, Dorsal Neurons (DNs) and Lateral Posterior Neurons (LPNs) play a role in thermal information processing (Miyasako *et al.*, 2007; Busza *et al.*, 2007; described below). Recently, it has been shown that the *D. melanogaster* brain is not able to synchronise its circadian clock to temperature cycles but requires signals from the peripheral tissues. The organs involved in the temperature perception have been identified as the chordotonal organs which are impaired in *nocte* mutants (Sehadova *et al.*, 2009).

1.4.3. Social entrainment and feeding

Social events influence circadian clocks by changing their periods and phases. Experiments in which wild-type males were combined with *per⁰* mutants in DD, showed a weak rhythmicity and a broad dispersion of activity compared to *per⁺* flies not exposed to the mutants (Levine *et al.*, 2002). Olfactory mutants showed that circadian social behaviour depends on possible chemical signals (such as pheromones) released by flies. Indeed, flies carrying olfactory mutations in a *per⁺* genetic background do not experience any changes in their period if they are exposed to *per⁰* strains (Levine, 2004). Social interactions can also change the phase of the period: *per^s* flies (i.e. short period) influence strongly the phase of *per^l* flies (i.e. long period) rather than the opposite (Levine, 2004). The nature of this synchronisation, as mentioned before, derives from chemical signals released by flies. An original experiment showed that wild-type flies kept in DD can be synchronised using humidified air collected from a second population kept in LD condition. However, this synchronisation is impaired if the receiving population has defects in the olfactory system (Siddiqi, 1987).

Another cue that can entrain circadian clocks at the molecular level is feeding. Temporal restricted feeding entrains behavioural and endocrine circadian rhythms in mammals. When food is available for a limited period of the day, animals increase locomotor activity several hours before the onset of food availability (Fuller *et al.*, 2008). This distinctiveness is not restricted to mammals, because birds and bees show such food-anticipatory activity (Mistlberger, 1994). Furthermore, recent studies have demonstrated that daytime food restriction in nocturnal rodents can entrain peripheral oscillators (such as clockworks present in heart, liver and kidney) independently of the environmental light/dark cycles (Damiola *et al.*, 2000). The circadian expression of mammalian clock genes in the periphery becomes entrained to periodic meals whereas gene expression in the SCN (where the mammalian master clock is located) does not appear to be affected by temporal feeding (Hara *et al.*, 2001). Peripheral food-entrainable oscillators can work in SCN-lesioned mice,

suggesting that the synchronisation process of food-entrainable oscillators is essentially independent of the SCN (Hara *et al.*, 2001).

Recently, food entrainment has also been investigated in *D. melanogaster*. In general, wild animals tend to eat at specific times of the day and this pattern may also vary from one species to another. In addition to this, food-uptake behaviour is often maintained in animals kept in experimentally controlled laboratory regimes. In the case of *Drosophila*, experiments have also pointed out that flies tend to eat during the daytime in the presence of LD cycles. This feeding rhythm is driven by two mechanisms. One is the circadian clock, because even in constant darkness flies maintain a rhythmic feeding pattern and moreover the DD rhythm is eliminated in clock mutant flies. The other process that can drive this rhythm is light, as *Clk^{irk}* flies display a rhythmic feeding pattern in LD cycles similar to that of wild-type flies (reviewed from Xu *et al.*, 2008).

1.5. Outputs

As mentioned before, the output pathway is the manifestation of the circadian core oscillations that influences biochemical or physiological behaviours of organisms.

In fruit flies there are diverse rhythmic behaviours:

- Eclosion: it is defined as the emergence of insect from their pupal case. This event occurs prevalently at daybreak in order to prevent a possible desiccation due to high temperatures. This process is *gated* since fully developed adults can remain inside the pupal case waiting for the following dawn (Qiu and Hardin, 1996). Furthermore, pupae entrain during their development in a 12:12 LD regime and when released in constant darkness, they emerge when the light should be on (subjective dawn). This is strong evidence that this phenotype is under control of an endogenous oscillator (Pittendrigh, 1967).
- Locomotor activity: this is defined as the alternation between phases of activity or inactivity during 24 h. An adult fly presents most of its activity during the day (looking for food or mating) and inactivity during the night, sleeping or reducing at the minimum the capability to respond to *stimuli*

(Shaw *et al.*, 2000). In the presence of light/dark cycles, the distribution of locomotor activity is prevalent during the light phase of the day (Ewer *et al.*, 1992).

- Olfactory response: it has been shown that circadian clock mutants do not show any rhythmicity in their olfactory response, which is maximal in the middle of the night, returning to basal level at the end of the night. This pattern is in opposite phase to the locomotor behaviour, probably because it facilitates the detection of predators or contributes to opportunistic feeding at the time when the animals are relatively inactive (Krishnan *et al.*, 1999).
- Mating: it has been shown that the timing of this behaviour is species-specific. *per* is one gene that determines this specification. Not only does it regulate the love song of *D. melanogaster* (Kyriacou and Hall 1989; Alt *et al.*, 1998), but also determines a temporal window for the mating which is usually at the beginning of the night (Tauber *et al.*, 2003). Moreover, it has also been established that in a social interactive context, this behaviour is governed by the circadian clock and olfactory system of the male individuals (Fujii *et al.*, 2007).
- Oviposition: In *D. melanogaster* this phenomenon has been reported to be rhythmic, entrainable stably by a wide range of LD cycles, and with a free-running circadian period in DD. Furthermore, the periodicity of egg-laying rhythm does not vary greatly with changes in temperature or with the level of protein in the food (reviewed by Howlader and Sharma, 2006).

Another way to identify candidate circadian outputs is to search for rhythmic transcripts that oscillate even in the absence of environmental cues. Five independent studies have described the cycling transcriptome (Claridge-Chang *et al.*, 2001; McDonald and Rosbash, 2001; Ceriani *et al.*, 2002; Lin *et al.*, 2002; Ueda *et al.*, 2002). All of these groups extracted transcripts specifically from fly heads using the Affymetrix oligonucleotide microarray, finding genes that are believed to be directly, or indirectly, under the control of clock genes. More recently, a new strategy has been applied to identify output genes which takes advantage of the

GAL4/UAS system. Specific sets of cells labeled through UAS-GFP, were dissociated from the whole brain and used as a template for microarray in order to determine the gene expression pattern among these labelled neurons (Nagoshi *et al.*, 2010).

In addition to this, genetic screens focused on diverse output of the circadian clock have also revealed functions for a number of genes that are downstream of the central oscillator. One of these genes is *lark* which has been identified during a study of genes implicated in eclosion by P-element enhancer trap element insertions (Newby and Jackson, 1993). LARK contains a RNA-binding and zinc finger domains that suggest a possible role in translation control. Moreover, null mutants for *lark* are lethal, indicating its implication not only in the eclosion event but also during larval development (McNeil *et al.*, 1998). Hemizygous flies carrying only one copy of *lark*, show an advance in the pupal eclosion rhythm whereas transgenic carrying more copies of *lark* present a delay in the pupal emergence (McNeil *et al.*, 1998; Newby and Jackson, 1996). At the molecular level, *lark* mRNA does not cycle, but the protein does with a maximal peak in the middle of the day and a minimum level in the middle of the night, an oscillation that is abolished in the *per*⁰ mutant (McNeil *et al.*, 1998).

takeout (to) is a gene expressed in the head, cardia, crop and antennae, which are all structures involved in feeding (Sarov-Blat *et al.*, 2000). Food deprivation induces the expression of *to* which is also under clock control, as its expression is absent in arrhythmic flies. In response to starvation, *to* mutants show increased locomotor activity and die rapidly compared to wild-type flies. Combinations of *per* or *tim* mutations with the *to* mutant, make these individuals die even more rapidly in response to starvation. In light of this, *to* is believed to provide a molecular link between the circadian clock and behavioural/metabolic changes caused by food deprivation (Sarov-Blat *et al.*, 2000).

Another downstream clock gene is *ebony* which affects locomotor activity rhythms since null mutants are arrhythmic (Suh and Jackson, 2007). This β -alanyl-biogenic amine synthase is expressed in glial cells and in particular in proximity to aminergic neurons indicating its function in dopaminergic signalling. Since there is a synergy between glia cells and motor neurons, it is possible that EBONY affects the

excitability of motor neurons responsible for locomotor activity (Suh and Jackson, 2007).

Finally, the most extensively studied output is *pdf* (Pigment Dispersing Factor) (Renn *et al.*, 1999) which was identified in *D. melanogaster* was first identified by using an antiserum against the crustacean neuropeptide (Helfrich-Forster, 1995). *pdf* encodes for a precursor peptide of 102 amino acids which consists of a peptide signal, an associated PDF peptide (PAP), mature PDF (consisting of 18 amino acids) and a signal for amidation (Park and Hall, 1998). Moreover the primary structure of *D. melanogaster* PDF is similar to the PDH/PDF family which is highly conserved among different species (Shirasu *et al.*, 2003). Flies which carry a null mutation for *pdf* behave normally in most respects but their circadian clock-regulated behaviours are highly abnormal (Renn *et al.*, 1999). While they entrain to LD regimes and light signals, their diurnal profile of rhythmic behaviour is altered: there is an absence of the morning peak of activity and the evening peak activity is advanced by 1.5 hours compared to wild-type (Renn *et al.*, 1999). Furthermore, when these mutants are released in constant DD, they maintain their rhythmicity for a few cycles before becoming arrhythmic. The localisation of PDF changes during the 24 h: it is always localised in the cellular bodies of LN_v neurons (see paragraph 1.6.1) but in their axon terminals it changes rhythmically (Park *et al.*, 2000). In fact in the small LN_v neurons, there is a diurnal and circadian rhythm in the antibody staining of PDF: it is highest 1 hour after light-on and lowest 1 hour after light-off and this rhythmicity is also maintained in DD (Park *et al.*, 2000). *pdf* RNA is positively regulated by the transcription factors CLK and CYC in an indirect way (Park *et al.*, 2000), however *vriille* mutants exhibit a reduced PDF immunostaining but normal *pdf* RNA levels (Blau and Young, 1999). Besides this, *per* and *tim* mutations do not affect *pdf* RNA level, but the level of PDF expression is affected in the small LN_v terminals (Park *et al.*, 2000).

1.6. Where are the “ticking cells” located?

1.6.1. Central clock

In *D. melanogaster*, rhythmic behaviour is guaranteed by the cooperative and rhythmic expression of clock genes in small groups of neurons located in the CNS

(Figure 1.7). Different genetic tools such as ablation, specific rescue of clock genes and physiological manipulation, as well as cytological staining (RNA and protein), provide the precise number and localisation of circadian pacemaker neurons. The initial studies using *per* as a probe (mRNA or protein) divided the brain in two parts: an anterior-lateral part and a dorsal protocerebrum (Ewer *et al.*, 1992). Furthermore PER was found also in photoreceptors and glia cells in the optic lobes (Zerr *et al.*, 1990).

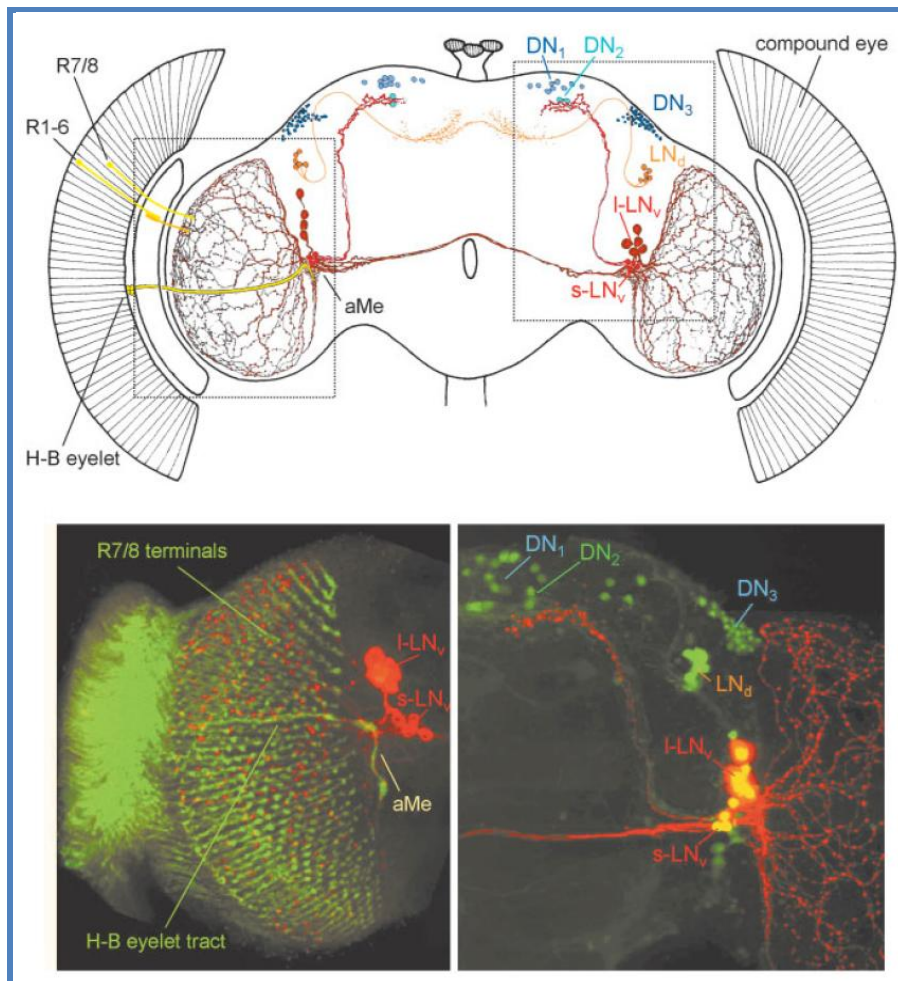


Figure 1.7: Arborisation pattern of all Lateral Neurons in relation to the localisation of the Dorsal Neurons. The lower pictures represent confocal images of wild-type brains. The left picture is stained with an antiserum against PDF (red) and against photoreceptor cells (green). The right image shows neurons stained against GFP expressed in transgenic flies under the control of *cry* promoter. *cry* labels all the LNs and DNs. Finally, the yellow staining is due to an overlap in the expression of PDF and CRY (Helfrich-Foster, 2002).

Subsequent experiments carried out using other clock proteins confirmed this general anatomical division leading to the lateral (LNs) and dorsal neuron (DNs) classification (Helfrich-Foster, 2003). Currently, the LNs and DNs are each divided

into 3 groups of clock neurons: the large ventrolateral neurons (l-LN_vs), the small ventrolateral neurons (s-LN_vs) and the dorsolateral neurons (LN_ds). The DNs are classified as DN1s, DN2s and DN3s. However, recent observations suggest that the number of neurons has to be increased to include: a single neuron in each hemisphere which does not express PDF called the 5th s-LN_v, a group consisting of lateral posterior neurons (LPNs) and a separation in the DN1s neurons dividing them in anterior and posterior neurons (Shafer *et al.*, 2006).

1.6.2. Ventral lateral neurons

- The small LN_vs appear to be the primary neurons responsible for the locomotor rhythm. This affirmation is emphasised by the following experiments: the level of PDF mRNA is not influenced in the large LN_vs but only in the small when *Clock* or *cycle* mutants are analysed (Park *et al.*, 2000);
- Under DD condition PER and TIM cycle in the small but not in the large LN_vs (Lin *et al.*, 2004). This fluctuation is maintained in the same condition in *cry^b* mutants (Stanewsky *et al.*, 1998);
- Genetic manipulations that allow the expression of PER in the small LN_vs, revealed that this is sufficient to rescue rhythmic activity (Grima *et al.*, 2004);
- Free-running of the other circadian neurons is guaranteed by small LN_vs (Stoleru *et al.*, 2005).

On the other hand, the function of the large LN_vs is not fully characterised even if they express PDF. Recent studies proposed that these neurons modulate arousal and wakefulness as well as sleep stability. In fact, when the excitability of these cells is altered, the normal pattern of light-driven activity during the day is reversed to a novel pattern of firing rate that favours higher activity in the night (Sheeba *et al.*, 2008).

1.6.3. Dorsal lateral neurons (LN_d)

This set of neurons represents critical pacemakers in *Drosophila*. This is supported by the fact that flies ablated of LN_vs and LN_ds present more severe arrhythmicity under constant conditions (such as DD) compared to flies lacking only the LN_vs (Renn *et al.*, 1999). Furthermore, these cells are considered to be important

for regulating the evening locomotor activity peak (Stoleru *et al.*, 2004; Grima *et al.*, 2004).

1.6.4. Dorsal neurons 1 (DN1s)

There are approximately 14 to 16 neurons of this type in each brain hemisphere. All of them apart from two express the transcriptional factor GLASS and are deleted in *glass* mutants (Klarsfeld *et al.*, 2004; Veleri *et al.*, 2003). Genetic studies revealed that GLASS-positive dorsal neurons contribute to the light sensitivity of the pacemaker network (Klarsfeld *et al.*, 2004) and act as *cryptochrome* independent deep brain photoreceptors (Rieger *et al.*, 2003). In addition to this, subsets of this group have been specifically implicated in driving oscillatory behaviour in constant light (LL) conditions (Stoleru *et al.*, 2007). The two GLASS-negative DN1s are distinguished from the others by their anterior position, by their survival in *glass* mutant background and by the expression of the neuropeptide IPNamide (IPNa) (Shafer *et al.*, 2006). On this basis, DN1s are further divided in two categories: “anterior DN1s” (aDN1s: GLASS-negative) and “posterior DN1s” (pDN1s: GLASS-positive). The neurochemical outputs of these latter are unknown (Shafer *et al.*, 2006).

1.6.5. Dorsal neurons 2 (DN2s)

The cell bodies of the two DN2s are closed to the terminal of the small LNvs. Their neurochemistry and function is unknown. Furthermore, their TIM and PER oscillation is in an opposite phase to the majority of circadian clock neurons (Kaneko *et al.*, 1997; Stoleru *et al.*, 2005).

1.6.6. Dorsal neurons 3 (DN3s)

Each hemisphere of the *D. melanogaster* brain displays approximately 40 of these neurons. Genetic analysis in which PER expression is driven only in these neurons showed that these pacemaker cells are not sufficient to maintain locomotor rhythms under constant conditions but they are able to direct the *per*-dependent evening peak of activity under LD conditions (Veleri *et al.*, 2003).

1.6.7. Lateral posterior neurons (LPNs)

These neurons were classified in a separate class since they cannot be defined as lateral or posterior neurons due to their position. Furthermore they were initially described as pacemaker cells expressing TIM but not PER (Kaneko and Hall, 2000). More recently, they were confirmed as *bona fide* neuronal clock cells and recently implicated specifically in temperature entrainment together with the DN2s (Miyasako *et al.*, 2007).

1.6.8. Networking between circadian neurons

Extended constant light desynchronises the internal pacemaker system. Pittendrigh and Daan (1976) observing behaviour of rodents in LL (lighting) condition, proposed a dual oscillator model in which light changes the period of the M (morning) and E (Evening) activity. This hypothesis provided an explanation for coordinated seasonal adaptations in the profile of daily behavioural activity.

D. melanogaster, in a light/dark regime presents a bimodal pattern of locomotor activity: a peak of activity that anticipates the lights-on point (defined as the morning peak) and a larger one that anticipates the lights-off event (defined as the evening peak, Figure 1.8).

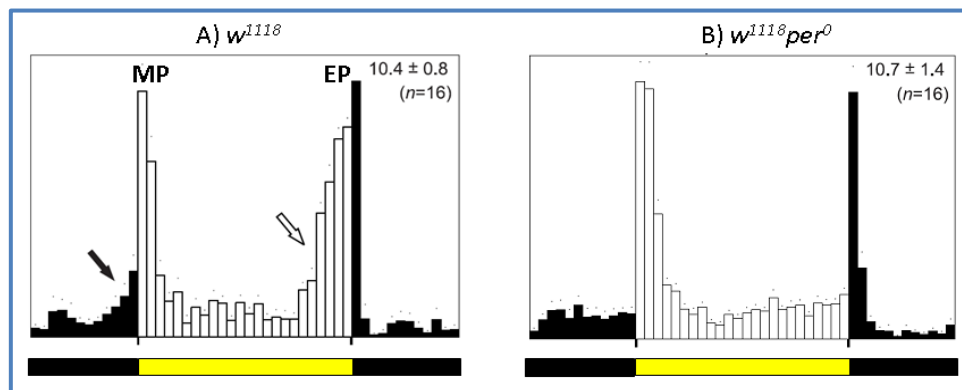


Figure 1.8: Averaged locomotor activity profiles of wild-type flies (A) and *per⁰* mutants (B) measured in LD 12:12 and constant temperature. The yellow bars indicate the light phase and black bars represent the dark phase of the LD cycle. Arrows show anticipatory activity which starts a few hours before the light transition itself. MP indicates morning peak and EP is for evening peak (adapted from Grima *et al.*, 2004).

This bimodal profile becomes unimodal when flies are released in DD, losing their morning peak within few cycles and maintaining only the evening one. Helfrich-Förster (2001) studying *per* mutants proposed that the M activity is *per* independent

whereas the E peak is dependent on *per*, suggesting that the evening peak could represent the coordination of the two oscillator systems proposed originally by Pittendrigh and Daan (1976). However in the past few years, the idea of a dual oscillator model has been reconsidered to explain the daily locomotor rhythm in flies and their circadian neuronal system. Thus different groups try to define potential pacemaker cells that control the different phases of daily locomotor activity (Grima *et al.*, 2004; Stoleru *et al.*, 2004). In these studies, gene expression was manipulated in different ways within clock neurons (ablating or restoring *per* expression in subsets of neurons in a *per*⁰ genetic background) reaching similar conclusions. These two studies concluded that:

- The morning peak in LD is exclusively driven by PDF-positive LN_vs hence called M cells;
- The evening peak in LD regime is driven by different clock groups that include the LN_ds, the 5th small LN_v and also 2 DN1 neurons hence called E cells.

Furthermore, M and E cells were shown to interact: lacking a functional clock in the M cells does not preclude the production of a morning peak in LD (Stoleru *et al.*, 2004). This suggests that E and M cells are coupled in a way that E cells can produce a rhythmic output in the M neurons despite the disruption of LN_vs pacemaking activity or E and M cells can drive morning and evening activity depending on the state of the network.

How does this coordination between M and E oscillators change in absence of light entrainment? Stoleru *et al.* (2005) answered this question by changing the period of M and E pacemaker neurons by selective expression of *shaggy* (Martinek *et al.*, 2001). The expression of *sgg* in the M cells reduced the period of the molecular cycle in the E cells and the behavioural activity cycle but left the relative phases of the M and E normal. However, the expression of *sgg* in the E cells did not change the behavioural activity period but generated an advancement of the E peak activity (Stoleru *et al.*, 2005). In light of this, M cells set the period of the network, resetting the period of the molecular cycling in the E cells and these latter pacemaker neurons are important in the setting of phase of the evening activity (Stoleru *et al.*, 2005).

Also, it has been shown that the clock in evening cells is dominant in extended light conditions (Murad *et al.*, 2007; Stoleru *et al.*, 2007), that light activates behavioural output from evening cells and inhibits it from morning cells, reinforcing their functions in light and dark respectively (Picot *et al.*, 2007). Thus, it has been hypothesised that the morning pacemaker neurons are dominant in short photoperiods which mimic winter conditions while the evening cells are important in the longer photoperiods present in summer (Stoleru *et al.*, 2007). This can explain how the circadian clock adapts to different seasons.

Another fundamental aspect that has been studied is the relationship between the circadian neurons, temperature and locomotor activity. Both M and E cells play a role in the behaviour synchronisation to temperature cycles. M cells appear to be less sensitive to temperature variation compared to E cells. In fact, the E cells are more rapidly synchronised to temperature cycles, and even more if they are disconnected from the M cells by genetic manipulation (Busza *et al.*, 2007). Thus the circadian network is highly sensitive to temperature fluctuations but the interplay between different cells makes it more resilient, preventing flies from overreacting to temperature changes (Busza *et al.*, 2007).

1.6.9. Peripheral clocks

The circadian gene studied most intensively in terms of spatial expression patterns has been *per*. Immunocytochemistry using antibody against PER protein, *in situ* hybridisation and transgenic flies (for example carrying *per* promoter fused to β -galactosidase) have been used to detect the presence of *per* in organs and tissues outside the CNS and circadian cells within the brain (described above, paragraph 1.6). All these available techniques reveal a broad distribution of *per* mRNA and protein in photoreceptor and glial cells, endocrine glands, alimentary canal, ovaries and testes (reviewed in Giebultowicz, 2001). Nevertheless, in some tissues (such as epidermis, skeletal muscle and tracheal epithelium) the level of either PER or TIM is not detectable, demonstrating that *per/tim*-based oscillators are not found in all tissues but rather are limited to specific organs (Plautz *et al.*, 1997). However, as in the case of the clock machinery in the CNS, the peripheral circadian oscillators

display the ability to maintain self-sustained rhythm when explanted *in vitro* and to be entrained directly by environmental signals.

The optic lobes in *D. melanogaster* do not seem to contain *per*-positive neuronal cell bodies, but neurites from *per*-expressing LN_vs extensively arborise there (this data is also confirmed by anti-PDF staining). Glial cells of the medulla and lamina display cycling in the expression of *per* (Zerr *et al.*, 1990). The lamina glial cells, which envelope the optic cartridges in the lamina, may be involved in rhythms associated with visual processing. Optic cartridges are part of the first visual neuropile where photoreceptor terminals make synaptic contacts with the large monopolar neurons. These neurons exhibit circadian changes in the diameter of their axons and the clock that regulates them seems to be located in the glia associated with these neurons (Meinertzhagen and Pyza, 1996; Stanewsky *et al.*, 1997). Compound eyes and ocelli exhibit rhythmic expression and nuclear translocation of PER and TIM (Zerr *et al.*, 1990). Furthermore, experiments involving transgenic flies demonstrate that the rhythmicity in these structures is maintained also in absence of *per* expression in other parts of the CNS (Cheng and Hardin, 1998).

The sexual organs in flies also display expression of *per*. In females, the *per* signal is limited to the follicle cells associated with the small previtellogenic egg chambers and appears to be cytoplasmic with not nuclear translocation. In addition to this, *per* does not exhibit daily cycles in abundance in contrast with the oscillation displayed by the rest of the body (Hardin, 1994). The role of *per* in the ovaries is not clear but it seems to have a clock-related function: vitellogenesis and ovulation are reported to be rhythmic in flies; diapause levels depend on *per* since *per*⁰ flies display a short critical daylength compared to wild-type (Saunders, 1990). *D. melanogaster* males express *per* mRNA in their testes, in particular in the terminal epithelium at the basis and in the *vas deferens* epithelium (reviewed in Beaver *et al.*, 2002). Moreover, experiments have shown that loss of *per* function interferes with reproductive rhythms and decreases reproductive fitness of *D. melanogaster* males (Beaver *et al.*, 2002).

Segments of the alimentary canal of adult flies, such as esophagus, midgut, hindgut and rectum display strong *per* expression (Liu *et al.*, 1988). Therefore, PER is detected in all gut epithelium cells, showing cycling and nuclear translocation. The

role of this gene in the digestive system is not known but it is believed that it has an adaptive value. Daily cycles of rest and activity are likely associated with feeding cycles, which in turn may be matched by daily rhythms in production of digestive enzymes, absorption of nutrients and other processes related to digestion and metabolism. Malpighian tubules, which are non-innervated epithelial tubes comprising large secretory cells involved in urine excretion (reviewed in Giebultowicz and Hege, 1997), exhibit brain independent circadian mechanism which is self-sustained also in decapitated flies kept in LD and DD (Hege *et al.*, 1997). Furthermore, Malpighian tubules distinguish the role of CRY in the CNS and peripheral tissues. While CRY in the clock neurons appears to be an essential player in the photoreception, in the MT it does not seem to have a similar role since in *norpA^{D41};cry^b* double mutants the rhythmicity in PER and TIM protein level is not affected by light during the dark phase. Thus, in MTs CRY is an essential clock component because the clock oscillations in *cry^b* MTs are significantly modified in LD and completely abolished in DD regimes (Ivanchenko *et al.*, 2001). The same results have been found in *cry^b* antennae under various conditions: an abnormal rhythmicity of PER and a loss of physiological clock output (Krishnan *et al.*, 2001).

1.7 Clocks in other organisms

In unicellular as well as multicellular species, the core clock genes are conserved, as in mammals. Although orthologues of most of the genes involved in fly clockwork have been cloned in mice, and the general feedback-loop mechanism is similar, there are differences in specific functions between orthologues for several of the components. Furthermore, gene duplication has led to increased complexity among vertebrate clock genes (Reppert and Weaver, 2000). Therefore, understanding the molecular basis of the circadian clock in one organism helps to understand oscillator functions in others.

1.7.1 The circadian clock in *Neurospora crassa*

Studies in *N. crassa* have helped to understand many of the basic mechanisms that underlie circadian rhythms such as negative feedback and light and temperature entrainment, which are in common to all clocks. The clock of this organism controls

several rhythmic processes but the most frequently studied is the daily production of asexual conidiospores. In *N. crassa*, the positive elements WC-1 and WC-2 (encoded by *white collar-1* and *white collar-2* genes) transcribe a negative element encoded by *frequency (frq)*. FRQ undergoes phosphorylation in the cytoplasm under the control of a specific kinase and subsequently acts as inhibitor of its own transcription, determining a negative feedback loop (Bell-Pedersen *et al.*, 2005). This loop, called FRQ/WC oscillator (FWO), is entrained by light signals from the environment *via* the blue-light photoreceptor WC-1. However, strains that lack FWO still have rhythmic behaviour, indicating the presence of other regulating mechanisms (Bell-Pedersen *et al.*, 2005). In particular a second oscillator, named FRQ-less oscillator (FLO), is reset by temperature rather than light (Pregueiro *et al.*, 2005).

Components of FWO and FLO transfer the temporal information controlling the rhythmic expression of clock-controlled genes (*ccgs*). All the oscillators have to communicate with each other to co-ordinately regulate rhythmic processes, such as development.

1.6.2 The circadian clock in mammals

The CNS has been showed to be a circadian pacemaker in mammals although independent clocks have been identified in different cells and tissues (Table 1.1 for a comparison between species). Ablation of the mammalian SCN from mouse eliminates circadian pattern of activity, endocrine output and many biochemical processes throughout the organism (Turek, 1985). Furthermore, transplantation of SCN tissue to SCN-lesioned hamsters restores circadian behavioural rhythmicity (Ralph *et al.*, 1990). This indicates that the SCN contains a collection of cell autonomous oscillators that are coupled to each other to form the complete SCN pacemaker that is responsible for setting the phase and period of biological rhythms throughout the organism. Finally, it receives photic input through the retino-hypothalamic tract (RHT) which is required for the entrainment of mammalian circadian rhythm in LD cycles (Johnson *et al.*, 1988).

Organism	Oscillator or tissue with pacemaker function	Processes regulated by pacemaker	Presence of other oscillators	Processes regulated by other oscillators
<i>Neurospora crassa</i>	FRQ/WC oscillator	Conidiation, gene expression	FLO	Gene expression
<i>Drosophila melanogaster</i>	Ventral lateral neurons	Locomotor activity	Olfactory sensory neurons Malpighian Tubules	Odour-dependent electrophysiological responses Excretion
<i>Mammals</i>	SCN	Locomotor activity Neuronal electrical firing Cytosolic calcium level Neuropeptide secretion	Heart, Lung, Liver, Kidney, Fibroblasts, Pineal gland	Heart rate, systolic blood pressure, vasodilation, gene expression, metabolism, melatonin level

Table 1.1: Processes controlled by the central and peripheral oscillators in different model systems (reviewed from Bell-Pedersen *et al.*, 2005).

As in the case of *D. melanogaster*, the mammalian clocks, and in particular the mouse machinery, have negative and positive feedback loops. The negative feedback loop consists of three PER proteins (mPER1, mPER2 and mPER3) and two CRY proteins (mCRY1 and mCRY2; Figure 1.9). mPER1 and mPER2 have been shown to be essential components of the mammalian clock since null mutations in both *mPer1* and *mPer2* can cause arrhythmia (Zheng *et al.*, 2001). However, mPER1 and mPER2 can rescue independently robust circadian rhythms if they are expressed in *mPer2*^{-/-}/*mPer3*^{-/-} and *mPer1*^{-/-}/*mPer3*^{-/-} deficient mice, respectively (Lee *et al.*, 2004). mPER3, on the contrary, is not necessary for circadian rhythms since deficient mice show minor defects in their circadian machinery (Shearman *et al.*, 2000) and it is not able to rescue the rhythmicity in *mPer1/mPer2* deficient mice (Lee *et al.*, 2004).

Simultaneously null mutations in *mCry1* and *mCry2* generate loss of rhythm but mCRY1 or mCRY2 deficient mice show short and long periods respectively (van der Horst *et al.*, 1999). The mPERs and mCRYs form complexes which are necessary for nuclear localisation (Kume *et al.*, 1999). As in the case of *Drosophila*, the nuclear translocation time is regulated by casein kinase I ϵ and δ (CKI ϵ/δ) which phosphorylate the mPER proteins (Lee *et al.*, 2001). Once in the nucleus, the mCRY proteins downregulate their own synthesis by disrupting the heterodimer BMAL1/CLK (Shearman *et al.*, 2000). This latter heterodimer positively regulates the expression of PERs and CRYs binding to the E-box elements located in their promoters (Reppert and Weaver, 2002). BMAL1 is the mammalian homologue to *Drosophila* CYC, but instead of being constitutively expressed as in the case of fruit flies, its expression cycles (Shearman *et al.*, 2000).

The positive feedback loop involves REV-ERB α which generates a rhythmic inhibition of *Bmal1* transcription (Preitner *et al.*, 2002). The expression of *Rev-erba* is regulated positively by BMAL1/CLK and negatively by PERs and CRYs (Bell-Pedersen *et al.*, 2005). Surprisingly, *Rev-erba* mutant mice are still rhythmic and *mPer* and *mCry* mRNAs are rhythmically expressed. This indicates that the positive feedback loop is important to enhance the robustness of the circadian oscillator (Preitner *et al.*, 2002).

As mentioned before, the light entrainment to the clock pacemaker cells comes from the RHT but mTIM does not show the same light sensitivity as dTIM. Thus, the light sensitive role appears to have been taken over by the regulation of the expression of *mPer1* and *mPer2* (Reppert and Weaver, 2000). A light pulse during the early subjective night rapidly induces the expression of *mPer1* and a later induction of *mPer2* (Reppert and Weaver, 2002). The altered level of mPER proteins have been demonstrated to cause phase delays and advances depending on the time of the light pulse (Udo *et al.*, 2004).

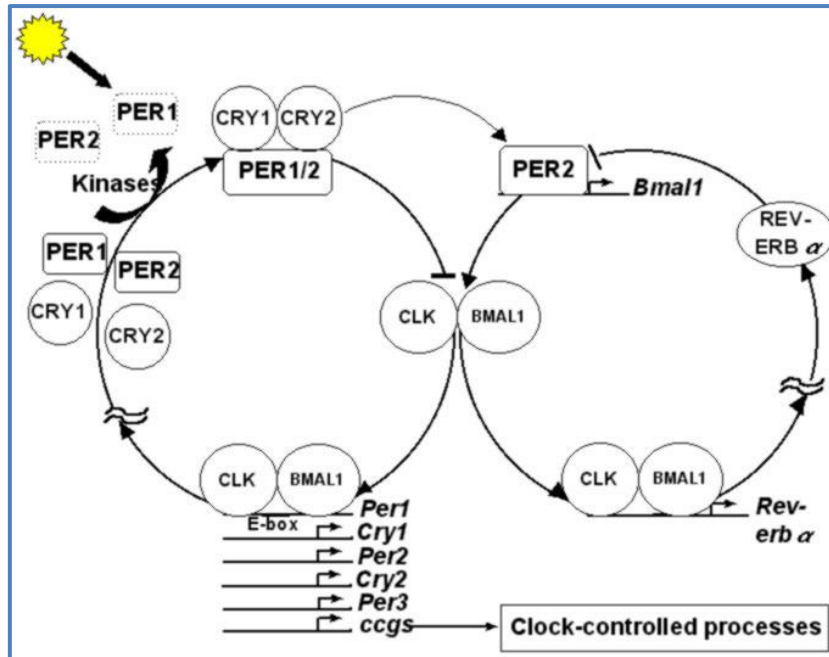


Figure 1.9: Model of circadian clock in mammals.

1.8 Aim of the project

Most of the information regarding the entrainment of the *Drosophila* circadian clock are related to light input pathway. The function and effect of temperature as a *Zeitgeber* has only recently been studied (Glaser and Stanewsky, 2005). *nocte* and *norpA* represent two genes involved in this pathway. The aim of this project is to understand this aspect with reference to *norpA*. NORPA has been shown to have a double effect in the synchronisation of the circadian clock, one, acting through the accumulation of PERIOD, and two, directly as a component of the temperature signalling pathway to the circadian pacemaker. In order to understand the role of *norpA* in both these mechanisms:

- NORPA expression has been investigated within circadian pacemaker cells *via* ICC and *in situ* hybridisation (Chapter 3);
- Transgenic flies generating *norpA* downregulation mediated by RNA interference have been created and analysed in LD 12:12 at low and warm temperature (Chapter 4) in order to define the cluster of the neurons in the *D. melanogaster* brain involved in temperature synchronisation.

- Transgenic *norpA* downregulated flies have been analysed also in temperature cycles regime subjecting them to temperature shifts. In addition to this, light input mutants have been investigated under the same conditions (Chapter 5).
- However, since the disruption of thermal circadian behaviour of *norpA* null is not as severe as in *nocte* mutants, I also investigated the role of another PLC β in this cascade (PLC21C). Flies downregulating *plc21C* were tested in LD 12:12 under two temperatures and their locomotor behaviour analysed (Chapter 6).

Another part of this project is focused on the characterisation of a new photoreceptive pathway. *glass^{60j}cry^b* mutants which are reported to be circadian and visual blind have revealed the presence of a possible set of neurons that are still able to be synchronised by light and could entrain the circadian clock. The aim of this second project is to:

- evaluate if these “blind flies” are able to synchronise to different LD regimes (Chapter 7).
- characterise the nature of a “new photoreceptor” among a set of orphan GPCRs (Chapter 8).

Chapter 2. Materials and methods

2.1. Genomic DNA extraction from *Drosophila* individuals

To obtain genomic DNA from a single fly, the following protocol was used. An individual fly or a maximum of two flies were placed in a 0.5 ml tube and mashed for 5-10 s with a yellow pipette tip containing 50 μ l of Squishing Buffer (SB, 10 mM Tris-HCl pH 8.2; 1 mM EDTA; 25 mM NaCl and 200 μ g/ml Proteinase K which was diluted fresh from a frozen stock). Then the remaining SB was expelled and the samples were incubated at room temperature (25-37°C) for 20-30 min. Finally the samples were heated to 95°C for 1-2 min to inactivate the proteinase K (Gloor *et al.*, 1993). 1 μ l of this preparation was used for 10-20 μ l PCR reaction volume.

2.2. RNA extraction from *Drosophila* individuals

D. melanogaster fly strains were collected at the required time points and snap frozen in liquid nitrogen. All flies were homogenised in 400 μ l TRIZOL reagent (Invitrogen) using a plastic pestel. A further 600 μ l of TRIZOL was then added and the homogenate was allowed to stand for 5 min. 200 μ l of chloroform was then added and the mixture shook vigorously for 15 s. It was then left to stand for 10 min before being centrifuged in a microfuge for 15 min at 4°C. The upper phase was then carefully collected and removed to another RNase-free tube. This is a key step, since the DNA is not completely separated from RNA; it was necessary, thus, to remove the very upper layer, leaving a little in the borderline, to avoid any DNA contamination. The 500 μ l of isopropanol was added to the RNA and left to stand at room temperature for 5-10 min. To precipitate the RNA, the tube was then centrifuged for 15 min at 4°C. The pellet was washed in 80% EtOH and then resuspended in 20 μ l of DEPC treated dH₂O. The quality and quantity of the isolated RNA was checked by a 1% agarose gel or by measuring the optical density (OD) at 595nm using a Spectrophotometer (Eppendorf) or using a NanoDropTM 1000 (Thermo Scientific).

2.3. cDNA synthesis

Before performing the cDNA synthesis, the RNA extracted was treated with DNase (Ambion) to prevent any DNA contamination. This treatment was carried out by adding the following components into an RNase-free microcentrifuge tube:

- 1 µg of RNA sample
- 1 µl 10X DNaseI reaction Buffer
- 1 µl DNase I, Amp Grade, 1 U/µl
- DEPC-treated water to 10 µl

The tube was incubated for 30 min at 37°C. The DNase was inactivated with the addition of 1 µl of 25 mM EDTA solution to the reaction mixture and heated for 10 min at 65°C or using the producer inactivation buffer. cDNA synthesis was performed using the ImProm-II Reverse Transcriptase (Promega). 5 µl of DNase-treated RNA from the previous step were mixed with 1 µl of oligo-dT primer (500 ng). This was incubated at 72°C for 5 min and then chilled on ice for 5 min. To this, 4 µl of 5X Buffer, 2.5 µl of 25 mM MgCl₂, 1 µl of dNTP mix (10 mM each), 0.5 µl of rRNasin Ribonuclease Inhibitor and 5 µl of DEPC treated dH₂O were added. This was mixed before adding 1 µl of ImProm-II Reverse Transcriptase. The reaction was then incubated at 25°C for 5 min, followed by 42°C for 1 h and then the reaction was terminated by heat inactivation at 70°C for 15 min on a thermocycler. The product was used directly for PCR amplification.

2.4. PCR (Polymerase Chain Reaction)

PCRs for cloning were performed principally using Phusion™ High-Fidelity DNA Polymerase (New England Biolabs Inc.). The PCR mix was set up as follows:

Reagents	Volume for 20 µl reaction
DEPC H ₂ O	up to 20 µl
5X Buffer Phusion	4 µl
10 mM dNTPs	0.4 µl
Primer A (10mM)	1 µl
Primer B (10mM)	1 µl
Template DNA or cDNA	1 µl
Phusion DNA Polymerase	0.2 µl

Table 2.1: List of PCR reagents used in each reaction.

PCR programs basically were varied each time to adapt the amplification to primer annealing temperatures and the expected length of the product. In general, the following thermal profile was used as a default program:

Step	Degrees (°C)	Time	Number of cycles
Initial denaturation	98	30 sec	1
Denaturation	98	5 or 10 sec	25 or 35 (for cloning 25 cycles were chosen to avoid possible mutations induced by the polymerase)
Annealing	42 or 72 (depending on primers)	10 or 30 sec	
Extension	72	15 or 30 sec (depending on the length of the fragment)	
Final extension	72	10 min	1
Hold	4	forever	

Initially, the PCR reaction was carried out using a gradient of temperatures in the primer annealing step. In the case of positive results even in the presence of a temperature gradient, PCR products were used for the following steps.

For fly genotyping, a standard Taq Polymerase was used (Kappa TAQ Polymerase, Biosystem). In the following tables the standard components and standard cycling conditions for a PCR reaction are reported. 11.1X Buffer consists of 45 mM Tris-HCl pH 8.8, 11 mM Ammonium Sulphate, 4.5 mM Magnesium Chloride, 6.7 mM 2-Mercaptoethanol, 4.4 μ M EDTA pH 8.8, dNTPs 1mM each and 113 μ l/ml BSA.

PCR Component	Concentration
DNA	Up to 1 μ g
11.1X Buffer	1X
Forward Primer	5pmoles
Reverse Primer	5pmoles
<i>Taq</i> DNA Polymerase	1Unit
DEPC Water	To make final volume of 20 or 50 μ l

Table 2.2: Standard components of a PCR.

PCR Step	Temperature	Time (min:sec)
Initial Denaturation	92°C	2:00
Denaturation	92°C	0:30
Annealing	42°C to 72°C depending on primers used	0:30
Extension	72°C	0:30 – 1:10 (dependent on size of PCR fragment)
Repeated steps 2, 3 and 4 for 35 cycles		
Final Extension	72°C	10:00
Hold	10°C	Forever

Table 2.3: Standard cycling conditions for PCR.

All PCR reactions were performed using the DYAD™ DNA Engine Peltier Thermal Cycler.

2.5. Agarose Gel Electrophoresis

Amplified DNA fragments were loaded in an agarose gel after being mixed with loading buffer (0.25% bromophenol Blue; 0.25% cyanole). Agarose was melted in 0.5X TBE (109 g/L Tris, 55 g/L Boric Acid, 9.3 g/L EDTA de-ionized water up to volume buffer, and its concentration was between 0.7% and 2%, depending on the dimensions of the fragments. Gels were run between 80-120 Volts for 60-90 min. The DNA was visualised under UV light, with ethidium bromide added in the gel. The signals were detected and the images elaborated by Gene Genius from the Bio-Imaging System (Bio-Imaging System Inc, UK). The length of the fragments was determined by comparison with fragments from a known molecular weight marker.

2.6. Recovery of DNA from an agarose gel

Standard QIAquick Gel Extraction Kit (Quiagen®) was used to purify the DNA from the agarose gel following the maker's protocol. At the last step, DNA was eluted in 30 µl of Elution Buffer (instead of the recommended 50 µl in order to get more concentrated material) and 2 µl of it were used to determine the efficiency of the purification and concentration.

2.7. Sequencing

Samples were sent to the Protein and Nucleic Acid Chemistry (PNAAC, University of Leicester) to be run on an ABI 377 sequencer. The sequence were analysed by FinchTV (Geospiza™).

2.8. Vectors

2.8.1. pBluescript II KS (pBS)

pBluescript® II KS vector (Stratagene) was utilised as a intermediary cloning plasmid between the PCR amplification and the final vectors. The former is for PCR products, the latter for transformation. For example pBS was used for the cloning of the single fragments of the gene *norpA* and the *norpA*-IR construct. pBS possesses a wide range of

restriction sites in the multiple cloning region, so it allows the correct and specific orientation of fragments within the vector. Moreover, its small dimensions are ideal for multi-way ligation of low molecular-weight fragments. Finally, pBS is a very efficient bacteria transformation and confers ampicillin resistance.

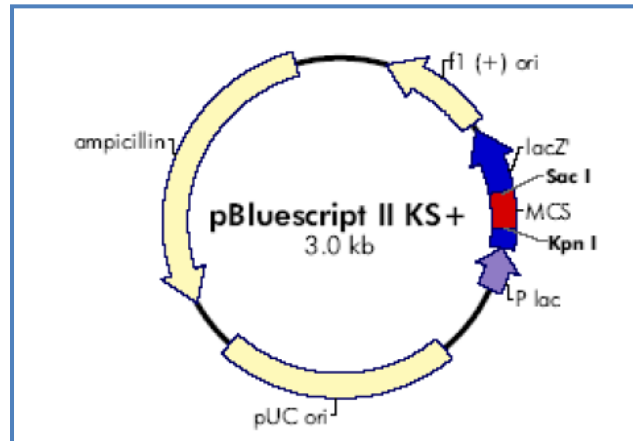


Figure 2.1: pBS vector map. It is shown the ampicillin resistance and the multiple cloning site (MCS).

2.8.2. pUAST

pUAST is a *D. melanogaster* transformation vector. It is used for this purpose because it possesses many functional features. Firstly, it carries the wild allele of *white* (*w⁺*) that acts as a marker and allows easy identification of transformants. pUAST carries the sequence of *D. melanogaster* P-elements, which allow the transposition of sequence within the genome of the host; moreover, it has the *E. coli* TATA Box under the control of *hsp70* promoter. In addition the vector contains the *UAS* (upstream activation sequence) for the binding of the transcriptional activator GAL4. Finally, the multiple cloning sequence is followed by the terminator sequence SV40 that acts as the stop signal for the transgene. This vector was used to generate transgenic flies by sending it to BestGene which microinject it.

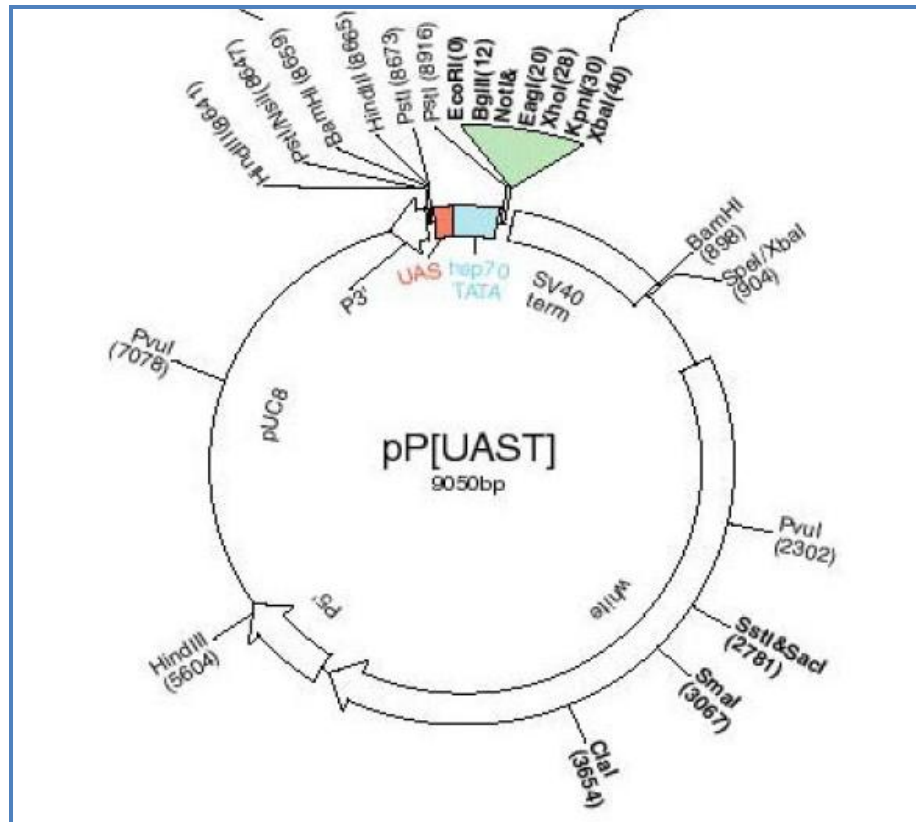


Figure 2.2: pUAST map vector. All features such as white gene, UAS, TATA box, multiple cloning sites and terminator sequences are reported.

2.9. Bacteria transformation by electroporation

Preparation of competent cells:

- A single colony of *E coli* XL1 BLUE MFR' strain (Stratagene) was grown overnight at 37°C in 10 ml of LB medium (10 g/L bacteria triptone; 5 g/L yeast extract; 10 g/L NaCl; distilled water to volume) with tetracycline antibiotic.
- The overnight cultures was poured in new 400 ml of LB with tetracycline and incubated with shaking until reaching a concentration equal to $OD_{600}=0.5$.
- It was centrifuged at 4000 rpm on a Sorvall GSA rotor for 15 min at 4°C and the pellet resuspended in 200 ml of sterile water at 4°C.
- After centrifugation as above the pellet was suspended again in 100 ml of sterile water at 4°C.
- Again the cell suspension was spun down as above and this time resuspended in 5 ml of 10% ice-cold glycerol.

- The suspension was centrifuged on a Sorvall SS34 rotor at 5000 rpm for 15 min at 4°C.
- Finally, the pellet was resuspended in 1.6 ml of 10% glycerol and aliquoted in eppendorf tubes of 40 µl. Each aliquot was snap frozen in liquid nitrogen and stored at -80°C.

2.10. Transformation

Transformation was carried out by mixing 40 µl of electrocompetent XL1 BLUE cells with 3 µl of DNA in an electroporation cuvette, which was subjected to electroporation (1.5 kV, 1000 Ω and 25 µF) in a Biorad Biopulser. After electroporation, the cells were rescued with 1 ml of LB liquid and incubated at 37° C for 1 h. The cells were then diluted 1:1, 1:10 and 1:100 in the same medium and plated on LB plates containing the appropriate antibiotic for selection. Where possible (for example with pBS vector), X-Gal and IPTG were added to the media to enable blue/white selection of transformants. If the X-Gal assay was negative (due to the lack of *lacZ* expression), a second ligation reaction with positive (vector and insert) and negative (vector empty and insert separately) controls was performed. The plates were incubated at 37°C overnight. Single putative transformant colonies were isolated and grown in ~5 ml of LB and antibiotic at 37°C with shaking overnight. These cultures were consequently used for the “mini-prep” (speed preparations of the plasmid DNA).

2.11. Speed preparation of the plasmid DNA (“Mini-prep”)

1.5 ml of bacterial culture was centrifuged to pellet the bacteria at 13000 rpm for 20 min. The pellet was then resuspended in 100 µl of solution A (50mM Tris-HCl pH = 8.0, 4% Triton X-100, 2.5 mM LiCl and 62.5 mM EDTA). 100 µl of phenol/chloroform/isoamyl alcohol (solution 25:24:1) were added to the latter mixture and vortexed for 10 s. This was then centrifuged at 13000 rpm in a microfuge for 2 min to separate DNA (aqueous phase) from proteins and contaminants (phenolic phase). The resulting upper aqueous phase was collected. 200 µl of cold 100% EtOH were added to this and the contents mixed. The mixture was centrifuged at 13000 rpm to pellet the

precipitated DNA, and the EtOH removed. The pellet was then washed in 80% EtOH and resuspended in 20 μ l of TE (10 mM Tris-HCl pH 8.8 1 mM EDTA) and RNase (10 μ g/ml).

When clean plasmid DNA for following ligation reaction or sequencing was needed QIAprep Miniprep[®] kit (Qiagen) was used. The DNA at the final step of the protocol was eluted in 30 μ l of Elution Buffer in order to concentrate the final material rescued.

2.12. Restriction digest of DNA

To digest DNA with a restriction endonuclease, the required amount of DNA was incubated with the enzyme (or enzymes) of choice in a solution containing the appropriate reaction buffer at the optimum temperature for the enzyme for 1-2 h. A small sample of the reaction was then run out on an appropriate percentage agarose gel to check the efficiency of the restriction reaction. If this was performed to isolate a band of DNA from, for example a plasmid, then the rest of the digest was run out on the gel in a large well and then recovered.

2.13. Western Blotting

2.13.1. Protein extraction from *Drosophila* heads

Flies were collected at different conditions by freezing in liquid nitrogen, stored at -80°C and their heads were used for western blots. Heads were collected in eppendorf tubes kept on dry ice by vortexing the samples and using a sieve to separate the heads from the bodies. A volume of extraction buffer (0.1% TritonX, 10 mM EDTA, 1m M DTT, 0.5 mM PMSF, 10 μ g/ml Apsotinin, 5 μ g/ml Leupeptin, 5 μ g/ml Pepstatin in HEMG; HEMG is 0.1 M KCl, 20mM HEPES pH 7.5, 50% Glycerol) which was double that of the approximate volume of heads was added to the samples. The heads were homogenised for approximately 1 min using a sterile plastic pestle while keeping the samples on wet ice the entire time. The debris were separated by spinning the samples at 13,000 rpm for 5 min at 4°C. The supernatant containing the proteins was retained and quantified by mixing 1 μ l of sample with 1ml of 1:5 dilution of Bradford's Reagent (Sigma-Aldrich) and measuring the optical density (OD) at 595nm using a Spectrophotometer

(Eppendorf). The samples were equalised using extraction buffer before loading onto an SDS-polyacrylamide gel.

2.13.2. SDS-Polyacrylamide Gel Electrophoresis (SDS-PAGE)

Appropriate amounts of 3X loading buffer (188 mM Tris HCl pH 6.8, 6% v/v SDS, 30% v/v Glycerol, 15% v/v β MerCaptoethanol, 0.03% w/v Bromophenol Blue) were added to the samples and they were boiled for 3 min at 95°C. They were then loaded onto the gel along with a pre-stained broad range molecular weight marker (BioRad). An acrylamide gel is divided into two parts - the stacking and the resolving gel. Their components are listed in Tables 2.4 and 2.5 respectively. The gel was run using running buffer (2.5 mM Tris, 0.25 M Glycine, 0.1% v/v SDS) at 15 mA for approximately 2 h.

Component (Stock)	Volume used in ~10ml
1M Tris HCl pH 6.8	1 ml
20% SDS	50 μ l
25% APS	20 μ l
TEMED	10 μ l
30% Acrylamide	1.5 ml
Water	7.3 ml

Table 2.4: Components of the stacking gel portion of a polyacrylamide gel.

Component (Stock)	6% Gel (Volume used in ~10ml)
2M Tris HCl pH 8.8	2 ml
20% SDS	50 μ l
25% APS	80 μ l
TEMED	12 μ l
30% Acrylamide	2 ml
Water	5.8 ml

Table 2.5: Components of a 6% resolving gel portion of a polyacrylamide gel

2.13.3. Transfer onto Nitrocellulose Membrane

After running the polyacrylamide gel allowing separation of the proteins, they were electrically transferred onto a nitrocellulose membrane (PROTRAN, Schleicher and Schuell). This blotting of proteins was done using the BioRad mini Trans Blot kit. The gel

and membrane were surrounded on either side by 3 layers of absorbent filter papers (Whatman) to facilitate the absorbance of transfer buffer (40mM Tris, 40mM Glycine, 0.375% v/v SDS, 20% Methanol) which was used for this procedure. The blotting of the proteins was done at 400mA for approximately 2 h and the apparatus was surrounded with ice to prevent overheating.

2.13.4. Immunostaining with Antibodies

The proteins were fixed onto the nitrocellulose membrane by incubating with 5% (w/v) milk buffer (milk powder in TBST; TBST consists of 10mM Tris HCl pH7.5, 150mM NaCl, 0.05% w/v Tween 20) for 1 h. The membrane was then probed with the primary antibody (anti-NORPA in rabbit, 1 in 10000 dilution in milk buffer) at 4°C overnight with continuous slight agitation. The membrane was then washed 3 times for 30 min each using TBST. The secondary antibody used (anti-rabbit from Sigma, 1 in 6000 dilution in milk buffer) had a horse-radish peroxidase moiety essential for detecting the protein. The blot was probed with the secondary antibody for 1 h at 4°C with continuous slight agitation. The membrane was then again washed three times for approximately 15 min each using TBST.

2.13.5. Protein Detection

The membrane was incubated for 1 min with the solution used for signal detection (0.1 M Tris HCl pH 6.8, 6.25 μ M Luminol, 6.38 μ M pCumaric Acid, 2.7 mM H₂O₂). It was then wrapped in cling film and exposed for different times (1, 5 and 10 s) to photographic film (Fuji) and subsequently developed.

2.14. *in situ* hybridisation

2.14.1. Synthesis of RNA probes

The synthesis of the probes was carried out starting from PCR products generated from wild-type fly cDNA. In all syntheses a nested PCR was set up, first amplifying a larger region including the region for the probe, and then amplifying the probe using

primers that include the T7 or T3 RNA polymerase recognition sites. At each stage the PCR products were sequenced in order to check for mutations generated by the polymerase.

For the synthesis of the RNA probes the following reagents were used:

- PCR template DNA (100 ng)
- 5X transcription buffer: 4 μ l
- DDT (0.1M): 2 μ l
- Biotin (or DIG) nucleotide mix (including 10 mM GTP, 10 mM ATP, 10 mM CTP, 6 mM UTP, 3.5 mM DIG or Bio-UTP) : 2 μ l
- RNase inhibitor (100U/ μ l): 1 μ l
- T3 or T7 RNA Polymerase (40U/ μ l): 2.5 μ l
- dH₂O: to 20 μ l

This mix was incubated at 37°C for 2-3 h and 1 μ l of products was run on a 1% agarose gel to check the efficiency of the reaction. The samples were treated with DNase I (RNase free) and incubated for 20 min at 37°C to eliminate the template DNA.

The RNA obtained was passed through a mini-spin column (Roche) to eliminate unbound nucleotides and unused reagents. 100 μ L of Hybridisation Buffer (HB, see below) were added to the mix and stored at -20°C.

2.14.2. Brain dissection

Flies were collected at the appropriate time points and fixed in 4% Paraformaldehyde (PFA) by incubating them for approximately 2 h on a rotating wheel at room temperature or at 4°C ON. They were then washed three times for 15 min each in Phosphate Buffer Saline (PBS) which is composed of 140 mM NaCl, 2.7 mM KCl, 10 mM Na₂HPO₄, 1.8 mM KH₂PO₄. Brains were then dissected under a microscope with two pairs of fine forceps. A small Petri dish containing a few drops of PBS on a layer of silicon was placed under the microscope. A fly was placed in the drop of PBS and the head was held with the forceps in the right hand and the body in the left hand. The body was removed and discarded and the head retained in the right hand. The proboscis of the fly

was firstly removed and discarded. The right forceps were then used to hold one eye through the hole created by the removal of the proboscis and the left forceps were also inserted into that hole to hold the right eye. By gently applying pressure, the two eyes were pulled apart in opposite directions to reveal the brain underneath. Before continuing, it was ensured that all the cuticles and connective tissue were removed from the surface of the brain to minimise non-specific fluorescence. The brains were then transferred in Methanol (MetOH) in order to prevent RNA and protein degradation until they were used. These steps were also used for processing brain for immunocytochemistry.

2.14.3. *in situ* protocol

Brains were rehydrated through downgrading 90%, 70%, 50%, 30% methanol/0.2% PBT series (1X PBS plus 0.2% Triton-X) and finally washed for five times in PBT. Brains were then treated with proteinase K in order to increase the probe penetration for 3 min at room temperature and subsequently for 1 hr at 4°C. Proteinase K treatment was concluded by three washes with glycine (10 mg/mL) and subjecting brains to 4% paraformaldehyde in PBS fixation. After being washed for 5 times in PBT, samples were incubated for 5 min in a 1:1 mixture of PBT:HYB (50% formamide, 5X SSC-DEPC, 0.1% Triton-X, 100 µg/ml heparin, 100 µg/ml salmon sperm DNA and 500 µg/ml of yeast t-RNA) at room temperature. This mix was replaced with HYB and brains were incubated for 2h at 60°C. Subsequently, samples were incubated with serial dilutions (50, 100 or 150 ng) of RNA probe dissolved in HYB buffer at 60 °C ON. After overnight hybridisation, the excess of probe was removed through two downgrading washes: the first of 3:2, 1:1, 2:3 ratio of HB:2XSSCT at 60°C (10X SSC: 3 M NaCl, 0.3 M sodium citrate, DEPC H₂O) and the second with a 3:2, 1:1, 2:3 ratio of 0.2 X SSCT:PBT at room temperature. Subsequently brains were washed three times with TNT (0.1 M Tris HCl pH 7.5, 0.15 M NaCl and 0.05% Tween 20) before being incubated for 2 h in TNB (0.5% Blocking Buffer supplied with Tyramide Detection Kit dissolved in TNT). Brains were then incubated ON with antibody diluted in TNT (dilution 1:100). Two different set of antibody, which

recognise the modified nucleotide included during the RNA probe synthesis, have been used separately: one with horse-radish peroxidase epitope and another one conjugated with biotin. In the case of this latter, a secondary antibody has been used which recognises biotin and it is conjugated with horseradish peroxidase. In both cases, the luminescence signal was generated by the peroxidase which cleaves the Tyramide molecules. In order to remove the excess unbound antibody, brains were washed five times in TNT for 15 min each and, subsequently, incubated for 2-3 h in a solution containing Tyramide (Cyanine 3, diluted 1:50 in amplification buffer). At the end of the detection reaction, brains were washed three times with TNT for 15 min each and mounted in a slide using Vectashield to amplify and protect the fluorophore signal. The samples were further processed to detect PDF protein or LACZ. In this case, brains were treated with TNB buffer and the ICC protocol (described below) was followed.

2.15. Immunocytochemistry in *Drosophila* brain (ICC)

The dissected brains were washed for 5 min in 75% MetOH in PBT (PBS plus 0.5% of Triton-X). Two subsequent 5 min washes were performed with 50% and 25% MetOH in PBT, respectively, and finally three 5 min washes with 0.5% PBT in order to be permeabilised for the following steps. Subsequently, dissected brains were blocked for 2 h with 1% Bovine Serum Albumin (BSA) to minimise non-specific binding of the primary antibody. After blocking, the brains were incubated with the primary antibody which was diluted in 1% PBT which also contained 1% BSA and 0.1% Sodium azide. The presence of sodium azide prevents the contamination of the antibody solution with bacteria and thereby allows the re-use of the antibody. The brains were incubated in primary antibody for the required period of time (between 1 and 3 days) at 4°C every day mixing by pipetting the solution. They were then washed five times for 5 min each in 1% PBT. After being washed the brains were incubated for 2 h at room temperature in the appropriate secondary antibody (raised against the animal in which the primary antibody was generated) which was conjugated with a fluorophore. In the table below, the antibodies used for the immunocytochemistry experiments conducted are listed.

<u>Antibody</u>	<u>Source</u>	<u>Animal in which it was raised</u>	<u>Fluorophore</u>	<u>Working Concentration</u>
α -NORPA	Gift from Prof. Rouyer	Rabbit		1:1000
α -LAC	ABCam Ltd	Mouse		1:1000
α -PDF	Developmental Studies Hybridoma Bank	Mouse		1:600
α -GFP	ABCam Ltd	Rabbit/Mouse		1:1500
α -Rabbit	ABCam Ltd	Goat	Cy2	1:500
α -Mouse	Sigma-Aldrich	Goat	Cy5	1:500

Table 2.6: List of primary and secondary antibodies used for immunocytochemistry

Once the protein of interest had been labelled with the appropriate antibody, the brain was mounted onto slides (VWR) with a drop of mounting medium which comprises of 80% glycerol and 3% propyl gallate and covered with a coverslip of 0.1 mm thickness (VWR). The slides were stored in the dark at 4°C. They were visualised on an Olympus FV1000 confocal microscope. Individual images were taken of planes at different depths in order to create a Z-series for each brain. The size of the sections forming a Z-series was either 0.44 μ M (if using 40X objective) or 1.4 μ M (if using 20X objective). The optimal microscopic settings, in particular the laser gain, amplifier gain and offset and laser intensity were adjusted for each experiment in order to maximise the quality of the images.

2.16. Fly Stocks

All experiments were done using *D. melanogaster* adult flies grown on standard sucrose-yeast medium (46.3 g/L of sucrose, 46.3 g/L of dry yeast, 7.1 g/L of agar and 50 ml 20% Nipagen in ethanol). All stocks were maintained either at 18°C or 25°C under a cycle of 12 h of light and dark (LD 12:12). The *D. melanogaster* strains used are described below:

- Canton-S : a laboratory wild type strain.
- Oregon-R: another wild-type strain.
- w^{1118} : strain carries a null mutant for *white* gene that produces white coloured eyes. This strain is used as standard for the production of transgenic flies and in general is used as a control in activity experiment (to normalise the genetic background).
- $w; timGAL4$; : strain in a w^{1118} genetic background carrying a P-element on the second chromosome in which a promoter for the clock gene *timeless* drives the expression of the yeast *S. cerevisiae* protein GAL4.
- $yw; pdfGAL4$; : a *yellow white* strain carrying the *pdf* (Pigment-Dispersing Factor) promoter fused to GAL4
- Other GAL4 strains are $yw;; actinGAL4/TM6B$; $w; ninaEGMRGAL4;; elavGAL4;;$; $w;;cryGAL4$; $w; timGAL4; cryGAL80$; $w;; FGAL4$
- $yw;;cry^b$: strain that carries a missense mutation in *cryptochrome* gene (Stanewsky *et al.*, 1998).
- $yw;;glass^{60j}$: strain that carries an insertion of unknown DNA in *glass* (Moses *et al.*, 1989).
- Also, $yw;;glass^{60j}cry^b$: Obtained from Helfrich-Foster.
- $w^{1118}; Cyo/Sco; MKRS/TM6B$: strain carrying chromosome balancers for the second and third chromosomes. These flies carry some visible markers that are useful and allow following genes in crosses scheme.
- $FM7a;;$: strain that carries chromosome balancer for the sexual chromosome and associate with visible marker.
- Also $FM7a; Cyo/Sco$; and $FM7a;; MRKS/TM6B$
- $norpA^{p41};;$ and $norpA^{p41};;cry^b$: strains carrying a deletion of 351 bp in the coding sequence of *norpA* that generates a null mutant (Stanewsky, Personal communication) in *norpA*

- *w;;cry^{out}*: mutant strain characterised by the a deletion of 1490 nucleotides in *cry* sequence which includes the transcriptional start, exon 1, intron 1 and almost all of exon 2 (Yoshii *et al.*, 2008).
- *wUASdicer2;;*: strain carrying a P-element on the first chromosome that allows the expression of DICER2 under control of the yeast *S. cerevisiae* protein UAS sequence (Obtained from VDRC, Dietzl *et al.*, 2007). Also *w; UASdicer2;* and *w; timGAL4 UASdicer2;* strains
- R32: transgenic line carrying an expressing *lacZ* transgene on the third chromosome. In this line LACZ has a cytoplasmatic expression in the circadian neurons (Shafer *et al.*, 2006).
- *gal¹¹¹⁸GFP*: transgenic line carrying an expressing *UASgfp* transgene under the control of *gal¹¹¹⁸* promoter which is an unmapped P-GAL4 enhancer-trap line (Blanchardon *et al.*, 2001).
- Transgenic flies were obtained from VDRC or BestGene after been microinjected.

2.17. Locomotor activity

Locomotor activity was recorded by the Trikinetics locomotor monitoring system and software (Waltham, Massachussets, USA). Each male fly (about 1-4 days old) was loaded in a glass tube containing sugar food at one end and a cotton bung at the other. The food containing end was sealed with a plastic cap to avoid desiccation. Each tube was then placed in the monitoring apparatus, which consists of an infrared emitter and a detector, so that each time the fly breaks the infrared beam, one unit of locomotor activity is recorded by a computer connected to the detector. The number of times the beam is interrupted within a 30 min window is recorded as the locomotor activity of that specific time bin. The average activity histogram (actogram) was plotted using Microsoft Excel 2003 or 2007 using flies that survived until the end of the experiment.

The monitors were housed in light boxes equipped with 15 light emitting diodes (LEDs) programmed to turn on and off using timers (Müller) according to the

experimental light regime. The light boxes were placed into incubators (Scientific Laboratories Supplies Ltd) that maintained constant temperature.

2.18. Data collection and Analysis

The locomotor activity monitors were connected to a PC using a Power Supply Interface Unit (TriKinetics Inc) and the data from them was collected using the DAMSystem2.1.3 software (TriKinetics Inc). Only flies that survived till the end of the experiment were used for all subsequent analysis. The average activity histogram (actogram) was plotted using in house macros in Microsoft Excel 2003 or 2007. The period of each individual fly was calculated by Autocorrelation and also by using Python 2.2 for high resolution spectral analysis using the CLEAN algorithm which confirm or reject the biological significance of the autocorrelation. In the autocorrelation analysis, the data (collected in 30 minute bins) is shifted point by point and compared to itself to create correlation coefficients (thus called autocorrelation) which are then plotted together. The spectral analysis breaks down the signal to its sine and cosine waves, and the frequencies that provided the closest matches to the data are displayed as a spectrogram. Monte Carlo simulations were used to generate the confidence limits of 95% and 99% by doing 100 randomisations on the data for each fly (Rosato & Kyriacou, 2006). The data obtained after CLEAN was assembled together and further processed using a collection of macros generated in the laboratory by Dr. Edward Green (BeFly!). Flies were considered rhythmic in the case that they presented a clear and significant autocorrelation and spectral analysis. If an individual showed a single detectable peak above the 99% confidence limit in the CLEAN analysis, this was taken as the period. Individuals with multiple peaks above the 99% confidence limit were regarded to have multiple rhythms. Any other pattern that falls below the 99% confidence limits was considered arrhythmic.

The average activity histogram (actogram) of entrained flies was plotted using Microsoft Excel[®] 2003. Actograms for each individual fly were then used to determine the onset and offset of the morning and evening activity.

For all the genotypes studied, the time of onset and offset of the morning burst of activity was determined fly-by-fly for each day throughout the entire duration of the every experiment. Below are described the criteria adopted for determining the onsets and offsets (referring to Figure 2.3):

- A burst of activity was considered as, for example, morning burst if it occurred after a long period of rest during the dark phase of a day.
- Activity bursts have to present a steady increase and decrease in activity levels and finally a clear peak.
- The burst of activity had to be based on a continuous movement of the fly with “no-activity gap” longer than half an hour (one bin).
- The window of time taken in consideration to define a burst of activity was 4-5 h before the light transition (light off/on in the case of morning onset or light on/off for the evening onset).

The average bin value of the onset and offset of morning and evening activity bursts for each genotype were computed for each day and subtracted from the bin value of the light transition. The bin values among the entire experiment were averaged within the same fly to obtain an average morning onset bin value. This criteria was used for the other parameters such as morning offset, evening onset and evening offset.

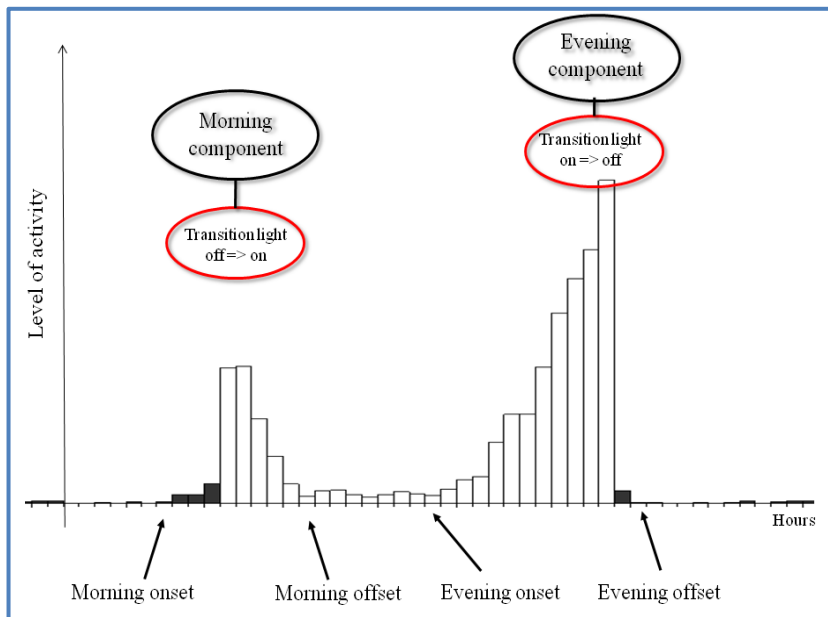


Figure 2.3:
Diagrammatic representation of locomotor activity recorded in 12:12 LD regime (light: white bars, dark: black bars). The morning and evening onsets and offsets of activity were determined for each fly for every genotype used.

Chapter 3 NORPA as a component of temperature entrainment

norpA has been shown to modify the level of *per* splicing and behavioural phenotype in relation to the environmental temperature. The aim of this chapter is to understand whether the *norpA* mRNA and protein expression is localised among the circadian neurons responsible for the locomotor behaviour.

3.1. Introduction

The *norpA* gene in *D. melanogaster* encodes for a phospholipase C (PLC). This enzyme cleaves phosphatidylinositol 4,5-bisphosphate (PIP₂) to two second messengers: inositol trisphosphate (IP₃) and diacylglycerol (DAG). These messengers are associated with a variety of cellular processes including, for example, cell growth, differentiation, secretion, memory and phototransduction (Bloomquist *et al.*, 1988). In the latter process, the role of *norpA* is generally understood: the photoisomerisation of rhodopsin to metarhodopsin (Rh → M, encoded by the *ninaE* gene) activates heterotrimeric G_q protein *via* GTP-GDP exchange, releasing the G_{qα} subunit (Figure 3.1). This activates phospholipase C (PLC; encoded by *norpA*), generating inositol 1,4,5-trisphosphate (IP₃) and diacylglycerol (DAG) from phosphatidyl inositol 4,5- bisphosphate (PIP₂). Two classes of light-sensitive channel (TRP and TRPL) are activated, but by an unknown mechanism.

Several components of the cascade, including the ion channel TRP, protein kinase C (PKC, *inaC* gene) and PLC are coordinated into a signalling complex by the scaffolding protein, INAD, which contains five PDZ domains. At the base of the microvilli, a system of submicrovillar cisternae (SMC) has been presumed to represent Ca²⁺ stores endowed with IP₃ receptors (IP₃R; *dip* gene) and smooth endoplasmic reticulum Ca²⁺-ATPase; however, the SMC may play a more important role in phosphoinositide turnover: DAG is converted to phosphatidic acid (PA) *via* DAG kinase (*rdgA* gene) and to CDP-DAG *via* CD synthase (*cds* gene) in the SMC. After the conversion to phosphatidyl inositol (PI) by PI synthase, PI is transported back to the microvillar membrane by a PI transfer protein (*rdgB* gene). PI is

converted to PIP₂ via sequential phosphorylation (PI kinase and PIP kinase; reviewed from Hardie, 2001; Figure 3.1).

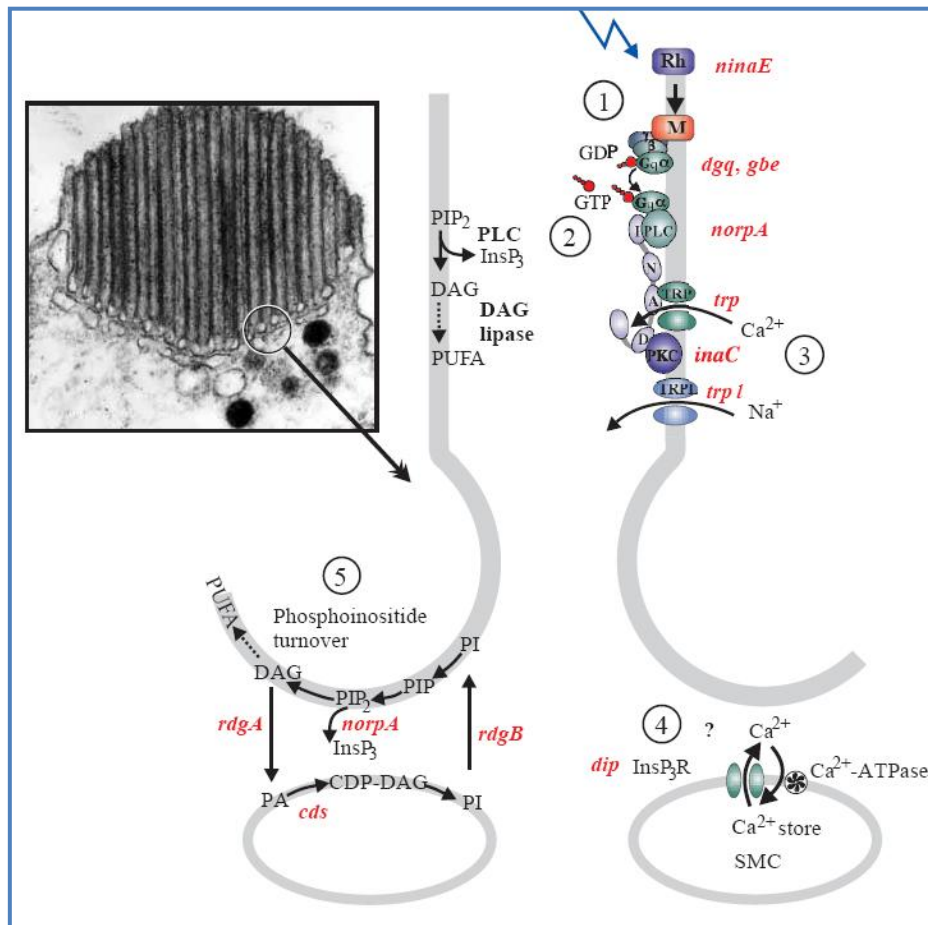


Figure 3.1: *D. melanogaster* phototransduction cascade. Cross-section of a *Drosophila* rhabdomere (electron micrograph), which is composed of about 30000 microvilli, each approximately 1-2 mm in length and 60 nm in diameter. Each microvillus contains approximately 1000 molecules of rhodopsin and most elements of the phototransduction machinery. An enlargement of the circled area, showing the base of one microvillus with associated phototransduction machinery is also shown schematically in the right hand panel (taken from Hardie, 2001).

A behavioural role for *norpA* in the circadian mechanism has also been established regarding seasonal and temperature synchronisation. *norpA*^{P41} mutants show an early upswing of PERIOD protein and a consequential advance of the evening component of the locomotor activity at low and high temperatures. Molecularly, this is determined by a high level of splicing in the 3'UTR *period* mRNA in both conditions. Thus *norpA* seems to be important for communicating the temperature information to the circadian clock (Collins *et al.*, 2004; Majercak *et al.*, 2004). Furthermore, another study has shown that *norpA*^{P41} mutation affects

molecular and behavioural entrainment to temperature cycles independently to the splicing event in *per* gene (Glaser and Stanewsky, 2005).

In this chapter, the spatial expression of NORPA has been investigated *via* immunocytochemistry (ICC) and *in situ* hybridisation, in order to analyse possible structures in common between the circadian machinery and NORPA.

3.2. Materials and Methods

3.2.1. Synthesis of *norpA* RNA probes

Primers used to generate *norpA* RNA probes and subsequently subjected to *in situ* hybridisation procedure are reported in the table below (3.1).

Primer	DNA sequence	In Figure 3.11
NRPext F	5' - TGTACCACAAGGTGTGTC CCC - 3'	Black
NRPext R	5' - TTCTCCTGGCGCAGAGATTC - 3'	Black
T3NRPF I	5'- AATTAACCCCTCACTAAAGGGAGAACGGAGAAAATTGGGTACACG - 3'	Orange
T7NRPR I	5' - TAATACGACTCACTATAGGGAGATGATCTGGTAGCGGCTCC - 3'	Orange
T3NRPF II	5' - AATTAACCCCTCACTAAAGGGAGAACCAGATCATCCGCTGGATC - 3'	Blue
T7NRPR II	5' - TAATACGACTCACTATAGGGAGATGCCCACTTTCTTGTCGGA - 3'	Blue
T3NRPF III	5' - AATTAACCCCTCACTAAAGGGAGATTGATCCGTTTGCCGATG - 3'	Green
T7NRPR III	5' - TAATACGACTCACTATAGGGAGAGGTCTTTGCACCGAGGTG - 3'	Green
T3NRPF IV	5' - AATTAACCCCTCACTAAAGGGAGAAGATGCTGGCAAGGCCAA - 3'	Violet
T7NRPR IV	5' - TAATACGACTCACTATAGGGAGACGCCTCCTCGATTTTG - 3'	Violet

Table 3.1: Primer sequences used to generate *norpA* probes.

PCR were carried out using Phusion Polymerase (Finnzymes®). PCR reactions were set up according to primer annealing temperatures and length of the amplified fragment. The lines used, the antibody concentration and other details are reported in Chapter 2 (section 2.14, 2.15 and 2.16).

3.3. Results

3.3.1. Spatial localisation of NORPA in fly adult brains *via* ICC

norpA spatial expression was investigated in two ways: by immunocytochemistry (ICC) and *in situ* hybridisation. In the first case, an antibody against NORPA protein was used in fixed brains (Zhu *et al.*, 1993). In general, ICC methodology gives better and more specific results than *in situ* protocols due to the nature of the probing.

However, this depends on the characteristics of the antibody: its specificity for the epitope and the natural folding of the protein (tertiary structure). This aspect is determined by the way the animals have been immunised: the full-length (or fragment) of folded wild-type protein or a denatured peptide.

The localisation of NORPA was investigated in whole mounted *Drosophila* brains using a NORPA antibody (1:1000 dilution; Zhu *et al.*, 1993). In previous experiments conducted by ICC in larval brains, NORPA was localised in the Bolwig nerve fibers (BN; Section 3.3.2; Malpel *et al.*, 2002). In *D. melanogaster* larvae the visual system consists of a pair of 12-cell Bolwig organs (BO) which are responsible for several light induced larval behaviours (Hassan *et al.*, 2000). This structure sends axonal projections (the Bolwig nerves or BNs) into the brain and in particular they terminate in the vicinity of the LNs, suggesting that the clock cells could be their direct targets (Kaneko *et al.*, 1997). Moreover Zhu and co-workers (1993) demonstrated that NORPA is mostly expressed in the retina, optic lobes, ocelli and brain (cerebrum) of adult brains. This data was in agreement with the spatial localisation of *norpa* mRNA in tissue sections of head (Bloomquist *et al.*, 1988) and the spatial distribution of PIP₂ which is a relevant substrate of the PLC (Suzuki and Hirose, 1992). Since all these published data have been obtained in tissue sections, a localisation of NORPA in whole mounted fly brain might give a more accurate spatial expression in relation to circadian structures. In order to investigate this point, NORPA antibody was used together with lacZ in flies that express this exogenous gene in the circadian neurons (hereafter named *R32*, Shafer *et al.*, 2006) or to coincide with PDF antibody in wild-type strain (i.e. *w¹¹¹⁸*).

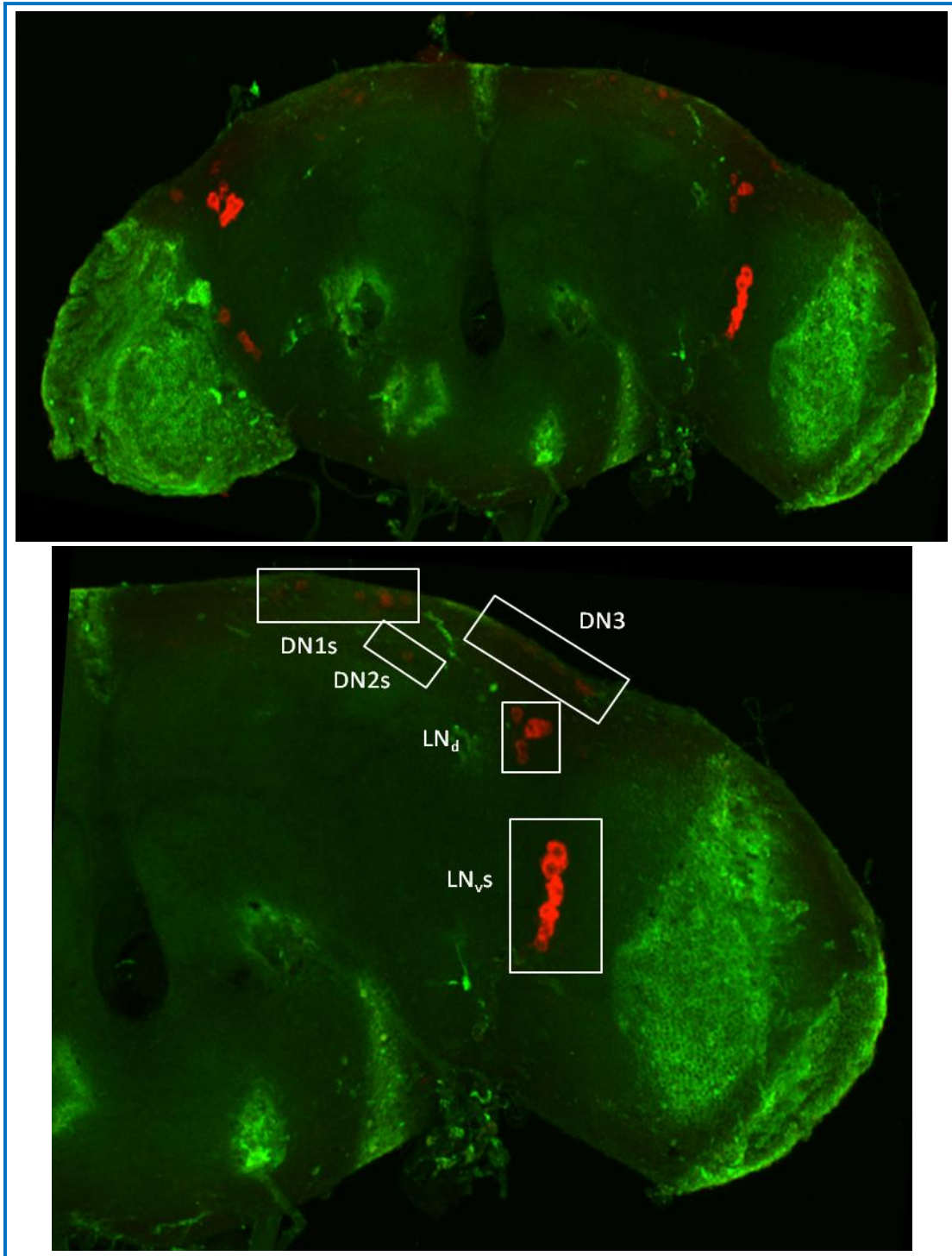


Figure 3.2: Representative R32 *Drosophila* brain (20X, upper panel) and enlargement of the right hemisphere (bottom panel). Confocal images were merged together in order to create a full structure of the brain. The red signal (Cy5) corresponds to LACZ antibody whereas green signal (Cy2) localises NORPA antibody. Flies were entrained under LD 12:12 at 25°C.

Figure 3.2 shows R32 transgenic *Drosophila* brains expressing *lacZ* in circadian neurons which were subjected to an ICC protocol using *lacZ* and NORPA antibodies. The expression pattern displayed by the α -LACZ (CWO reporter) antibody was

specific and localised in all circadian neurons (s-LN_vs, l-LN_vs, LN_ds as well as most of DNs; Figure 3.2 and Shafer *et al.*, 2006). On the other hand, the expression profile of NORPA appeared to be widely dispersed. The examination of a single layer obtained from the confocal identified NORPA expression mostly on the surface of the brain. Surprisingly no signal emerged from the inner portions of the brain where the circadian clock cells are located. All images analysed appeared to give a consistent labelling at the level of the cellular membrane but none from the nucleus. This result is in accordance with the molecular and physiological role of NORPA within the cells: an intermediate enzyme between the signal and the signalling pathway cascade.

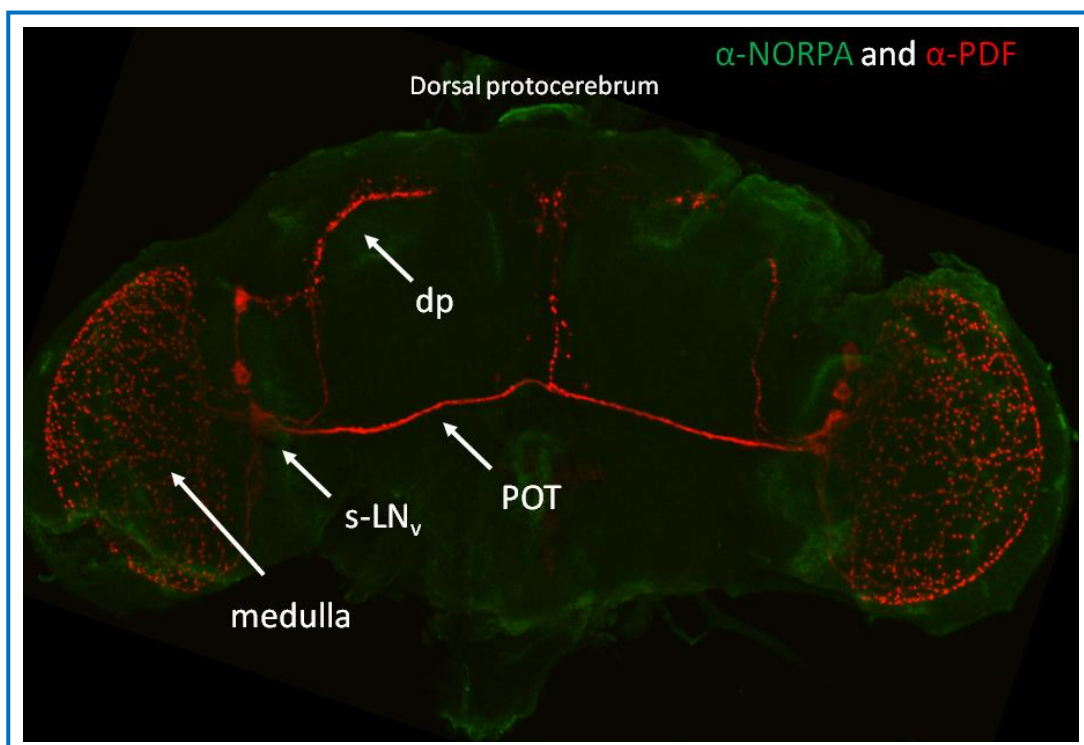


Figure 3.3: *w*¹¹¹⁸ brain labelled with PDF (red; Cy5) and NORPA (green; Cy2) antibodies. The brain presented is an image of 30 independent layers merged together. Flies were entrained under LD 12:12 at 25°C.

The results described for *R32* lines were also confirmed in *w*¹¹¹⁸ brains (Figure 3.3). In this case, ICC was carried out using α-NORPA and α-PDF antibodies. The expression pattern displayed by NORPA was similar to the *R32* transgenic. PDF antigen labelled the LN_v neurons (s-LN_vs and l-LN_vs) that express this neuropeptide (e.g. Grima *et al.*, 2004). The s-LN_vs send dorsal projection (dp) to the dorsal brain whereas the l-LN_vs send projections to the other hemisphere (POT) and arborise in the optic lobe.

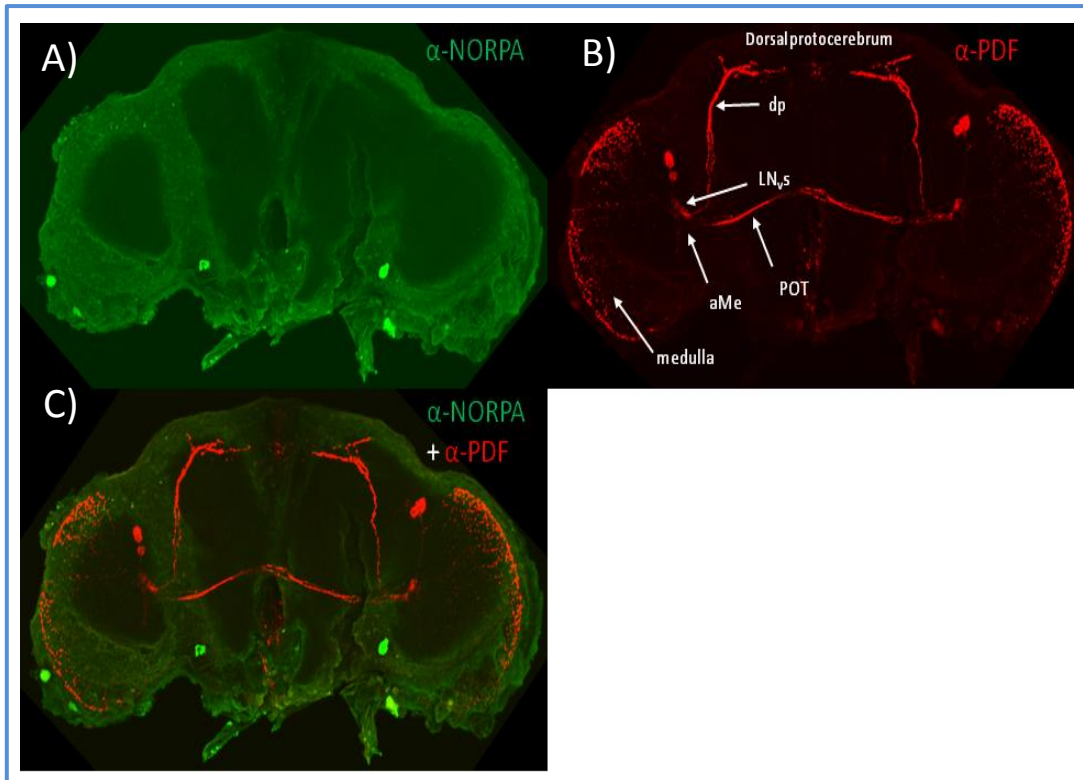


Figure 3.4: *Drosophila* brain in which NORPA was over-expressed in the morning neurons via *PdfGAL4* driver. A) NORPA signal (Cy2). B) PDF signal (Cy5). C) Merge of images A and B. Flies were entrained under LD 12:12 at 25°C.

However, neither in the case of *R32* nor *w¹¹¹⁸*, overlapping signals generated by co-localisation of NORPA and circadian neurons (yellow = green + red) were detected, suggesting three possibilities: 1) NORPA may be not expressed in the circadian clock neurons; 2) the NORPA antibody is not of sufficient quality although it works perfectly in western blots (Section 4.3.1, Figure 4.5) or 3) the antibody may be not able to penetrate the packed structure of the brain.

Therefore, flies over-expressing NORPA in the LN_{v,s} (*w; PdfGAL4/+; UAS norpA/+*) [Material and Method, section 2.16 and Appendix 1]) were examined. As shown in Figure 3.4, a co-labelling of α-NORPA and α-PDF was not found in the LN_{v,s}. Remarkably, as described before, NORPA signal was distributed mostly in the optic lobes and its localisation appeared to be on the surface of the brain.

However, when an enlargement of the optic lobe and LN_{v,s} was analysed, overlapping signals were observed only in the contact area between the optic lobe surface and the termination of the PDF arborisation (Figure 3.5).

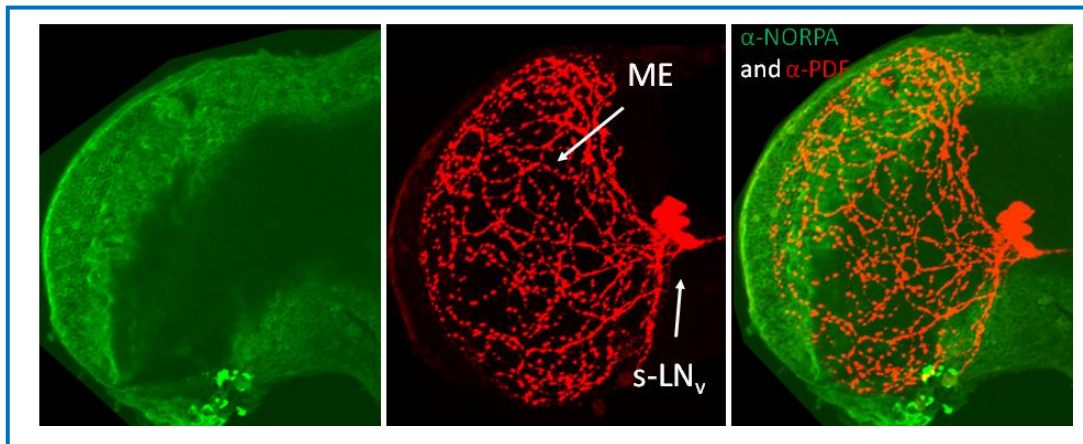


Figure 3.5: Enlargement of an optic lobe over-expressing NORPA in PDF neurons. A) NORPA (Cy2), B) PDF (Cy5) signals. C) Merge of A and B images. Flies were entrained under LD 12:12 at 25°C.

From these results, it is evident that the NORPA antibody is not able to penetrate the brain structures, otherwise a signal would be expected in the LN_vs under “extreme” conditions such as GAL4 over-expression. Alternatively, steric hindrance of the antibody or its folding may cause penetration failure through the pore created by the washes. However, the brain surface displayed a NORPA signal.

Thus, the specificity of this was investigated incubating brains just with the secondary antibody (Cy2; Figure 3.6).

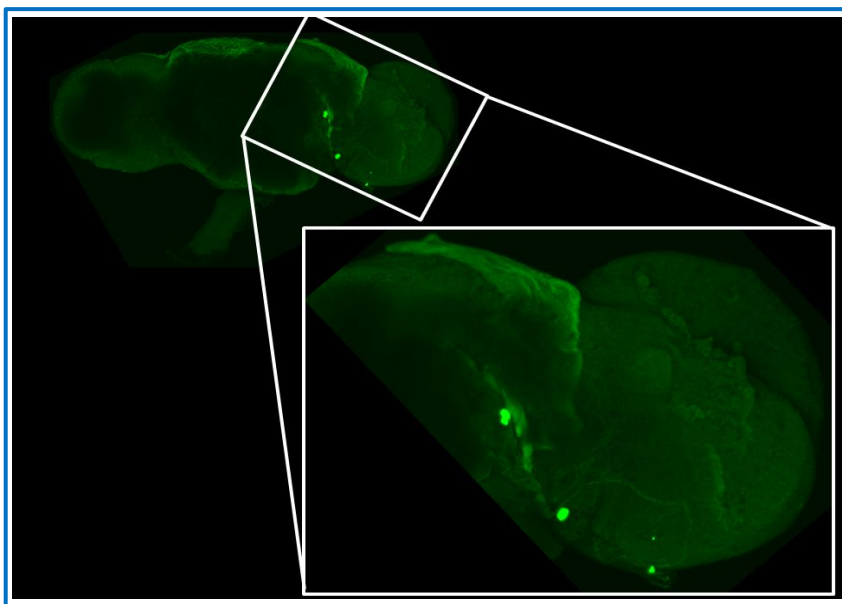


Figure 3.6: w^{1118} brain subjected to the secondary antibody labelling (Cy2). Flies were entrained to LD 12:12 at 25°C.

As shown in Figure 3.6, no specific brain structures were labelled in the absence of NORPA primary antibody. Fluorescent signal was homogeneously distributed: cellular membranes were not marked as in the presence of NORPA antibody.

Finally, the NORPA labelling was also analysed in *norpA* null mutants but as expected, no specific staining was observed. In the figure below (3.7), a representative brain is shown stained with α -NORPA and α -LACZ antibodies (which recognises circadian neurons in *R32*).

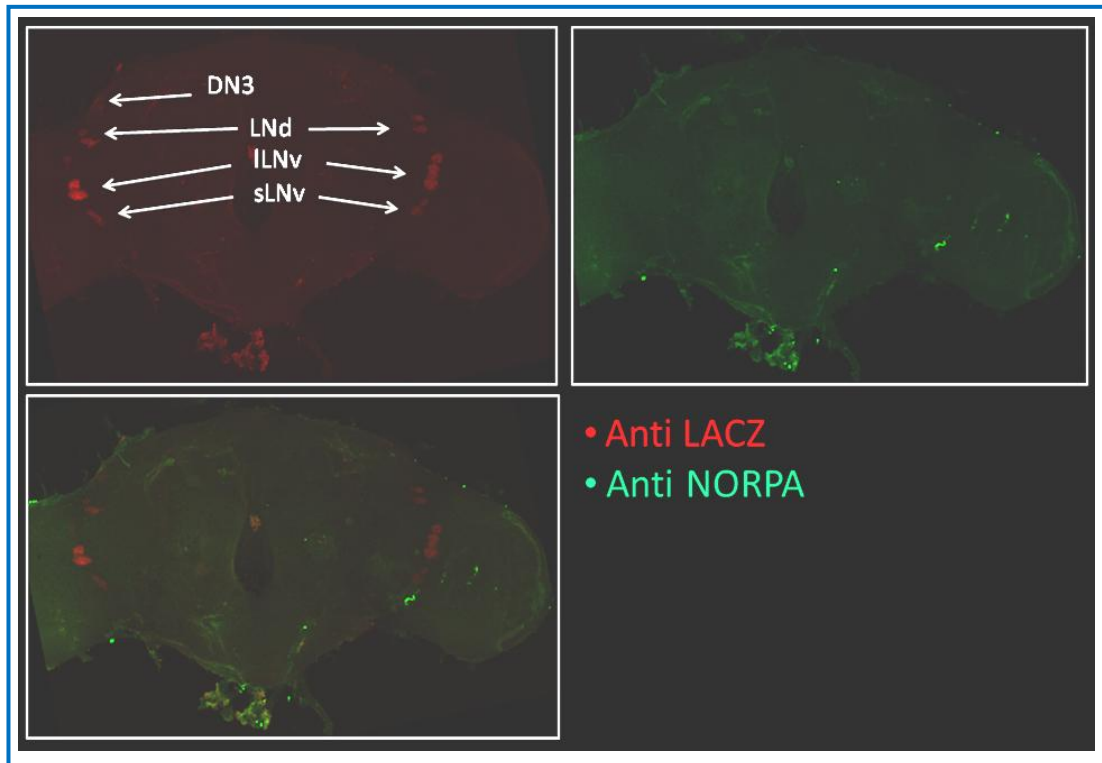


Figure 3.7: Representative *norpA^{P41}*; *R32* adult brain. Confocal images were merged together in order to create a full tridimensional structure of the brain. The red signal (Cy5, in the top left panel) corresponds to LACZ antibody whereas green signal (Cy2, right top panel) localises NORPA antibody. Flies were entrained under LD 12:12 at 25°C.

3.3.2. Spatial localisation of NORPA in fly larval brains *via* ICC

In order to verify the efficiency of NORPA antibody (Zhu *et al.*, 1993), *w¹¹¹⁸* larval brains were subjected to immunocytochemistry together with PDF antibody. In the Figure below (3.8), NORPA (green, Cy2) and PDF (red, Cy5) signals are shown in a representative brain. PDF labeled the LN_vs and their dorsal projections whereas NORPA signal was found in the Bolwig nerve fibers (BN). This last result is in agreement with results published by Malpel *et al.* (2002).

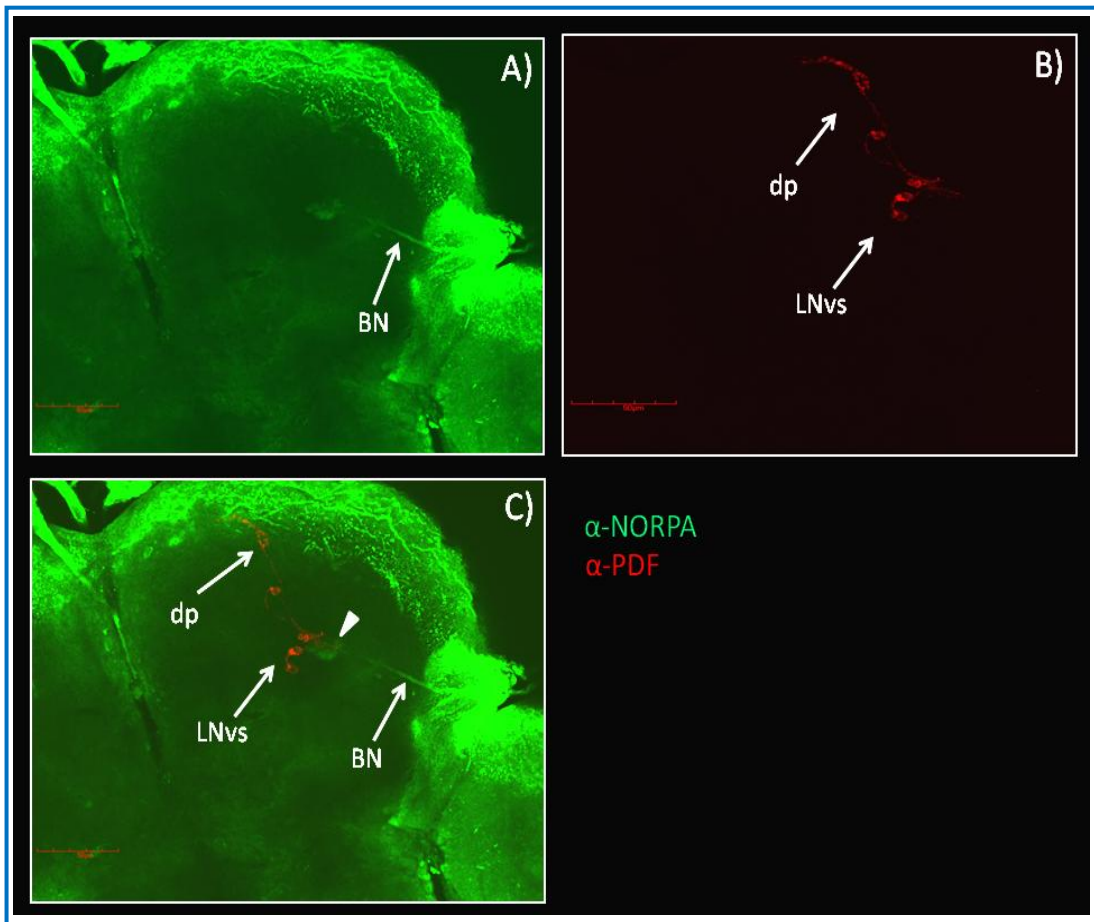


Figure 3.8: A projected Z-series montage of a larval w^{118} brain labeled with α -NORPA (green, Cy2, A) and α -PDF (red, B, right top panel). Flies were entrained under LD 12:12 at 25°C.

Furthermore, w^{118} larvae were entrained at 18°C and their brain dissected (Figure 3.9 and 3.10). This temperature was chosen to detect any possible differences with flies kept at higher temperatures (i.e. 25°C). As before, NORPA antibody was used together with PDF in order to have a positive control and a circadian marker.

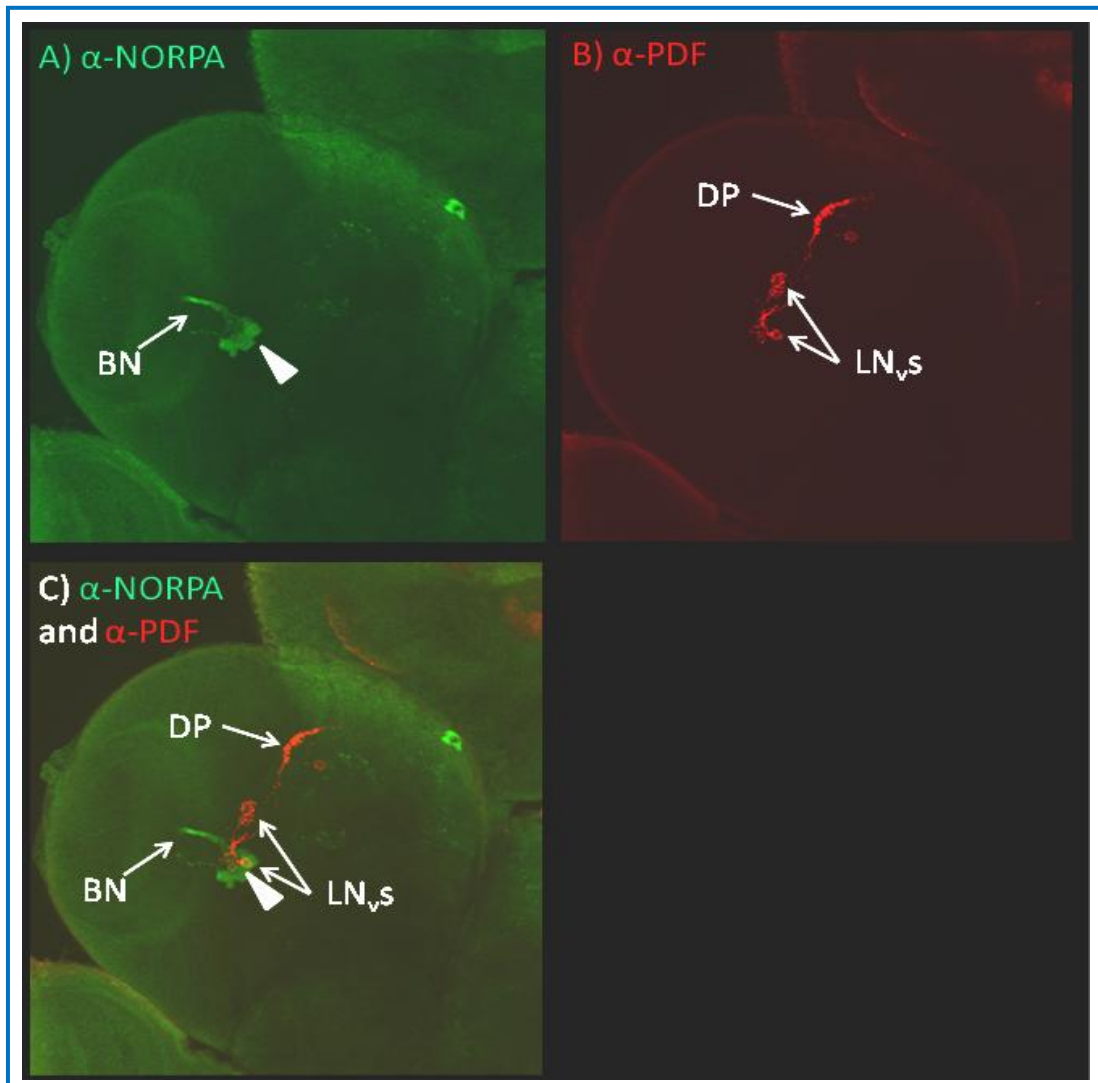


Figure 3.9: Representative larval *w¹¹¹⁸* brain entrained at 18°C (ventral view). Confocal images were merged together in order to create a full tridimensional structure of the brain. NORPA (A, green signal, Cy2) and PDF (B, red signal, Cy5) antibodies. In panel C, A and B were overimposed. Arrow head indicates a costaining of NORPA and LN_vs.

At low temperature, more larval brain structures were labelled by NORPA antibody compared to 25°C. In fact, an overlapping signal between an LN_v neuron and the end of the Bolwig nerves was found in the ventral part of the brain (Figure 3.9). Moreover, the termination of the BN was characterised by a large number of cells (which are visible in Figure 3.9). In the dorsal part of the brain two cluster of cells (indicated with arrow heads in Figure 3.10) were found which, due to their location, may be DNs.

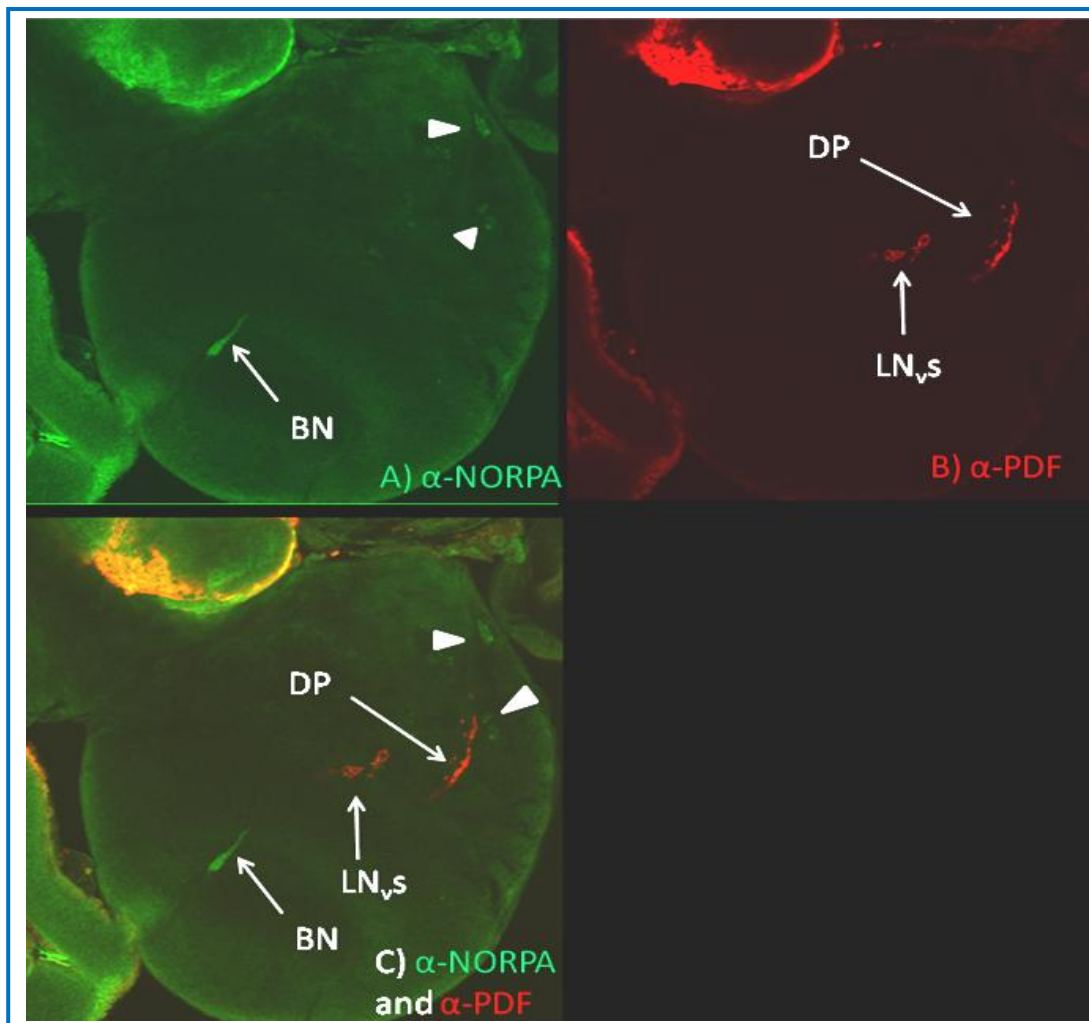


Figure 3.10: Representative larval w^{1118} brain entrained at 18°C (dorsal view). Confocal images were merged together in order to create a full tridimensional structure of the brain. NORPA (A, green signal, Cy2) and PDF (B, red signal, Cy5) antibodies. In panel C, A and B were overlaid. Arrow heads indicate possible staining in the DNs.

3.3.3. Spatial localisation of *norpA* in fly brain *via in situ* hybridisation

Initially, *norpA* expression has been evaluated following Wülbeck and Helfrich-Förster protocol (2007). w^{1118} cDNA was used as template from which the *norpA* probe was synthesised by a nested PCR strategy. First a large region that included the template for the *norpA* probe was amplified and used as a source of DNA for the subsequent PCR reactions. These were carried out utilising two sets of primers that include in their sequence either T7 or T3 RNA polymerase promoters. The product of this PCR was subjected to RNA transcription in order to obtain a sense *norpA* probe and an anti-sense *norpA* probe (Figure 3.11). In both probes, a ribonucleotide conjugated with Digoxigenin (DIG) was incorporated in the reaction in order to be recognised by a specific antibody in the following *in situ* steps.

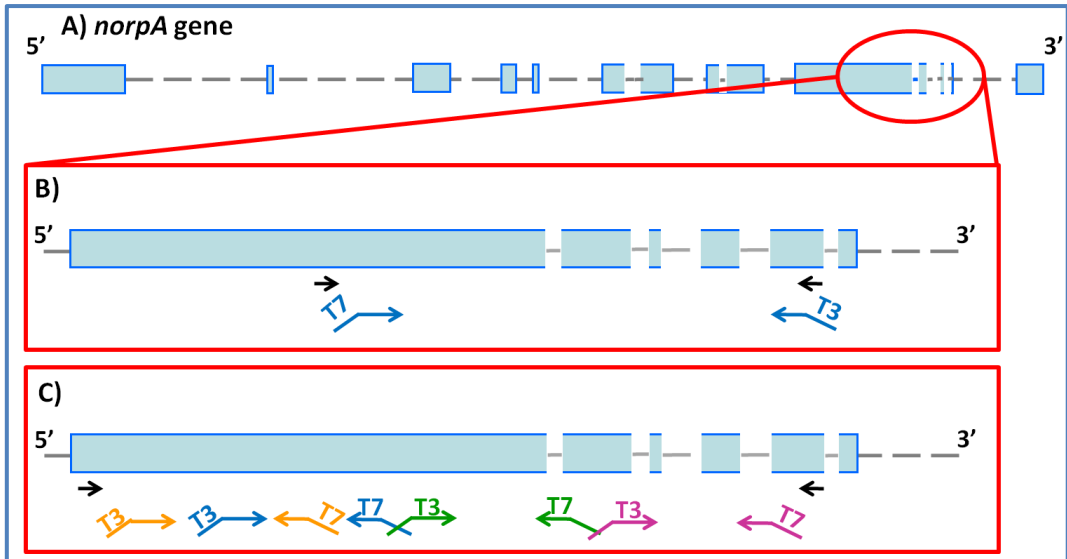


Figure 3.11: Representation of the strategy adopted to generate the sense and anti-sense probes used for the *in situ* hybridisation. In panel A full length *norpA* is reported including exons and introns. In B and C, an enlargement of the region amplified for generating the probes is shown. Black arrows indicate the first set of primers utilised for amplifying a larger region that has been used as template for the following PCR reactions for the T7 and T3 probes (different color arrows).

Initially, as shown in Figure 3.11 panel B, a single probe of 1400 bp was generated and subjected to the *in situ* protocol. Strong non-specific labelling, mostly generated by tracheas, was detected and no *norpA* expression in circadian neurons emerged suggesting a problem with the penetration of the probe (Figure 3.12).

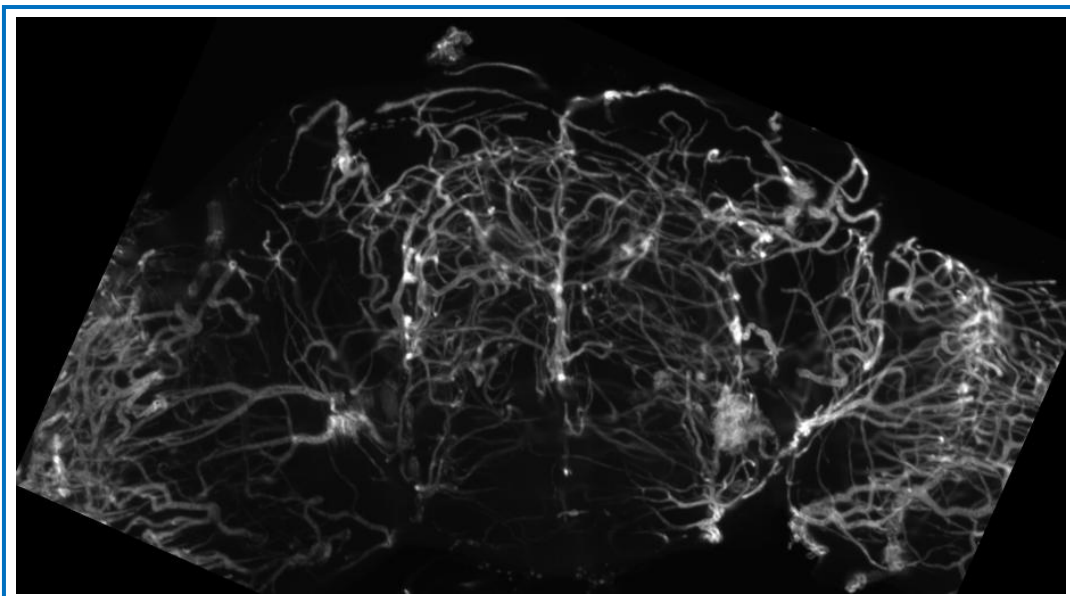


Figure 3.12: Canton-S brain probed with α -*norpA* probe (1400 bp). The brain shown is an image of 20 independent confocal layers merged together.

In order to increase the penetration of the probe and reduce the background as much as possible, a new probe was designed. The same region was used as template but divided in four fragments each one \approx 800 bp in size (Figure 3.11, panel C). Furthermore, the Helfrich-Förster protocol was slightly adjusted by increasing the proteinase K treatment timing (to 1 hr at 4°C) and washing the brains in a cell culture plate. In addition to this, the detection of *norpA* transcript was carried out by indirect labelling. Thus, two antibodies were used in succession: one against DIG and conjugated with Biotin and a second conjugated with HRP which recognises the BIO epitope. This strategy was used to detect *norpA* in larval (Figure 3.13) and adult brains (Figure 3.14 and 3.15). In the case of larval brain, a transgenic line expressing GFP under control of *gal¹¹¹⁸* promoter which help to localise the LN_vs was used (Blanchardon *et al.*, 2001). *norpA* probes displayed a broad labelling. Diverse layers of the brain were scanned finding *norpA* signal distribution in all of them (Figure 3.13, B). Furthermore, a co-localisation between *norpA* transcript and the ventral circadian neurons was detected when the two signals were merged together (Figure 3.13, C). Unfortunately, the *gal¹¹¹⁸* line does not mark the DN (dorsal neuron) subset of pacemakers, thus it was not possible to detect the presence of the *plc β* transcript in these cells. However, given the broad labelling of the probe, the presence of the transcript may be assumed also among them. Furthermore, the *norpA* probe labelled two dorsal clusters of dorsal neurons, dg1^L and dg2^L, which were reported to express no PER (Figure 3.13, F; Blanchardon *et al.*, 2001). Finally, when the sense *norpA* probe (double concentrated compared to the α -sense) was used as control, weak and non specific staining was observed (Figure 3.13, E and F).

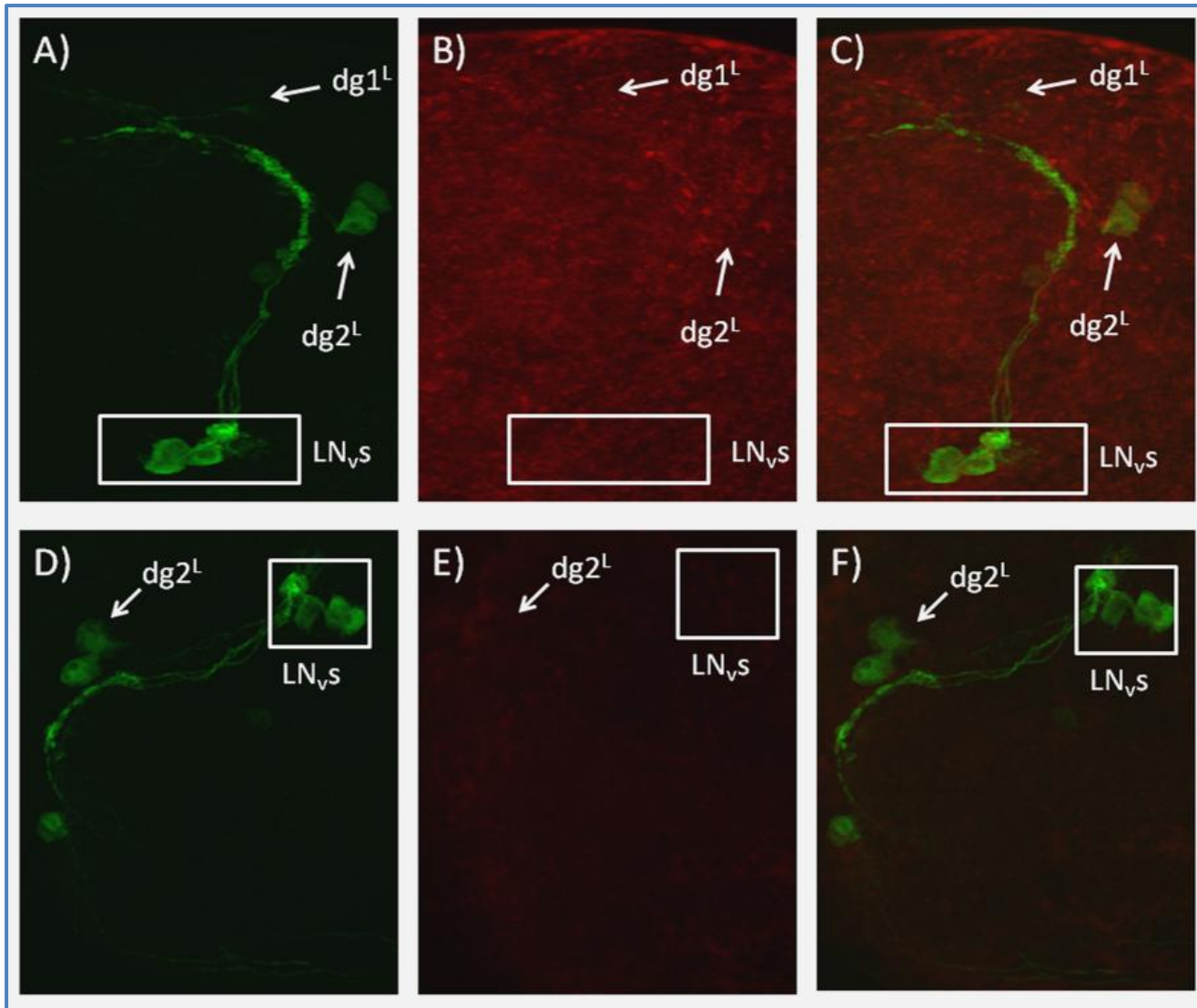


Figure 3.13: Representative larval brain of *gal¹¹¹⁸GFP* fly probed with GFP antibody (A and D), α -sense *norpA* probes (concentrated 75 ng, B) and sense *norpA* probes (concentrated 150 ng, E). C and F are a merge of A-B and D-E, respectively. dg1-2^L refers to dorsal *gal¹¹¹⁸* larval neurons (Blanchardon *et al.*, 2001). The brain presented is an image of 10 independent layers merged together. Larvae were entrained under LD 12:12 at 25°C.

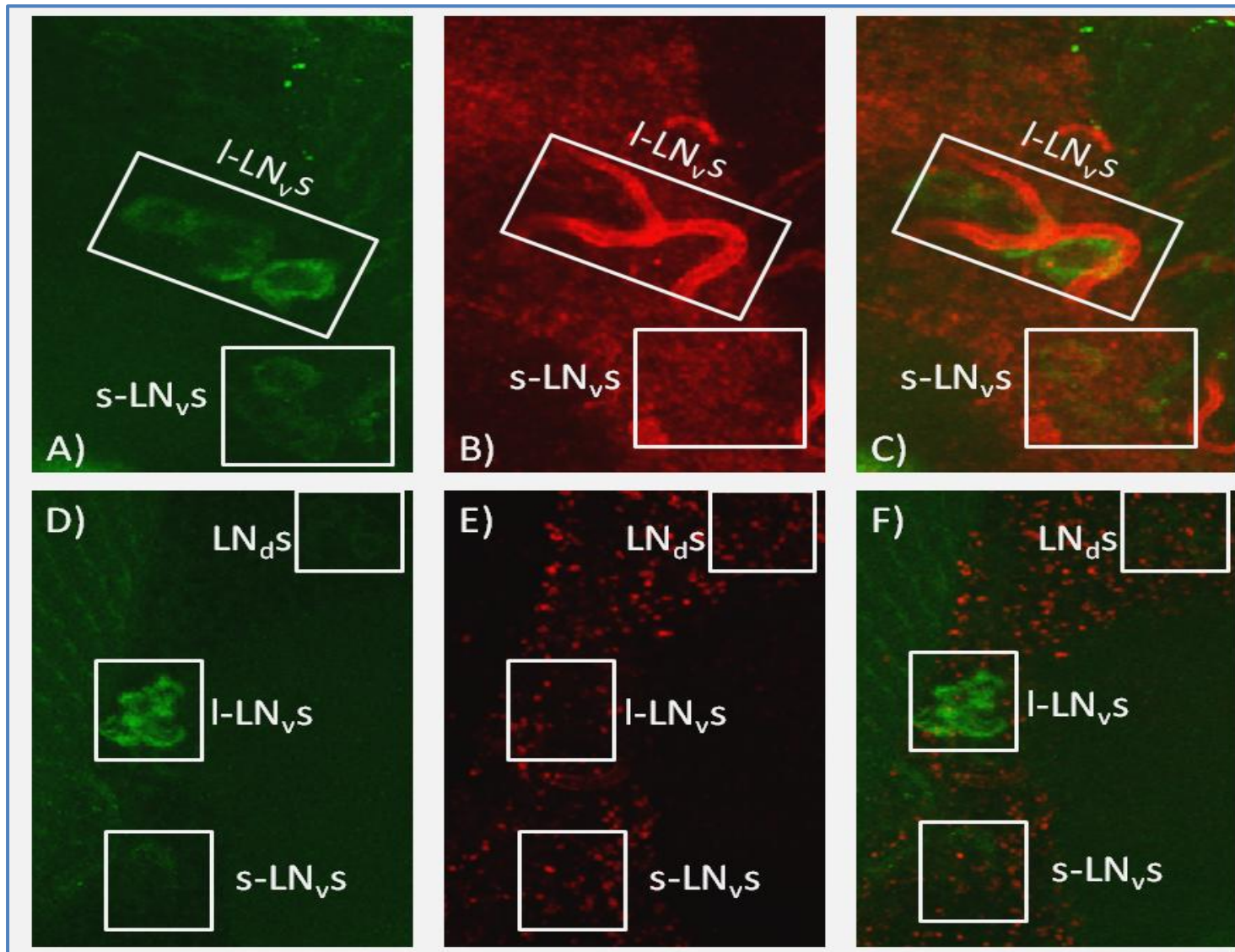


Figure 3.14: Ventral views of representative R32 adult brains probed with β -LAC antibody (A and D), α -sense *norpA* probe (concentrated 75 ng, B) and sense *norpA* probe (concentrated 150 ng, E). C and F are a merge of A-B and D-E, respectively. The brains presented are images of 10 independent layers merged together. Flies were entrained under LD 12:12 at 25°C.

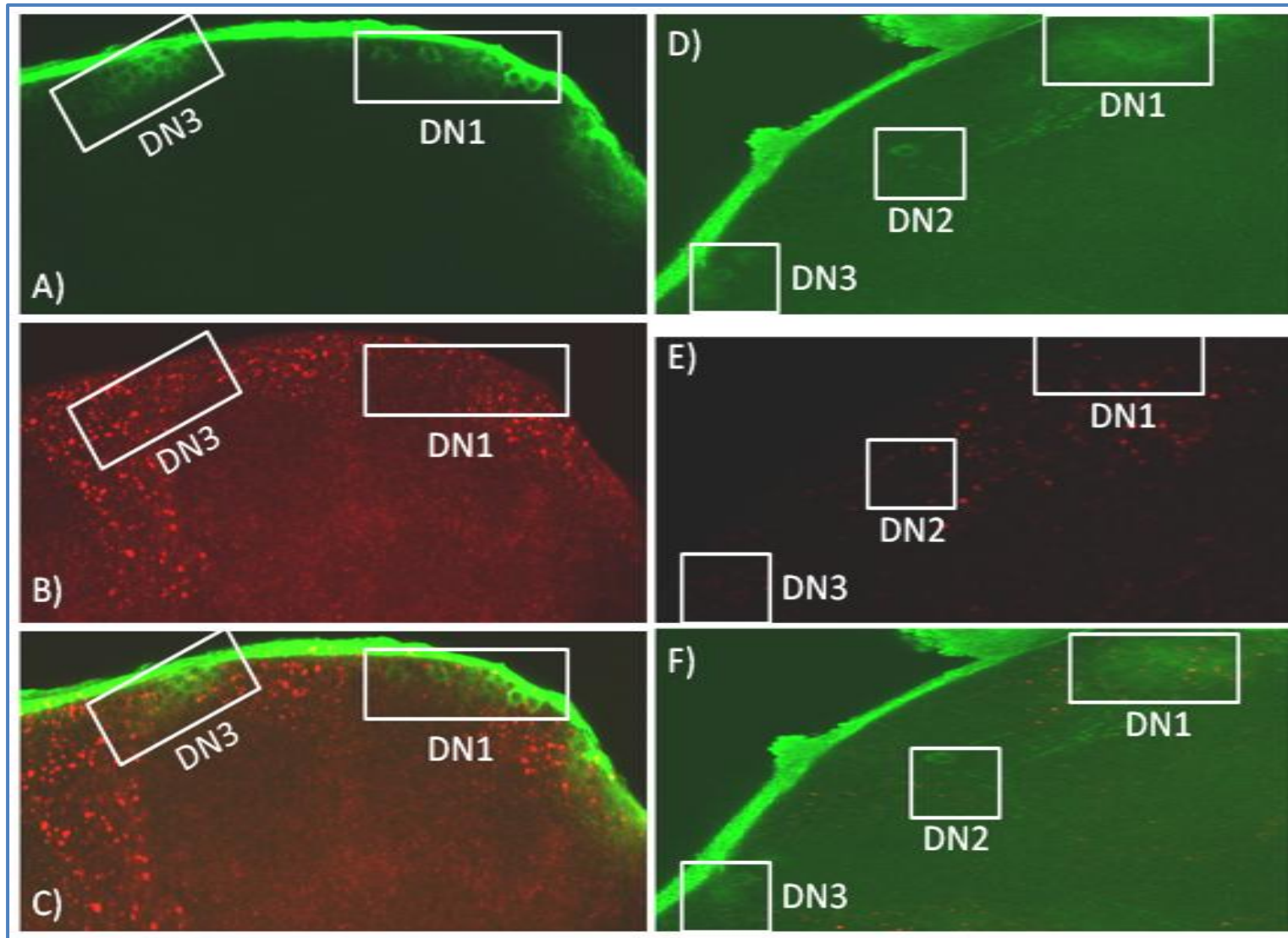


Figure 3.15: Dorsal views of representative R32 adult brains probed with β -LAC antibody (A and D), α -sense *norpA* probe (concentrated 75 ng, B) and sense *norpA* probe (concentrated 150 ng, E). C and F are a merge of A-B and D-E, respectively. The brains presented are images of 10 independent layers merged together. Flies were entrained under LD 12:12 at 25°C.

Adult brains were also analysed with the same methodology. In this case, *R32* (Shafer *et al.*, 2006) was used in order to distinguish among the populations of circadian neurons. In all the layers of the brains analysed, *norpA* was broadly distributed in CNS tissues. Furthermore, when the analysis was focused on the LN_vs and DNs, *norpA* signal emerged from these cells (Figure 3.14 C and 3.15 C, respectively). In most cells analysed, *norpA* signal was not perfectly overlapping with the LACZ marker but included in the cells. The *R32* brains were also processed with *norpA* sense probe as control for verifying the hybridisation efficiency (Figure 3.14 F and 3.15 F). The concentration of this control probe was double to the α -sense (150 ng) resulting in a weaker and non specific signals especially at the level of the circadian neurons.

3.4. Discussion

The localisation of a transcript or its protein are complementary methods. The presence of a mRNA does not necessarily imply the presence of the protein, since the mRNA can degrade or diffuse. However if protein is not detectable, there may be several reasons such as low expression, or poor antibody quality. The latter appeared to be the case for NORPA. I attempted to extend the results of previous investigations that used tissue sections of brains, where penetration of the antibody should not be problematic (Zhu *et al.*, 1993; Malpel *et al.*, 2002). These results however, do not offer a global view of NORPA expression because cryosections show just a portion of the brain without giving any tridimensional information and larval brains are not characterised by the full cluster of circadian clock neurons (reviewed from Picot *et al.*, 2009). In order to visualise precisely the circadian pacemakers, transgenic flies expressing LacZ in clock neurons (Shafer *et al.*, 2006) or PDF antibody were used. NORPA was not detected in circadian neurons (Figure 3.2 and 3.3). However, it appeared that the absence of signals was mostly due to the penetration inefficiency of the antibody because over-expressing NORPA in LN_vs cells did not reveal any signal (Figure 3.4 and 3.5, Appendix 1). On the other hand, NORPA signal was found at the superficial level of the brain and at the level of the arborisations of LN_vs in the medulla. This was not observed in the *norpA^{p41}* mutant (Figure 3.7) nor

using only the secondary antibody (Cy2, Figure 3.6), so it would appear to represent specific NORPA expression.

Larval brains were also subjected to NORPA, entraining individuals to different temperatures (18 and 25°C). Broader NORPA signal emerged at lower than higher temperature (Figure 3.9 and 3.10 at 18°C; Figure 3.8 at 25°C). At both temperatures, Bolwig Nerves were labelled by NORPA anti-serum (as expected, Malpel *et al.*, 2002). However, at low temperature, more cells were visible at the BN termini as well as a possible colocalisation of NORPA and a PDF⁺ cell (Figure 3.9). Moreover, in the dorsal region of the brain, two clusters of cells were positively marked by the NORPA antibody (Figure 3.10). Due to their location, these may putatively be DN2s and DN1s. Thus, these data suggest a higher level of NORPA expression at lower temperature. This is in contrast with western blot analysis where no differences in NORPA level were noted between control flies entrained at 18 or 29°C (section 4.3.2.1, Figure 4.6). However, the western blot may not be a sensitive method to assess small changes in cellular protein level regarding a few cells. Furthermore, analysis needs to be done in order to verify this possible difference in NORPA expression and colocalise its expression pattern in the DNs (e.g. colabeling with TIM antibody). It is clear that even overexpressing *norpa* in clock neurons *via PdfGAL4*, does not permit colocalisation of NORPA antibody with clock cells, so clearly the antibody has problems penetrating the inner brain in whole mounts (Figure 3.4 and 3.5).

For this reason, *in situ* hybridisation was used as an alternative method. The Helfrich-Förster protocol was inefficient (Yoshii *et al.*, 2008; Wülbeck and Helfrich-Förster, 2007), in the case of *norpa* as tracheal structures were mainly detected by using a single long probe (Figure 3.12). Therefore, shorter multiple probes were designed and background staining was profoundly decreased leading to the visualisation of neurons. The *norpa* mRNA was localised in a broad pattern in transgenic lines that express exogenous markers in the pacemaker cells such as GFP or LacZ (larval and adult brains, Figure 3.13 and 3.14-15, respectively).

In larval as well as adult brains *norpa* transcripts were located among the LN_vs (Figure 3.13 and 3.14). In particular, in adults the mRNA was detected in both s- and

l-LN_vs (Figure 3.14). Furthermore, the analysis of dorsal neurons in adult brains revealed the presence of *norpA* in these cluster (Figure 3.15). In larval brain, *norpA* signal in the DNs was only hypothesised since a proper marker which labelled these neurons was not used (Figure 3.13). At cellular level the *norpA* localisation appeared to be peculiar. Both markers used in these experiments were cytoplasmic, however in most of the cases, an overlapping signal was not found but included in the central part of the cells. The specificity of this labelling was tested with sense probes which were doubly concentrated. These controls confirmed the reliability of the α -sense probes showing weak and non specific signals. Thus, it is possible that *norpA*, at the transcription level, may be expressed and localised in specific cytoplasmic area of the cells. Nevertheless, the fact that *norpA* transcript has been localised in the circadian neurons is perfectly in agreement with the results describe in the following chapter in which its downregulation determines behavioural phenotypes (Chapter 4).

Finally, since *norpA* encodes for two alternative splicing isoforms (Appendix 1, Kim *et al.*, 1995), it was not possible to distinguish between them in these experiments. Therefore, it is also plausible that the LN_vs and DNs may possess different patterns of expression of these two *norpA* subtypes which may be involved in different signalling pathways.

3.5. Conclusions

- NORPA protein was not detected among the circadian clock neurons in adult brains possibly due to the penetration inefficiency of the antibody.
- In larval brain at low temperature (i.e. 18°C), a PDF⁺ cell and Dorsal Neurons were labelled by NORPA antibody.
- *norpA* mRNA, in larval and adult brains, was detected among LN_vs and Dorsal Neurons.

Chapter 4. RNA interference of *norpA*

norpA mRNA has been localised among the circadian neurons *via in situ* hybridisation (Chapter 3). In this chapter, *norpA* expression has been downregulated by RNAi. The aim was to clarify how the *norpA* KD in specific circadian pacemaker neurons could influence the locomotor behaviour in relation to the temperature.

4.1. Introduction

As mentioned before, *norpA*^{p41} null mutants have circadian implications. In this chapter I will describe the use of *norpA* RNA interference (Sharp, 1999) in order to tissue-specifically downregulate this gene. The RNAi phenomenon was described initially in *Caenorhabditis elegans* (Fire *et al.*, 1998), but has since been studied in many other organisms from plants to mammals. Thus, RNAi is likely to be a general feature for gene regulation and may be critical for many developmental and antiviral processes (Stanislawska & Olszewsky, 2005).

The interference process is reversible, since in the F₂ progeny from RNAi treated organisms, the normal phenotype is rescued. This is because RNAi is a type of post-transcriptional regulation, which does not act on the gene sequence, but only on the mRNA. Introduced into a cell, a double-stranded RNA of a transcript triggers specific degradation of a target mRNA, by activating an enzymatic apparatus, called Dicer, which recognises it. This enzymatic complex cuts the mRNA into small fragments of about 25 bp, called small interference RNA (siRNA; reviewed from Tijsterman and Plasterk, 2004 and shown in Figure 4.1). siRNAs are duplicated by RNA-dependent RNA polymerase in high copy numbers and these fragments bind to all copies of the endogenous RNA, forming other double-stranded structures, which are successively degraded. In this way, all the target mRNAs of a cell are destroyed, giving, in theory, a knock-out of the respective gene. This mechanism is highly conserved to prevent viral infections and to provide a fine-tuned gene expression (Stanislawska and Olszewsky, 2005).

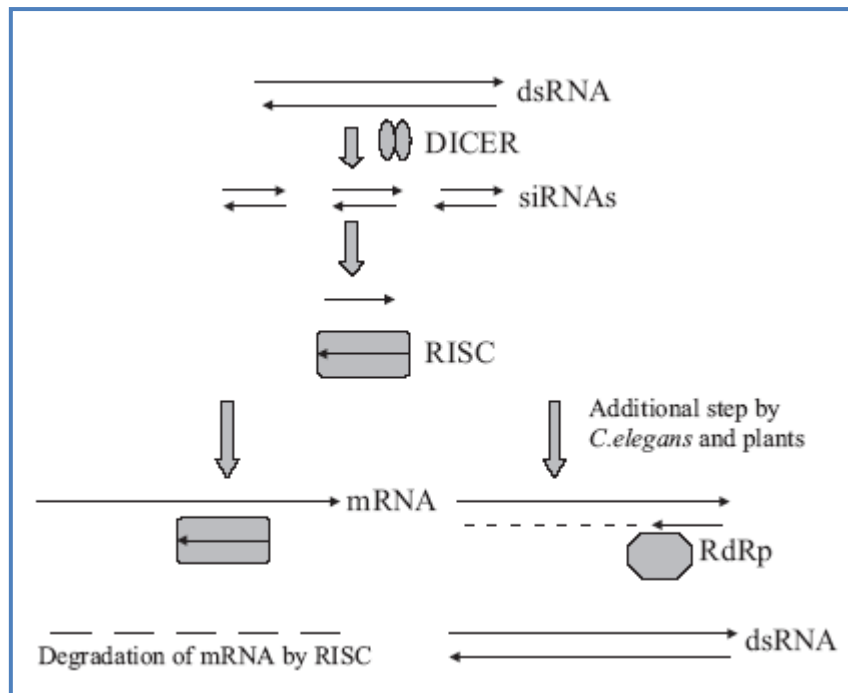


Figure 4.1: Schematic model of the RNAi mechanism. The cellular enzyme Dicer cleaves intracellularly synthesised or exogenously administered dsRNA into 21-25 nucleotide siRNAs. The siRNAs are incorporated into the RNA-induced silencing complex (RISC), which uses the antisense strand of the siRNA to find and destroy the target mRNA. The siRNAs can also be used as primers for the generation of new dsRNA by RNA-dependent RNA polymerase (RdRp). This step has only been found in plants and *C. elegans* (Stanislawska and Olszewsky, 2005).

The reversible feature of the RNAi phenomenon, are not heritable in a Mendelian fashion so, each individual is the result of direct manipulation, making the collection of large data sets extremely labour intensive (Piccin *et al.*, 2001). In *D. melanogaster*, an efficient alternative is the transcription from an integrated construct consisting of two inverted repeated sequences (IR) separated by a spacer. This type of construct generates the expression of an hairpin-loop shaped RNA that can trigger interference as a normal dsRNA (Piccin *et al.*, 2001). If this construct is associated with the *GAL4*-binding UAS (Upstream Activating Sequence [Brand and Perrimon, 1993]), it is possible to drive expression of the transgene under the control of specific promoters (Figure 4.2). This technique is efficient and heritable (Piccin *et al.*, 2001).

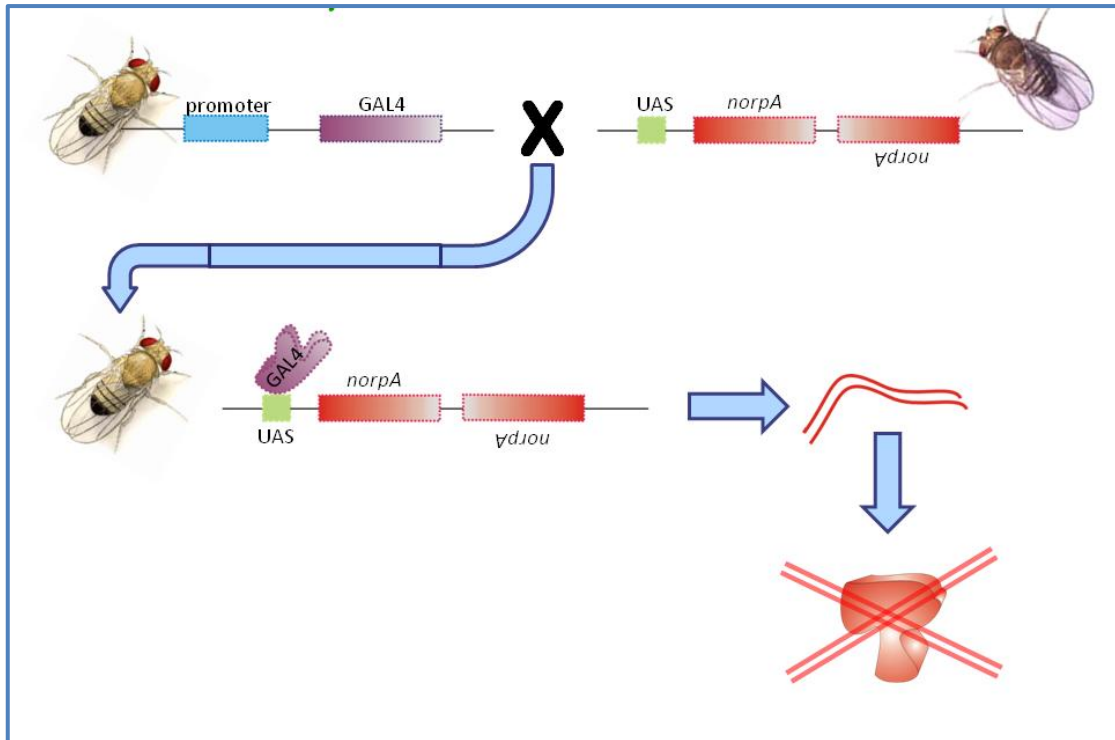


Figure 4.2: Principle of *GAL4/UAS* system. A first transgenic fly carrying a target cell or tissue specific gene promoter in front of the *GAL4* sequence is crossed to a second transgenic fly carrying a RNAi construct (inverted repeated sequences) downstream of Upstream Activating Sequence (UAS). The progeny of this cross possesses both *GAL4* and UAS elements. In the cells where the promoter is active, it drives the expression of *GAL4*, which binds to the UAS sequences and activates the expression of double strand of RNA.

In order to increase the efficiency of the RNAi mechanism in *D. melanogaster*, a construct containing a portion of genomic DNA and a cDNA fragment in the opposite orientation separated by an extra genomic fragment without using an exogenous spacer, guarantees a strong signal for the interference mechanism (Kalidas and Smith, 2002).

In this chapter, the strategy adopted for the generation of *D. melanogaster norpA* RNAi strains is presented in addition to the results obtained on the level of their downregulation and their locomotor activity profiles. Furthermore, Dietzl and co-workers generated a genome-wide library of *Drosophila* transgenic UAS-RNAi strains rendering it publically available (Dietzl *et al.*, 2007, VDRC stock center). The behaviour of the VRDC *norpA* RNAi line was also tested.

4.2. Materials and Methods

4.2.1. *norpA* RNAi VDRC lines

A single line that generates RNA interference of *norpA* was obtained from the VDRC (Vienna Drosophila RNAi Center, code 21490). This strain carries the transgenic insertion on the third chromosome but it is also associated with an off-target (*frazzled, fra*). Transgenic flies that trigger *fra* RNAi were also ordered and obtained from VDRC (code: 29909 and 29910).

4.2.2. Cloning strategy to generate “our” *norpA* silencing lines

Before the VDRC lines were available, *norpA* RNAi transgenic lines were generated in our laboratory. In Figure 4.3 are shown the steps adopted for obtaining several *norpA* RNAi transgenic strains.

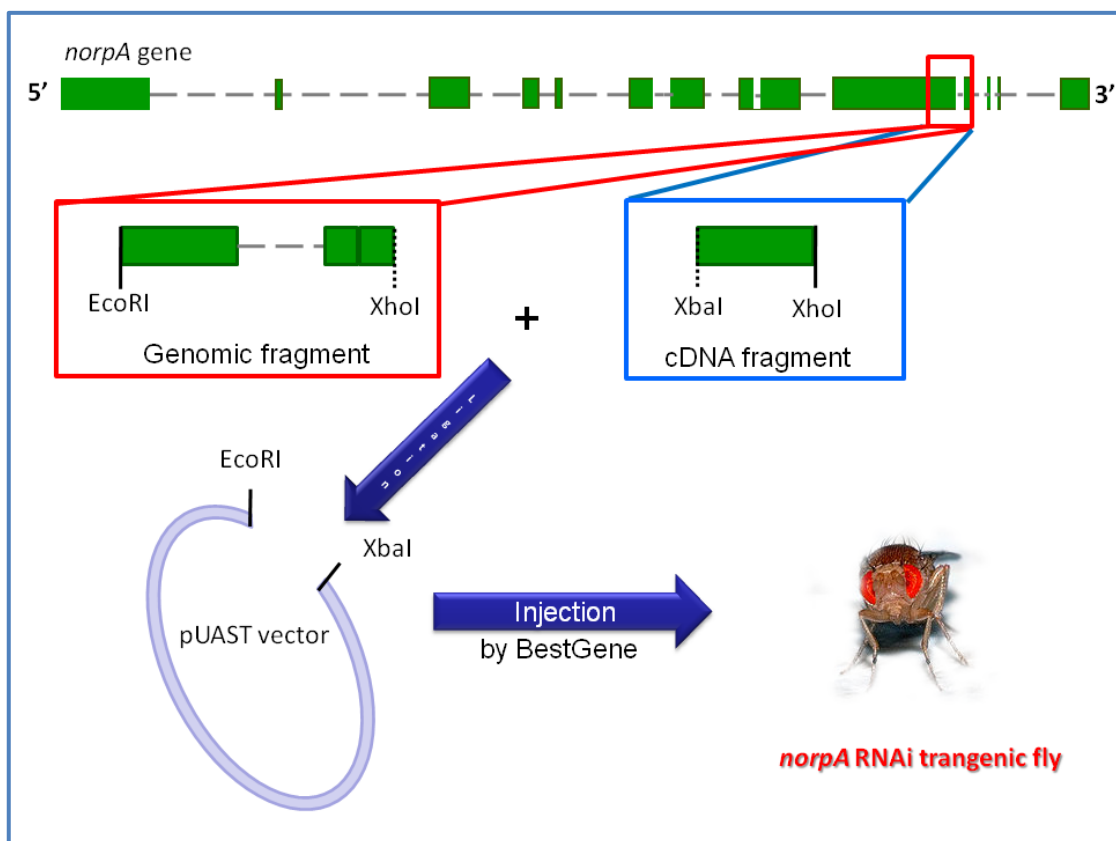


Figure 4.3: Schematic representation of molecular steps followed for creating *norpA* RNAi flies.

The region chosen as a template for obtaining the genomic and cDNA fragments was inserted in a specific vector that allows transformation in w^{1118} *Drosophila* strain using a specific set of restriction enzymes (Figure 4.3). Eight independent lines, which

differ for the position of the insertion, were generated and tested. The rescue of red eyes phenotype in the transgenic flies indicated the presence and insertion of the construct. Molecularly, this latter aspect can also be checked by PCR primers that recognise specifically the transgene and not the endogenous *norpA* gene.

4.3. Results

4.3.1. Testing the silencing level in *norpA* RNAi flies

To check the level of the downregulation of NORPA in *our* and VDRC transgenic flies, western blots were performed. Flies were entrained at 29°C for 3 days in LD 12:12 and collected in the middle of the photophase (ZT 6). The high temperature was chosen in order to stimulate as much as possible the expression of *GAL4* (Brand and Perrimon, 1993; Duffy, 2002). Male drivers ($w; +; \frac{actinGAL4}{TM6b}$) were crossed to virgin females carrying the RNAi construct ($w; +; \frac{UASnorpARNAi}{UASnorpARNAi}$). As controls both driver and UAS strains were crossed to w^{1118} flies (Rosato and Kyriacou, 2006; Figure 4.4). Figure 4.5 shows an example of western blot obtained using NORPA antibody and the level of downregulation of NORPA in relation to HSP70 (an housekeeping protein used as internal and loading control), in wild-type flies (i.e. Canton-S), null mutants ($norpA^{p41}$) and interfered flies ($w; +; \frac{actinGAL4}{norpARNAi}$). The data shown are obtained from a single collection.



Figure 4.4: Crossing scheme adopted to generate flies that possess the *norpA* RNAi construct activated by *actinGAL4* and the controls for both the driver and the UAS construct. The colours for each cross are the same used in all the figures of the chapter.

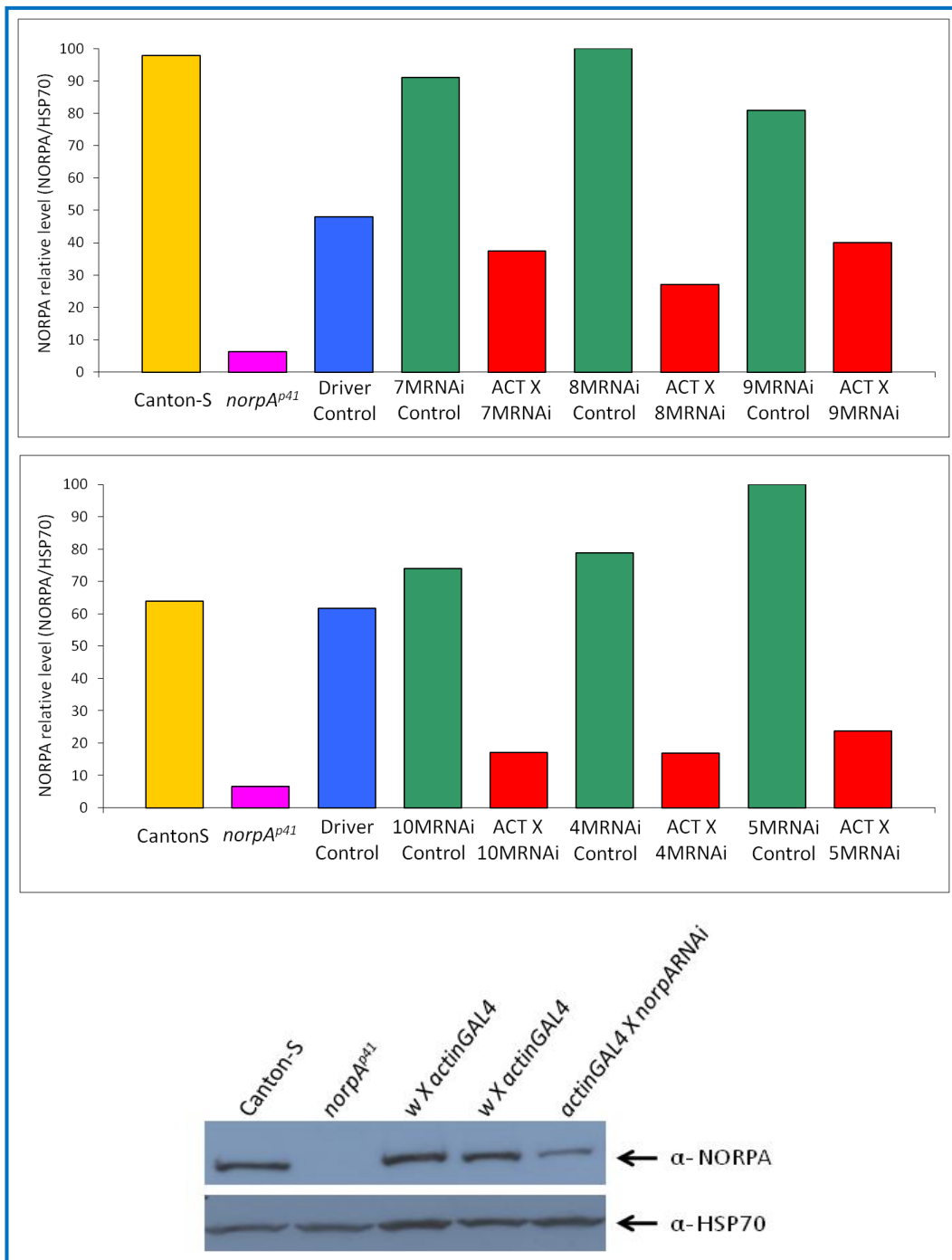


Figure 4.5: Relative level of NORPA in wild-type flies, null mutants, several independent RNAi genotypes and relevant controls. NORPA level was quantified in relation to HSP70. In the lower picture a western blot film probed with α -NORPA and α -HSP70 is shown.

Levels of NORPA in the experimental genotypes compared to both controls are given in Table 4.1.

Genotype	Reduction (%) NORPA compared to control	
	w X <i>actinGAL4</i> Driver Control	w X <i>UASnorpARNai</i> UAS Control
<i>actinGAL4 X 4M</i>	45	62
<i>actinGAL4 X 5M</i>	38	76
<i>actinGAL4 X 7M</i>	11	54
<i>actinGAL4 X 8M</i>	21	73
<i>actinGAL4 X 9M</i>	8	41
<i>actinGAL4 X 10M</i>	45	57

Table 4.1: Percentage of NORPA downregulation in interfered flies compared to their relative controls.

In order to evaluate the efficiency of silencing generated by VDRC transgenic line, NORPA levels were again analysed by western blots (Figure 4.6). The *norpA* KD was driven ubiquitously by *actinGAL4*. The level of NORPA was evaluated in experimental and control flies entrained in LD 12:12 at 12, 18 and 29°C.

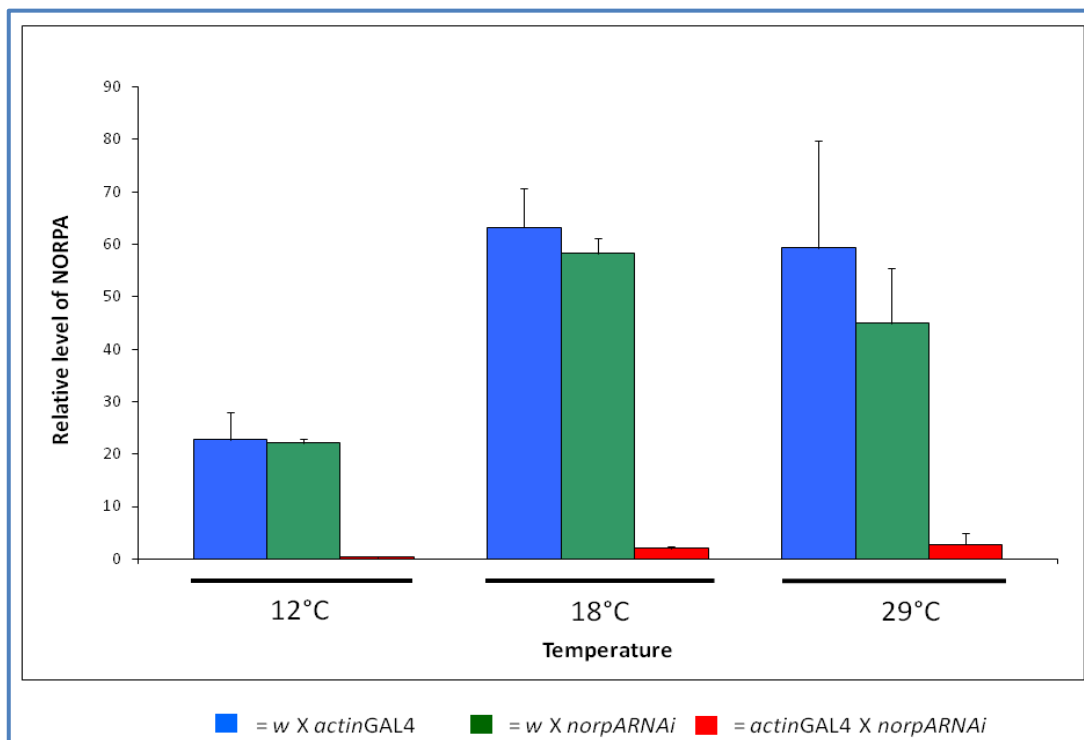


Figure 4.6: Relative amount of NORPA in interfered flies and controls at 12, 18 and 29°C in LD regime (N=3). Bars indicate SEM. Intensity of bands have been analysed for each gel separately and results have been pooled in order to normalise all data together within the three different temperatures.

Statistical analysis (ANOVA) revealed significant Genotype and Temperature effects ($F_{2,24} = 27.50$, $p \ll 0.001$; $F_{2,24} = 8.15$, $p \ll 0.05$, respectively). The level of

NORPA in knocked-down flies was high in all cases compared to controls (Figure 4.6, Appendix 2.1) revealing a higher efficiency of this VDRC line than the ones generated in our laboratory. For this reason, all the experiments and results presented in this chapter refer to VDRC transgenic line.

4.3.2. Behaviour analysis

4.3.2.1. *actinGAL4* driver: *norpA* downregulation in whole *Drosophila*

The transgenic flies downregulating *norpA* via *actinGAL4* driver were used for further experiments in which locomotor activity profiles were tested at low (18°C) and high (29°C) temperatures in 12:12 LD regime for 6 days. In these conditions, the locomotor activity pattern of each genotype and each day was superimposed for the entire length of the experiment in order to obtain an averaged actogram (Figure 4.7). Furthermore, the morning and evening onsets and offsets were determined for each individual evaluating the bin number in which a fly started to increase or decrease its activity in relation to the light transitions (Materials and Methods, Section 2.18).

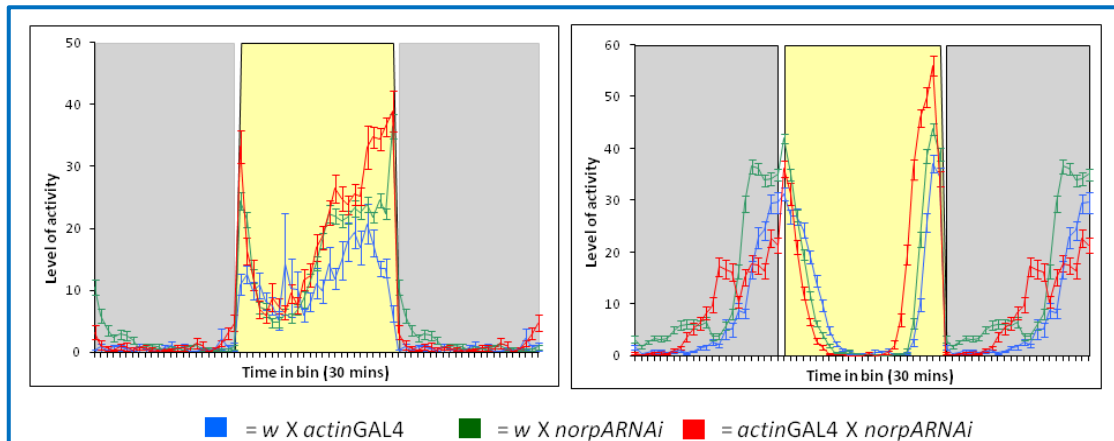


Figure 4.7: Averaged locomotor profiles (\pm SEM) of *norpA* silencing using *actinGAL4* driver and controls at 18°C (left panel) and 29°C (right panel) in LD.

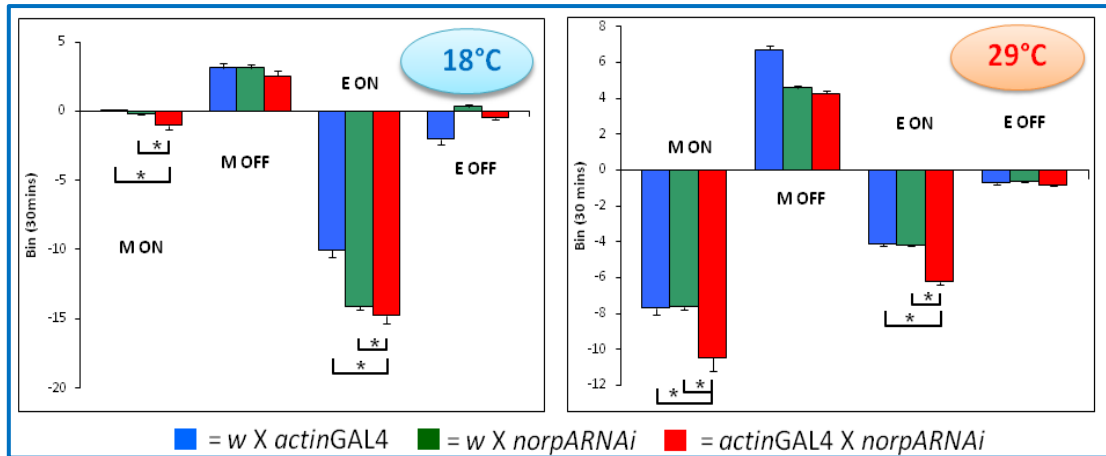


Figure 4.8: Averaged morning and evening onsets and offsets of transgenic flies in which *norpA* was silenced by *actinGAL4* and relevant controls at 18 (left) and 29°C (right graph). Asterisks indicate significant values.

Genotype	18°C					29°C				
	N	Morning onset	Morning offset	Evening onset	Evening offset	N	Morning onset	Morning offset	Evening onset	Evening offset
<i>w X actinGAL4</i>	1 4	0.01	1.56	-5.02	-1.02	2 6	-3.85	3.35	-2.05	-0.25
<i>w X norpARNAi</i>	3 0	-0.08	1.56	-7.05	0.16	4 5	-3.82	2.28	-2.09	-0.32
<i>actinGAL4 X norpARNAi</i>	1 3	-0.52	1.28	-7.38	-0.24	2 2	-5.23	2.12	-3.12	-0.44

Table 4.2: Morning and evening onsets and offsets of *norpA* interfered flies and controls (expressed in h) related to light off/on transition and *vice versa*. 0 represents the light transition therefore negative values indicate locomotor activity starting before this event. Significant values are highlighted.

Figure 4.8 shows that the morning onset was advanced compared to both transgenic controls at 18°C as well as 29°C ($F_{2,54} = 12.2$, $p < 0.001$; $F_{2,90} = 7.63$, $p < 0.001$; respectively). Moreover, the evening onsets also displayed an advance ($F_{2,54} = 32.64$, $p < 0.001$; $F_{2,90} = 40.89$, $p < 0.001$; respectively). Morning and evening offsets in experimental flies were not significantly different to controls (Table 4.2). Thus ubiquitous *norpA* KD generates an advance of the morning and evening components, in agreement with results observed in *norpA^{p41}* (Collins *et al.*, 2004).

The free running periods of locomotor activity of these genotypes were also analysed in continuous darkness for six days (DD) at two temperatures but no significant differences were observed since experimental lines displayed intermediate values (Table 4.3).

Genotype	18°C		29°C	
	Period ± SEM	N	Period ± SEM	N
<i>w X actinGAL4</i>	24.02 ± 0.25	10	23.93 ± 0.30	10
<i>w X norpARNAi</i>	23.28 ± 0.12	30	23.13 ± 0.09	30
<i>actinGAL4 X norpARNAi</i>	23.87 ± 0.12	14	23.15 ± 0.17	14

Table 4.3: Free running locomotor activity rhythms for *norpA* RNAi and control genotypes at 18°C and 29°C. The endogenous periods were determined by Autocorrelation .

Interestingly, analysing the behaviour profile of experimental flies in DD at 29°C, it was observed a reduction of the early subjective morning peak of activity compared to controls. These latter appeared to adapt to the hot conditions advancing this surge of activity in the middle of the night, whereas *norpA* KD individuals lose it after a few days (arrows in Figure 2.1.1 and 2.1.2, Appendix 2.1).

4.3.2.2. *norpA* off-targeting: *frazzled* gene

The VDRC *norpA* RNAi has an off-target sequence in the *CG8581* gene named *frazzled* (*fra*) which is reported to be involved in several biological processes such as motor axon guidance and axon midline choice point recognition (Hiramoto *et al.*, 2000).

The aim of this section is to reveal the specificity of *norpA* RNAi construct by investigating the circadian behaviour of *frazzled* RNAi transgenic flies. Thus, I tried to address the question if the effects observed above on behaviour are due in part to *fra* KD. Five independent UAS*fra* RNAi strains were crossed to *actinGAL4* but none of the offspring in which the interfered construct was active shown any level of survival. The KD of FRA was lethal at the pupal stage whereas the controls (RNAi constructs or driver) showed a normal level of survival. This indicates that the behavioural effects found by *norpA* KD are not depending by the off-target in *fra*.

4.3.2.3. *ninaEGMRGAL4* driver: *norpA* silencing in photoreceptor cells

Since NORPA is mainly expressed in phototransduction structures such as the retina (Bloomquist *et al.*, 1988), its KD was next triggered by the *ninaEGMRGAL4* driver (hereafter named *gmrGAL4*). This driver is commonly used for the expression of transgenes in the developing eyes (Freeman, 1996). Initially, the level of NORPA

downregulation of interfered line (*w; gmrGAL4/+; norpARNAi/+*) was investigated comparing it against controls: driver (*w; gmrGAL4/+; +*) and RNAi construct (*w; +; norpARNAi/+*) by western blot. These strains were entrained for 3 days to 12:12 LD at 29°C and protein were extracted from heads after being collected in the middle of the photophase (\approx ZT6). Figure 4.9 shows the level of NORPA in these strains.

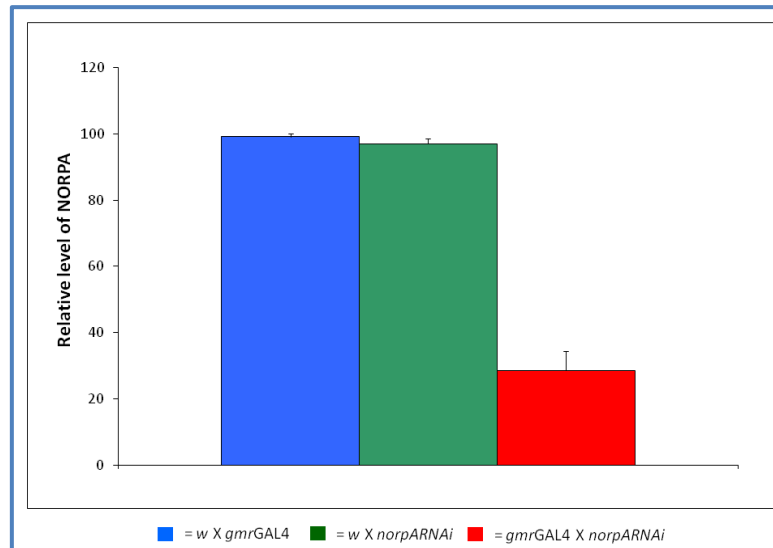


Figure 4.9: Downregulation level of NORPA (\pm SEM, N = 4) by *gmrGAL4*.

The RNA interference of *norpA* by *gmrGAL4* driver generates a significant reduction of the NORPA of about 70 % ($F_{2,9} = 137.5$ and $p \ll 0.001$). However, a significant difference exists between the *norpA* KD triggered by *actin* and *gmr* drivers ($p \ll 0.001$). This indicates that structures outside photoreceptor cells but within the *Drosophila* heads express NORPA in agreement with data published by Zhu and co-workers (Zhu *et al.*, 1993).

The locomotor activity of these flies was monitored in LD 12:12 at 18 and 29°C (Figure 4.10).

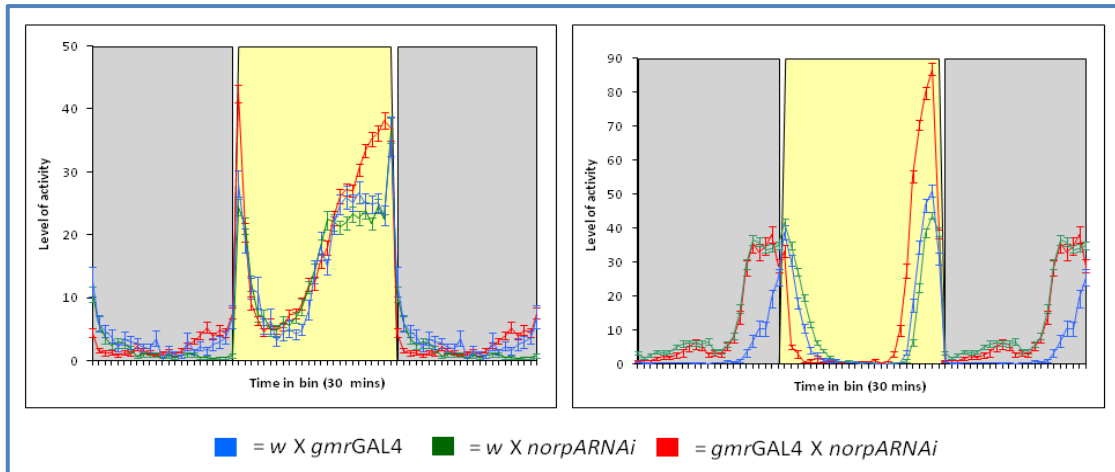


Figure 4.10: Averaged locomotor activity profiles (\pm SEM) of *norpA* silencing triggered by *gmrGAL4* driver and relative controls at 18°C (left panel) and 29°C (right panel).

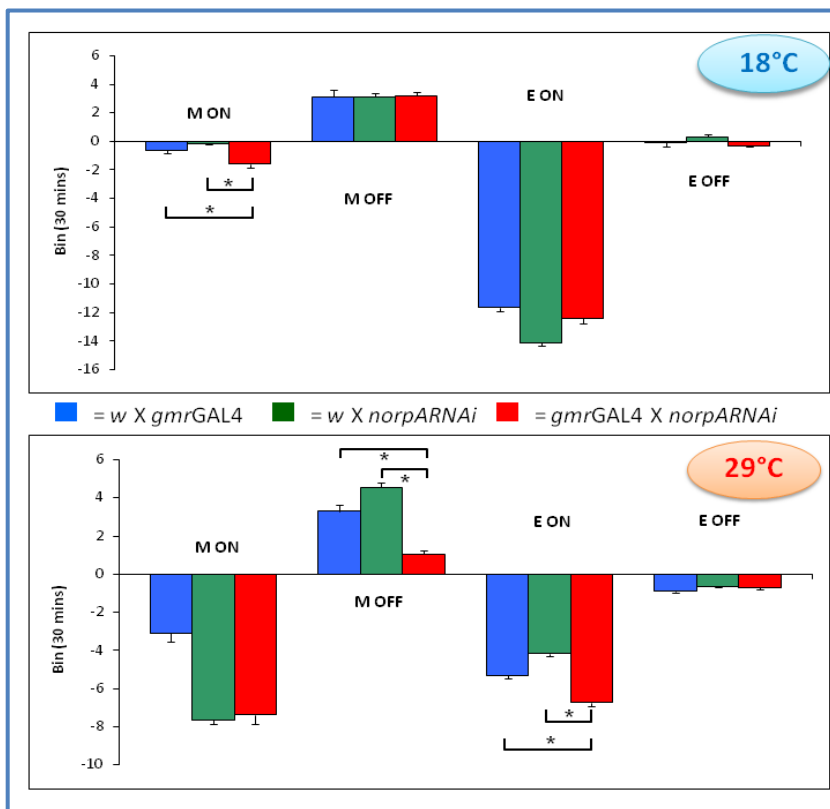


Figure 4.11: Averaged morning and evening onsets and offsets of *gmrGAL4* UAS*norpA* RNAi and controls at 18°C and 29°C in LD 12:12. Asterisks indicate significant values.

Genotype	18°C					29°C				
	N	Morning onset	Morning offset	Evening onset	Evening offset	N	Morning onset	Morning offset	Evening onset	Evening offset
<i>w X gmrGAL4</i>	16	-0.31	1.56	-5.82	-0.03	14	-1.55	1.64	-2.65	-0.45
<i>w X norpARNAi</i>	30	-0.08	1.56	-7.05	0.16	45	-3.82	2.28	-2.09	-0.32
<i>gmrGAL4 X norpARNAi</i>	31	-0.80	1.59	-6.20	-0.15	29	-3.69	0.53	-3.37	-0.35

Table 4.3: Morning and evening onsets and offsets obtained from flies silencing *norpA* in photoreceptor cells by *gmrGAL4* driver and controls (in h). Significant values are highlighted.

At low temperature (18°C) the morning onset was the only component affected in *norpA* RNAi ($F_{2,74} = 20.31$, $p \ll 0.001$) presenting an advance in its upswing compared to controls (Figure 4.11 and Table 4.3). At high temperature, the offset of the morning activity as well as the evening onset produced significant advances compared to controls ($F_{2,85} = 55.11$, $p \ll 0.001$; $F_{2,85} = 83.12$, $p \ll 0.001$; respectively).

The period length in DD for six days was also investigated but no significant differences among lines at either temperature were observed due to the fact that KD flies displayed intermediate periods compared the controls.

4.3.2.4. Pan-neuronal *elavGAL4* driver

norpA was then KD pan-neuronally with *elavGAL4* (Luo *et al.*, 1994; Soller and White, 2004). Due to the genomic location of the driver on the X chromosome, driver females were crossed to RNAi males (*elavGAL4*; +; *norpARNAi*). The same direction of cross was applied to the controls. NORPA levels in heads revealed a highly significant downregulation in RNAi flies ($F_{2,6} = 51.75$, $p < 0.001$; Figure 4.12).

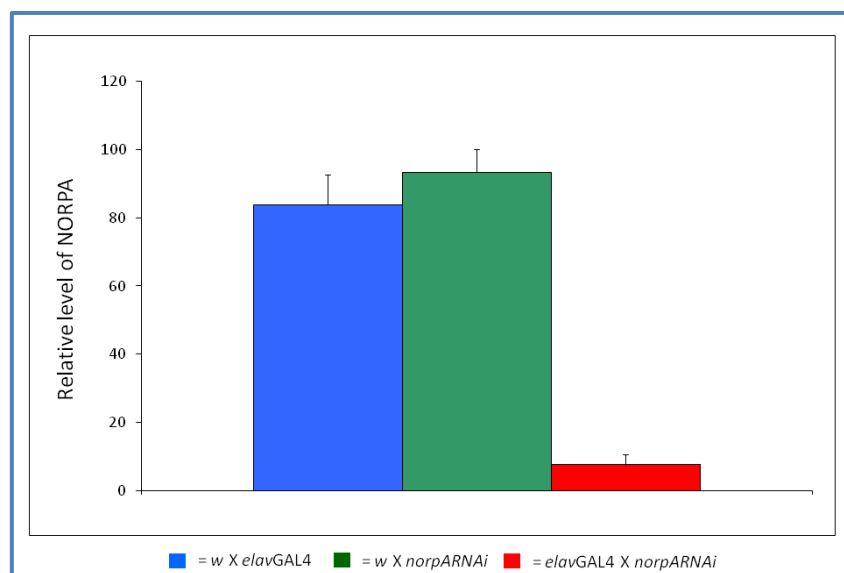


Figure 4.12: Percentage of NORPA downregulation (\pm SEM, N = 3) generated by *elavGAL4* driver and controls.

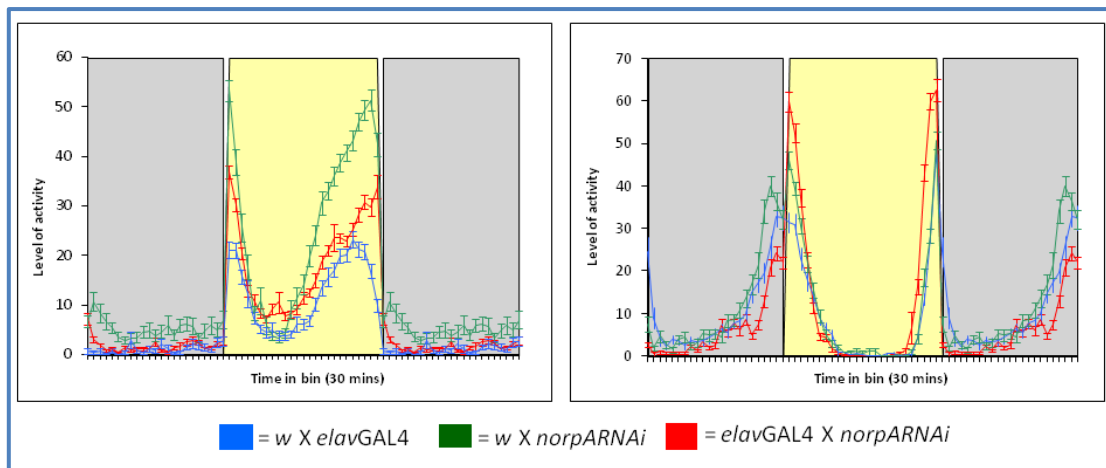


Figure 4.13: Averaged locomotor activity of *elavGAL4*; *norpARNAi* flies and controls in LD 12:12 at 18°C (left panel) and 29°C (right panel).

Behaviourally, the characteristic that distinguishes *norpa* RNAi from controls at both temperatures was the upswing of the evening locomotor activity. In both cases this was advanced when compared to driver and RNAi control strains ($F_{2,59} = 10.56$, $p \ll 0.001$ at 18°C; $F_{2,53} = 8.27$, $p \ll 0.001$ at 29°C). Other components such as the morning onset were affected only at high temperature (delayed compared to control, $F_{2,53} = 6.41$, $p \ll 0.001$). Finally, morning and evening offsets were not influenced by the NORPA KD neither at 18°C nor 29°C (Figure 4.14 and Table 4.4).

Genotype	18°C					29°C				
	N	Morning onset	Morning offset	Evening onset	Evening offset	N	Morning onset	Morning offset	Evening onset	Evening offset
<i>w X elavGAL4</i>	15	-0.21	1.98	-5.80	-0.64	14	-2.85	2.13	-1.65	0.16
<i>w X norpARNAi</i>	15	-0.49	1.85	-6.21	0.41	12	-3.11	2.33	-1.57	-0.15
<i>elavGAL4 X norpARNAi</i>	32	-0.30	2.03	-7.04	-0.28	30	-2.29	2.02	-1.97	-0.31

Table 4.4: Averaged phases (in h) of *norpa* interference driven by *elavGAL4* and controls at 18°C and 29°C. Significant effects highlighted in yellow.

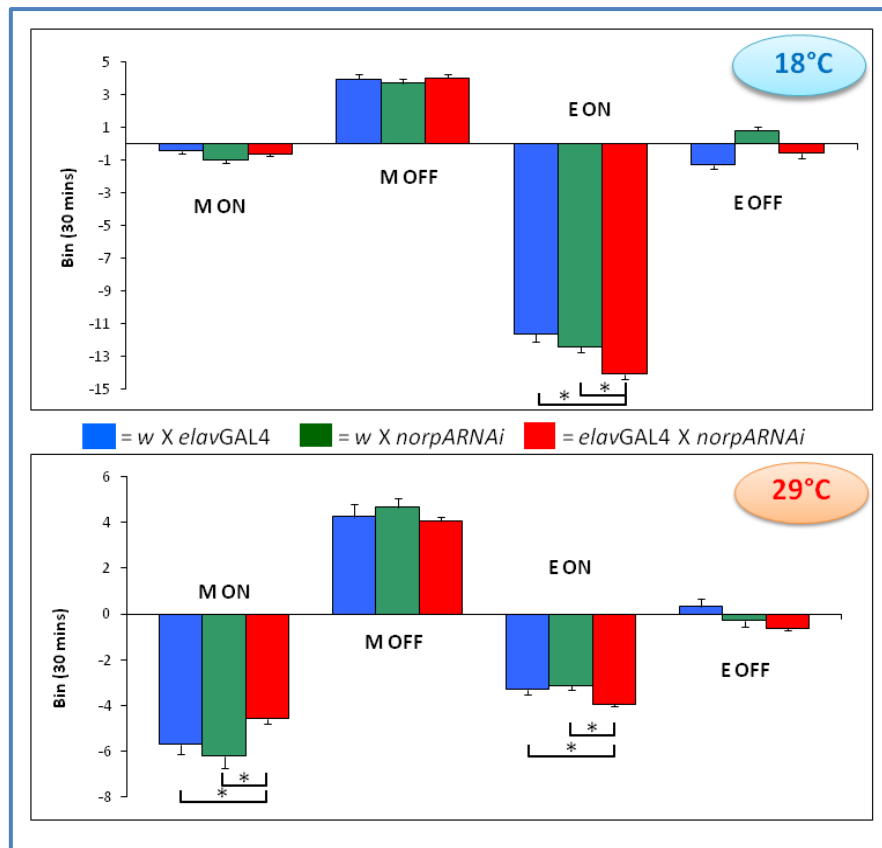


Figure 4.14: Averaged morning and evening onsets and offsets (± SEM) for *elavGAL4 norpA RNAi* and controls at 18 and 29°C. Asterisks indicate significant values.

The rhythmicity of interfered flies and controls was tested in DD regimes at 18°C and 29°C for 6 days and again no significant difference were found.

4.3.2.5. *timGAL4* driver: *norpA* silencing in circadian cells

In order to dissect a possible role of *norpA* in the circadian mechanism and structures, *timGAL4* was utilised, which drives UAS expression in about 150 circadian cells which are responsible for the circadian behaviour (Helfrich-Foster, 2003). Thus, lateral and dorsal neurons as well as photoreceptor cells can be manipulated with this driver. The effect of *norpA* KD mediated in these cells was firstly assessed by western blots and successively by behavioural activity essays. As for the experiments described before, interfered flies (*w; timGAL4/+; norpARNAi/+*) were compared to controls: the driver (*w; timGAL4/+; +*) and the RNAi control (*w; +; norpARNAi/+*). These lines were raised at 29°C in 12:12 LD and three days old individuals were collected for extracting proteins from their heads.

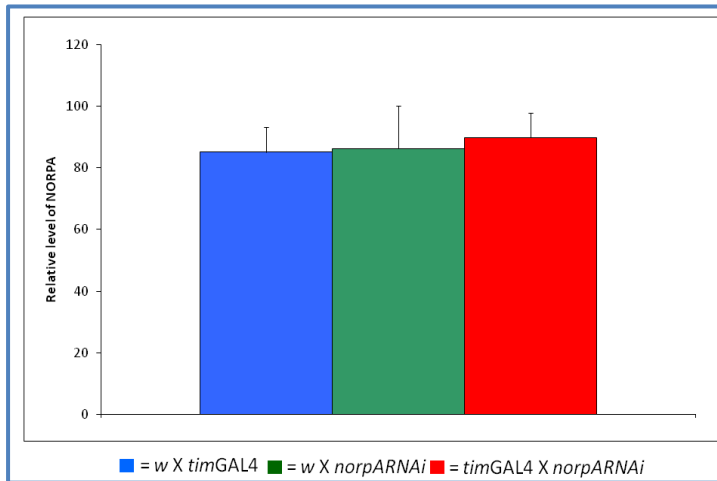


Figure 4.15: Analysis by western blot of NORPA level (\pm SEM) in *timGAL4 norpA* RNAi and controls. N = 3.

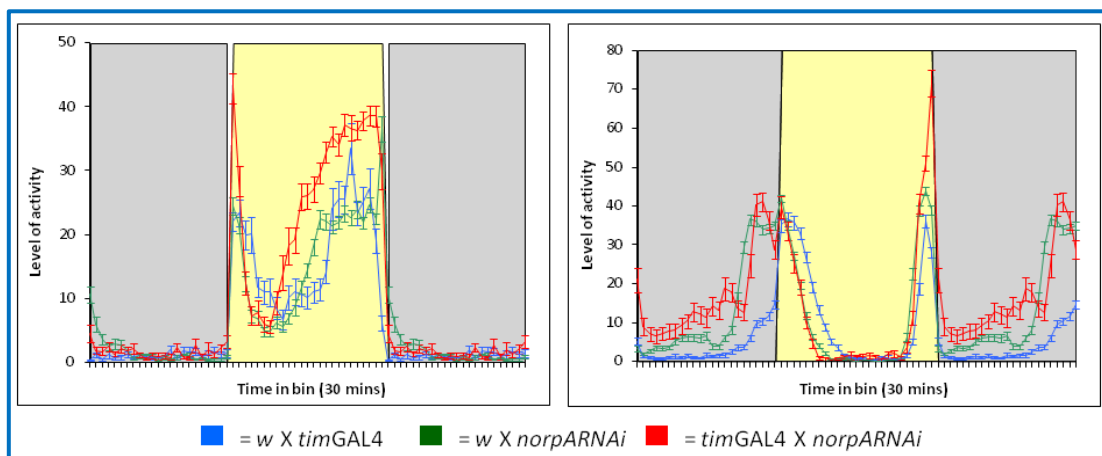


Figure 4.16: Averaged activity profiles for *norpA* silenced in circadian neurons and controls subjected to 12:12 LD cycles for 6 days at 18°C (left panel) and 29°C (right panel).

As *norpA* downregulated is very restricted in *timGAL4* cells, it was not surprising that downregulation did not give an overall reduction in NORPA expression in heads ($F_{2,6} = 0.57$, $p = n.s.$; Figure 4.15). At low temperature, the morning upswing was the only component influenced by *norpA* KD which was advanced in interfered flies ($F_{2,85} = 6.70$, $p < 0.001$; Figure 4.17 and Table 4.5). At 29°C, the evening offset of interfered flies was delayed compared to controls ($F_{2,72} = 22.56$, $p < 0.001$).

Genotype	18°C					29°C				
	N	Morning onset	Morning offset	Evening onset	Evening offset	N	Morning onset	Morning offset	Evening onset	Evening offset
<i>w X timGAL4</i>	43	-0.15	1.89	-4.77	-1.31	45	-1.27	2.86	-1.22	-0.13
<i>w X norpARNAi</i>	30	-0.08	1.56	-7.05	0.16	45	-3.82	2.28	-2.09	-0.32
<i>timGAL4 X norpARNAi</i>	15	-0.45	1.55	-7.45	-0.19	15	-3.15	1.86	-2.09	0.31

Table 4.5: Averaged phases (in h) of *norpA* silencing driven by *timGAL4* and controls at 18°C and 29°C. Significant values are highlighted.

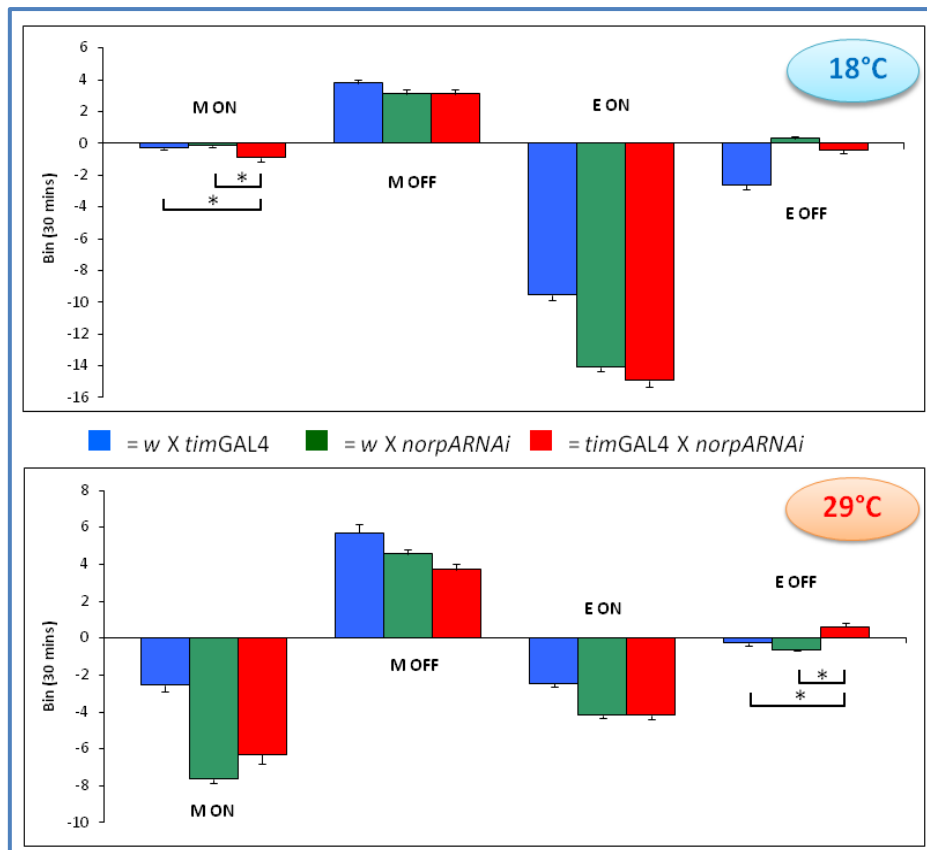


Figure 4.17: Averaged morning and evening onsets and offsets of *timGAL4norpA RNAi* and controls at 18 and 29°C. Asterisks indicate significant values.

The effect of *norpA* downregulation in *timeless* cells was also investigated in DD (Table 4.6). Although at high temperature the interfered line displayed a slightly longer period, this did not result significant by *a posteriori* comparison (Appendix 2.1).

Genotype	DD at 18°C		DD at 29°C	
	Period ± SEM	N	Period ± SEM	N
<i>w X timGAL4</i>	24.34 ± 0.34	18	23.43 ± 0.14	35
<i>w X norpARNAi</i>	23.28 ± 0.12	30	23.13 ± 0.09	30
<i>timGAL4 X norpARNAi</i>	24.17 ± 0.28	12	23.93 ± 0.11	13

Table 4.6: Averaged periods (± SEM) of flies downregulating *norpA* in circadian cells and controls. Periods obtained at 18 and 29°C in DD are shown.

The western blot experiments showed that the downregulation of *norpA* mediated by *timGAL4* driver was not detectable, even though photoreceptor cells express *tim* and these contribute about 1500 neurons (plus 150 clock cells; Kaneko and Hall, 2000). Perhaps *tim* is also not as strong a driver as *actin* and *gmr* at least in the eyes which are the main source of head extracted proteins. I therefore combined

timGAL4 to *UASdicer2* in order to enhance the RNAi mechanism (Dietzl *et al.*, 2007) and evaluated NORPA downregulation using western blots (*w; timGAL4UASdicer2/+; norpARNAi/+* versus driver control *w; timGAL4UASdicer2/+; +* and RNAi construct controls *w; +; norpARNAi/+*; Figure 4.18). As in the case of the results obtained without the co-expression of DICER2, NORPA did not show any significant decrease in its expression ($F_{2,12} = 0.67$, $p = \text{n.s.}$).

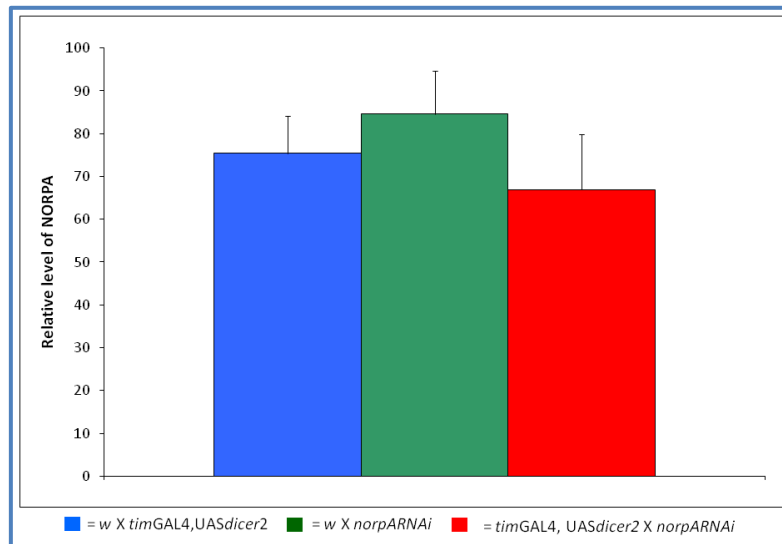


Figure 4.18: Averaged NORPA level in *w; timGAL4UASdicer2/+; norpARNAi/+* flies and controls. N = 3.

In a second set of experiments, the *norpa* RNAi lines generated in our laboratory were tested. In this experiment, the locomotor activity of line 4M, 5M, and 9M was monitored in LD 12:12 at 29°C.

Figure 4.19 reveals a bimodal locomotor activity characterised by a morning peak at “lights on” and an evening peak component at the on/off transition. The activity profile of silencing lines (*timGAL4 X norpARNAi*) was compared to lines carrying a single copy of the driver and the RNAi construct in a *w¹¹¹⁸* genetic background. The “expressing” lines presented an intermediate behaviour profile compared to controls. None of the activity components, such as morning and evening onsets and offsets, were affected by the absence of NORPA in *tim* cells.

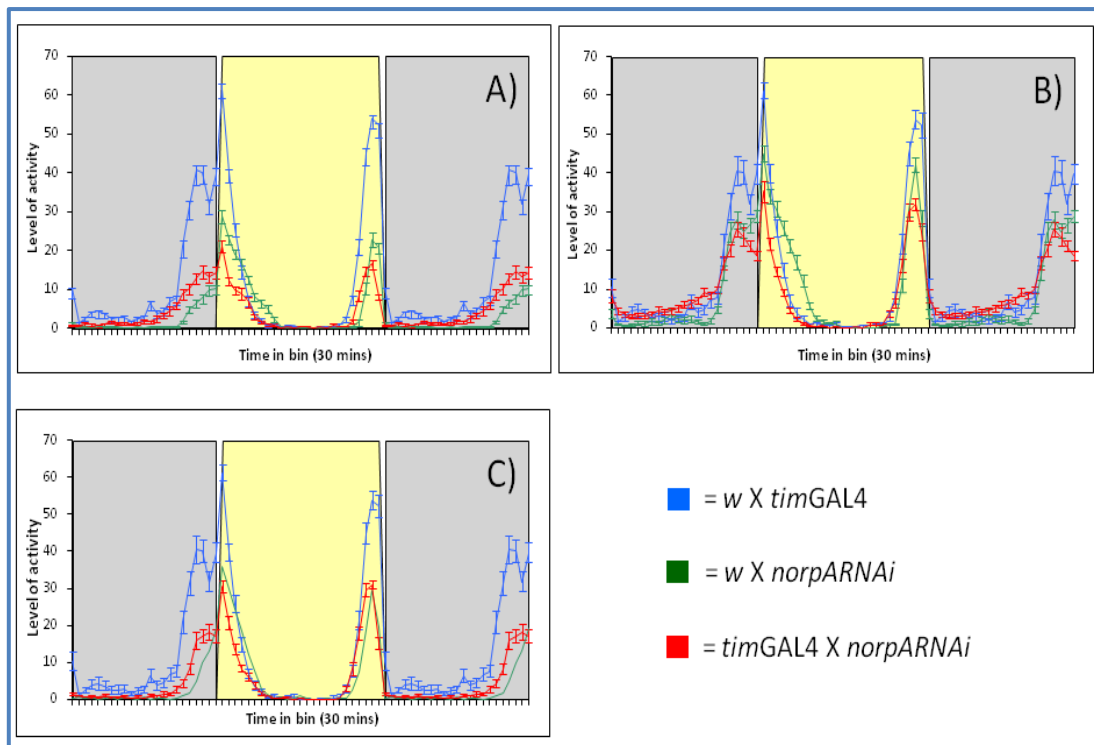


Figure 4.19: Locomotor activity profiles of flies (4M, 5M and 9M) expressing the UAS-*norpA* RNAi triggered by *timGAL4* and compared to controls in LD 12:12 at 29°C.

4.3.2.6. *pdfGAL4* driver: *norpA* silencing in morning cells

The KD of *norpA* using the *tim* promoter gives a global downregulation in all circadian cells. However, the *PdfGAL4* driver expresses only in the ‘morning cells’ (s-LN_vs and l-LN_vs; Park and Hall, 1998; [Section 1.5]). In particular, the s-LN_vs drive circadian rhythms in DD (Grima *et al.*, 2004). The importance of PDF in the circadian clock is supported by null mutants (i.e. *Pdf⁰¹*) which are characterised by the absence of the morning peak of activity in LD regimes (Grima *et al.*, 2004) and lack of the rhythmicity in DD (Renn *et al.*, 1999).

The locomotor pattern of flies in which *norpA* was downregulated in the LN_vs (*w*; *PdfGAL4/+*; *norpARNAi/+*) was compared to driver (*w*; *PdfGAL4/+*; +) and RNAi (*w*; +; *norpARNAi/+*) controls. These individuals were tested in the usual way (Figure 4.20).

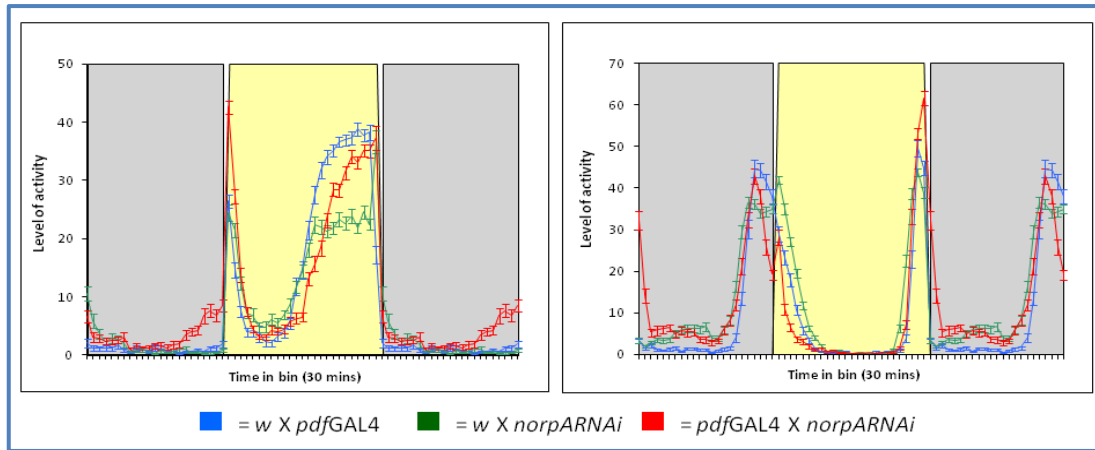


Figure 4.20: Averaged locomotor activity profiles of flies in which *norpA* was silenced in the M cells (via *PdfGAL4* driver) and controls at 18°C (left panel) and 29°C (right panel).

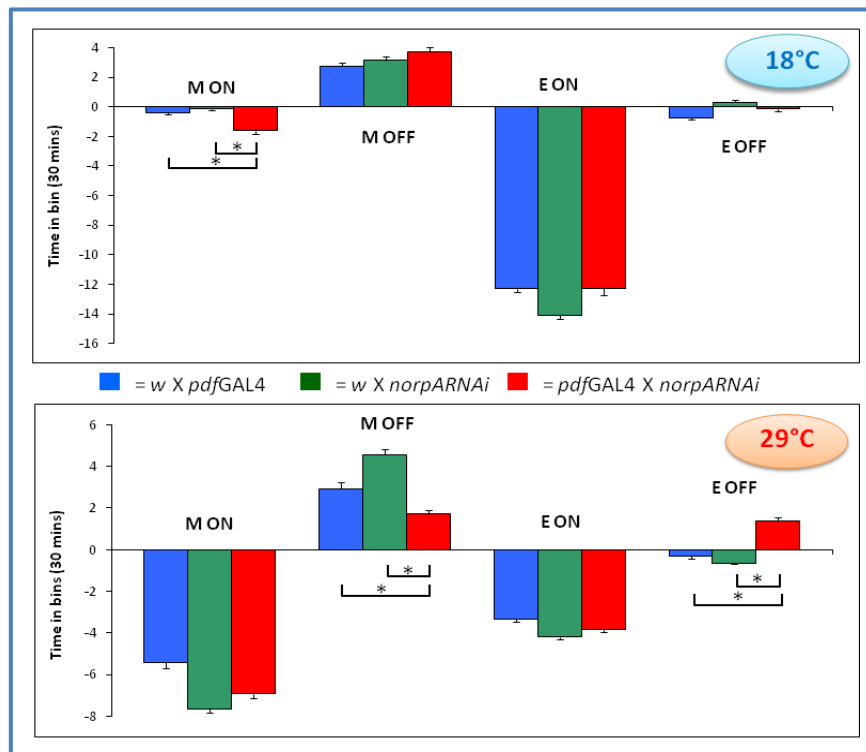


Figure 4.21: Averaged phases of *w*; *pdfGAL4/+*; *norpARNAi/+* and controls at 18 and 29°C. Asterisks indicate significant values.

Genotype	18°C					29°C				
	N	Morning onset	Morning offset	Evening onset	Evening offset	N	Morning onset	Morning offset	Evening onset	Evening offset
<i>w X pdfGAL4</i>	29	-0.20	1.38	-6.15	-0.38	31	-2.71	1.47	-1.66	-0.15
<i>w X norpARNAi</i>	30	-0.08	1.56	-7.05	0.16	45	-3.82	2.28	-2.09	-0.32
<i>pdfGAL4 X norpARNAi</i>	31	-0.81	1.86	-6.14	-0.06	28	-3.46	0.86	-1.91	0.68

Table 4.7: Averaged phases at 18 and 29°C for the morning and evening onsets and offsets determined in PDF *norpA* downregulating flies and relevant controls. Significant values are highlighted.

At 18°C, the morning onset was the only activity component that significantly different between controls and experimental flies. Its upswing was dramatically advanced in the interfered flies ($F_{2,87} = 29.37$, $p \ll 0.001$; Figure 4.21 and Table 4.7). At 29°C, the offset of the morning and evening activity components were affected. The morning offset of *norpA* KD flies was advanced compared to controls ($F_{2,101} = 31.81$, $p \ll 0.001$), while the evening offset was delayed ($F_{2,101} = 59.44$, $p \ll 0.001$).

Genotypes	DD at 18°C		DD at 29°C	
	Period ± SEM	N	Period ± SEM	N
<i>w X pdfGAL4</i>	23.61 ± 0.11	41	23.28 ± 0.12	28
<i>w X norpARNAi</i>	23.28 ± 0.12	30	23.13. ± 0.09	30
<i>pdfGAL4 X norpARNAi</i>	23.83 ± 0.22	16	23.50 ± 0.08	15

Table 4.8: DD Averaged periods (± SEM) of *norpA* downregulation in PDF cells and controls at 18 and 29°C.

w; pdfGAL4/+; norpARNAi/+ in DD at both temperatures showed no differences in period compared to controls (Table 4.8; Appendix 2.1).

4.3.2.7. *cryGAL4* driver: *norpA* silencing in CRY cells

To further dissect the role of *norpA* in circadian neurons, a *cryGAL4*₁₃ driver was used which expresses in most clock neurons (LN_vs, LN_ds, DN1_as, two DN1_ps and two DN3s; Emery *et al.*, 2000) and in the compound eyes (Yoshii *et al.*, 2008).

The locomotor activity of male flies that downregulated *norpA* in CRY cells (*w; +; cryGAL4/norpARNAi*) was tested at 18° and 29°C in LD. Their activity patterns were compared to controls: driver (*w; +; cryGAL4/+*) and RNA interference construct (*w; +; norpARNAi/+*) controls. In the Figure below (4.22) the averaged locomotor patterns of these three lines are shown at both temperatures.

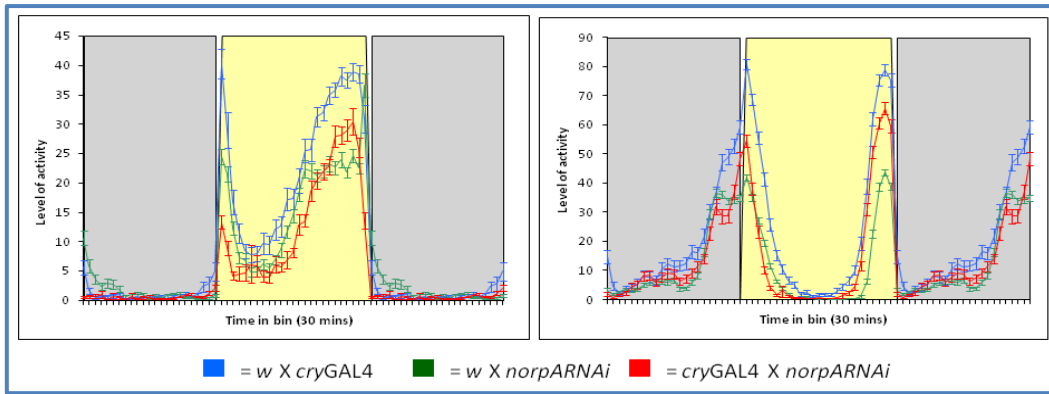


Figure 4.22: Averaged activity profile of transgenic flies downregulating *norpA* in *CRY*⁺ cells and controls. 18°C locomotor activity is shown in the left panel and 29°C in the right panel.

The KD of *norpA* driven by *cryGAL4* did not affect the ability of flies to entrain to the LD cycle. Averaged *norpA* RNAi locomotor activity levels of the morning component were significantly lower than controls at low temperature ($F_{2, 372} = 61.18$, $p << 0.001$).

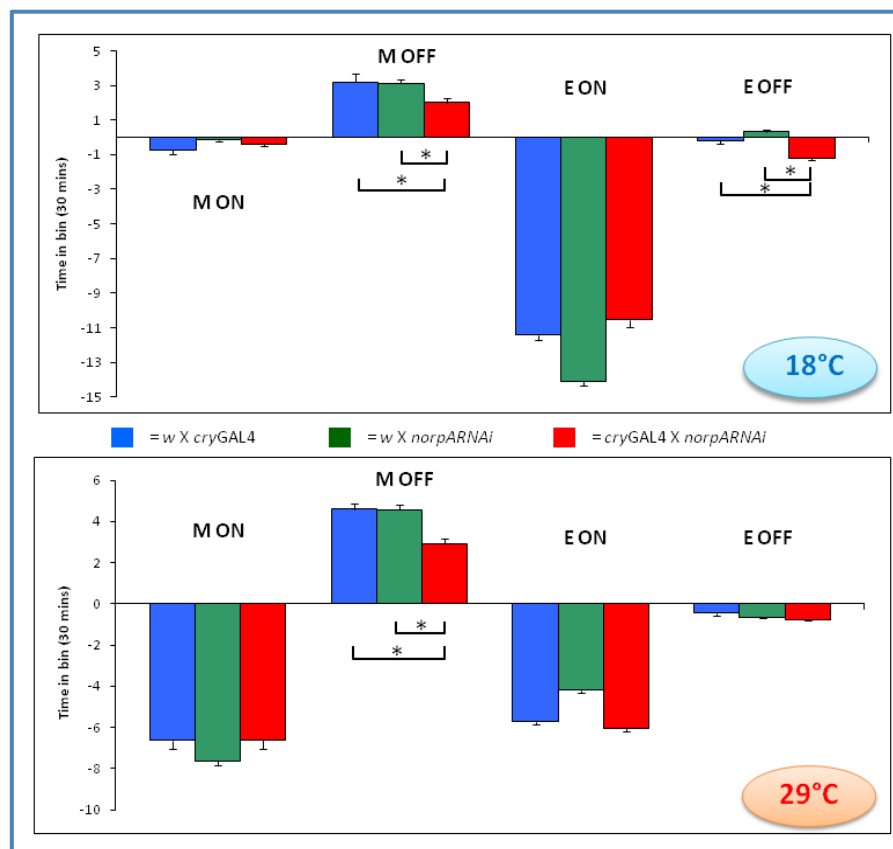


Figure 4.23: Averaged phases of *w*; +; *cryGAL4/norpARNAi* and controls at 18 and 29°C. Asterisks indicate significant values.

At 18°C, the silencing of *norpA* in *CRY* cells revealed an advance in the morning and evening offsets compared to the controls ($F_{2,72} = 5.50$, $p << 0.05$ for the morning

offset; $F_{2,72} = 29.00$, $p \ll 0.001$ for the evening offset; Figure 4.23 and Table 4.9). At higher temperature, the morning offset was advanced when compared to controls ($F_{2,105} = 13.37$, $p \ll 0.001$).

Genotype	18°C					29°C				
	N	Morning onset	Morning offset	Evening onset	Evening offset	N	Morning onset	Morning offset	Evening onset	Evening offset
<i>w X cryGAL4</i>	16	-0.37	1.59	-5.71	-0.10	32	-3.32	2.30	-2.86	-0.23
<i>w X norpARNAi</i>	30	-0.08	1.56	-7.05	0.16	45	-3.82	2.28	-2.09	-0.32
<i>cryGAL4 X norpARNAi</i>	29	-0.19	1.01	-5.28	-0.59	31	-3.31	1.46	-3.02	-0.39

Table 4.9: Averaged phases (in h) at 18 and 29°C for morning and evening onsets and offsets determined from flies downregulating *norpA* in the CRY cells and controls. Significant values are highlighted.

The circadian periodicity of these strains was tested in DD at both temperature conditions.

Genotypes	DD at 18°C		DD at 29°C	
	Period ± SEM	N	Period ± SEM	N
<i>w X cryGAL4</i>	23.92 ± 0.14	29	23.83 ± 0.19	30
<i>w X norpARNAi</i>	23.28 ± 0.12	30	23.13 ± 0.09	30
<i>cryGAL4 X norpARNAi</i>	23.97 ± 0.20	16	23.25 ± 0.11	32

Table 4.10: DD averaged periods (± SEM) of line downregulating *norpA* in CRY cells and controls at 18 and 29°C.

2 way ANOVA revealed significant Genotype and Temperature effects ($F_{2,161} = 12.29$, $p \ll 0.001$; $F_{1,161} = 7.41$, $p \ll 0.05$, respectively) but not significant interaction between them (Table 4.10; Appendix 2.1).

4.3.2.8. Implementation of GAL80 element

Another powerful feature of *GAL4/UAS* system is the possibility to co-express in parallel the *GAL80* element. In yeast, the *GAL80* protein antagonises the *GAL4* activity by binding to the activation domain of *GAL4* and preventing its interaction with the transcriptional machinery (Ma and Ptashne, 1987). This also works in *D. melanogaster* where *GAL80* can suppress any *GAL4* induced effect (Lee and Luo, 1999). I used a combination of *timGAL4*; *cryGAL80* to generate a specific knock-down predominantly in the Dorsal Neurons (in particular in the DN1_{ps}, DN2s and DN3s).

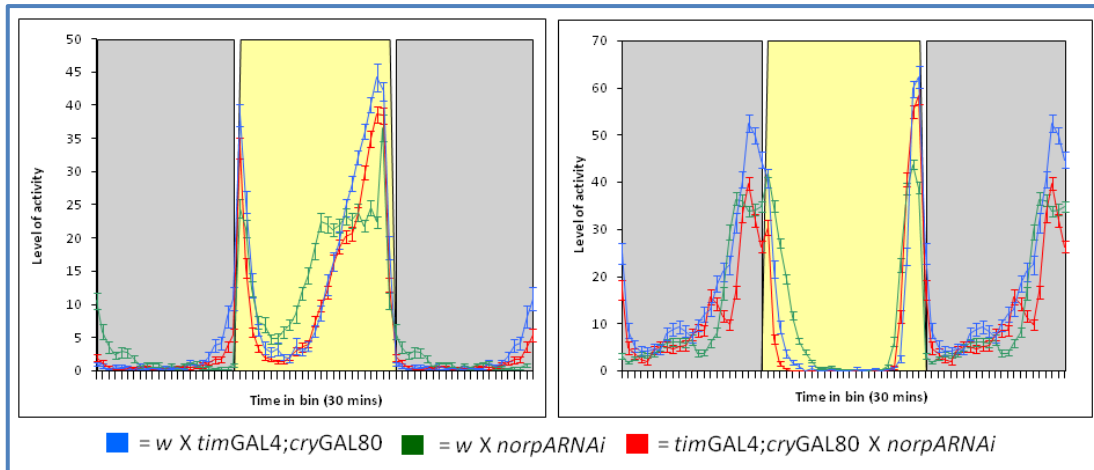


Figure 4.24: Averaged activity profile of transgenic flies downregulating *norpA* in Dorsal Neurons (via *timGAL4*; *cryGAL80* driver) and controls at 18° and 29°C.

KD of *norpA* in the DNs, as shown in Figure 4.24 and 4.25, significantly advanced the morning offsets at high temperature only ($F_{2,97} = 84.86, p < 0.001$; Table 4.11).

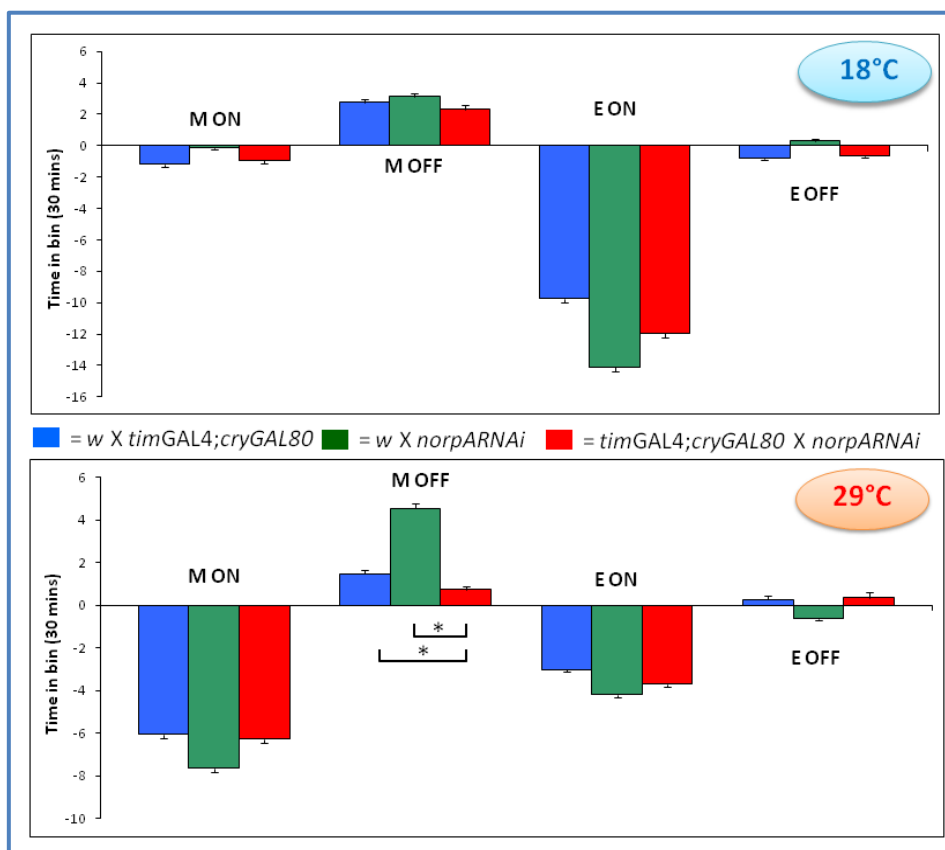


Figure 4.25: Averaged morning and evening onset and offset phases (\pm SEM) of flies downregulating *norpA* in the DNs and controls at 18 and 29°C. Asterisks indicate significant values.

Genotype	18°C					29°C				
	N	Morning onset	Morning offset	Evening onset	Evening offset	N	Morning onset	Morning offset	Evening onset	Evening offset
<i>w X timGAL4; cryGAL80</i>	31	-0.58	1.38	-4.87	-0.4	31	-3.02	0.74	-1.50	0.14
<i>w X norpARNAi</i>	30	-0.08	1.56	-7.05	0.16	45	-3.82	2.28	-2.09	-0.32
<i>timGAL4; cryGAL80 X norpARNAi</i>	30	-0.46	1.16	-5.97	-0.32	24	-3.13	0.37	-1.85	0.18

Table 4.11: Averaged phases (in h) at 18 and 29°C for morning and evening onsets and offsets determined from flies downregulating *norpA* in the Dorsal Neurons and controls. Significant values are highlighted.

As in the case of the other lines described in previous paragraph, the period lengths of these strains were tested in DD. In this condition, the circadian periods were not influenced by *norpA* KD neither at low nor high temperature.

4.3.2.9. *FGAL4: norpA* downregulation in chordotonal organs

Recently, it has been shown that chordotonal organs are involved *via nocte* in the temperature entrainment pathway (Sehadova *et al.*, 2009). These organs in adult individuals are located at the joints between limb segments attached to the cuticle where they function as stretch receptors (Kernan, 2007). *nocte* mutants exhibit ch organ defects implying a possible role of this gene in the correct development of these structures. Since *norpA* is also involved in the temperature entrainment pathway (Glaser and Stanewsky, 2005), its KD was directed to the Ch Organs *via* the *FGAL4* driver (Kim *et al.*, 2003). Thus the locomotor activity of experimental flies (*w; +; FGAL4/UASnorpARNAi*) was monitored at 29°C in LD and compared to driver (*w; +; FGAL4/+*) and RNAi (*w; +; UASnorpARNAi/+*) controls.

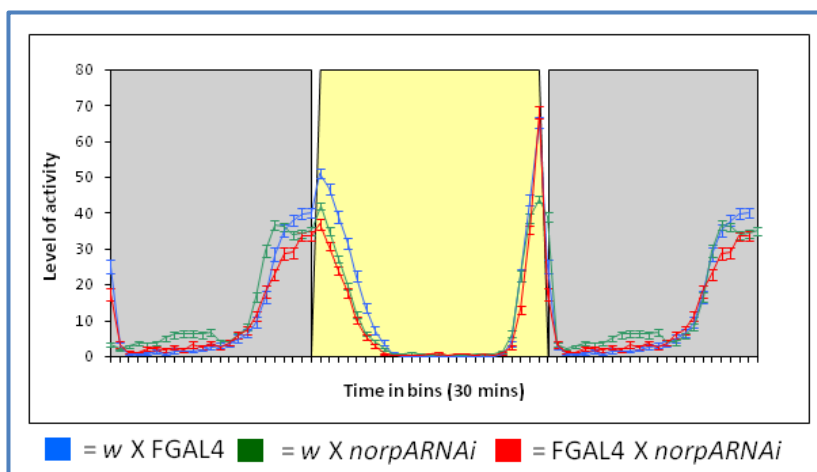


Figure 4.26: Averaged activity profile of transgenic flies downregulating *norpA* in chordotonal organs (*via FGAL4* driver) and controls at 29°C in LD.

Analysis of the averaged profile of ch organs *norpA* KD flies did not show any impairment in the ability to entrain to LD (Figure 4.26). Experimental flies as well as controls displayed a bimodal activity. Furthermore, the onset and offset of the morning and evening components were not influenced by the downregulation of *norpA* in these temperature organs.

4.4. Discussion

In this chapter, the role of NORPA has been examined under different molecular and behavioural perspectives. This work was stimulated by the finding that the splicing levels of an intron in the *per* 3'UTR is determined by temperature and the *norpA* encoded phospholipase C (Collins *et al.*, 2004; Majercak *et al.*, 2004). Also under temperature entrainment cycles *norpA* mutants are effectively thermally blind (Glaser and Stanewsky, 2005). However, all the splicing experiments are performed *in vivo* on heads and largely reflect *per* expression in the eyes. This does not permit a detailed discrimination among the NORPA expressing *per* cells and their involved in the “splicing cold” phenotype. Thus, in parallel to mRNA location among pacemaker neurons, RNA interference is an additional way to investigate the functional involvement of a gene in a specific subset of tissues by reducing the levels of its product (Stanislawska and Olszewsky, 2005).

The UAS/*GAL4* system and variety of driver lines including their combinations provide a powerful tool for numerous manipulations targeting the silencing of a gene in diverse cell subsets without perturbing others (Brand and Perrimon, 1993). In this case, two different transgenic *norpA* RNAi lines were subjected to studies. One set of lines was generated in our laboratory while the other was obtained from VDRC stock center (Vienna Drosophila RNAi Center, Dietzl *et al.*, 2007). The interference efficiency of these lines was investigated by western blots which revealed a significantly higher level of *norpA* downregulation in VDRC line as well as more dramatic behavioural effects. The VDRC transgenic construct has been generated using software that maximises silencing and minimises off-targets while in our case the fragment was chosen to facilitate the cloning process; both constructs contain an intron which enhances nuclear export of the transgenic transcript (Maniatis and Reed, 2002). This intron, however, differs between the two lines. In the strain

generated in our laboratory an endogenous small intron within two coding sequences has been used (Kalidas and Smith, 2002) whereas in VDRC line a standard intron has been cloned downstream to the reverted repeats (Dietzl *et al.*, 2007). The vector used for microinjection in VDRC lines carries 10 UAS repeats whereas “our pUAST” vector only 5. Clearly one or a combination of these factors enhanced the downregulation of *norpA* in VDRC line.

The downregulation levels of NORPA have been tested using diverse drivers. As expected *actin*, *gmr* and *elavGAL4* lines generated significant decrease of endogenous NORPA in the experimental lines (Figures 4.6, 4.9 and 4.12, respectively). No effect was found when the knock-down was targeted specifically to the circadian cells (*via timGAL4*, Figure 4.15) even with over-expressing DICER2 (Figure 4.18, Dietzl *et al.*, 2007). The high NORPA amount displayed by these flies may simply be because less than 2000 neurons express *tim* and this cannot be seen over the background of total NORPA expression. Alternatively, *timGAL4* may be a weak driver in the eyes. Whatever the reason, the level of NORPA was therefore not evaluated for *cry* or *pdf* drivers which express in subsets of *tim* cells.

Once established that the NORPA downregulation is efficient at least with some drivers, the locomotor activity profiles of experimental lines were investigated subjecting them to cold and hot temperatures. The intention of these experiments was to upregulate *per* splicing in diverse circadian neurons responsible for the morning and evening behaviours since *norpA* mutants upregulate *per* splicing; (Collins *et al.*, 2004; Majercak *et al.*, 2004). The phasing of morning and evening locomotor activity components in experimental flies was compared to controls focusing predominantly on the onsets and offsets. The analyses revealed that different circadian cells are implicated in the regulation of the locomotor activity *via* NORPA (Table 4.12).

Driver	Locomotor components			
	M on	M off	E on	E off
<i>actin</i> GAL4	← ←	/ /	← ←	/ /
<i>gmr</i> GAL4	← /	/ ←	/ ←	/ /
<i>elav</i> GAL4	/ →	/ /	← ←	/ /
<i>tim</i> GAL4	← /	/ /	/ /	/ →
<i>pdf</i> GAL4	← /	/ ←	/ /	/ →
<i>cry</i> GAL4	/ /	← ←	/ /	/ /
<i>tim</i> GAL4; <i>cry</i> GAL80	/ /	← ←	/ /	/ /

← = advance → = delay / = no effect ■ = 18°C ■ = 29°C

Table 4.12: *norpA* KD effects on the circadian locomotor components.

Table 4.12 reveals a number of interesting conclusions (referring to Figure 4.27):

1. The M onset is advanced by *pdf* expressing cells and photoreceptor cells (s and I-LN_vs) and these are sensitive to temperature (the advances are in cold not hot temperatures). The *cry* driver includes expression in the 5th PDF-null s-LN_v (but not in *PdfGAL4*), and this may delay the behavioural response, just as it does under moonlight (Bachleitner *et al.*, 2007). Alternatively the CRY⁺ neurons in the LN_d and DN subsets might suppress the PDF⁺ advance;
2. The M offset is similarly advanced by photoreceptor and *pdf* expressing cells that are sensitive to hot conditions. These advances can also be observed in a non temperature-sensitive way when expressing in CRY⁻ DNs and in CRY⁺ cells. These results are difficult to explain because if CRY⁺ and CRY⁻ clock cells can generate non-temperature sensitive advances, so should *timGAL4*, unless CRY⁻ and CRY⁺ neurons repress each other;
3. The evening onset is advanced at hot temperatures by at least the photoreceptors, but also by a non-clock CNS structure in the cold.

- Evening offset gives rather unusual results with delays in the offsets at warmer temperatures mediated by *pdf* cells. It appears that this behaviour is related to the off-target sequence in *fra* gene generated by *norpA* RNAi line (Appendix 2.2).

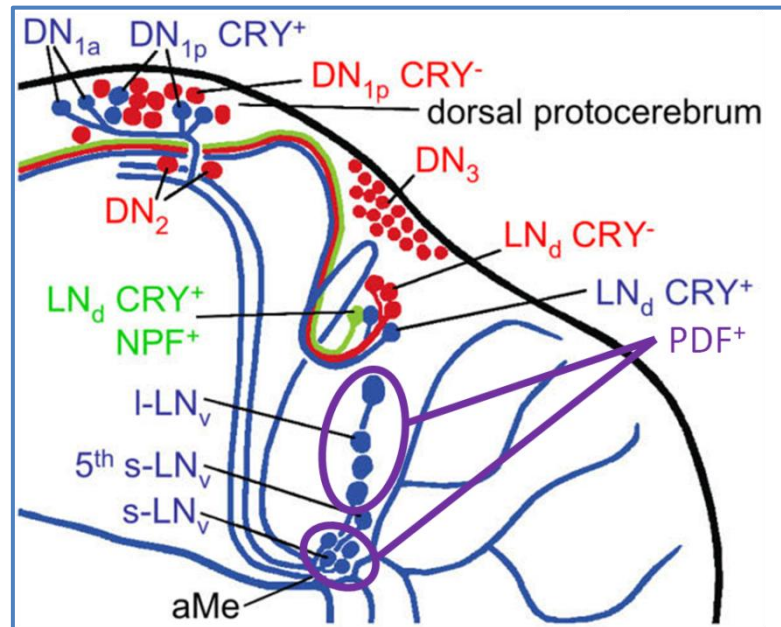


Figure 4.27: Cartoon showing the circadian pacemakers and their clock gene expression. Taken from Yoshii *et al.*, 2008.

Thus disturbing the network with *norpA* downregulation can give some rather intriguing results, but in general the results are consistent with the known effects of *norpA* on *per* splicing.

When the *norpA* interference was directed to the chordotonal organs, which have been reported to be temperature responsive structure (Sehadova *et al.*, 2009), no appreciable changes in the locomotor components were observed at 29°C. This is consistent with the finding that no circadian clock is required in these peripheral organs (Sehadova *et al.*, 2009).

Analysis of *per* splicing level was carried out in flies downregulating *norpA* via *actin* and *gmr* drivers (Karsisiotis and Breda, undergraduate report, 2009). In these strains at high temperature, an increased level of *per* spliced isoform was observed compared to controls. At 18°C, there was no significant difference between interfered and controls, probably due to the lower efficiency of *GAL4/UAS* system at low temperature (Duffy, 2002). Furthermore, when the analysis was extended to

tim, particularly to a splicing event that is enhanced at low temperature (Boothroyd *et al.* 2007), *norpA*^{p41} null mutants displayed a significantly higher level of the spliced *tim*^{cold} isoform compared to Canton-S and *w*¹¹¹⁸ controls. Thus *norpA* downregulation by either *GAL4* or the null mutant, enhances the temperature-sensitive splicing of both *per* and *tim*, at least in the heads, which predominantly reflect photoreceptor contributions. Therefore, my behavioural results presume that *per* can also be spliced *via norpA* downregulation in the clock cells subtypes.

Another possible way might be to study *per* splicing by PCR within the circadian neurons by dissecting out the photoreceptor (Ivanchenko *et al.*, 2001) or “disassembling” in a neuron-specific manner, the fly brains (Nagoshi *et al.*, 2010). Alternatively, *per* can be locked into the spliced mode using transgenic flies engineered to express only one splice isoform (Cheng *et al.*, 1998). The splicing event *per se*, not the isoforms is responsible for generating high steady level of *per* RNA during cold days (Majercak *et al.*, 1999). Thus, blocking the *per* alternative splicing whilst knocking down *norpA* should not result in any locomotor phenotype. If in this case activity is affected, then *norpA* might also be involved in a pathway other than “seasonal *per* splicing”. In fact, it has been documented that one isoform of *norpA*, generated by alternative splicing, is expressed throughout development in adult head and body (Kim *et al.*, 1995). As the RNAi does not discriminate between the two isoforms, it is possible that the development of some circadian structures may be influenced by the early *norpA* absence, although *norpA*^{p41} (which affects the expression of both variants) brains did not show any lack of circadian neurons (Section 3.3.1, Figure 3.7).

4.5. Conclusions

- The *norpA* KD via *actin*, *gmr* and *elavGAL4* drivers reduces dramatically the level of endogenous NORPA.
- *per* splicing level results increased in flies downregulating *norpA*.
- The locomotor activity is affected by NORPA downregulation in a temperature dependent manner:

- The morning behaviour is shifted *via* morning and evening cells in addition to photoreceptors at both temperatures analysed.
- The evening behaviour is shifted by no circadian CNS structures and photoreceptors at low and hot temperatures, respectively.

Chapter 5. Temperature synchronisation of the *Drosophila* circadian clock

Drosophila melanogaster needs to synchronise its locomotor behaviour to daily temperature fluctuations. In this chapter, the temperature synchronisation of wild-type, several entrainment mutants and *norpA* downregulating strains have been tested.

5.1. Introduction

In order to be in tune with environmental conditions, circadian clocks need to respond to changes in light and temperature. While the understanding of how light acts as a Zeitgeber, the manner in which its signal is transmitted and influences the circadian clockwork is increasing, less is known about how temperature information is received and processed by the circadian oscillator. However, what is certain is that ambient-temperature fluctuations are detected and used by the clock as a synchronisation signal in order to adjust accordingly the fly behaviour, despite its cardinal ability to maintain a periodicity close to the 24 h i.e. temperature compensation, over a range of physiological temperatures (Hall, 1997).

However, when flies are exposed to temperature fluctuation, characterised by a difference of only 3°C between the thermophase and cryophase, they are able to synchronise their behaviour accordingly (Wheeler *et al.*, 1993). This is characterised by an increase of their locomotor activity during the warm phase with a maximum before the transition to the cold phase, whereas *per*⁰¹ mutants merely respond to temperature changes (Glaser and Stanewsky, 2005). However, *tim* and *per* loss of function flies retain some aspects of temperature entrainment, which are completely lost in *Clk*^{irk} and *cyc*⁰¹ (Yoshii *et al.*, 2002). Furthermore, temperature cycles can also override constant light conditions (LL) which would otherwise make flies behaviourally arrhythmic (Yoshii *et al.*, 2002).

Molecularly, it has been shown that PER and TIM profiles are synchronised to temperature cycles in DD and LL, indicating a communication between the thermal signalling pathway and the core clock (Yoshii *et al.*, 2002). Moreover, temperature pulses (of 37°C), like light pulses, produce a rapid fall in the level of PER and TIM

(Sidote *et al.*, 1998). Light and temperature act on the behaviour in different ways so that a light pulse at early night leads to a significant reduction in TIM and then PER levels determining a delay in the following day activity. In contrast, heat pulses induce an immediate reduction in PER and TIM levels. In addition, a heat pulse administered in the early night generates a stable phase delay but no advances when given in the late night (Sidote *et al.*, 1998).

Temperature entrainment is independent of the antennae but is disrupted in *nocte* (no circadian temperature entrainment) and *norpA* mutants (Glaser and Stanewsky, 2005). The former cannot be entrained by temperature cycles whereas their locomotor activity remains normal in LD regimes. This might mean that *nocte* encodes for a thermoreceptor or a molecule involved in the transduction of the thermal signal to the clock (Glaser and Stanewsky, 2005). *norpA*, as mentioned before, in addition to the splicing event at the *per* 3' UTR (Collins *et al.*, 2004), is also involved in temperature entrainment. *norpA* mutants show an impaired molecular and behavioural synchronisation to these thermal cues (Glaser and Stanewsky, 2005). Nevertheless, behavioural desynchronisation in *norpA* appears to be less severe than in *nocte* mutants, probably because other PLCs are encoded (see Chapter 6).

In this chapter, the temperature synchronisation of wild-type, several entrainment mutants and *norpA* downregulating strains have been tested, after being exposed to temperature cycle shifts.

5.2. Materials and Methods

5.2.1. Stock flies

Fly strains used in these experiments have already been described in Materials and Methods (Chapter 2, section 2.16).

5.2.2. Locomotor activity

Locomotor activity profiles have been investigated in 12 h at 25°C and 12 h at 18°C in LL. At the 6th or 7th days these cycles were advanced by 6 h exposing flies to a short warm phase or to a 6 h cold phase. This latter paradigm has been used by Glaser and Stanewsky (2005) and therefore has been named the “Stanewsky

protocol". The other paradigm has not been described, and has been modestly named the "Breda protocol".

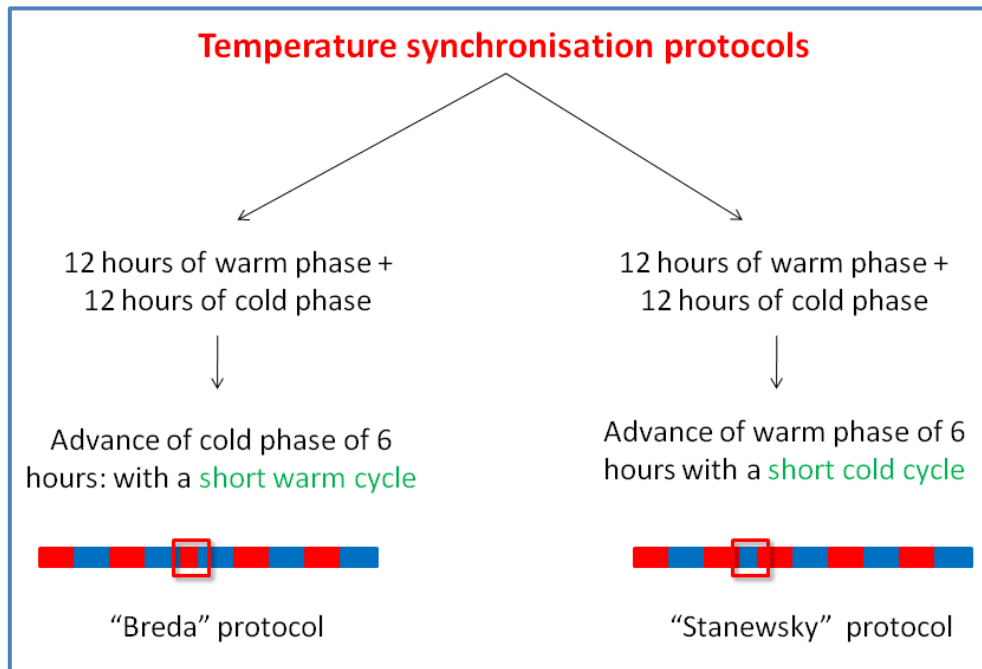


Figure 5.1: Schematic representation of temperature synchronisation protocols used in these experiments. Warm phase (red bars) indicates 25°C whereas cold phase refers to 18°C (blue bars).

The level of resynchronisation has been measured for each fly as the ratio between the amount of locomotor activity during the cold (18°C) over warm (25°C) phase for each single day during the entire experiment. Data were analysed using Microsoft Excel in order to generate averaged locomotor activity profiles. Statistical software was used to evaluate significant differences in the temperature response among and within strains.

5.3. Results

5.3.1. Temperature synchronisation of wild-type and *norpA^{D41}* mutant

Flies detect ambient temperature fluctuations and adjust their behaviour accordingly. In order to confirm this, Canton-S and *norpA^{D41}* mutant strains were tested under the "Stanewsky" or "Breda" protocols.

As shown in the Figure 5.2, Canton-S and *norpA^{D41}* mutants were able to entrain to LL when associated with temperature cycles. The wild-type showed a peak of activity that started to increase in the middle of the thermophase and extended into

the cold phase. *norpA^{p41}* mutants, on the other hand, increased their activity during the thermophase reaching a maximum peak in the middle of it, and decreasing it as soon as the warm phase ceased .

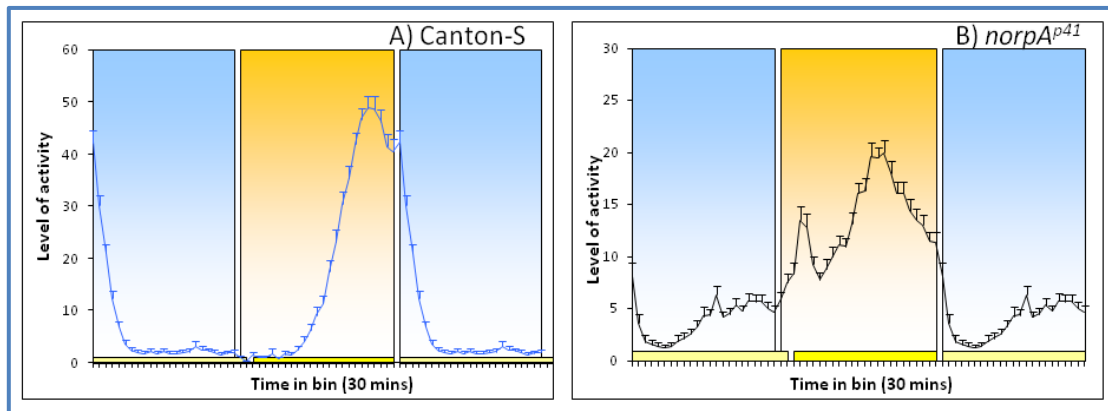


Figure 5.2: Averaged locomotor activity profiles of Canton-S (left panel, N = 24) and *norpA^{p41}* (right panel, N = 31) in LL and temperature cycles. Data from 6 consecutive days were averaged.

These two strains present a different picture when they were subjected to a temperature shift (Figure 5.3). Wild-type responded to both temperature shift paradigms whereas *norpA^{p41}* did not. This was easily observable by comparing the ratio of activity during the cryophase against the thermophase (Figure 5.4). This method appeared more reliable than the evaluation of the phase hot-cold transition locomotor activity. In the “Breda” protocol, the level of temperature shift response of a individual was evaluated dividing the 12 h cold activity over 6 h hot for the day of the change.

Vice versa, in the “Stanewsky” paradigm, the responsiveness of the flies was defined as the total activity during the cold 6 h over the one in the following hot 12 h. Canton-S flies responded when the temperature shift was applied, while *norpA^{p41}* behaviour was characterised by the same ratio throughout the entire experiment. This latter result indicates a response to the new temperature cycle, rather than an active resynchronisation, which takes a cycle for the circadian clock to negotiate. Moreover the diversity in the response to the two new shifted temperature cycles was significantly different between the two strains. Statistical analysis revealed an interaction between Genotype and Days of the experiment for both protocols ($F_{11,312} = 6.44$, $p < 0.001$ “Breda”; $F_{11,631} = 5.44$, $p < 0.001$ “Stanewsky”) caused by the difference between Canton-S and *norpA^{p41}* at day 6th ($p < 0.001$ *a posteriori*

comparisons). This was also confirmed when flies were entrained to a new temperature cycle after being subjected to a 6 h cryophase (i.e. “Stanewsky” protocol). Canton-S and *norpA*^{p41} responded to this new temperature cycle in a different manner: wild-type took two cycles before re-entrainment whereas *norpA*^{p41} simply reacted to the temperature shift adjusting their activity immediately ($p \ll 0.001$ at the 7th day; $p = \text{n.s.}$ at the 8th day). These results are consistent with those that revealed an inability of *norpA*^{p41} to resynchronise to a new temperature cycle (Glaser and Stanewsky, 2005).

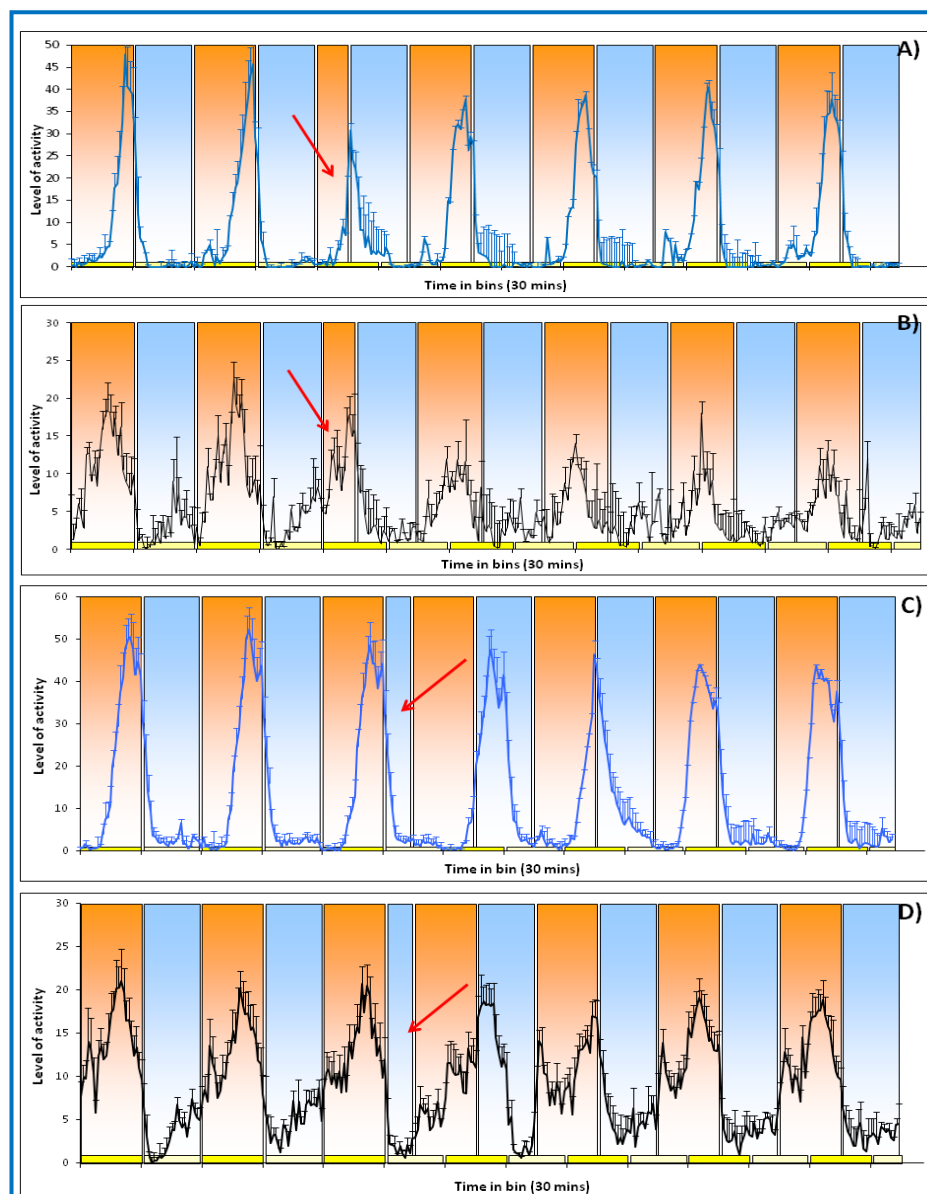


Figure 5.3: Averaged locomotor activity profile of Canton-S (A; N = 12) and *norpA*^{p41} (B; N = 16) subjected to “Breda” protocol. In C and D, Canton-S (C; N = 24) and *norpA*^{p41} (D; N = 31) subjected to “Stanewsky” protocol. Arrows indicate the day in which temperature cycle has been shifted. Orange and blue bars indicate cycle of 25°C and 18°C, respectively.

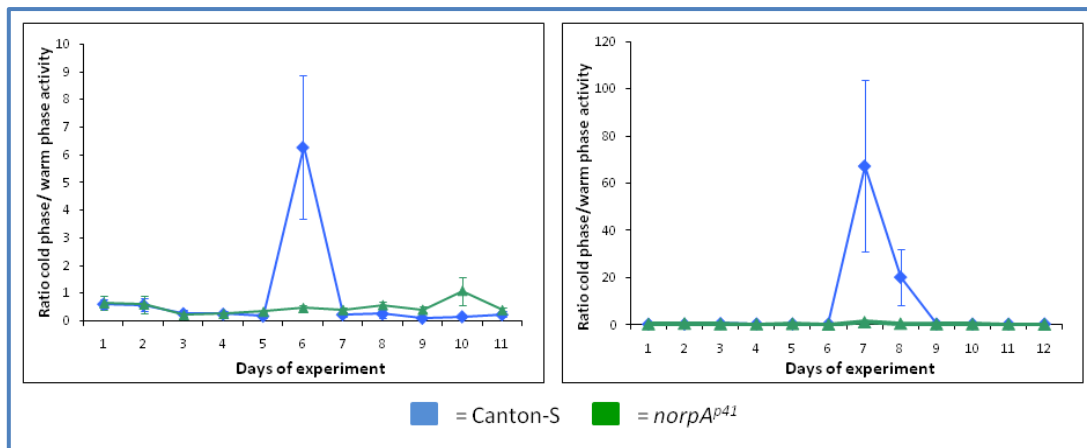


Figure 5.4: Resynchronisation of Canton-S and *norpA*^{p41} mutant to new temperature cycle shifted by 6 h. “Breda” protocol on the left panel and “Stanewsky” protocol on the right panel. The level of resynchronisation has been measured for each fly as the ratio between the amount of locomotor activity during the cold (18°C) over warm (25°C) phase for each single day during the entire experiment.

5.3.2. Temperature resynchronisation in photoreceptor mutants

The ability to synchronise to a temperature cycle shift was investigated in flies carrying mutations in the light input pathway. Thus, *cry*^b, *cry*^{out} and *gl*^{60j} were tested using the two temperature shift protocols. The first two strains are characterised by a miss-expression of *cry*. *cry*^b is a missense point mutation that determines a non-functional CRY (Stanewsky *et al.*, 1998) whereas *cry*^{out} mutants are characterised by a deletion in *cry* (Dolezelova *et al.*, 2007). *glass* encodes a transcription factor necessary for the general development of photoreceptor cells and *glass*^{60j} lack all ommatidial photoreceptors and the ocelli, as well as the primary and secondary pigment cells in the compound eyes (Moses *et al.*, 1989). *glass*^{60j} also disrupts the development of a subset of DN₁s (Moses *et al.*, 1989). In the Figure below (5.5), the responses of these mutants to a shifted temperature cycle are shown and analysed.

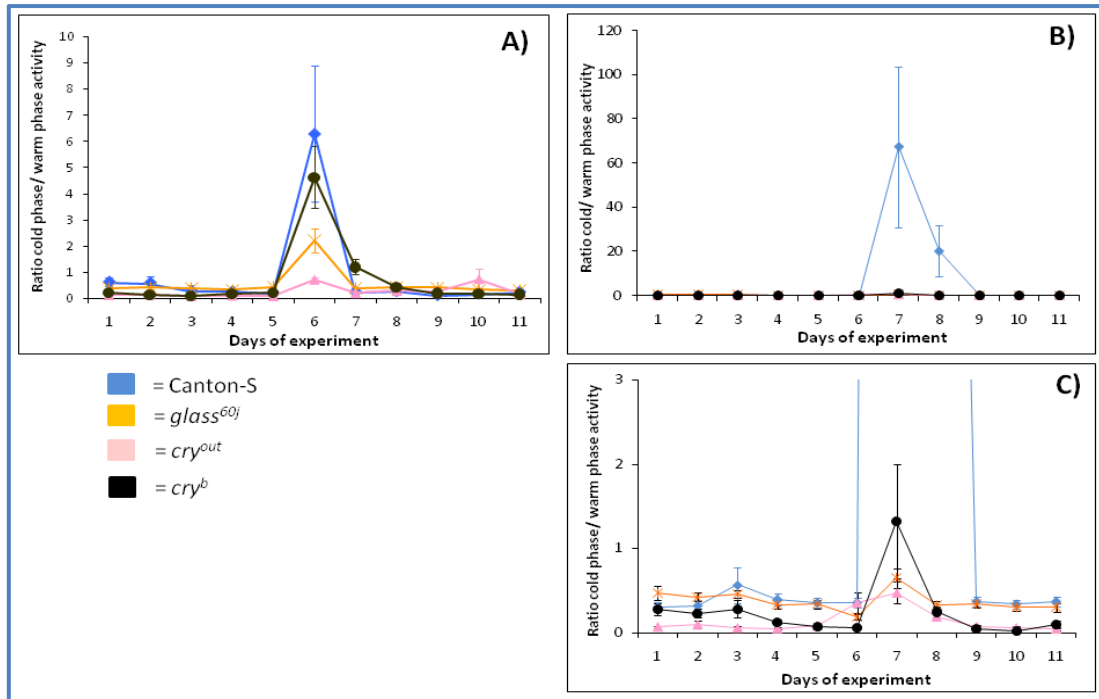


Figure 5.5: Canton-S, $glass^{60j}$, cry^b and cry^{out} responses to a temperature cycles shifted by 6 h. A “Breda”. B and C “Stanewsky protocol”. C is an enlargement of B.

Both experiments revealed different responses to temperature cycle shifts among the mutants. This was confirmed by statistical analysis (ANOVA/MANOVA) which showed a significant difference between genotypes in both “Breda” and “Stanewsky” protocols ($F_{3,612} = 4.00$, $p \ll 0.001$, $F_{3,679} = 4.00$, $p \ll 0.001$, respectively; Appendix 2.3). Finally, an interaction between Genotype and Days was present in both experimental paradigms ($F_{33, 612}$ “Breda” = 3.62 and $p \ll 0.001$, $F_{33, 679}$ “Stanewsky” = 2.13 and $p \ll 0.001$, Appendix 2.3). Under “Breda” all the mutant strains significantly differ from the wild-type and among themselves in their response to the temperature shift although cry^b has the mildest effect (Table 3.1).

Probabilities for <i>Post Hoc</i> Test Newman-Keuls Test		Re-synchronisation at 6 th day			
		N	$glass^{60j}$	cry^{out}	cry^b
Re-synchronisation at 6 th day	$glass^{60j}$	15			
	cry^{out}	15	$p < 0.05$		
	cry^b	13	$p \ll 0.001$	$p \ll 0.001$	
	Canton-S	12	$p \ll 0.001$	$p \ll 0.001$	$p \ll 0.05$

Table 3.1: Significant differences between mutant strains and wild-type under “Breda” protocol.

The same mutant strains were also tested subjecting them to the “Stanewsky” experimental paradigm. The response of wild-type to the temperature shift was significantly different to the mutants, but there were no differences among the latter genotypes.

Probabilities for <i>Post Hoc</i> Test Newman-Keuls Test		Re-synchronisation at 7 th day			
		N	<i>glass</i> ^{60j}	<i>cry</i> ^{out}	<i>cry</i> ^b
Re-synchronisation at 7 th day	<i>glass</i> ^{60j}	12			
	<i>cry</i> ^{out}	13	n.s.		
	<i>cry</i> ^b	12	n.s.	n.s.	
	Canton-S	24	p << 0.001	p << 0.001	p << 0.001

Table 3.2: Significant differences between mutant strains and wild-type under “Stanewsky” protocol.

5.3.3. Temperature resynchronisation in *norpA*;*cry* mutants

The experiments presented above reveal a putative role for *cry* in the temperature pathway signalling. Thus, in this section *cry*^b mutation was combined with *norpA*^{p41} in order to generate “temperature blind” strains. These strains were subjected to temperature shift paradigms (Figure 5.6).

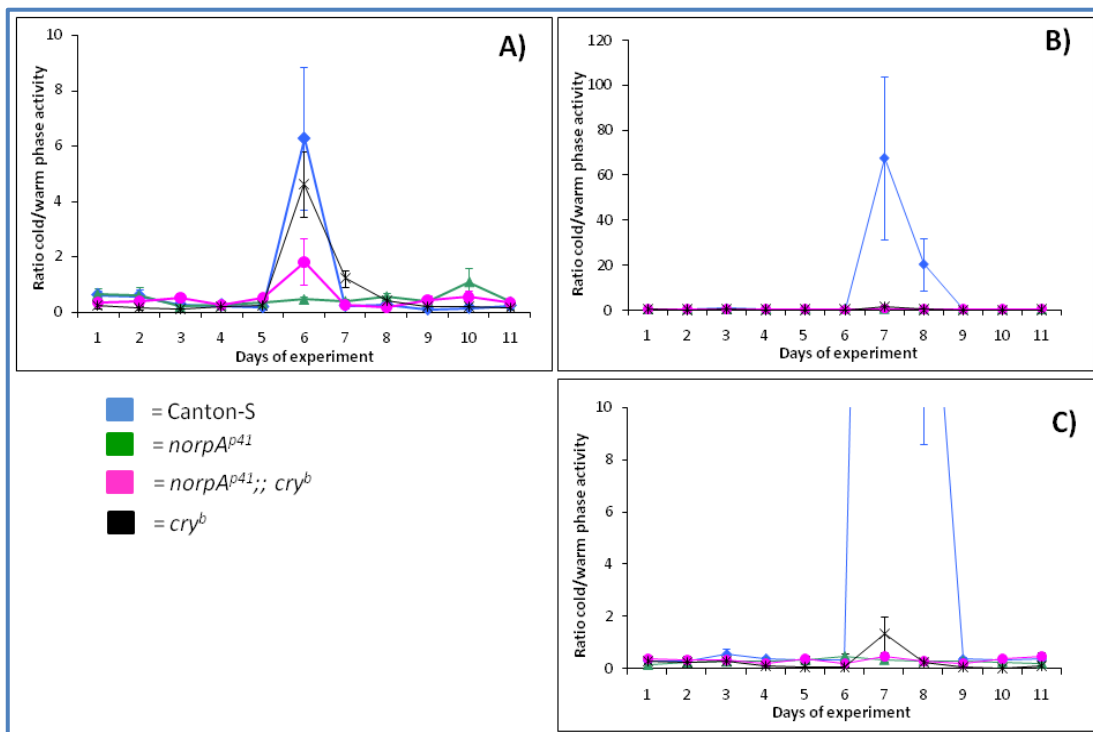


Figure 5.6: Canton-S, *norpA*^{p41}, *cry*^b and *norpA*^{p41};*cry*^b responses to a new temperature cycle shifted by 6 h. A “Breda”. B and C “Stanewsky protocol”. C is an enlargement of B.

The temperature shifts generated a significantly different response among genotypes ($F_{33,612}$ “Breda” = 3.93, $p \ll 0.001$; $F_{33,919}$ “Stanewsky” = 3.25, $p \ll 0.001$ with WT different from the mutants, and the Breda protocol revealing differences among mutants; Appendix 2.3).

Probabilities for <i>Post Hoc</i> Test Newman-Keuls Test		N	Re-synchronisation at 6 th day		
			<i>norpA^{p41};;cry^b</i>	<i>norpA^{p41}</i>	<i>cry^b</i>
Re-synchronisation at 6 th day	<i>norpA^{p41};;cry^b</i>	14			
	<i>norpA^{p41}</i>	16	n.s.		
	<i>cry^b</i>	13	$p \ll 0.001$	$p \ll 0.001$	
	Canton-S	12	$p \ll 0.001$	$p \ll 0.001$	$p \ll 0.05$

Table 3.3: Significant differences between mutant strains and wild-type under “Breda” protocol.

Probabilities for <i>Post Hoc</i> Test Newman-Keuls Test		N	Re-synchronisation at 7 th day		
			<i>norpA^{p41};;cry^b</i>	<i>norpA^{p41}</i>	<i>cry^b</i>
Re-synchronisation at 7 ^h day	<i>norpA^{p41};;cry^b</i>	14			
	<i>norpA^{p41}</i>	11	n.s.		
	<i>cry^b</i>	12	n.s.	n.s.	
	Canton-S	24	$p \ll 0.001$	$p \ll 0.001$	$p \ll 0.001$

Table 3.4: Significant differences between mutant strains and wild-type under “Stanewsky” protocol.

5.3.4. Temperature resynchronisation of *norpA* interference flies

In order to further dissect the role of *norpA* in the temperature synchronisation pathway, VDRC transgenic flies that allow the downregulation of *norpA* were tested. Thus, *norpA* was knocked-down by *actinGAL4*, *ninaEGMRGAL4*, *timGAL4* and *pdfGAL4* drivers. Interfered flies, as well as controls, were subjected and tested under the two described temperature shift protocols.

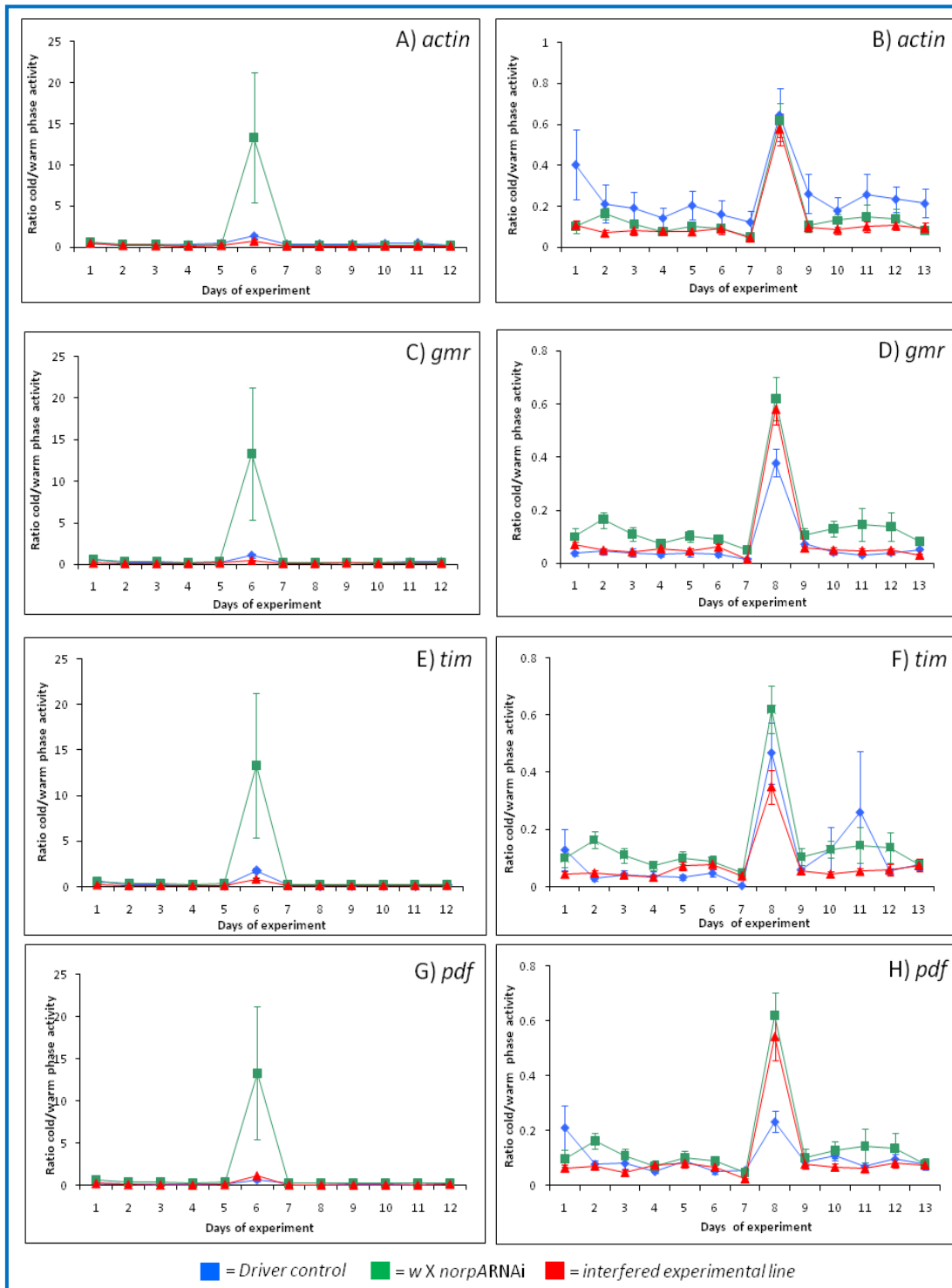


Figure 5.7: Synchronisation responses to temperature cycle shifts of *norpA* interference flies. “Breda” (graphs A, C, E and G) and “Stanewsky” protocol (graphs B, D, F and H) are shown together with the number of flies analysed (in the following page).

Flies under "Breda" protocol			Flies under "Stanewsky" protocol		
Genotype	N	Figure	Genotype	N	Figure
<i>w X norpARNAi</i>	25	A;C;E;G	<i>w X norpARNAi</i>	23	B;D;F;H
<i>w X actinGAL4</i>	11	A	<i>w X actinGAL4</i>	8	B
<i>actinGAL4 X norpARNAi</i>	11	A	<i>actinGAL4 X norpARNAi</i>	24	B
<i>w X gmrGAL4</i>	12	C	<i>w X gmrGAL4</i>	31	D
<i>gmrGAL4 X norpARNAi</i>	14	C	<i>gmrGAL4 X norpARNAi</i>	29	D
<i>w X timGAL4</i>	13	E	<i>w X timGAL4</i>	27	F
<i>timGAL4 X norpARNAi</i>	16	E	<i>timGAL4 X norpARNAi</i>	26	F
<i>w X pdfGAL4</i>	7	G	<i>w X pdfGAL4</i>	30	H
<i>pdfGAL4 X norpARNAi</i>	13	G	<i>pdfGAL4 X norpARNAi</i>	30	H

Under the "Breda" protocol, control flies carrying a single copy of the RNA interference construct displayed a large response to the temperature shift. On the other hand, driver controls as well as *norpA* silencing flies did not respond to the temperature alteration. These lines displayed little variation. Knocking-down lines presented slightly more difficulties to synchronise to the new temperature cycle than controls. This is evident when *actin*, *gmr* and *tim* were used as drivers but not in the case of *pdf*. However, in general the statistical comparison between lines and days did not show any significant difference (Appendix 2.3).

Under the "Stanewsky" paradigm, the temperature shift response was not dramatically different between lines (i.e. interfered and controls). In fact, statistical analysis did not reveal any notable diversity. It is worth mentioning that generally silenced flies behaved more similarly to the RNAi than to the driver controls. The only case in which a downregulated line displayed a response to the temperature shift was in the case of *timGAL4* driver which, however, was not significant.

5.3.5. Temperature resynchronisation: *norpA* KD in chordotonal organs

As mentioned in the previous chapter (Section 4.3.2.9), recently it has been reported that ch organs are involved in the temperature "sensation" *via nocte* (Sehadova *et al.*, 2009). Since *norpA*^{p41} mutants show temperature synchronisation impairment, the role of *norpA* in these organs has been investigated by downregulation triggered by the *FGAL4* driver (Kim *et al.*, 2003). In the Figure below (5.8), results obtained by "Breda Protocol" (left panel) and "Stanewsky Protocol" (right panel) are shown.

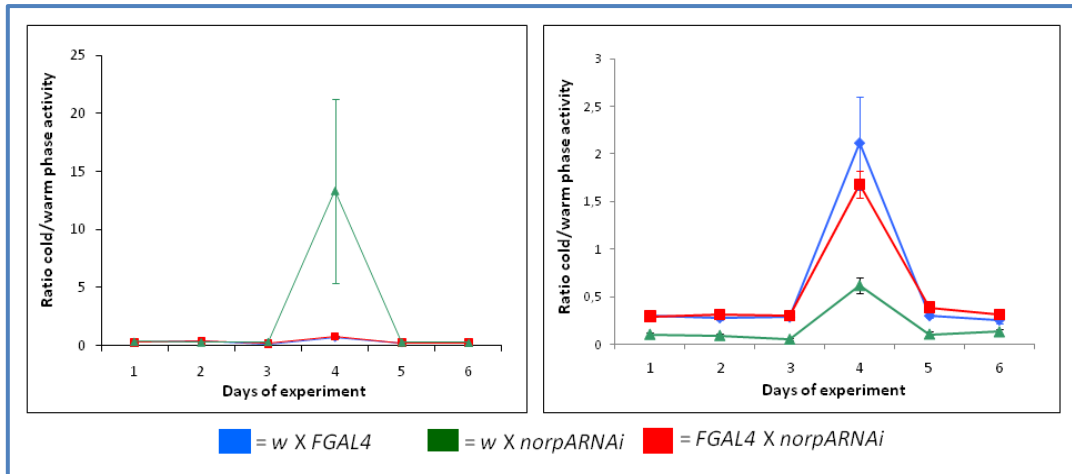


Figure 5.8: Synchronisation responses to temperature cycle shifts of *norpA* interfered in Ch organs. “Breda” (left panel) and “Stanewsky” protocols (right panel) are shown.

The KD of *norpA* mediated by *FGAL4* did not impair the ability of the flies to synchronise to a new shifted cycle of temperature. A significant interaction between the strains and the days of experiment was found in both paradigms ($F_{10, 492}$ “Breda” = 3.03, $p \ll 0.001$; $F_{10, 462}$ “Stanewsky” = 3.83, $p \ll 0.001$). However, a *posteriori* comparisons did not reveal any difference between experimental and driver control lines (Appendix 2.3). Thus, it is clear as in the case of the circadian drivers (described in the previous paragraph), that somehow the presence of GAL4 determined some impairment in temperature synchronisation of the flies.

5.4. Discussion

Light and temperature entrain behavioural and molecular rhythms in *Drosophila* under natural conditions. However in the wild, the intensity of light and its spectra, and temperature change gradually during a day and may differ between two consecutive days. It has been shown that the presence of cycles of temperature can synchronise the circadian mechanism in LL, a condition that would otherwise make flies arrhythmic (Glaser and Stanewsky, 2005). Moreover, in mammals, blood temperature changes daily by $\sim 1.5^{\circ}\text{C}$ serving as cue for the synchronisation of peripheral clocks (Kornmann *et al.*, 2007). So how is temperature perceived and processed, and which are the circadian cells involved?

In this chapter, the activity profile of light entrainment mutants as well as *norpA* RNA interference flies has been re-evaluated by subjecting flies to temperature cycles in LL and subsequently shifting them by six hours. In addition to this, a new

paradigm has been designed alongside the protocol described by Glaser and Stanewsky (2005). Moreover, an intuitive method to quantify the entrainment response has been defined which is based on the ratio between the total activity during the cold over the warm phase. Thus, a zero value indicates an immediate response (i.e. masking) of locomotor behaviour to the new temperature cycle, whereas a higher ratio suggests that the circadian clock is actively resynchronising its molecular cycles to meet the new environmental requirements. In light of this, Canton-S displayed high synchronisation values in agreement with the observation that they “overcompensate” an advanced temperature cycle regime, reaching a stable phase after 4-5 days (Figure 5.3 and 5.4; Glaser and Stanewsky, 2005). On the other hand, *norpA^{p41}*, merely reacts to the new temperature regime, in effect, bypassing its circadian re-entrainment (Figure 5.3 and 5.4; Glaser and Stanewsky, 2005).

To further investigate the role of NORPA in the temperature pathway, the effect of *norpA* knock-down was investigated in photoreceptor structures or in circadian cells applying different drivers and subjecting flies to both temperature shift protocols (Figure 5.7). Unfortunately, no clear picture emerged from these experiments. It is unlikely that the low temperature affected the GAL4 induced KD because Western blots revealed a dramatic downregulation of NORPA at low constant temperatures (chapter 4). Very recently, it has been proposed that the temperature signals are perceived by peripheral chordotonal organs and transmitted to brain where they are processed (Sehadova *et al.*, 2009). If *norpA^{p41}* is involved in the development of these organs (as shown for *nocte*, Sehadova *et al.*, 2009), then perhaps the acute shift in the temperature cycle may be processed by these organs. The fact that the *actin* driver does not give an effect may simply be due to the fact that the KD is not complete, whereas in the mutant, *norpA^{p41}*, it is. Unfortunately, when the *norpA* KD was driven specifically in these chordotonal organs a significant response was not found (Figure 5.8).

From these experiments, an additional role for CRY emerged. CRY has been implicated in circadian temperature compensation because *cry^b* mutants are able to rescue the lack of compensation displayed by *per^l* flies (Kaushik *et al.*, 2007). This is in contrast with the fact that *cry⁰* and *cry^b* are perfectly temperature compensated

(Dolezelova *et al.*, 2007). Thus, it appears that *cry^b* may manifest an altered thermal phenotype due to the modified binding properties of CRY^B to PER^L and/or TIM (Kaushik *et al.*, 2007). Here, *cry^b* and *cry^{out}* mutants were tested in the two protocols finding that the null mutation makes flies insensitive to the temperature changes (Figure 5.5).

5.5. Conclusions

- *norpA^{p41}* mutants do not re-entrain/resynchronise to temperature cycle shifts
- CRY appears to be involved in the temperature pathway through the mutation *cry^{out}*
- *glass* also impairs responses to temperature cycle shifts. However, this effect may be due to the absence of some Dorsal Neurons (i.e. DN1s) rather than the absence of photoreceptor structures (Figure 5.5).

Chapter 6. *plc21C*: is the phospholipase C located at 21C involved in the same pathway as *norpA*?

plc21C is a PLC β which share with *norpA* a 32% of identity. The aim of this chapter is to understand if this second phospholipase is involved in the same pathway of *norpA*. Moreover, the effects of *plc21C* downregulation by RNAi have been tested subjecting flies to LD 12:12 and two different temperatures.

6.1. Introduction

The protein product of *norpA* has been reported to be a crucial component in the visual and temperature signaling pathway. Flies carrying a null mutation in *norpA* (i.e. *norpA*^{*p41*}) fail to entrain to temperature cycles. This impaired behaviour is even more evident when a temperature shift of 6 hours is applied. The clock of wild-type flies resists this change, taking 5 circadian cycles to resynchronise, whereas, *norpA*^{*p41*} and *nocte* mutants passively react to the new regime in one cycle (Glaser and Stanewsky, 2005). However in this experimental condition, the *norpA*^{*p41*} response is not as severe as *nocte* mutants, leading to the possibility that other phospholipase C molecules, such as *plc21C*, may compensate for NORPA in certain tissues.

plc21C was identified in a screen using *norpA* cDNA as probe and mapped in the second chromosome. The gene encodes two proteins *via* alternative splicing which differ by only seven amino acids (Shortridge *et al.*, 1991). Furthermore, a comparison between PLC21C with known PLC sequences revealed that is similar in primary sequence and overall structure to NORPA and to the β -class of mammalian PLCs (Rhee *et al.*, 1989). Overall, the highest amino acid identity was observed between PLC21C and the *Drosophila* NORPA (32%), rat brain PLC β (37%) and bovine brain PLC β (37%) in comparison with other classes of PLCs (Shortridge *et al.*, 1991). Studies on *plc21C* spatial expression revealed a presence of this transcript in the cortical regions of the optic lobe, central brain and thoracic ganglia of adults and the cortical regions of the larval brain which correspond to the location of the neuronal cell bodies (Shortridge *et al.*, 1991).

In order to understand whether PLC21C is able to replace NORPA, I initially evaluated its expression over 24 h and whether there are differences in its

expression at different temperatures using RT-PCR. Moreover, a possible role of this phospholipase C in the circadian mechanism, light and temperature pathways was investigated using transgenic flies that allow RNA interference. As in the case of *norpA*, *plc21C* downregulation was driven in different tissues and locomotor activity profiles were monitored at two temperatures (i.e. 18 and 29 °C).

6.2. Materials and Methods

6.2.1. Fly strains

Two independent lines that generate RNA interference of *plc21C* have been used in these experiments and obtained from the VDRC stock center (Vienna Drosophila RNAi Center). Both strains carry the same RNA interference construct but differ in the location of the insertion on the second chromosome.

Name given	VDRC Code	Insertion (Chromosome)	Off-targets
Line A	26557	2	0
Line B	26558	2	0

Table 6.1: Code given to simplify strain identification, VDRC ordering code, location of the insert in the chromosomes and putative off-targets.

As in the case of *norpA*, several drivers have been used to specifically silence *plc21C* in different tissues. The drivers described in section 2.16 and used in these experiments were: *actinGAL4*, *ninaEgmrGAL4*, *timGAL4*, *PdfGAL4* and *cryGAL4*. The *GAL4/UAS* combinations were placed on a *w¹¹¹⁸* background.

6.2.2. Locomotor analysis

All locomotor analysis was performed for 3 days in LD followed by 7 days in LD or DD at 18 and 29°C. The LD data was used to evaluate the activity profile by superimposing successive days of activity to present an average activity pattern over several days. For each experiment, the morning and evening onsets and offsets were evaluated manually as described in section 2.18. DD data was used for both autocorrelation and spectral analysis (Section 2.17). Statistical analysis and comparisons among different genotypes for each experiment were carried out using STATISTICA (Statsoft).

6.2.3. RNA extraction from *Drosophila* individuals and cDNA synthesis

The procedure used to extract and synthesise cDNA was the same described in section 2.2.

6.2.4. RT-PCR

To evaluate the total mRNA of *plc21C* and the level of silencing in interfered flies, a multiplex PCR reaction was performed comprising of *rp49* (Ribosomal protein L32 used as an internal and loading control; O'Connell and Rosbash, 1984) and *plc21C* primers. In the following table the sequence of primers used is reported.

Primer	DNA sequence and numbering	Reference
<i>plc21C</i> F	5' - CCGGCCAGAAATCCAGTC - 3'	FlyBase IDFBgn0004611
<i>plc21C</i> R	5' - CGATGCTGTTGTGCGACTT - 3'	FlyBase IDFBgn0004611
<i>rp49</i> F	5' - ATCGGTTACGGATCGAACAA - 3'	FlyBase IDFBgn0002626
<i>rp49</i> R	5' - GACAATCTCCTTGCGCTTCT - 3'	FlyBase IDFBgn0002626

Table 6.2: Primers used in the PCR reactions together with the numbering according to the corresponding reference are indicated.

Optimal annealing temperature for these primers was 63°C and the number of cycles was 28. The products obtained from PCR amplifications were run in a 2% agarose gel. Finally, ImageJ software was used for the quantification of the PCR bands (measuring the mean gray value) and STATISTICA software was used for statistical analysis.

In order to quantify the level of *plc21C* in KD flies, the sets of primers listed in the table below have been used in addition to *rp49*.

Primer	DNA sequence and numbering	Region amplified
<i>plc21C int</i> F	5' – TTTATGACGAGGAGCCGTTC -3'	Interference
<i>plc21C int</i> R	5' –CGCGCTTCTCTAGCTCACTT -3'	Interference
<i>plc21C rnd</i> F	5' –GGCTTGGAACCGCTTATACA -3'	External
<i>plc21C rnd</i> R	5' –GCGGCAACTAATCAAATCGT -3'	External

Table 6.3: Primers for amplifying the interference and external region of *plc21C* and evaluating its expression in KD flies.

6.3. RESULTS

6.3.1. *plc21C* mRNA level in wild-type flies and *norpA* mutants

The level of expression of *plc21C* was tested in wild-type strains (Canton-S and *w¹¹¹⁸*) and *norpA^{p41}* mutants. Flies were raised at two temperatures (18 and 29°C) and subjected to LD 12:12. Every 3 h flies were collected and the total RNA was extracted from male heads. This genetic material was used as a template for the cDNA synthesis in the subsequent steps. cDNA was used as a template to perform RT-PCR in which two sets of primer were used: one that recognises a region in the 3' of *plc21C* mRNA and another as a control amplifying a fragment of *rp49* (i.e. an housekeeping gene used as an internal control, O'Connell and Rosbash, 1984). As showed in Figure 6.1, two bands were expected: one of 834 bp generated by the amplification of the phospholipase C and another one of around 200 bp amplifying the *rp49* fragment.

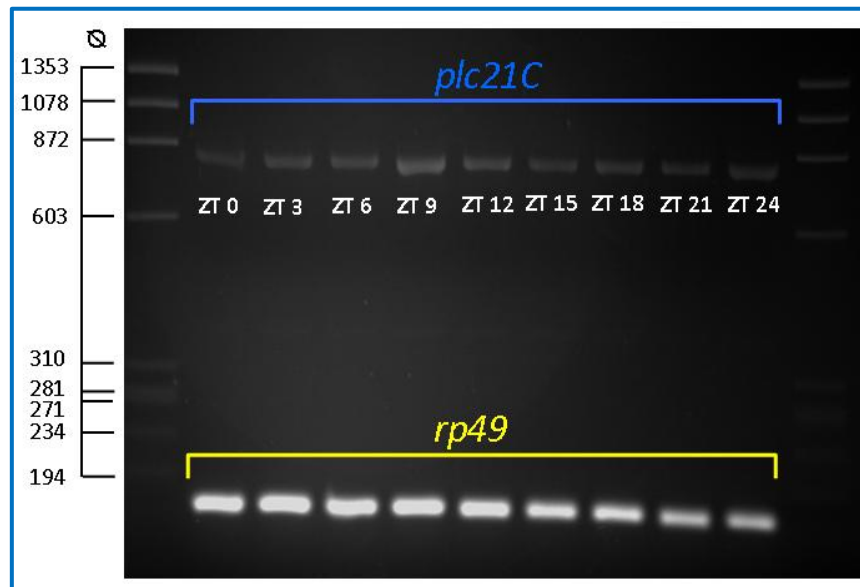


Figure 6.1: Electrophoresis of PCR products amplified from *w¹¹¹⁸* cDNA entrained at 29°C. All ZTs were tested and in each reaction *plc21C* and *rp49* were amplified together.

In the following graphs (Figure 6.2), the *plc21C* relative expression levels obtained from three independent replicas and two temperatures are reported. *plc21C* level was evaluated by removing the background effects and then normalising (dividing) with the control band *rp49*.

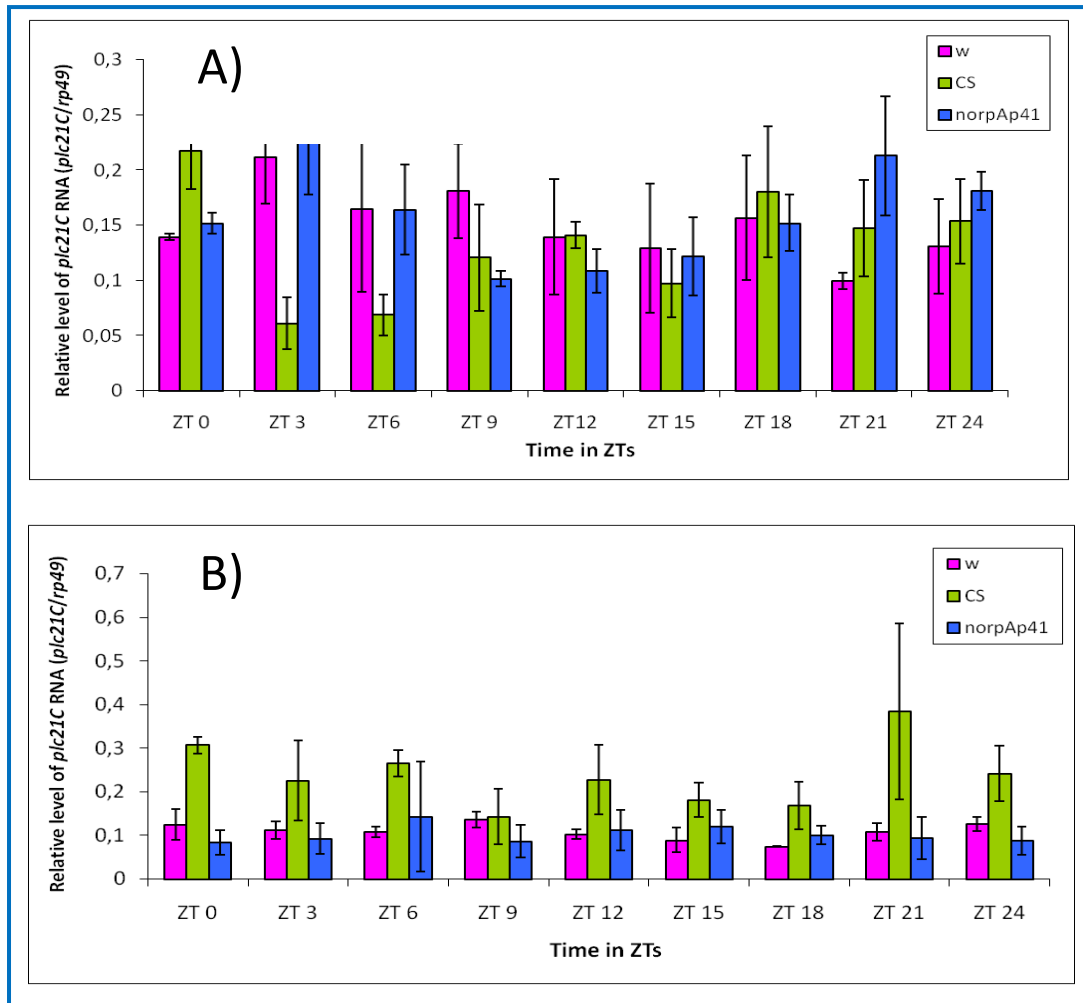


Figure 6.2: Total level of *plc21C* mRNA at 18°C (panel A) and 29°C (panel B) in *w*¹¹¹⁸, CantonS and *norpA*⁴¹ mutants at different Zeitgebers (ZTs).

Statistical analysis revealed a significant difference between genotypes ($F_{2, 216} = 5.98$, $p < 0.05$) and a Genotype/Temperature interaction ($F_{2, 216} = 25.00$, $p < 0.0001$) but no main Temperature effect (see Figure 6.3). *A posteriori* comparison revealed that Canton-S showed generally higher levels of *plc21C* than *w*¹¹¹⁸ and *norpA*⁴¹ ($p < 0.05$ in both cases, Appendix 2.4), whereas the two mutants did not significantly differ between each other at both temperatures. The interaction is due to Canton-S showing a higher level of *plc21C* at higher temperature than the two mutants and the opposite profile at low temperature (Figure 6.3). There was no compelling evidence for rhythmicity in these profiles ($p = \text{n.s.}$).

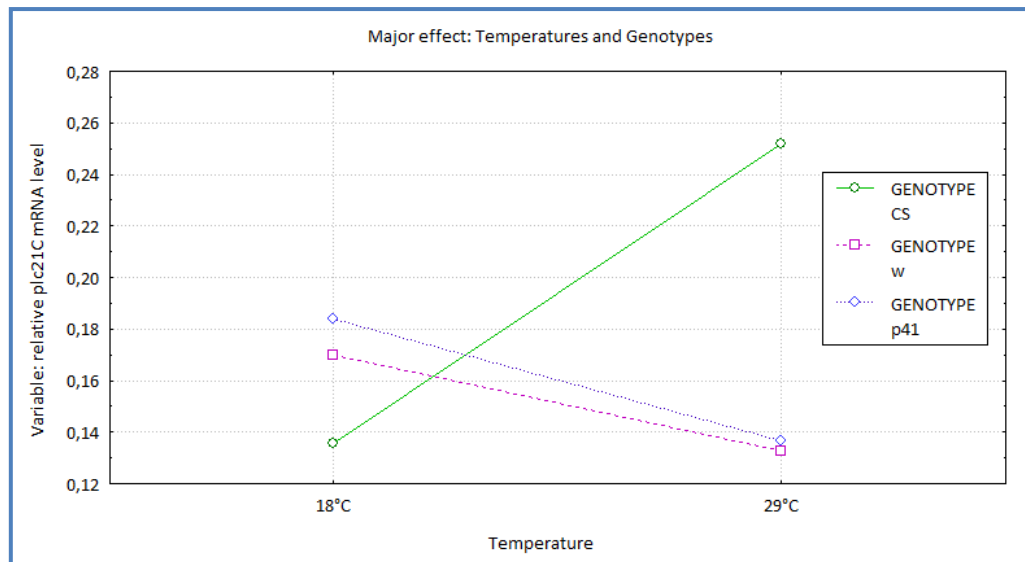


Figure 6.3: The Temperatures X Genotypes interaction in *plc21C* mRNA level.

6.3.2. Analysis of locomotor activity

6.3.2.1. Silencing *plc21C* in all *Drosophila* tissues via the *actinGAL4* driver

A putative role for PLC21C in the entrainment of the circadian clock was evaluated throughout the analysis of lines with reduced levels of the protein. In particular, PLC21C was first reduced with RNAi ubiquitously via *actinGAL4*. To assess the level of downregulation of *plc21C*, flies were entrained for four days at 18 and 29°C. Total RNA was extracted from these lines and cDNA was synthesised from heads at ZT 0 (light on) and ZT 12 (light off) as representative time points. The level of knock-down was assessed using two pairs of primers. The first set was generated within the target region for which the transgenic construct was directed. Additionally, the other set of primers amplified an upstream region to the interference sequence with the aim of verifying whether the silencing occurs in both isoforms of the full length *plc21C* mRNA. *rp49* was used as a loading and positive control.

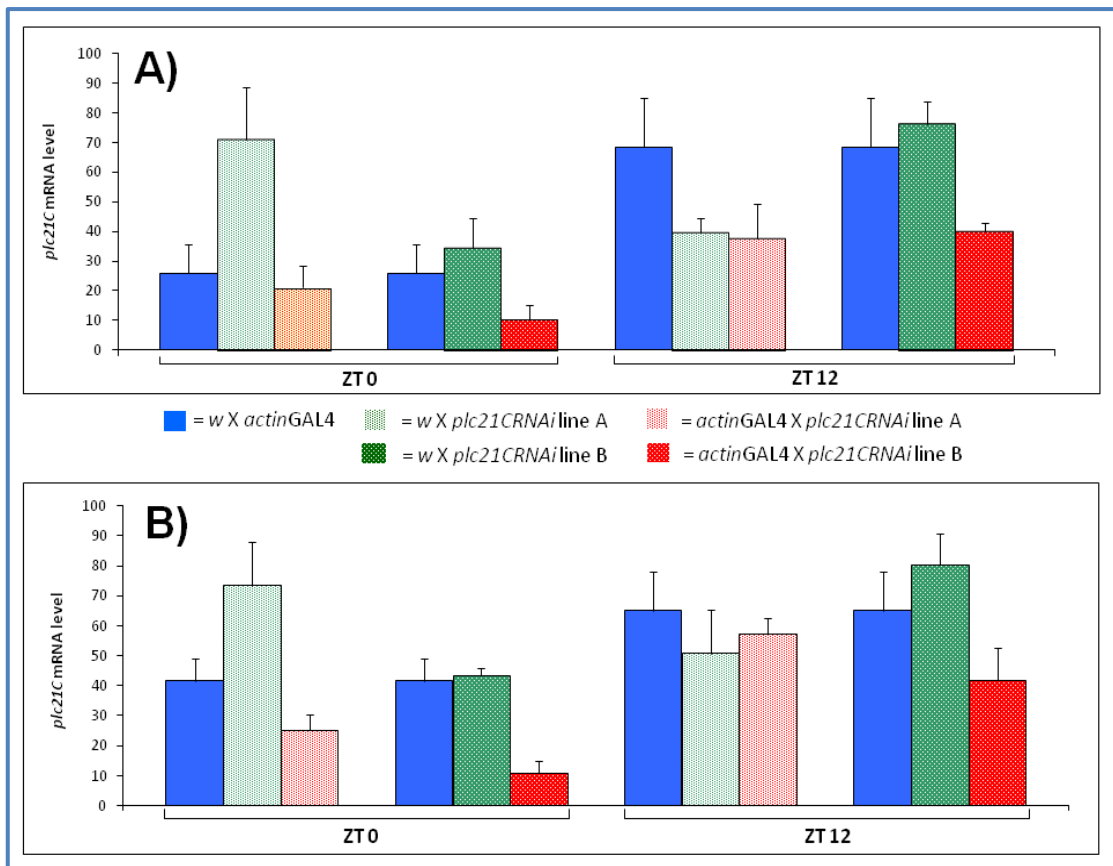


Figure 6.4: Downregulation of *plc21C* mRNA analysed in KD flies (line A and B) and controls at 18°C. Graph A represents the level of silencing within the region where the interference construct has been designed. The *plc21C* downregulation has also been assessed in an external region upstream the interference region (graph B). The graphs are based on averaged results (\pm SEM) obtained for three independent replicas.

In the Figure above (6.4), the level of *plc21C* transcript was evaluated in transgenic flies ($w; actinGAL4/plc21CRNAi; +$) and controls ($w; actinGAL4/+; +$ and $w; plc21CRNAi/+; +$) after being entrained at 18°C. In this thermal condition, line B appeared to display a better level of downregulation compared to line A when both regions and ZTs were considered. However, statistical analysis did not show any significant interaction between the interference or external regions in the two lines and ZTs (Appendix 2.4).

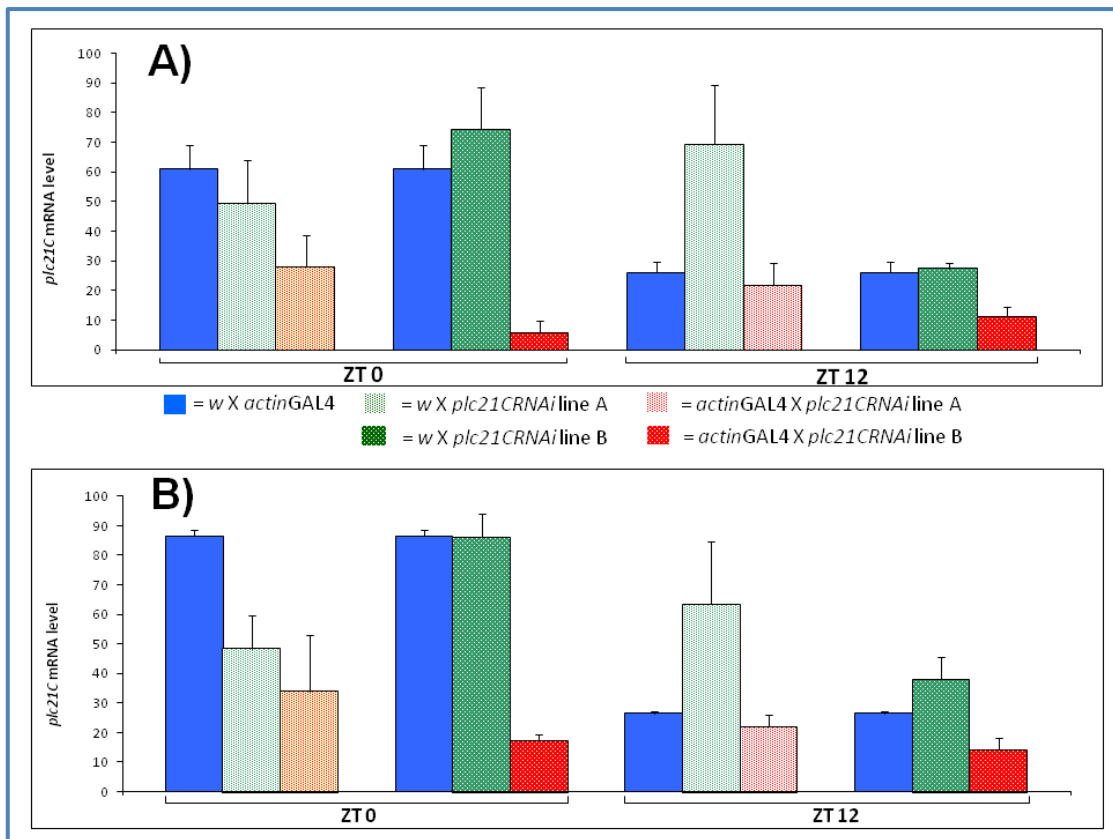


Figure 6.5: Downregulation of *plc21C* mRNA analysed in KD flies (line A and B) and controls at 29°C. Graph A refers to the silencing level within the interference region. The *plc21C* downregulation has also been assessed in an external region upstream the interference region (graph B). N = 3.

The downregulation of *plc21C* was also evaluated at 29 °C: a condition that should enhance the UAS-RNAi expression (*GAL4* is temperature-sensitive; Duffy, 2002) and give a better view of the downregulation efficiency among the two lines. *actinGAL4* driven RNAi displayed a lower *plc21C* level in relation to their controls. Regarding the interference region, line B was characterised by an higher and significant decrease of *plc21C* transcript compared to line A ($F_{2,12 \text{ Line B}} = 7.53$, $p \ll 0.05$). This effect was more marked at ZT 0 than ZT 12. The same trend of downregulation existed when the second region external to that interfered was considered. Also in this case, line B showed a greater diminished *plc21C* transcript level which was significant at both ZTs ($p < 0.001$). These data together indicate that the downregulation of *plc21C* is more efficient in line B than line A.

Since NORPA and PLC21C proteins share a 32% of homology in their primary sequence (Shortridge *et al.*, 1991), it is possible that the RNAi flies may have as off-targets *norpa*. To test this possibility, flies in which the downregulation of *plc21C*

was induced by *actinGAL4* were used in western blots to detect the level of NORPA. Figure 6.6a shows an example of results from a western blot and Figure 6.6b the results obtained from the two *plc21C* RNAi independent lines after being entrained for 3 days at 29°C.

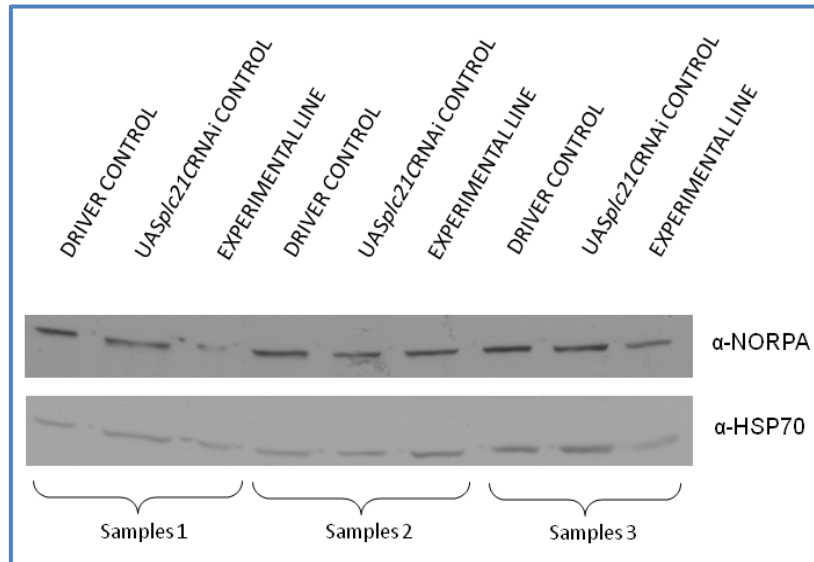


Figure 6.6a: Western blot analysis of NORPA in flies downregulating *plc21C* (line B) and their controls (N = 3). HSP70 was used as a loading control. Lanes 1, 4 and 7 are driver controls (*w; +; actinGAL4/+*); lanes 2, 5 and 8 are RNAi controls (*w; plc21CRNAi/+; +*) and lanes 3, 6 and 9 *plc21C* interfered flies (*w; plc21CRNAi/+; actinGAL4/+*).

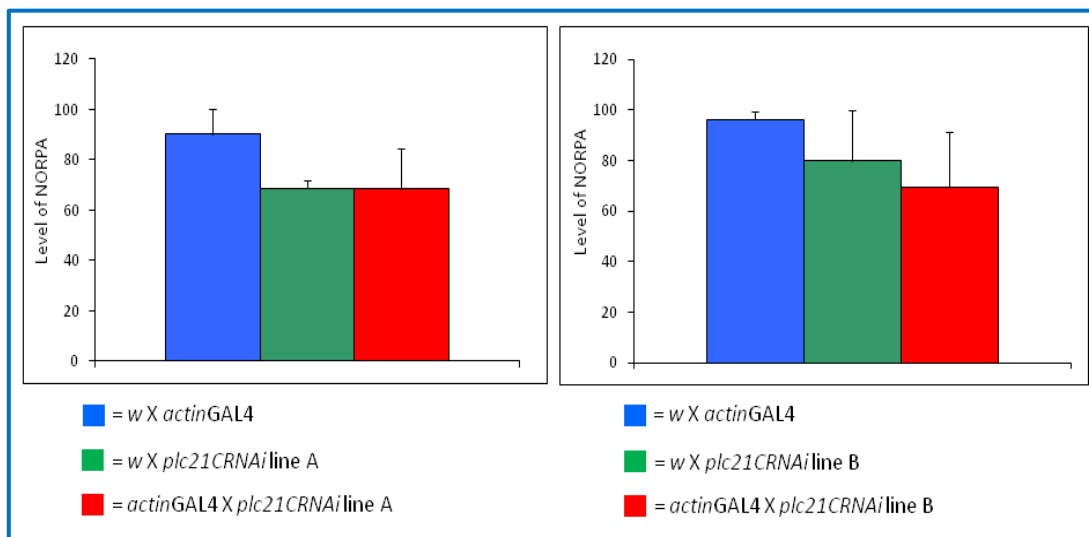


Figure 6.6b: Level of NORPA in flies downregulating PLC21C (line A on the left and line B on the right) and controls (N = 3). Bars indicate SEM. For each gel the strongest band was set equal to 100 and the others were normalised accordingly.

The difference between controls (driver and RNAi constructs) and interfered flies was not significant for line A or line B (ANOVA; $F_{2,6} = 1.24$, $p = n.s.$; $F_{2,6} = 0.61$, $p = n.s.$, respectively). This indicates that locomotor activity profiles, which will be shown

in the following sections, are due to the clear *plc21C* downregulation rather than a non-specific silencing of *norpA*.

The locomotor profiles of these strains were analysed at 18 and 29°C in LD 12:12 as well as DD. In order to correlate the level of *plc21C* downregulation to locomotor activity pattern, both line A and B are shown in Figure 6.7. At both temperatures, a bimodal locomotor behaviour was observed for all flies examined. Thus, PLC21C downregulation did not affect entrainment under LD conditions. In fact, the silenced flies showed the same bimodal pattern as the controls (Rosato and Kyriacou, 2006). However, while at low temperature the evening averaged amount of locomotor activity was affected by the KD of *plc21C*, at high temperature the morning and evening activity peaks were impaired compared to controls in both lines (Figure 6.7). In addition to this, the onsets and offsets of the morning and evening components appeared to be influenced by the PLC21C KD (Figure 6.8 and Table 6.4). At 18°C, the morning component of PLC21C silencing strains was advanced regarding its onset as well for its offset. These effects were displayed by both lines and supported by statistical analysis ($F_{\text{morning onset line A, 2,61}} = 14.36$, $p \ll 0.001$; $F_{\text{morning onset line B, 2,60}} = 16.64$, $p \ll 0.001$; $F_{\text{morning offset line, 2,61}} = 4.01$, $p < 0.05$; $F_{\text{morning offset line B, 2,60}} = 3.23$, $p < 0.05$). At 29°C, despite the phenotype at low temperature, the morning upswing was delayed compared to controls while its offset was advanced. Both line A and B showed these significant phenotypes when compared to their controls ($F_{\text{morning onset line A, 2,80}} = 10.21$, $p \ll 0.001$; $F_{\text{morning onset line B, 2,76}} = 6.57$, $p \ll 0.05$; $F_{\text{morning offset line A, 2,80}} = 33.26$, $p \ll 0.001$; $F_{\text{morning offset line B, 2,76}} = 13.06$, $p \ll 0.001$).

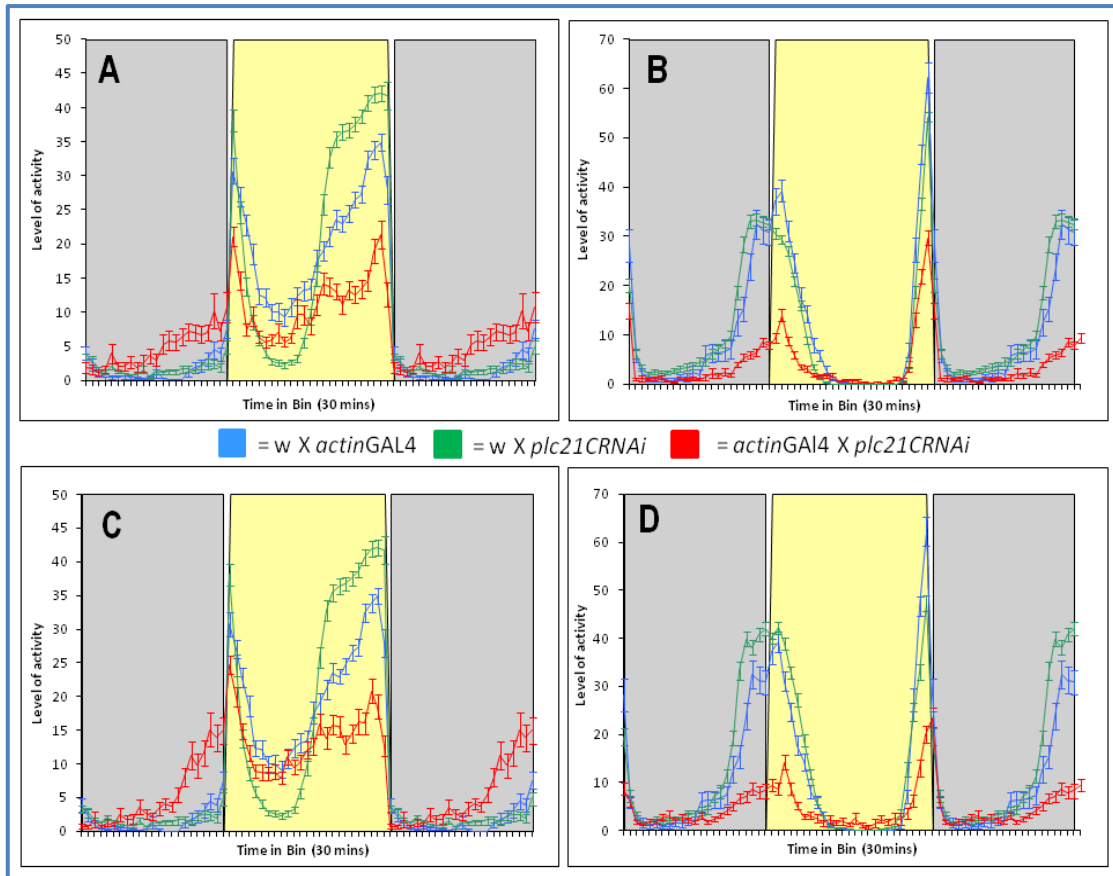


Figure 6.7: Averaged activity of flies in which *plc21C* was silenced by *actinGAL4* driver. A and B show the activity profile of line A at 18 and 29°C respectively whereas C and D, line B at the same temperature conditions.

The evening activity components of *plc21C* interfered flies were more affected at low than high temperature. In fact at 18°C, the evening onset showed a significant delay in its upswing in the two lines ($F_{\text{evening onset line A, } 2,61} = 18.61$, $p \ll 0.001$; $F_{\text{evening onset line B, } 2,60} = 5.48$, $p \ll 0.05$). At the same temperature condition, a significant advance in the offset of the evening activity was observed in the transgenic flies ($F_{\text{evening offset line A, } 2,61} = 50.23$, $p \ll 0.001$; $F_{\text{evening offset line B, } 2,60} = 83.48$, $p \ll 0.001$). At 29°C no significant differences in the evening component were observed.

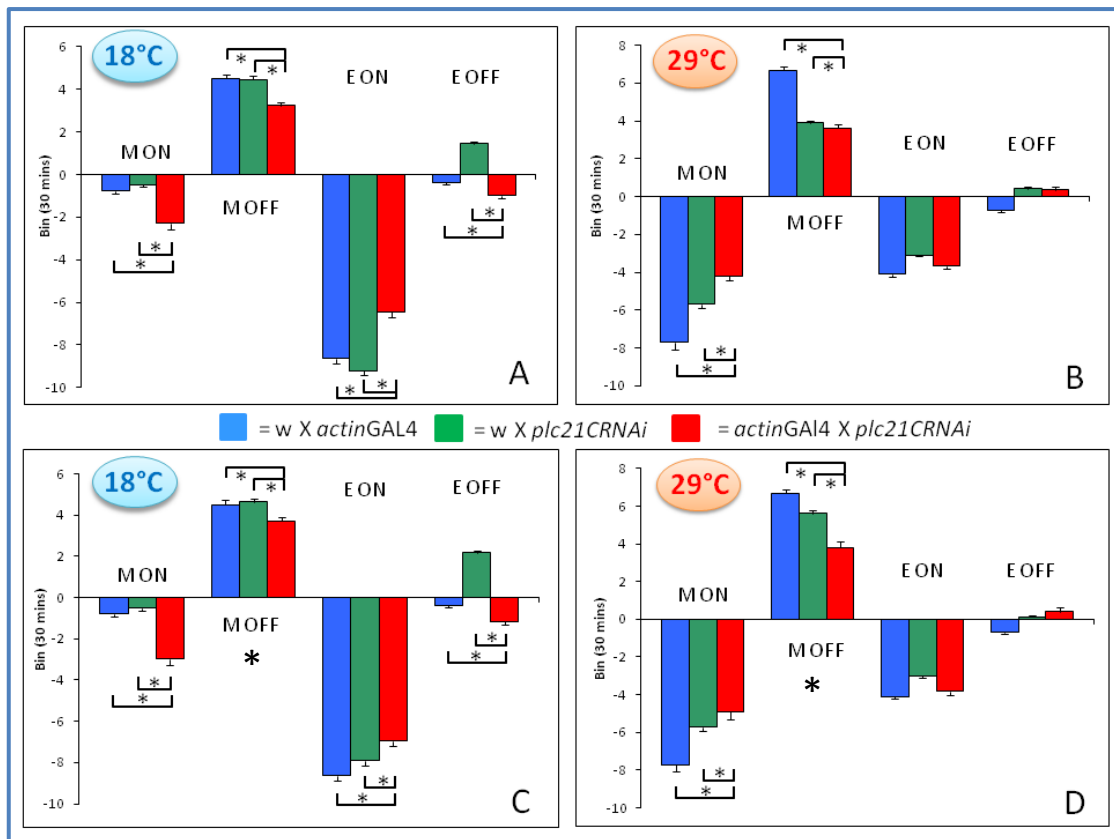


Figure 6.8: Averaged morning and evening onsets and offsets of *plc21C* KD flies and controls. The silencing was driven by *actinGAL4*. A and B show phase results for *plc21CRNAi* line A whereas C and D for line B. A and C represent phase results obtained from flies entrained at 18°C whereas B and D for flies kept at 29°C. Asterisks indicate significant values.

Genotype	N	18°C				29°C				
		Morning onset	Morning offset	Evening onset	Evening offset	N	Morning onset	Morning offset	Evening onset	Evening offset
<i>w X actinGAL4</i>	16	-0.39	2.26	-4.33	-0.19	26	-3.85	3.35	-2.05	-0.25
<i>w X plc21CRNAi</i> line A	32	-0.23	2.22	-4.60	0.73	37	-2.85	1.94	-1.54	0.22
<i>actinGAL4 X plc21CRNAi</i> line A	16	-1.15	1.61	-3.22	-0.49	20	-2.10	1.81	-1.84	0.19
<i>w X actinGAL4</i>	16	-0.39	2.26	-4.33	-0.19	26	-3.85	3.35	-2.05	-0.25
<i>w X plc21CRNAi</i> line B	31	-0.26	2.33	-3.95	1.08	40	-2.86	2.81	-1.50	0.06
<i>actinGAL4 X plc21CRNAi</i> line B	16	-1.49	1.86	-3.48	-0.58	13	-2.42	1.90	-1.90	0.19

Table 6.4: Averaged phases (in h) of *plc21C* interfered flies (line A and B) driven by *actinGAL4* and controls at 18 and 29°C. Significant values are highlighted.

Finally, the circadian periods for both lines A and B and their controls were evaluated in DD (Figure 6.9). Only line B at 29°C displayed a significantly longer period than controls ($F_{\text{period line B at } 29^{\circ}\text{C}, 2,56} = 15.25, p < 0.001$).

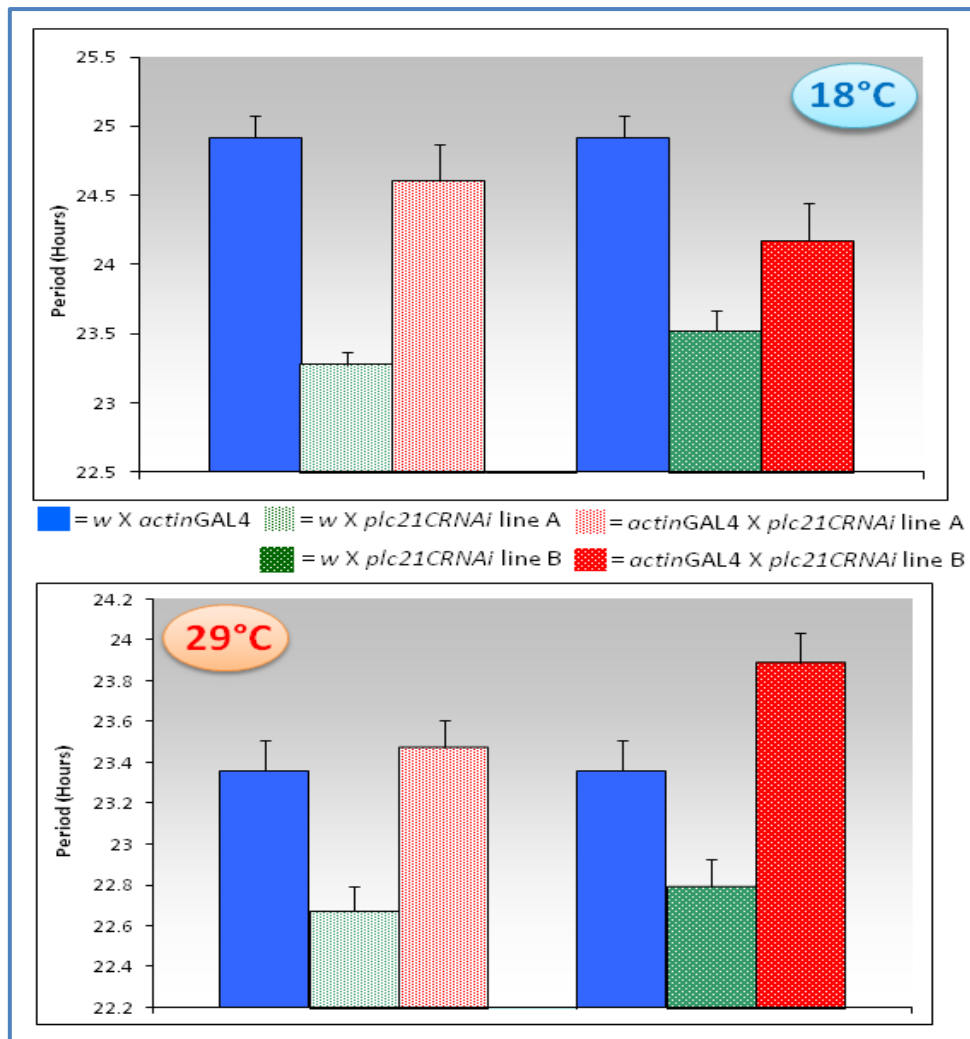


Figure 6.9: Free-running locomotor activity rhythms of flies downregulating PLC21C via *actinGAL4* and controls.

Since NORPA mediates the splicing event in the 3'UTR of *period* (Collins *et al.*, 2004), a possible involvement of PLC21C in this process was tested. As mentioned in Chapter 4, a RT-PCR was used as strategy to determine the total amount of *per* mRNA, spliced and unspliced, at ZT 0 and ZT12 at 18 and 29°C in *actinGAL4* PLC21C KD flies.

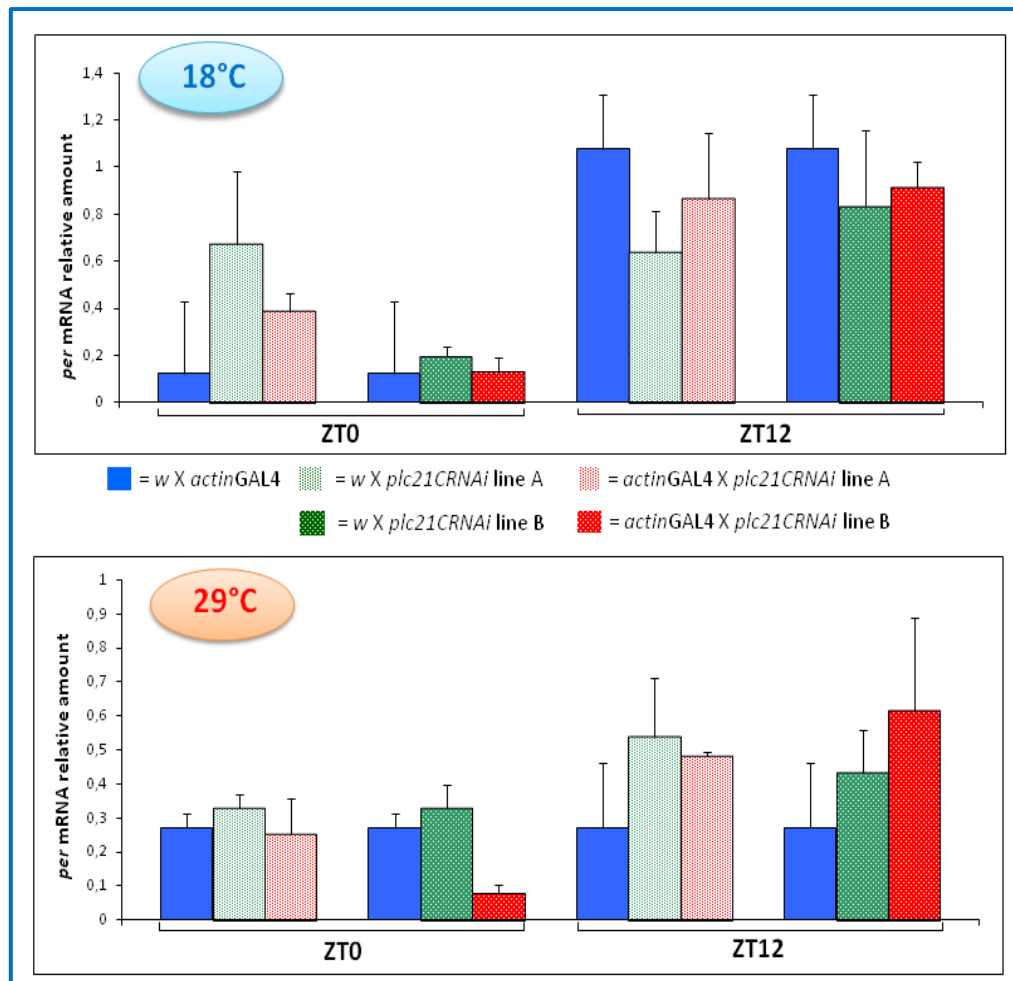


Figure 6.10: Total level of *per* mRNA (N = 3) in flies downregulating *plc21C* by *actinGAL4* driver at 18°C (upper graph) and 29°C (lower graph).

As shown in the Figure above (6.10), the *plc21C* interference did not affect the transcription of *per*. As expected a significant variation in the *per* level was found between the two ZTs examined ($F_{1,24}$ at 18°C = 32.01, $p < 0.001$; $F_{1,24}$ at 29°C = 4.40, $p < 0.05$) but no other effects emerged. The further quantification of the unspliced and spliced *per* products did not show any significant effects between lines at 18°C or 29°C, except that the level of unspliced *per* was significantly higher at ZT 12 compared to ZT 0 both only at high temperature ($F_{1,24}$ at 29°C = 9.65, $p < 0.05$; Appendix 2.4).

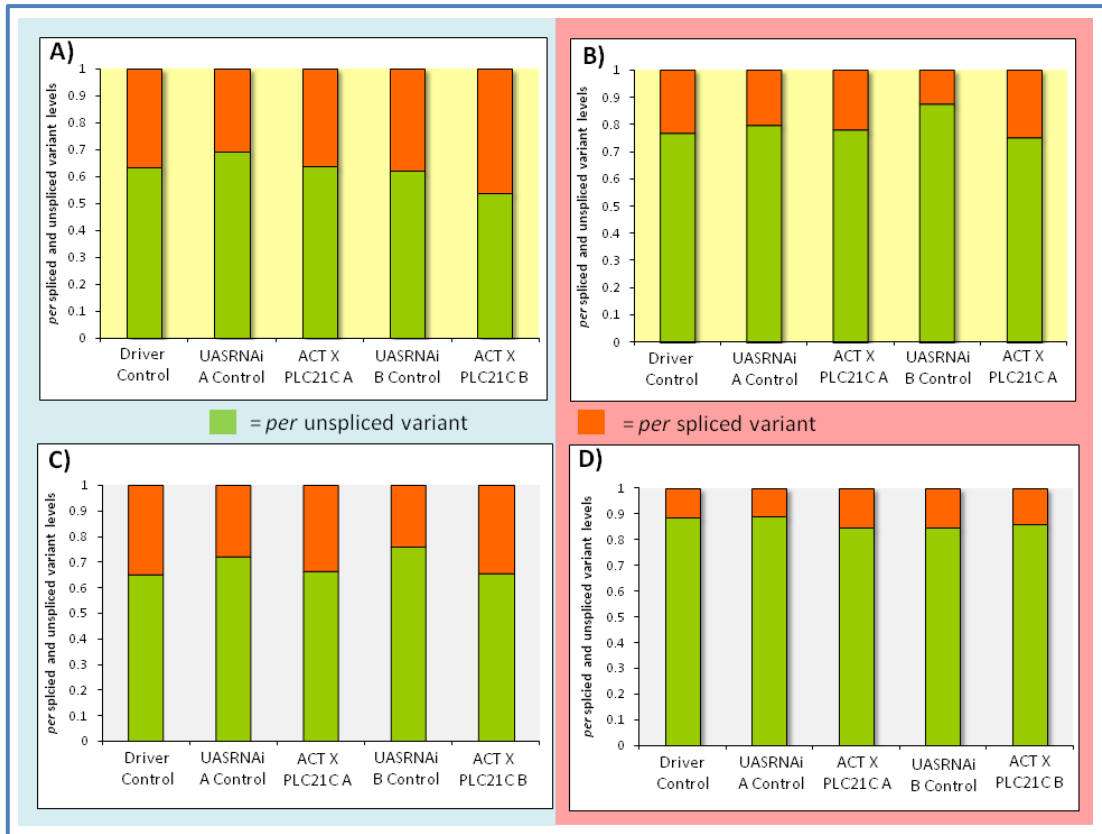


Figure 6.11: Level of spliced and unspliced *per* variants in *actinGAL4 X plc21C* RNAi lines at 18°C (A and C) and 29°C (B and D). The two ZTs analysed are ZT 0 (A and B) and ZT 12 (C and D).

I also tested whether the *tim^{cold}* splicing event might be regulated by PLC21C (Boothroyd *et al.*, 2007) using the same procedure as for *per*. The overall level of *tim* did not vary significantly between control and experimental lines indicating that the *plc21C* is not associated with the regulation of *tim* expression and no significant effect of downregulation was observed on the ratio of the spliced *tim^{cold}* isoform (Figure 6.12).

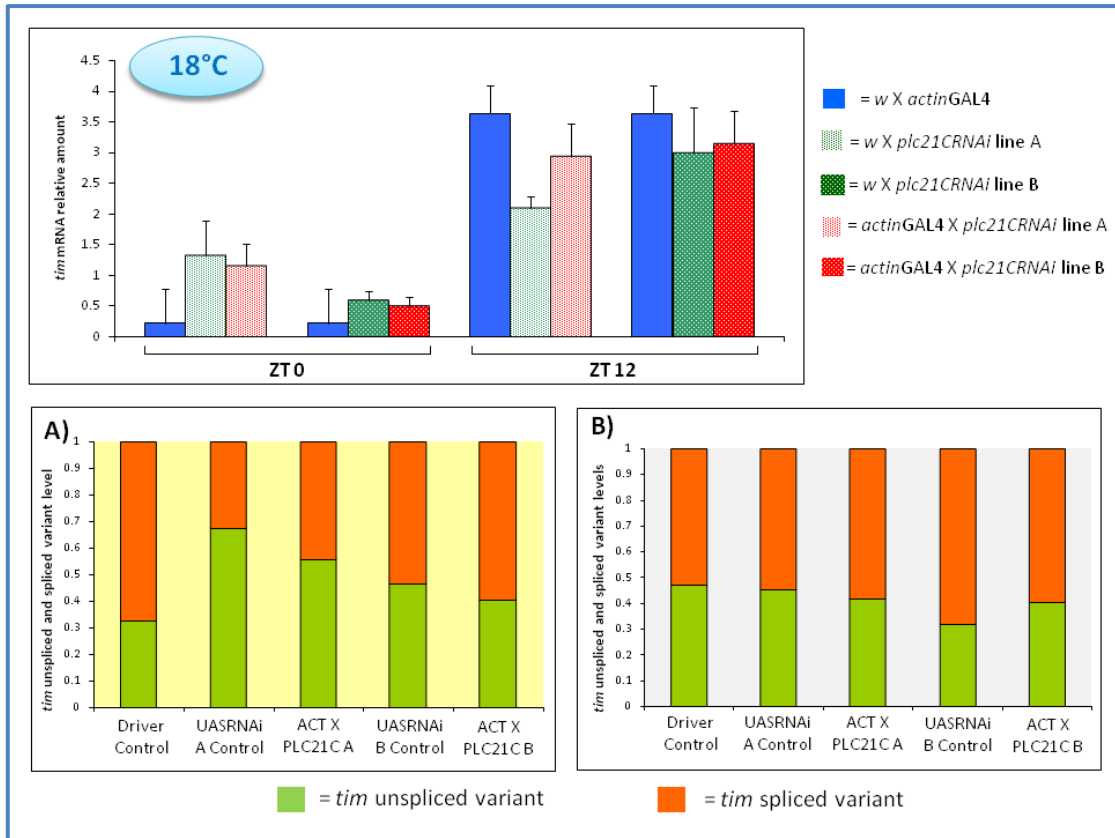


Figure 6.12: Total *tim* level at ZT 0 and ZT 12 in *actinGAL4 X plc21C* RNAi flies at 18°C. A and B show the unspliced and spliced level at ZT 0 and ZT 12, respectively.

6.3.2.2. *ninaEGMRGAL4* driver: silencing PLC21C in photoreceptor cells

Shortridge and co-workers (1991) described the spatial localisation of *plc21C* via *in situ* hybridisation in cryosections of larvae and adult tissues. In particular, they found a similar PLC21C expression pattern to NORPA in the cortical regions of the optic lobes. Therefore *plc21C* expression was knocked down in the phototransduction structures by using the *ninaEGMRGAL4* driver.

The behaviour of KD PLC21C (*w; ninaEGMRGAL4/plc21CRNAi* line B; +) was evaluated in 12:12 LD and DD regimes at 18 and 29°C. Their locomotor profiles were compared to driver (*w; ninaEGMRGAL4/+; +*) and the UAS interference construct (*w; plc21CRNAi* line B/+; +) controls. In the Figure below (6.13), the averaged activity profiles for the lines analysed at low and high temperatures are shown.

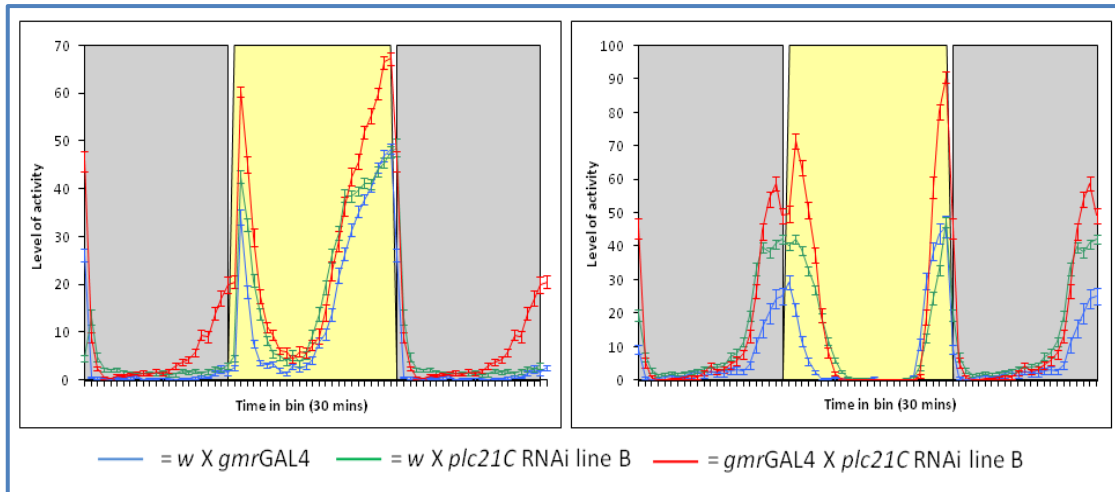


Figure 6.13: Averaged locomotor activity of flies downregulating PLC21C via GMRGAL4 driver and their controls at 18°C (left graph) and 29°C (right graph).

At both temperatures the experimental flies behaved similarly to controls, but the *plc21C* interfered strain was characterised by a higher level of locomotor activity compared to the controls at both transitions. At low temperature, the KD of *plc21C* in photoreceptors showed a significant advance in the morning onset ($F_{2,88} = 79.34$, $p < 0.001$), otherwise the other components showed no significant effects (Figure 6.14).

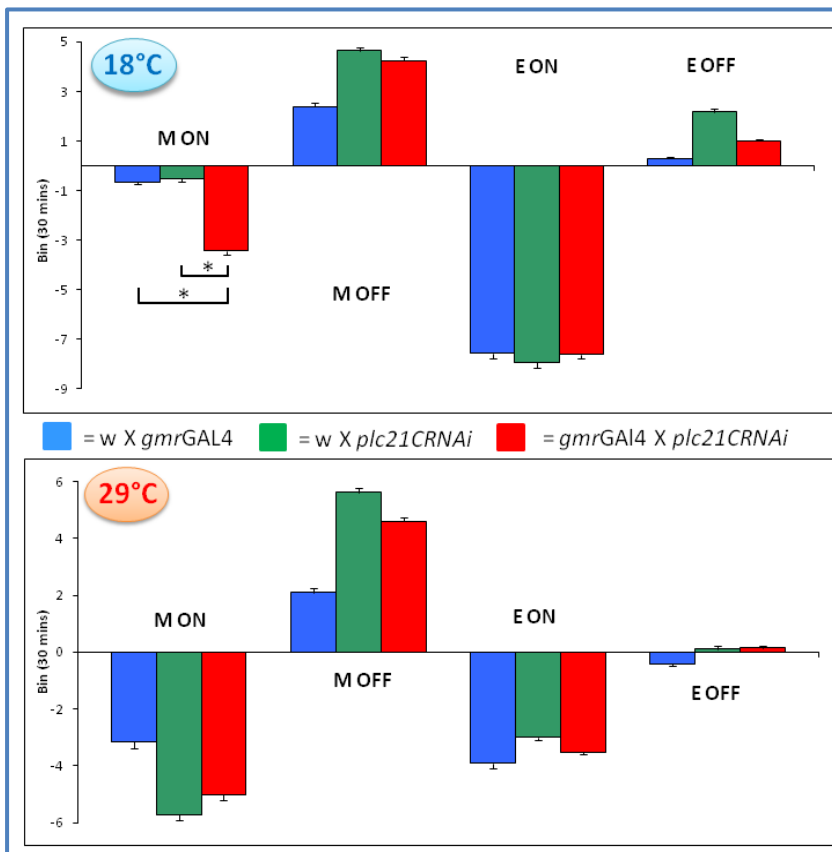


Figure 6.14: Averaged morning and evening onsets and offsets (± SEM) for flies downregulating PLC21C in photoreceptor cells by GMRGAL4 driver and controls. Results refer to 18°C in the upper graph and 29°C in the lower graph. Asterisks indicate significant values.

Rhythms were assessed in DD at both thermal conditions. No effects were found when *plc21C* was KD in flies.

6.3.2.3. *timGAL4: plc21C* silencing in circadian cells

As mentioned in previous chapter (Section 4.3.2.5), *timGAL4* driver allows the expression in about 150 circadian cells which are responsible for the circadian behaviour (Helfrich-Foster, 2003) including lateral and dorsal neurons as well as photoreceptor cells. Thus, PLC21C KD flies (*w; timGAL4/plc21CRNAi* line B; +) and controls (*w; timGAL4/+; +* and *w; plc21CRNAi/+; +*, driver and interference controls, respectively) were subjected to LD 12:12 at 18 and 29°C.

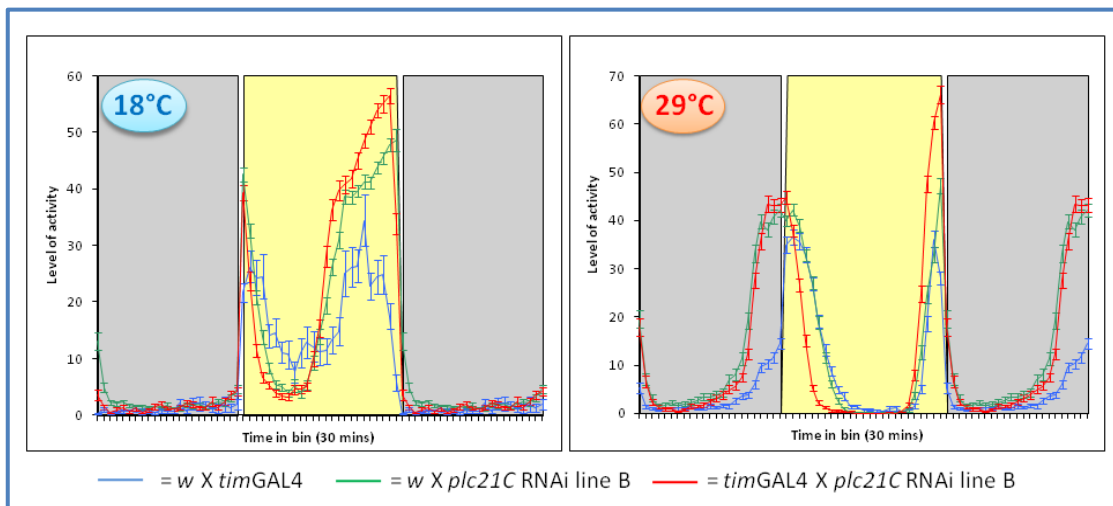


Figure 6.15: Averaged locomotor activity of flies downregulating PLC21C via *timGAL4* and controls at 18 (left panel) and 29°C (right panel).

Figure (6.15) shows how the PLC21C reduction in *tim* cells did not impair the ability of flies to entrain to LD cycles at 18 or 29°C.

The reduction of PLC21C protein in the circadian clock cells generated advances in the morning and evening components at the two temperatures (Figure 6.16 and Table 6.5). In particular, the morning upswing as well as its offset were affected at low temperature ($F_{\text{morning onset at } 18^{\circ}\text{C}, 2,98} = 7.72, p \ll 0.001$; $F_{\text{morning offset at } 18^{\circ}\text{C}, 2,98} = 9.82, p \ll 0.001$). The same profile for the morning offset was displayed at 29°C ($F_{\text{morning offset at } 29^{\circ}\text{C}, 2,103} = 51.93, p \ll 0.001$) whereas its upswing was not influenced. Regarding the evening activity, the silencing of PLC21C generated a significant advance in its onset at both temperatures ($F_{\text{evening onset at } 18^{\circ}\text{C}, 2,98} = 24.58, p \ll 0.001$; $F_{\text{evening onset at } 29^{\circ}\text{C}, 2, 103} = 15.75, p \ll 0.001$).

Genotype	18°C					29°C				
	N	Morning onset	Morning offset	Evening onset	Evening offset	N	Morning onset	Morning offset	Evening onset	Evening offset
<i>w X timGAL4</i>	43	-0.15	1.89	-4.77	-1.31	15	-1.27	2.86	-1.22	-0.13
<i>w X plc21CRNAi line B</i>	31	-0.26	2.33	-3.95	1.08	40	-2.86	2.81	-1.50	0.06
<i>timGAL4 X plc21CRNAi line B</i>	27	-0.54	1.56	-5.81	-0.21	51	-2.57	1.43	-2.01	-0.06

Table 6.5: Averaged phases (in h) of *plc21C* interfered flies (line B) driven by *timGAL4* and controls at 18 and 29°C. Significant values are highlighted.

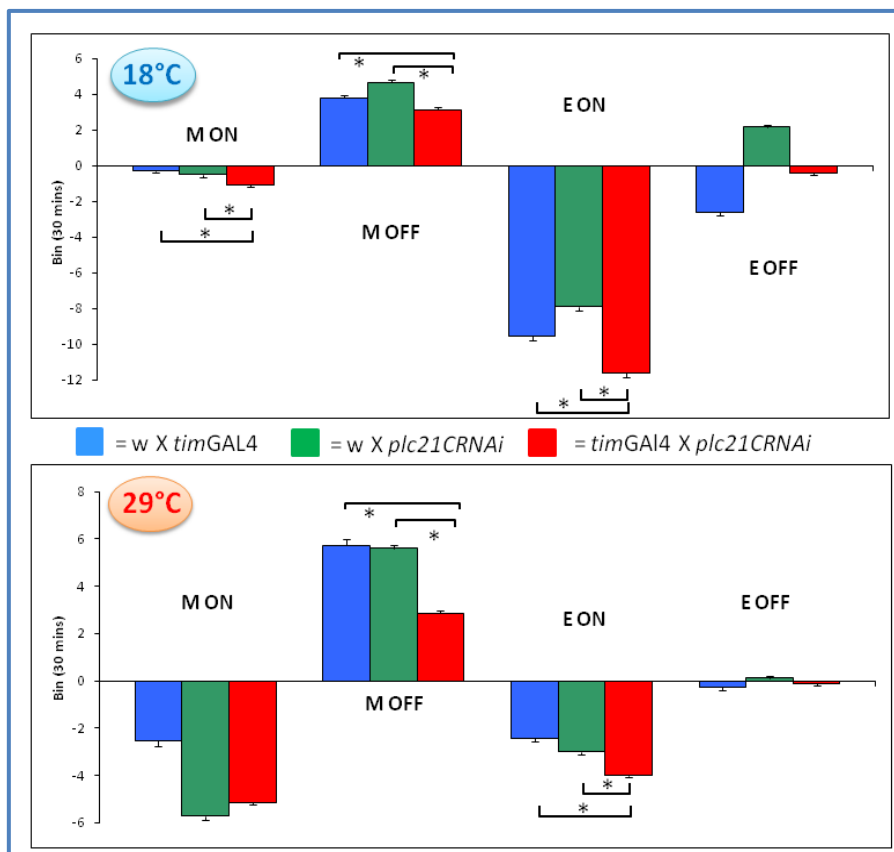


Figure 6.16: Averaged morning and evening onsets and offsets (\pm SEM) of flies downregulating PLC21C in circadian cells by *timGAL4* driver and controls. Results refer to 18°C in the upper graph and 29°C in the lower graph. Asterisks indicate significant values.

Finally, the rhythmicity of *plc21C* silencing flies was tested in DD, but no significant differences with both controls were observed at 18 and 29°C.

6.3.2.4. PdfGAL4: *plc21C* silencing in morning cells

timGAL4 does not permit discrimination among clock neurons. *PdfGAL4* drives expression in the small and large LN_vs which are specifically involved in the generation of the morning locomotor activity component (Grima *et al.*, 2004).

Consequently, *plc21C* was downregulated only in these Morning cells (*w*; *PdfGAL4/plc21CRNAi*; +) and compared to driver (*w*; *PdfGAL4/+*; +) and UASRNAi (*w*; *plc21CRNAi*; +) controls as before (Figure 6.17).

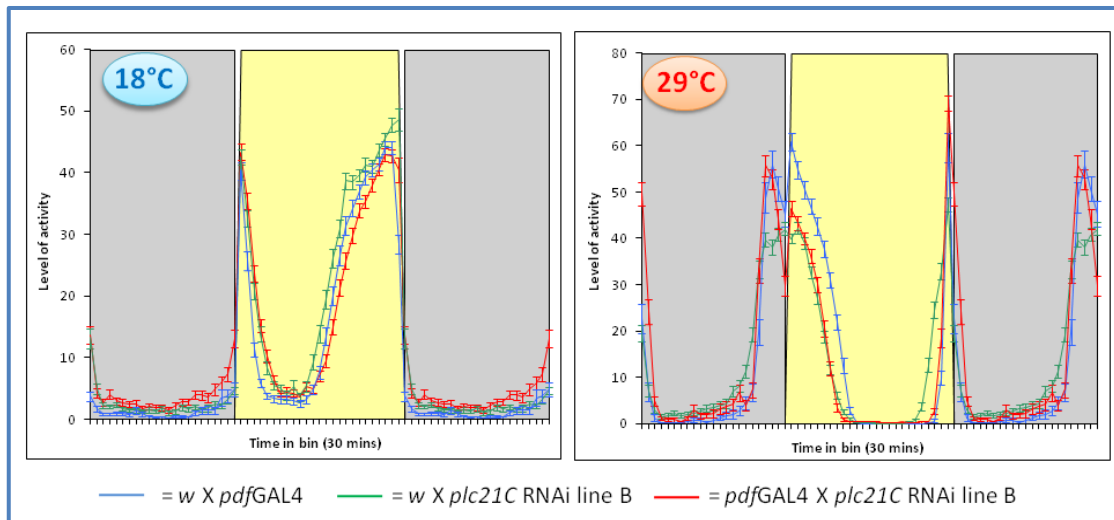


Figure 6.17: Averaged locomotor activity of flies downregulating PLC21C via PdfGAL4 and controls at 18 (left graph) and 29°C (right graph).

PLC21C KD in the morning cells did not affect the ability of flies to be entrained.

Morning activity onset was advanced in experimental flies at low temperature ($F_{\text{morning onset } 2,88} = 17.88$, $p < 0.001$, Figure 6.19 and Table 6.6). At 29°C, the evening offset was delayed ($F_{\text{evening offset } 2,84} = 13.96$, $p < 0.001$, Figure 6.18 and Table 6.6).

Genotype	18°C					29°C				
	N	Morning onset	Morning offset	Evening onset	Evening offset	N	Morning onset	Morning offset	Evening onset	Evening offset
<i>w X PdfGAL4</i>	29	-0.2	1.379	-6.151	-0.375	31	-2.709	1.467	-1.664	-0.145
<i>w X plc21CRNAi line B</i>	31	-0.258	2.326	-3.955	1.084	40	-2.860	2.808	-1.498	0.058
<i>PdfGAL4 X plc21CRNAi line B</i>	31	-0.767	2.212	-5.248	0.083	16	-3.170	2.962	-1.231	0.637

Table 6.6: Averaged phases (expressed in h) of *plc21C* interfered flies driven by PdfGAL4 and controls at 18 and 29°C. Significant values are highlighted.

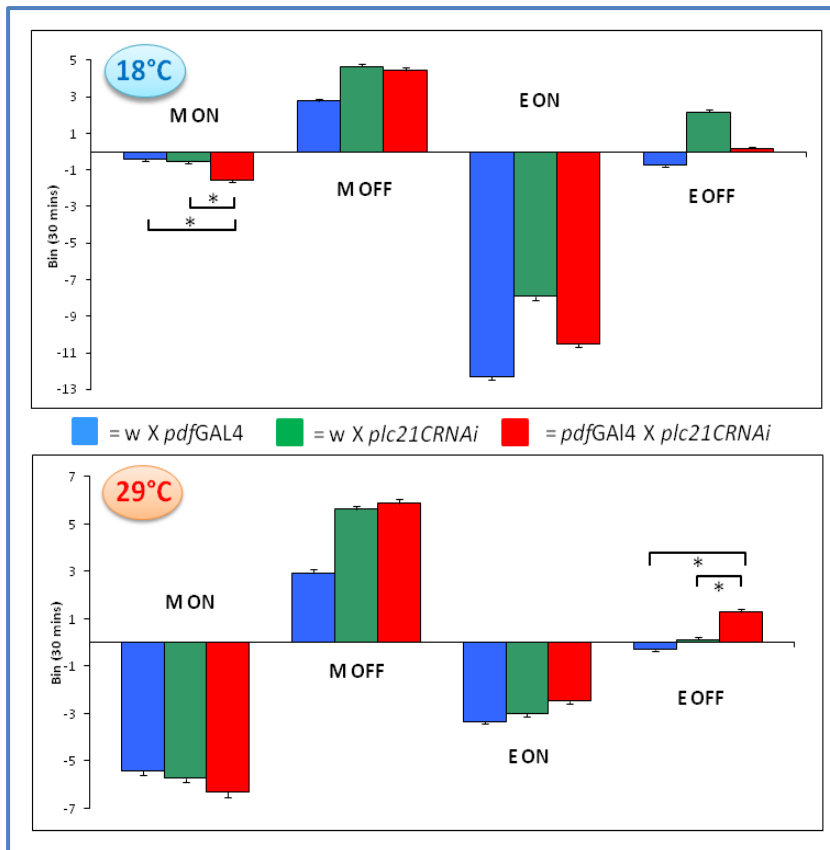


Figure 6.18: Averaged morning and evening onsets and offsets (\pm SEM) of flies downregulating PLC21C in morning cells by *PdfGAL4* driver and controls. Results refer to 18°C in the upper graph and 29°C in the lower graph. Asterisks indicate significant values.

Downregulation of *plc21C* mRNA increased the free-running period of flies compared to both controls only at 18°C ($F_{\text{period line B in DD at } 18^{\circ}\text{C, } 2,88} = 17.97, p < 0.001$, Figure 6.19).

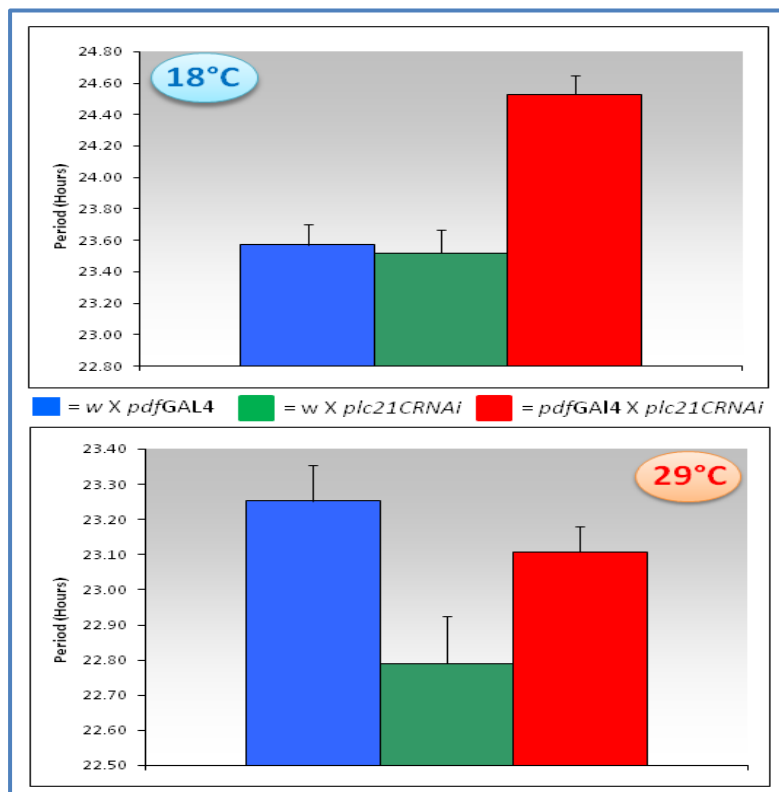


Figure 6.19: Free-running periods of flies downregulating PLC21C by *PdfGAL4* driver and controls in DD at 18 and 29°C.

6.3.2.5. *cryGAL4* driver: *plc21C* silencing in CRY cells

Finally, *plc21C* KD was specifically driven by *cryGAL4* driver which expresses in the LN_vs, LN_ds, DN1_as, two DN1_ps, and two DN3s neurons (Emery *et al.*, 2000; Yoshii *et al.*, 2008).

In the Figure below (6.20), the averaged LD 12:12 locomotor patterns of the three appropriate lines are shown at both temperatures.

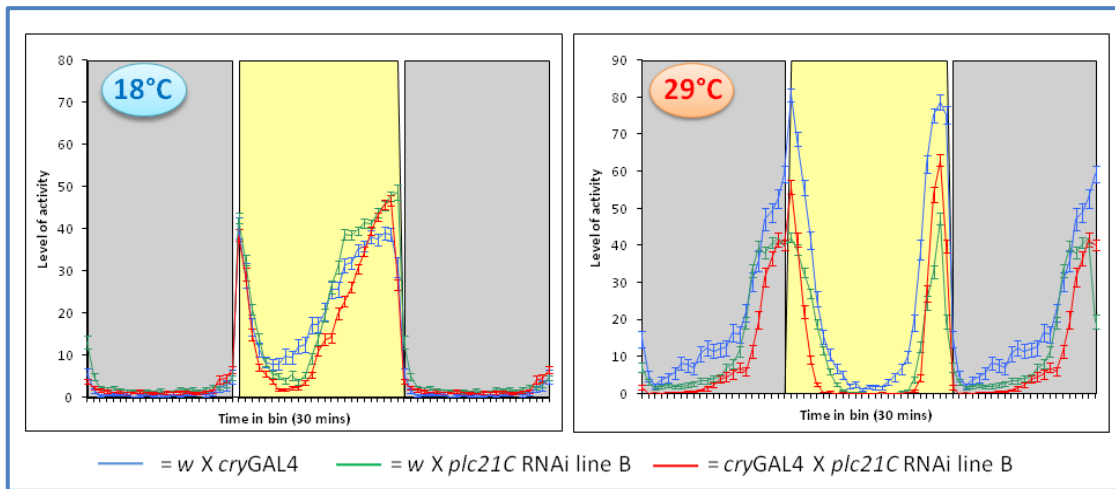


Figure 6.20: Averaged locomotor activity of flies downregulating PLC21C via *cryGAL4* and controls at 18 (left graph) and 29°C (right graph).

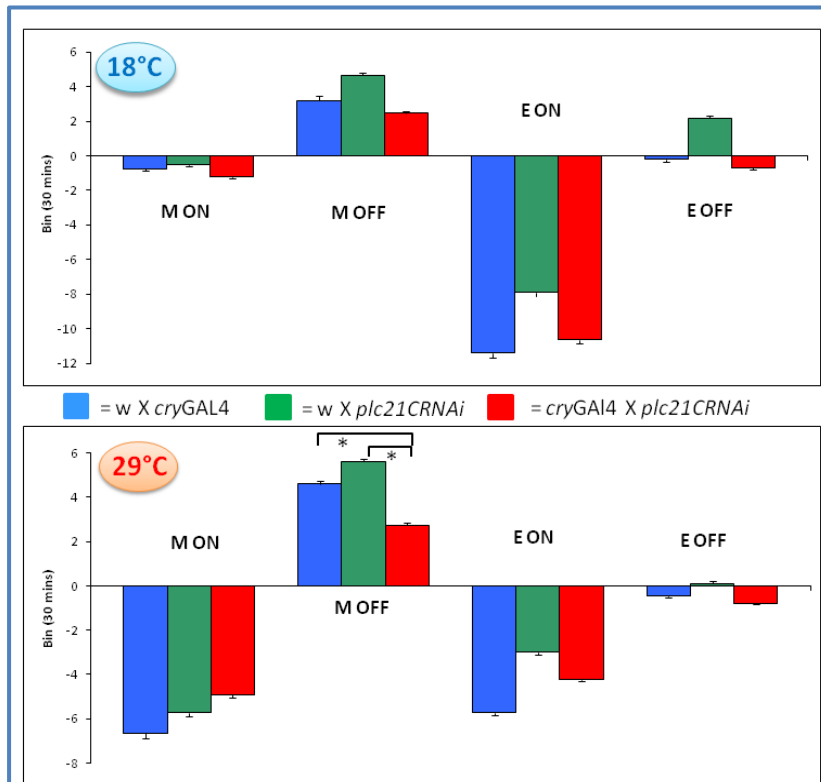


Figure 6.21: Averaged morning and evening onsets and offsets (\pm SEM) of flies downregulating PLC21C by *cryGAL4* driver and controls. Results refer to 18°C in the upper graph and 29°C in the lower graph. Asterisk indicates significant value.

Genotype	18°C					29°C				
	N	Morning onset	Morning offset	Evening onset	Evening offset	N	Morning onset	Morning offset	Evening onset	Evening offset
<i>w X cryGAL4</i>	16	-0.368	1.593	-5.706	-0.1	32	-3.318	2.3	-2.859	-0.225
<i>w X plc21CRNAi line B</i>	31	-0.258	2.326	-3.955	1.084	40	-2.860	2.808	-1.498	0.058
<i>cryGAL4 X plc21CRNAi line B</i>	28	-0.608	1.571	-5.328	-0.039	24	-2.45	1.370	-2.120	-0.391

Table 6.7: Averaged phases (expressed in h) of *plc21C* interfered flies (line B) driven by *cryGAL4* and controls at 18°C and 29°C. Significant values are highlighted.

Statistical analysis revealed a difference between controls and KD flies only in the case of the morning offset at 29°C ($F_{\text{morning offset at } 29^{\circ}\text{C}, 2,93} = 31.64, p = \ll 0.001$, Figure 6.21 and Table 6.7).

Under DD, no significant differences were obtained in free-running periods between the experimental flies and both controls.

6.4. Discussion

In order to entrain to external conditions diverse genes encoding for molecules involved in various signalling pathways are required. Moreover, the system is redundant, so impairments in one input pathway can be compensated by others. For example, in the light input to the clock, CRY and photoreceptor structures (such as compound eyes) “collaborate” for complete entrainment (Helfrich-Foster *et al.*, 2001). It is plausible that a similar *scenario* may exist for the temperature signalling cascade. In this chapter, a second phospholipase C, *plc21C* has been analysed (Shortridge *et al.*, 1991). PLC21C and NORPA share 32% of amino acids identity which is mainly based on a so called Box X, Box Y and C2 domains (Rhee *et al.*, 1989). Moreover, this second *plc21C* shares high levels of similarity with rat and bovine brain PLC β (37%, Shortridge *et al.*, 1991). In *Drosophila*, *in situ* hybridisation has detected *plc21C* signal in optic lobes and central brain (Shortridge *et al.*, 1991), where *norpa* is also localised, suggesting a possible convergence of function. Thus, in a presumptive *scenario* in which both enzymes belong to the same transduction cascade, the absence of one could be compensated by the other. Indeed, at low temperature, a higher level of *plc21C* was observed in *norpa* mutants, but transcript levels fall at 29°C (Figure 6.3). Furthermore NORPA levels revealed that the *plc21C* RNAi does not target *norpa* (Figure 6.6a and 6.6b). The level of *plc21C* was dramatically reduced in line B only compared to controls, not only for the region

recognised specifically by the siRNAs, but also for a second independent fragment upstream to the former, which excludes the existence of possible splicing variants that might escape the silencing (Figure 6.4 and 6.5).

Recently, PLC21B has been reported to be involved in olfactory transduction (Kain *et al.*, 2008) located in antennal sensory neurons. It has been shown that lack of *dgg* (a G_qα protein) together with an absence of *plc21C* gave impaired olfactory responses measured as a decrement of electrophysiological responses (using electroantennogram EAG) in these organs (Kain *et al.*, 2008). Moreover, PLC21C has also been documented to be preferentially expressed in mushroom bodies (MB, Shortridge and McKay, 1995). These are a paired neuropil structure each consisting of about 2500 neurons called Kenyon cells (Technau, 1984) which are involved in olfactory learning and memory as well as sex-specific behaviour (reviewed from Helfrich-Förster *et al.*, 2002). Behaviourally, flies carrying mutations ablating or impairing MB display aberrant locomotor phenotypes characterised by an increase in the overall level of locomotor activity (Martin *et al.*, 1998). However, the MBs are not involved in the control of the circadian activity rhythms, particularly in the output of the LN_vs pacemaker cells (Helfrich-Förster *et al.*, 2002).

Interestingly, the experiments presented in this chapter are at variance to what has been described above, because it would be expected to find an increased locomotor activity level in *plc21C* KD flies, especially when *actinGAL4* driver was used. However, an opposite effect was obtained. The global level of locomotor activity of KD *actin* driven flies resulted in a decrease of the morning and evening components at both temperatures.

Given these results and the similarity between PLC21C and NORPA proteins, a putative effect on the circadian core gene *period* was taken in consideration. As mentioned before, the absence of NORPA determines an enhancement of the “seasonal” splicing event in the 3’ UTR of *per*. Mutant flies for this PLCβ display a cold phenotype even if they are entrained at high temperature (Collins *et al.*, 2004, Majercak *et al.*, 2004). In order to investigate a possible involvement of PLC21C, unspliced and spliced variants were quantified from flies silencing *plc21C* in whole body. Since the level of *per* splicing was not significant different between experimental lines and controls at the time course analysed (Figure 6.10 and 6.11), I

further concluded and enforced the fact that these PLC21s do not share the same pathway and target. The same analysis was applied to investigate possible changes in *tim* splicing (Boothroyd *et al.*, 2007). No significant difference between the experimental lines and controls was found, indicating no involvement of PLC21C neither in this signaling cascade (Figure 6.12).

However, PLC21C does influence changes in the circadian activity profile particularly in relation to the onset and offset of morning as well as evening locomotor components. *actin*, *gmr*, *tim* and *pdf* drivers altered the morning onset mainly at low temperature (Figure 6.22). Thus, it appears that photoreceptor cells in addition to LN_vs may be important *via plc21C* to set the morning onset. Surprisingly, none of these circadian cells seems to be involved in morning onset at higher temperature. Possibly, the delay observed by *actinGAL4* at 29°C may be due to some glia cells which have been shown to be essential and crucial for a proper regulation of *Drosophila* circadian behaviour (Suh and Jackson, 2007).

The regulation of the morning offset is under circadian neuronal control (Grima *et al.*, 2004). The signal transduced by PLC21C in *tim* cells and in particular within *cry* cells, sets the timing of the morning offset at least at high temperature. The results suggest that all circadian cells apart for some DN1_{ps}, DN2 and some DN3s are involved in the perception of external temperature environmental conditions through PLC21C. At low temperature, the same cellular cluster may be involved although a significant effect was not found using *cryGAL4*. This may be due to the well documented reduction of *GAL4/UAS* efficiency at low temperature (Duffy, 2002).

The evening component was dramatically influenced when *plc21C* KD was triggered by *actin* and *tim* drivers. The first driver narrowed the evening activity at low temperature determining a delay in its upswing and an advance in the offset (Figure 6.22). The PLC21C KD by *timGAL4* generated an advance in the onset of evening activity at the two temperatures. However, it was not possible to further dissect the neurons important for this behaviour since the other silencing lines presented intermediate phenotypes. Strong candidates are Dorsal TIM⁺CRY⁻ Neurons which are affected only by *timGAL4* driver. Alternatively CNS glia cells may be affected by *plc21C* KD *via timGAL4* (Suh and Jackson, 2007). In these cells, PLC21B

may be an element important for the synchronisation of some output effectors in relation to temperature.

Driver	Locomotor components			
	M on	M off	E on	E off
<i>actin</i> GAL4	← →	← ←	→ /	← /
<i>gmr</i> GAL4	← /	/	/	/
<i>tim</i> GAL4	← /	← ←	← ←	/
<i>pdf</i> GAL4	← /	/	/	/
<i>cry</i> GAL4	/	/	/	/

← = advance → = delay / = no effect ■ = 18°C ■ = 29°C

Figure 6.22: *plc21C* KD effects on the circadian locomotor components.

As in the case of NORPA, PLC21C belongs to the β family of phospholipases which leads to the production of two second messengers, such as IP₃ and DAG. The activation of several protein kinase C isoforms (PKC) and the mobilisation of intracellular Ca²⁺ are the effects generated by the two messenger molecules (reviewed from Suh *et al.*, 2008). Both of these second messengers, interestingly, have been documented to be involved in certain aspects of circadian regulation. For instance, a role for mammal PKCs have been documented in the phosphorylation and enhancement of CLOCK transcription which culminates in a phase resetting of the circadian clock (Shim *et al.*, 2007). Therefore, it is possible that a PKC isoform in *Drosophila* triggered by PLC21C may be involved in a similar transcriptional regulating mechanism. However, it appears that the target of this process is not a core clock gene since dramatic changes in fly periodicities was not found. It is more reasonable to suggest that the effects may be directed to the regulation of some output genes which need to be thermally regulated. Ca²⁺ is also well documented to be an element involved in circadian control (review from Honma and Honma, 2003).

For instance, gene expression, PKC activation, membrane potential and neurotransmitter release are all functions modulated by this ion which is mainly stored in the endoplasmic reticulum. Therefore, it is plausible that a reduction of PLC21C would dramatically comprise the intracellular concentration of Ca^{2+} impairing several cellular processes.

Although the spatial localisation of this PLC21 β has not been investigated in this chapter, the effect obtained by downregulating *plc21C* with circadian drivers suggests the presence of this enzyme in some subset of circadian pacemakers. Additionally, the receptor biology for the PLC21C activation is not known nor the molecular and cellular output targets of this phospholipase. An interesting experiment would also be to downregulate *norpA* and *plc21C* at the same time in order to study the resulting behaviour and understand whether both phospholipase are sharing any common transduction pathway. This opens numerous gates for understanding the *plc21C* involvement for a proper regulation of *Drosophila* circadian behaviour.

6.5. Conclusions

- *plc21C* downregulation does not influence NORPA level nor *per* (or *tim*^{cold} splicing), so *plc21C* affects temperature responses *via* a *norpA* independent route.
- Circadian neurons express *plc21C* since its downregulation generates changes in the locomotor behaviour at the two temperatures analysed. In relation to the *plc21C* KD, I found that:
 - The morning behaviour is shifted *via* PDF⁺ cells and photoreceptors at cold temperature whereas by CRY⁺ cells in hot temperature.
 - The evening behaviour is shifted *via* DNs in both temperatures.

Chapter 7. Are *glass*^{60j}*cry*^b flies really circadian blind?

gl^{60j}*cry*^b flies have been reported to be circadian blind since they are not able to synchronise to any LD regime. In this chapter, their locomotor behaviour has been reevaluated in order to reveal any residual light entrainment.

7.1. Introduction

Light is the most salient environmental input into the circadian clock of *D. melanogaster*. The clock machinery is normally reset by light signals on a daily basis. These are transduced into the circadian clock by a rhodopsin mediated phototransduction cascade (Montell, 1999) but also *via* the *cryptochrome* mediated pathway (Stanewsky *et al.*, 1998; Figure 7.1). Phototransduction *via* rhodopsin is blocked in *norpA*^{p41} mutant flies. The *norpA* gene encodes for a phospholipase C (PLC), which is involved downstream of the rhodopsin phototransduction cascade (Montell, 1999). In *norpA*^{p41} mutants the phototransduction signalling in the compound eyes and ocelli is affected (Pearn *et al.*, 1996). *cry* encodes for a flavin based blue light photoreceptor cryptochrome and its function is completely or nearly abolished in *cry*^b mutant flies (Stanewsky *et al.*, 1998). In general, despite the fact that light resets the circadian clock, an uninterrupted light exposure results in arrhythmic behaviour in wild-type flies. In this condition, the constant light (LL) collapses the clock mechanism (Price *et al.*, 1995): TIM is continuously degraded by CRY, which ultimately results in the interruption of the negative feedback loop. The mutation in CRY "immunises" the circadian clock to the collapsing effect of LL, so *cry*^b flies show rhythmic free-running behaviour in LL, as if they were in DD conditions (Emery *et al.*, 2000). Double mutants, carrying *norpA* and *cry* mutations, are still able to synchronise to light-dark cycles but it takes them much longer to be entrained to a shifted LD cycle.

However, it has been reported that *cry*^b in association with a mutation in *glass* gene makes flies "circadian blind" (Helfrich-Förster *et al.*, 2001). *glass*^{60j}, arrests the development of photoreceptor cells (Moses *et al.*, 1989), and as GLASS is a transcriptional factor, its absence disrupts the development of photoreceptor structure in ocelli, all retinal photoreceptor cells, the primary and secondary

pigments in the compound eyes, H-B eyelets and some of the DN1s (Moses *et al.*, 1989; Helfrich-Förster *et al.*, 2001, Veleri *et al.*, 2003; Figure 7.1).

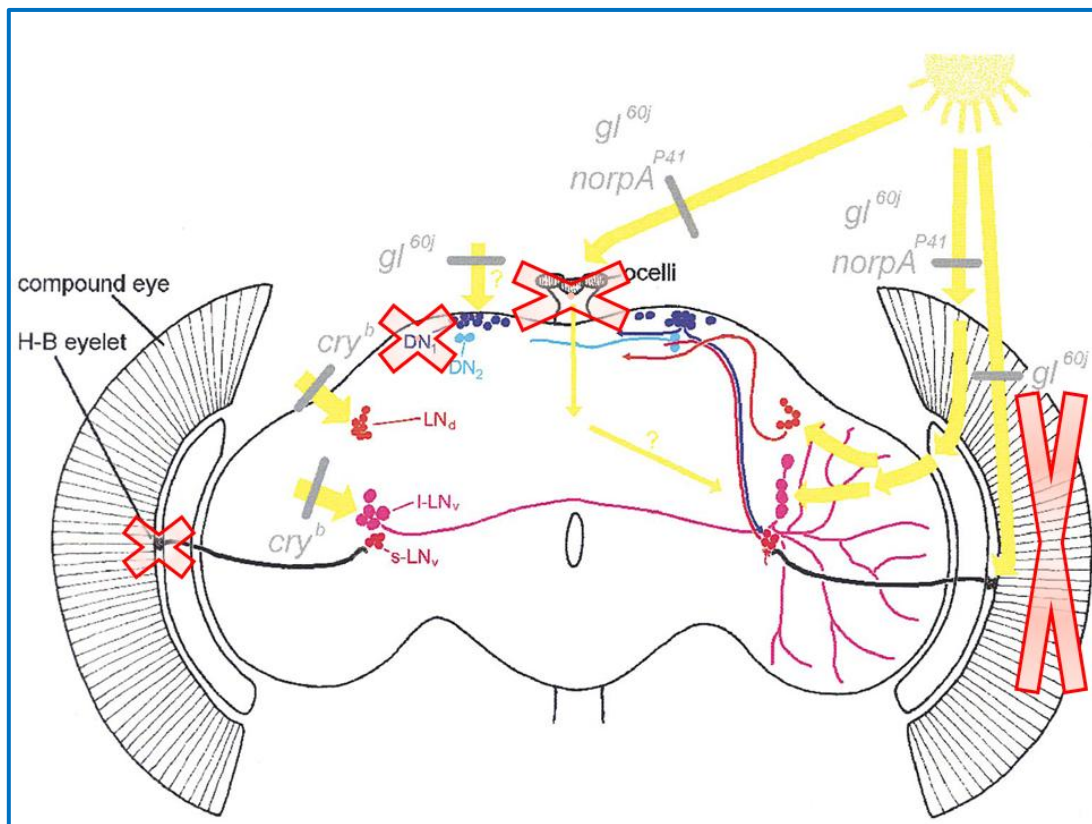


Figure 7.1: Schematic representation of $gl^{60j}cry^b$ brains. Crossed are the structures eliminated by the two mutations.

The locomotor activity profile of these double mutants has been described as a result of ‘masking’ by which the light/radiant energy directly influences the activity level bypassing the circadian clock. However, it has also been reported that DN3 neurons are still entrainable by light in flies lacking of CRY and GLASS (Veleri *et al.*, 2003). In this chapter the activity of this double mutant was re-analysed in order to understand if any residual light entrainment activity could be revealed.

7.2. Materials and Methods

7.2.1. $glass^{60j}$ and cry^b mutations

Before analysing locomotor activity profiles of $yw; +; gl^{60j}cry^b$ flies, they were tested to confirm their genotype. As mentioned before $glass^{60j}$ mutants are devoid

of all photoreceptor structures. The mutation is characterised by an insertion of a P-element in the *glass* coding sequence (Moses *et al.*, 1989). A molecular strategy to verify the mutation was not available but the mutant showed a specific phenotype that made the insertion easy to be spotted. In the Figure below (7.2), wild-type, *gl^{60j}* and a recombinant in *gl^{60j}cry^b* background (discussed in Chapter 8) are shown.

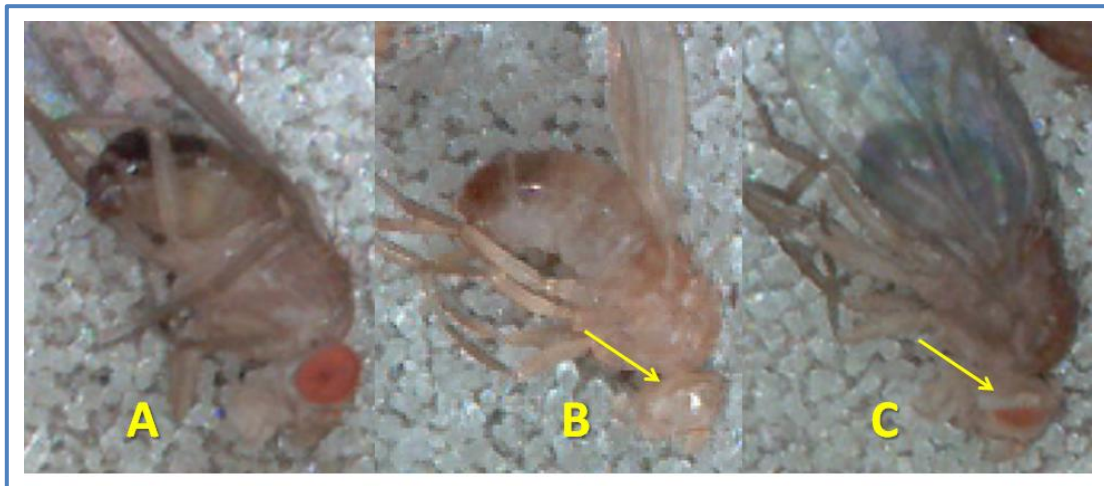


Figure 7.2: *glass^{60j}* phenotype. A) Canton-S; B) *glass^{60j}* and C) example of flies in which a RNA interference construct (described in the Chapter 8) was recombined with *glass^{60j}cry^b*. In this latter individual, *glass* phenotype is easily distinguishable: a reduction in the photoreceptor number which causes smaller eyes.

cry^b introduces a restriction site into the *cryptochrome* sequence, and this SNP was adopted as a diagnostic. The strategy used was based on a PCR amplification of a region including the mutation (from nucleotides 1116 to 1299) followed by a restriction reaction utilising the *BsmI* enzyme (restriction site introduced by the mutation). In Figure 7.3 is shown the difference between a wild-type *cry* sequence compared to *cry^b*.



Figure 7.3: Wild-type and *cry^b* sequences. The single nucleotide mutation is coloured in both sequence (red for the wild-type nucleotide and green for the missense mutation). *BsmI* restriction site, introduced by the mutation, is underlined.

Thus, in the presence of *cry^b* mutation, after PCR and restriction reactions, two bands were expected, whereas in the case of wild-type a single band was observed due to the inability of *BsmI* to cut the PCR product. In Figure 7.4 is shown an agarose

gel where five independent *glass^{60j}cry^b* flies were tested for the *cry* mutation together with Canton-S, *w¹¹¹⁸*, *cry^b* and *glass^{60j}* flies.

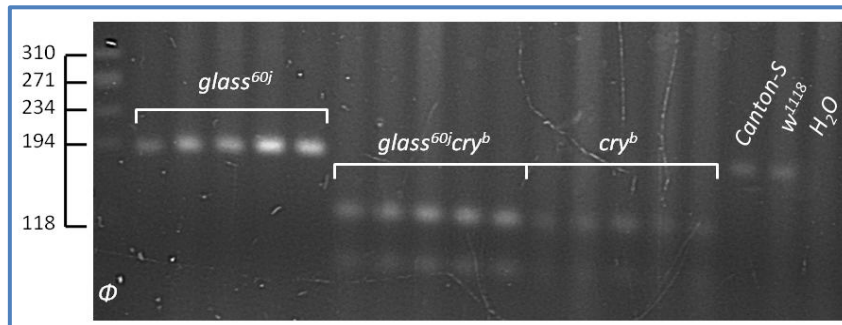


Figure 7.4: Electrophoresis in a 2% agarose gel of samples supplied to a restriction reaction with *BsmI*. Five independent samples of each genotype (*glass^{60j}*, *cry^b* and *glass^{60j}cry^b*) and controls (CantonS, *w¹¹¹⁸* and water) are shown.

7.3. Results: Locomotor activity of *glass^{60j}cry^b* mutants

7.3.1. *gl^{60j}cry^b* locomotor activity in LD regime

The locomotor activity profile of *glass^{60j}cry^b* double mutant was monitored under different temperatures at 18 and 25°C. In the Figure below (7.5), the activity profile is shown in LD 12:12 at 18 and 25°C.

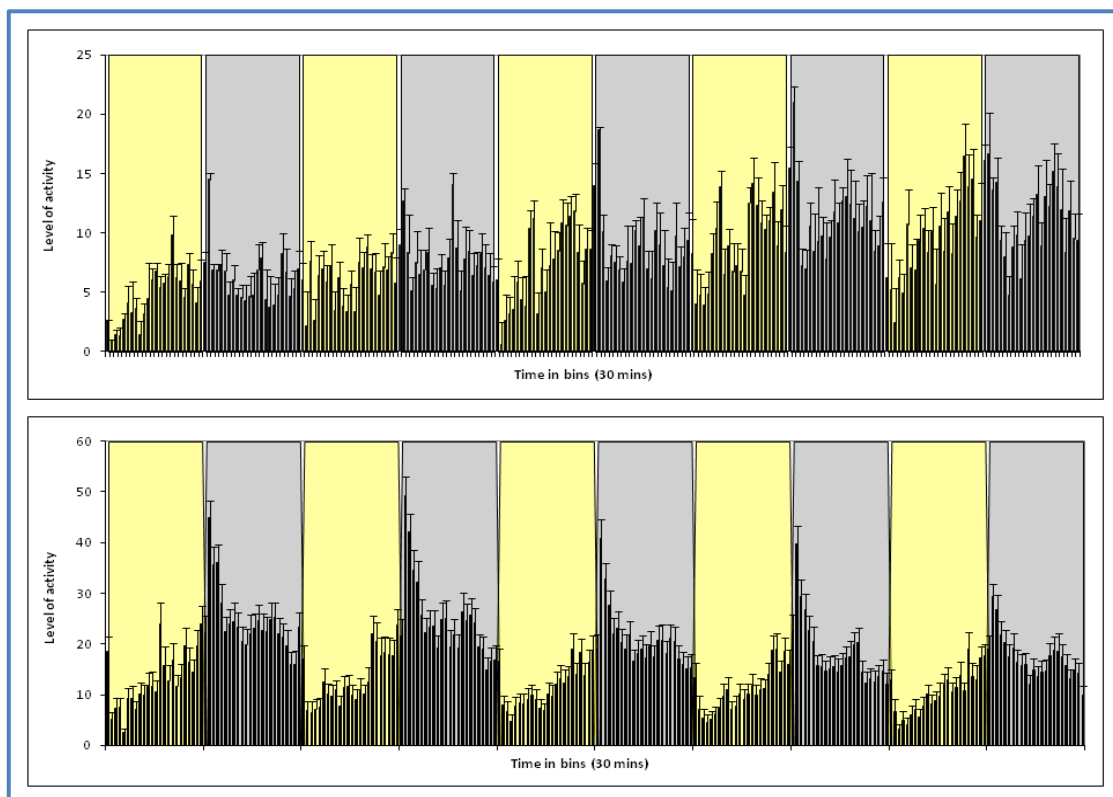


Figure 7.5: Averaged activity profiles of *glass^{60j}cry^b* flies subjected to 6 days under LD 12:12 at 18 (top; N= 54) and 25° C (bottom; N= 114). Yellow bars indicate the light phase whereas grey represents the dark phase.

The locomotor activity profile of *glass^{60j}cry^b* mutants has been reported to be unentrainable under LD cycles at 25°C (Helfrich-Forster *et al.*, 2001). As shown in the Figure 7.5, this was indeed the case for mutant flies tested at 18°C, but not for those at 25°C. In both temperatures, there was an absence of the morning peak but at 25°C activity began to increase before the light on/off transition, indicating entrainment in this condition. Furthermore the activity pattern at 25°C was more defined and rhythmic for the duration of the experiment than the lower temperature, where a clearly rhythmic profile was not present. The locomotor activity of individual flies was analysed by spectral and autocorrelation methods (see Section 2.18) at both temperatures for five days worth of data.

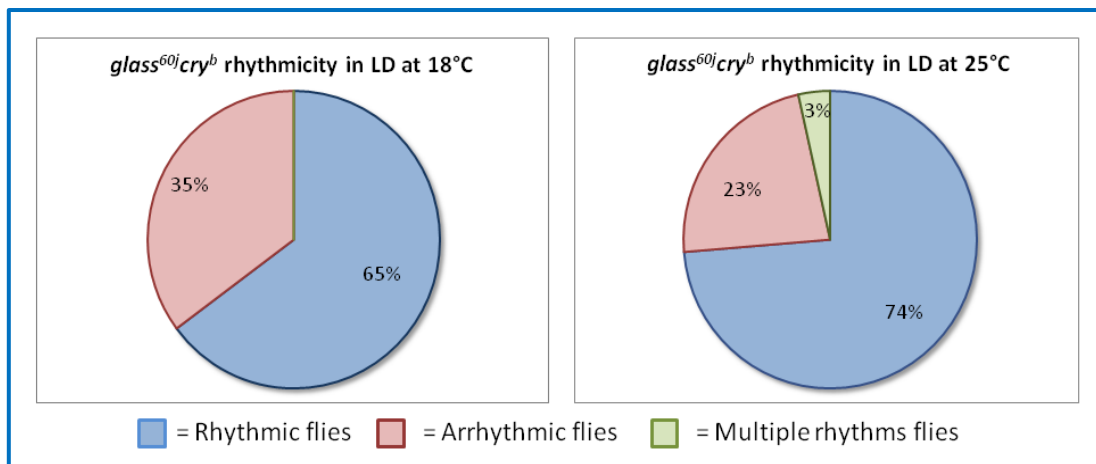


Figure 7.6: Percentage of rhythmic and arrhythmic *gl^{60j}cry^b* flies in LD at 18°C (left panel) and 25°C (right panel).

The great majority of flies behaved rhythmically, as expected, with a period in the circadian range of 23.85 ± 0.11 at 18°C and 23.68 ± 0.16 at the higher temperature. However at 25°C, a small portion of flies presented two significant peaks of rhythmicity varying between 20 and 24 hours. Thus the overall patterns of behaviour shown in Figure 7.6 reveal that flies are individually rhythmic, but not synchronised with respect to each other at 18 ° C, whereas this harmony is enhanced at 25° C (Figure 7.5).

7.3.2. *gl^{60j}cry^b* locomotor activity in DD regime

Mutant locomotor activity profiles were monitored for 6 days in constant darkness at 18 and 25°C. In this way, the endogenous periodicity of each fly could be

computed without any interference from external stimuli. As shown in Figure 7.7, the activity pattern of the double mutants was not synchronised once they were released in DD at both temperatures.

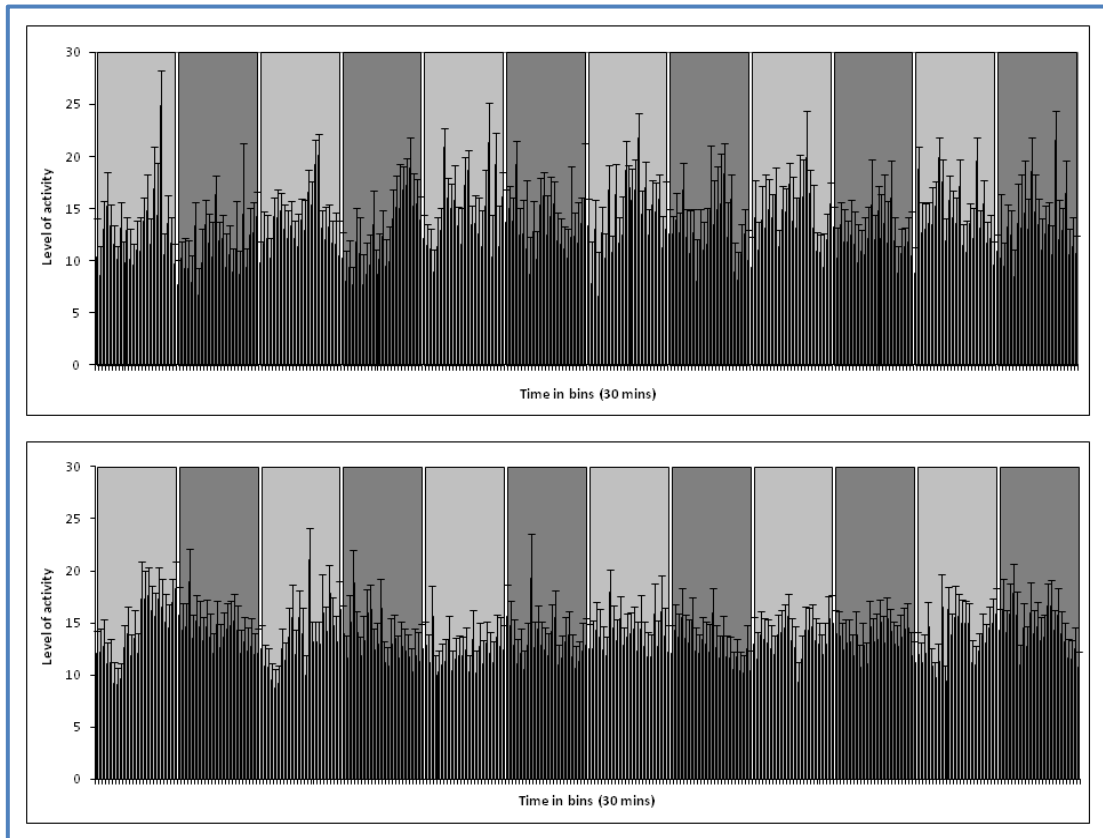


Figure 7.7: Averaged locomotor activity profiles of *glass^{60j}cry^b* flies subjected to 6 days in DD regime are shown at 18 (top; N= 49) and 25°C (bottom; N= 48). Grey bars indicate subjective days. The previous entrainment days are not shown.

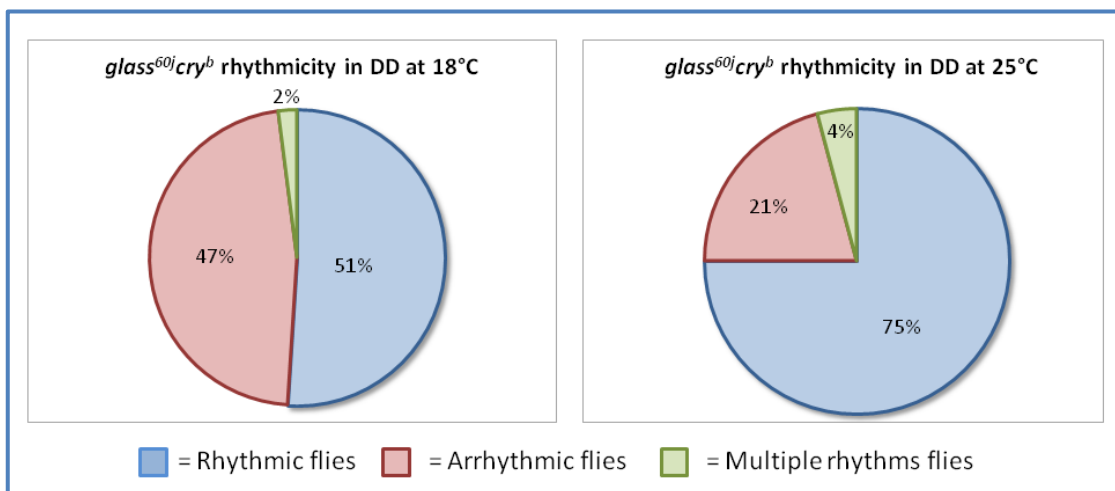


Figure 7.8: Percentage of rhythmic and arrhythmic flies in DD at 18 (left panel) and 25°C (right panel).

The averaged actogram presented in Figure 7.7 may be again interpreted as a loss of rhythmicity in the double mutant. However, analysis of each single individual revealed a large number of rhythmic flies especially at 25°C (Figure 7.8). The periods at both temperatures are characterised by circadian values (23.84 ± 0.17 at 18°C and 24.01 ± 0.13 at 25°C). The flies are thus simply desynchronised and each running with an independent phase. Furthermore, temperature has an effect in their ability to be synchronised with better synchrony observed in LD at the higher temperature.

7.3.3. *gl^{60j}cry^b* locomotor activity in LL regime

glass^{60j}cry^b mutants were tested under constant bright light (LL) at 18°C as well as 25°C. This condition generates arrhythmicity in wild-type flies since TIM protein is constantly degraded by activated CRY (Price *et al.*, 1995).

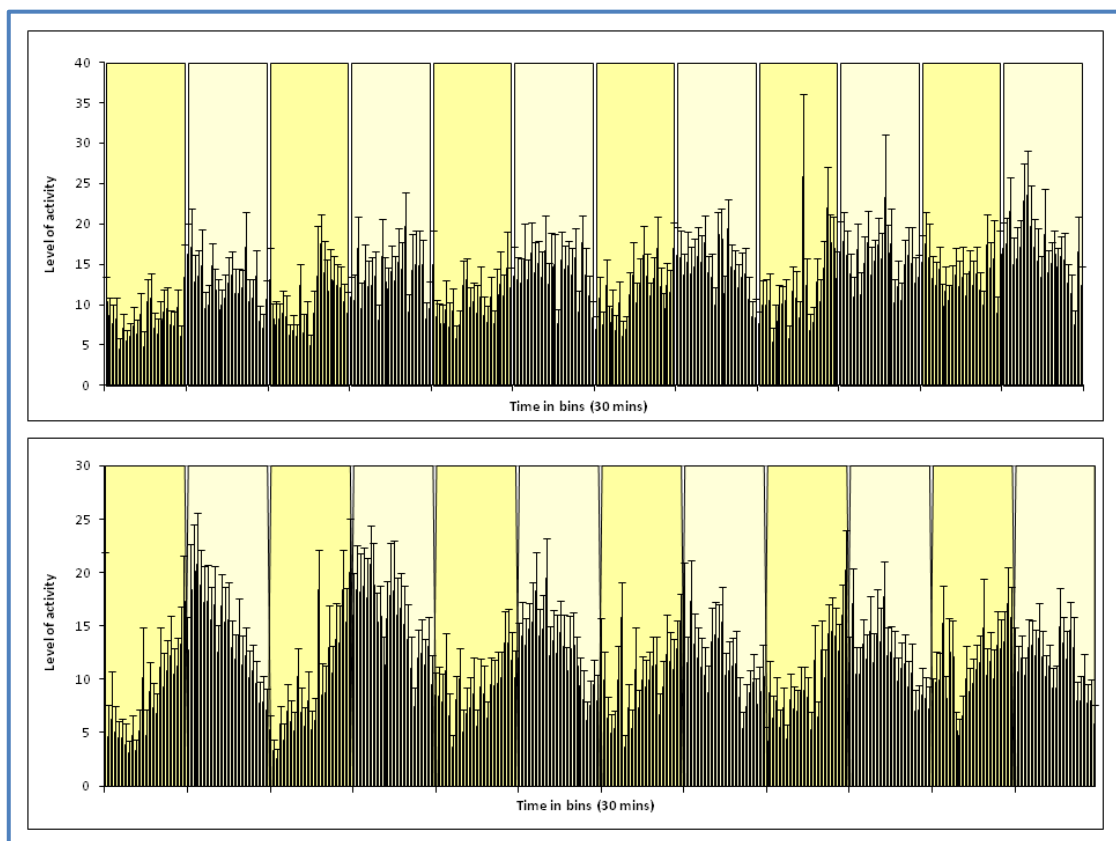


Figure 7.9: Averaged locomotor activity profiles of *glass^{60j}cry^b* flies. 6 days in LL regime are shown at 18 (top; N= 58) and 25°C (bottom; N= 38). Strong yellow bars indicate subjective days whereas light yellow bars subjective nights. The previous entrainment days are not shown.

Figure 7.9 shows how *glass^{60j}cry^b* activity profile at 25°C appeared to be more rhythmic than at 18°C. Mutants were characterised by an increase of activity before the subjective “light off” and a decrease of activity after the subjective light on/off transition, presenting constantly this profile pattern for the entire length of the experiment. Furthermore, this profile resembled the one observed in LD conditions. On the contrary, at 18°C flies did not present this clearly rhythmic behaviour. In order to confirm this observation, rhythmicity was analysed statistically in each individual (Figure 7.10).

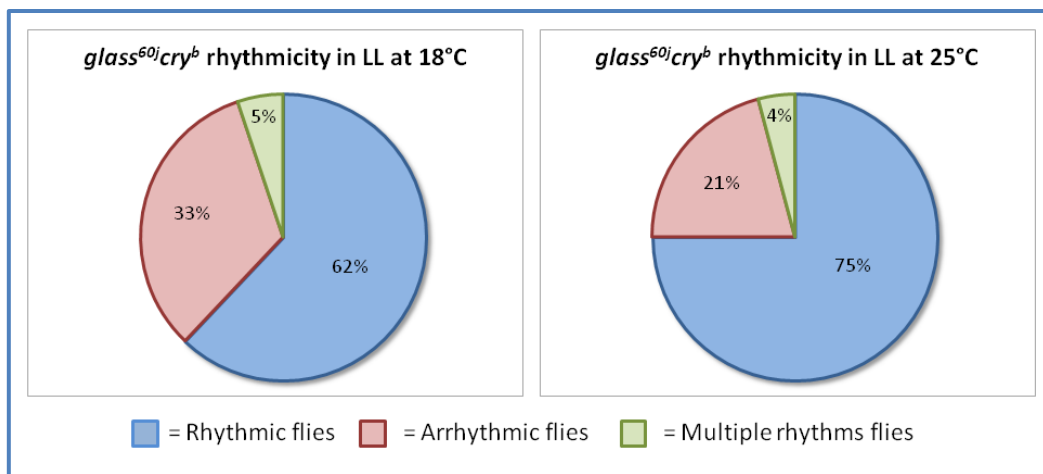


Figure 7.10: Percentage of rhythmic and arrhythmic flies subjected to LL regime at 18 (left panel) and 25°C (right panel).

Between 62-75% of flies displayed a significantly rhythmic behaviour by spectral analysis and autocorrelation. The period values fell between 24.00 ± 0.15 (N = 36) at 18°C and 24.01 ± 0.01 (N = 36) at 25°C. However, as in the case of LD and DD regimes, flies entrained better at high temperature than the lower one .

7.3.4. Are temperature fluctuations influencing *gl^{60j}cry^b* locomotor activity ?

In order to evaluate if “light on/off” transitions could affect the behaviour of flies *via* temperature changes, locomotor activity was recorded by maintaining the incubator in the LD 12:12 regime, but shielding flies from the light. In this way, flies were subjected to a free-running condition but synchronised by possible temperature change generated by the “light on/off” event. In Figure 7.11 are shown the locomotor profiles obtained at 18 and 25°C.

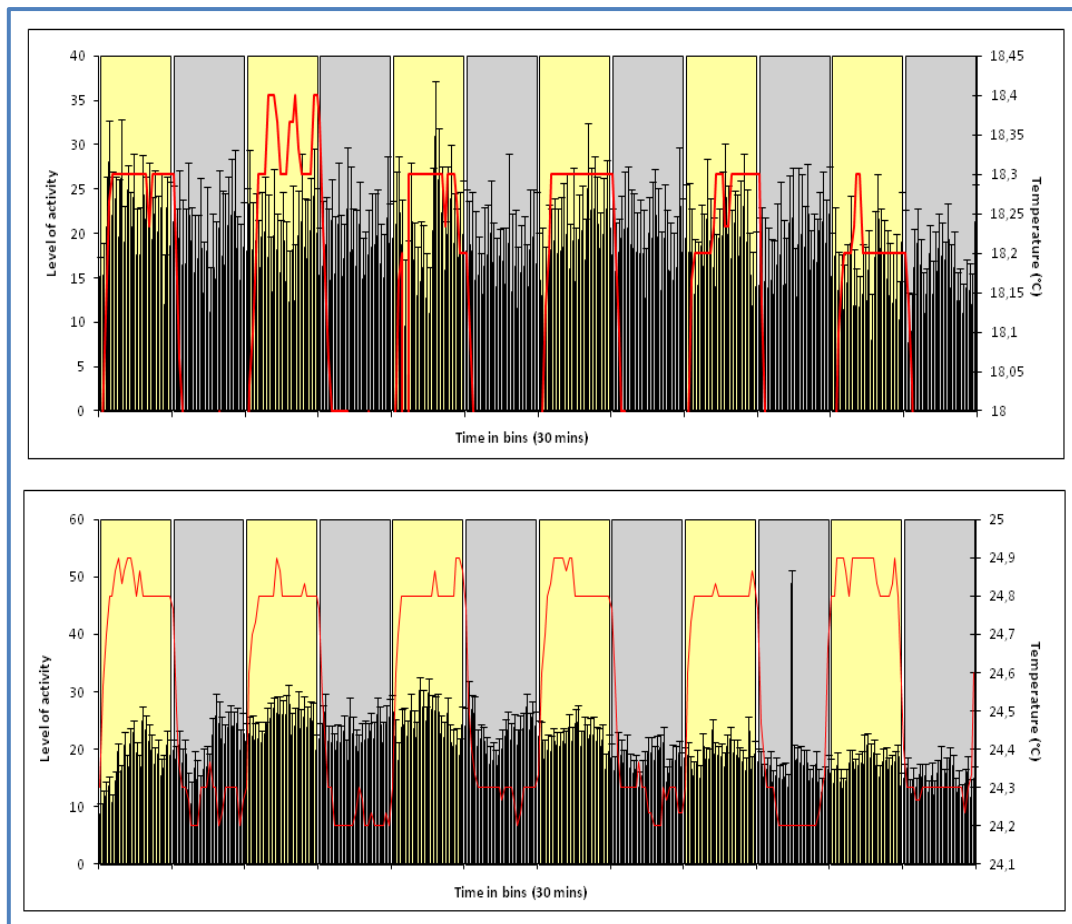


Figure 7.11: Averaged locomotor activity profiles of *glass^{60j} cry^b* flies at 18 (top; N= 47) and 25°C (bottom; N= 57). Locomotor activity was recorded in DD by shielding flies from the light but allowing entrainment by possible changes in temperature inside the incubator. Yellow bars indicate subjective days, whereas grey bars indicate subjective night. Red line indicates the measurement of temperature during the experiment.

At both temperatures, the behavioural activity profiles were not similar to those observed under LD. Even if the alteration between the photo and scotophase produced a variation in temperature within a range of 0.4°C at 18°C and 0.7°C at 25°C, this fluctuation was not sufficient to entrain the clock of this double mutant strain. In fact, the locomotor activity was very similar to the locomotor patterns found in DD at the respective temperatures, allowing us to conclude that light is the main cue that entrains the activity of this circadian ‘blind’ mutant. Furthermore when the locomotor activity periods were analysed, they were found to be characterised by circadian values (23.84 ± 0.15 [N = 25] at 18°C and 24.14 ± 0.11 [N = 43] at 25°C) and the number of rhythmic flies was not different from those described in DD (Figure 7.12). This experiment reveals that light is the stimulus that synchronises the activity of these double mutants, and not temperature fluctuations.

In fact, the variation between the light and dark phases was well below 3°C which is presumed to be the entrainment threshold to synchronise *D. melanogaster* locomotor activity through temperature cycles (Wheeler *et al.*, 1993). In other words, the double mutant is not circadian blind at higher temperatures.

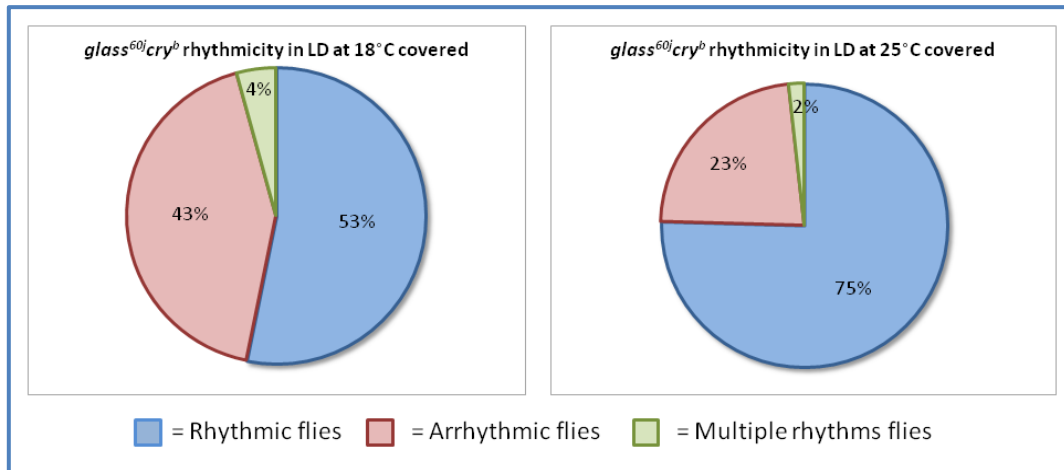


Figure 7.12: Percentage of arrhythmic and rhythmic flies at 18 and 25°C exposed to LD temperature fluctuations but subjected to free-running.

7.3.5. *gl^{60j}cry^b* locomotor activity under different LD regimes

In order to evaluate and confirm the ability of this double mutant to be synchronised by light, further experiments were carried out varying light/dark phases. Thus, the locomotor activity profiles of *glass^{60j}cry^b* flies were entrained under LD 12:12 conditions and subjected to a new photoperiod of LD 18:6 or to a shift of six hours at 25°C (Figure 7.13).

The figures below show how *glass^{60j}cry^b* flies were synchronised immediately to the new light/dark cycle. Under both conditions, these mutants showed an activity profile similar to the pattern described in the LD 12:12 regime at 25°C.

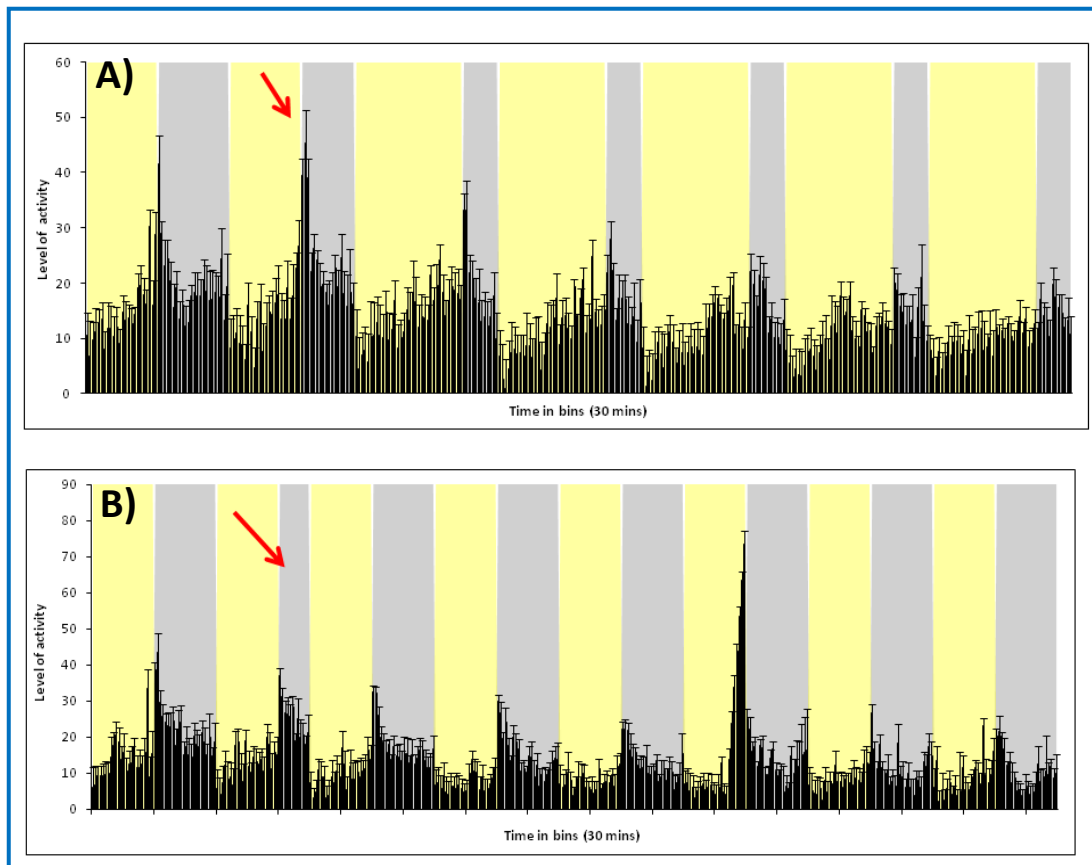


Figure 7.13: Averaged locomotor activity profiles of *glass^{60j}cry^b* flies at 25°C. Flies were entrained in LD 12:12 for 2 days and then sent to a LD 18:6 regime (panel A, N = 23) or to a new LD 12:12 regime shifted by 6 hours from the previous one (panel B, N = 24). The red arrow indicates the night in which the photoperiod was shifted.

Subsequently, another set of experiment was set up to evaluate the ability of this mutant to entrain to light phases. Flies were exposed to three days in LL or DD, after the canonical three days in LD 12:12 of entrainment. They were then released back to LD, LL or DD depending on which light/dark condition they were subjected in the previous three day cycle (Figure 7.14 and 7.15). The following figures show the results obtained in these experiments.

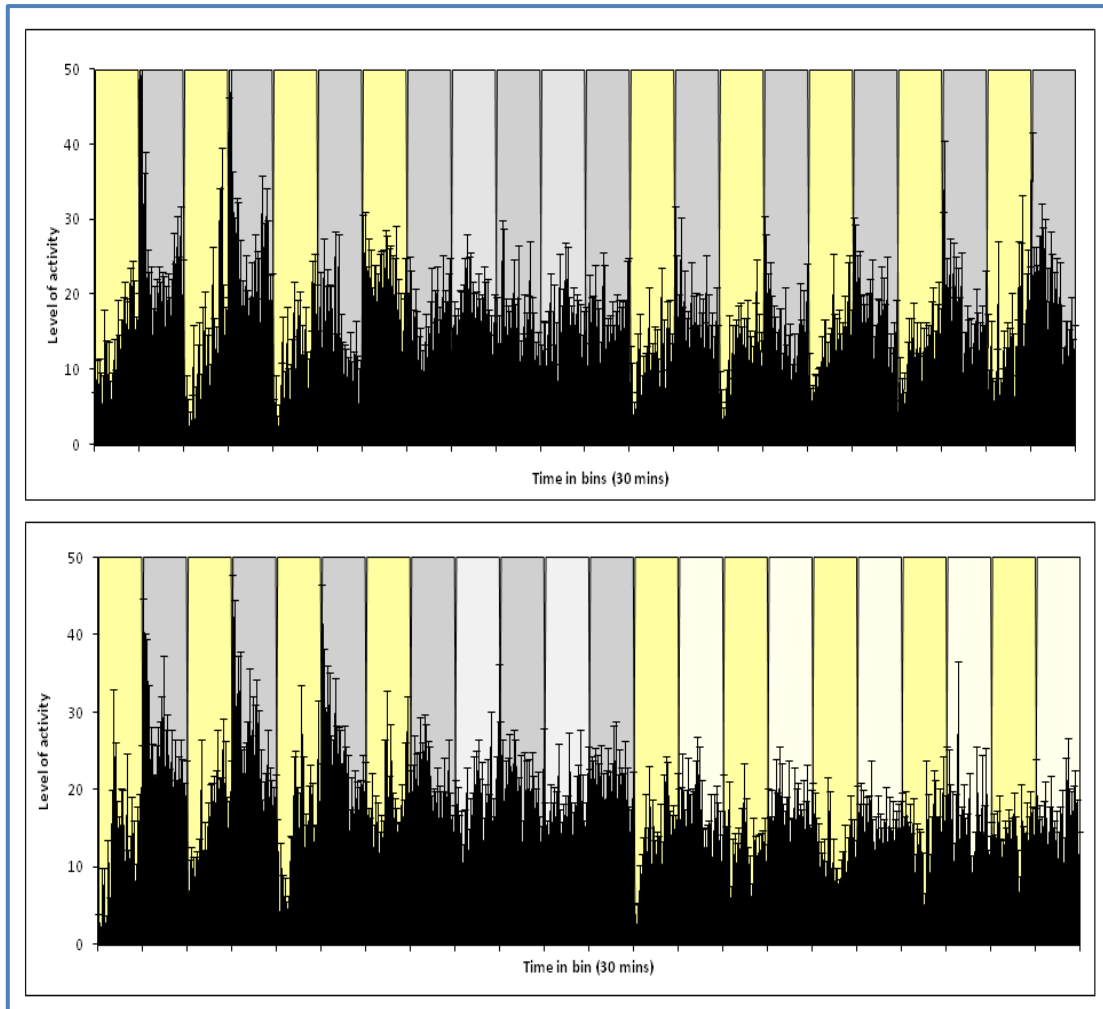


Figure 7.14: Averaged locomotor activity profiles of *glass^{60j}cry^b* flies at 25°C in different light/dark regimes. Flies were entrained for 3 days under LD 12:12 and then released in DD for other three days. Subsequently, their locomotor activity was monitored for 5 days in LD 12:12 (top; N= 21) or LL (bottom; N= 19).

gl^{60j}cry^b mutants were subjected to three days of constant darkness and subsequently, released back to LD or LL (Figure 7.14). The intermediate phase in DD did not appear to dramatically impair the ability of these strains to entrain to a further LD regime. However, in LD as well as LL, the strong anticipation of “light on/off” event became stable starting from the third cycle of LD. In LL this aspect was not as pronounced as in LD, although a weak anticipation was present.

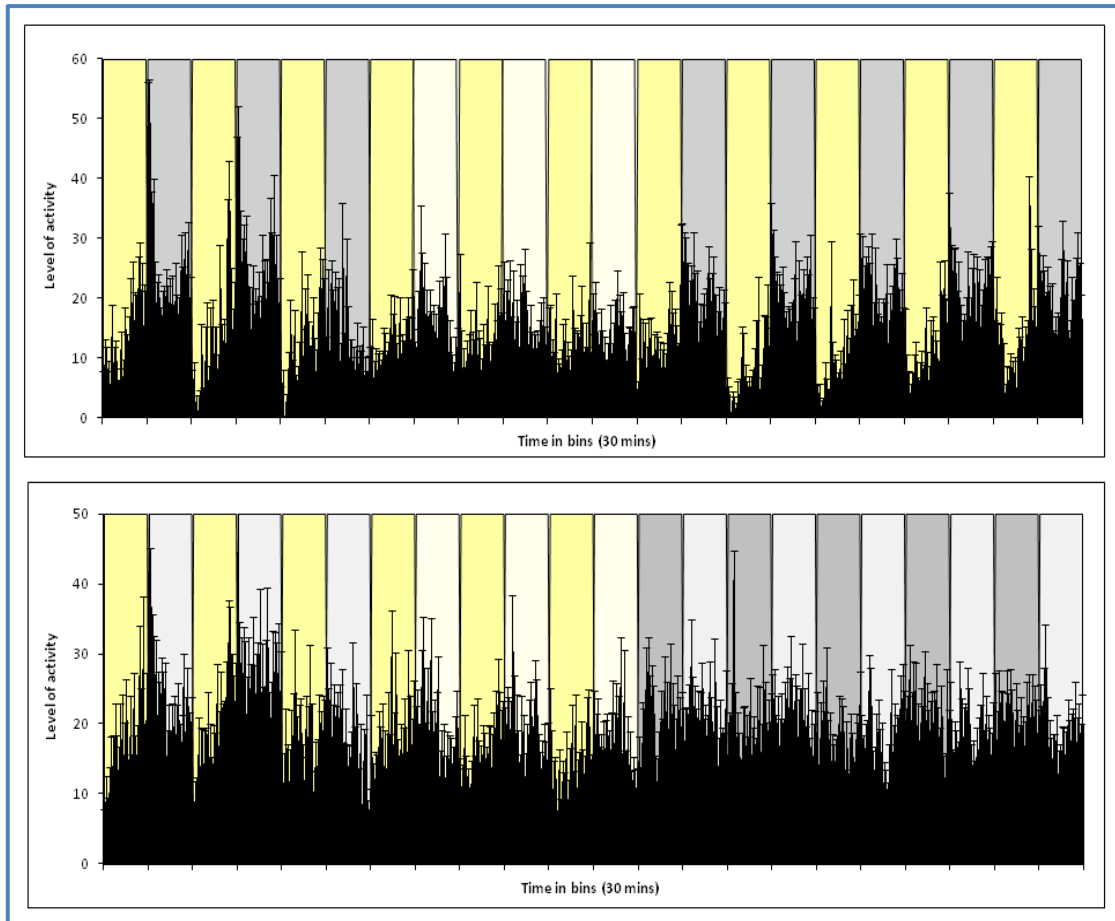


Figure 7.15: Averaged locomotor activity profiles of *glass^{60j}cry^b* flies at 25°C in different light/dark regimes. Flies were entrained for 3 days under LD 12:12 and then released in LL for three days. Subsequently, their locomotor activity was monitored for 5 days under LD 12:12 regime (top; N= 15) or DD (bottom; N= 16).

As in the case of the previous DD experiment, the synchronisation of mutants was not affected if they were placed for three days in LL (Figure 7.15). Flies easily restored the LD phenotype in a stable manner after two consecutive cycles. On the other hand, flies released into DD did not synchronise.

7.3.6. *gl^{60j}cry^b* locomotor activity under temperature cycles

Finally, the locomotor activity profiles of *glass^{60j}cry^b* mutants was analysed in diverse temperature cycling schedules in which thermal cycles were placed in opposition to normal photo and scotophases. In one case, the “light/day” portion was set at 25°C and the “night-time” at 18°C whereas the opposite was used in the second set of experiments, entraining flies at 18°C during the “light/day” part and at 25°C during the night-time. Furthermore, these temperature fluctuations were

combined with diverse lighting regimes, such as LD 12:12, DD or LL. In the figures below are presented the averaged locomotor activity profiles of *glass^{60j}cry^b* mutants in these regimes.

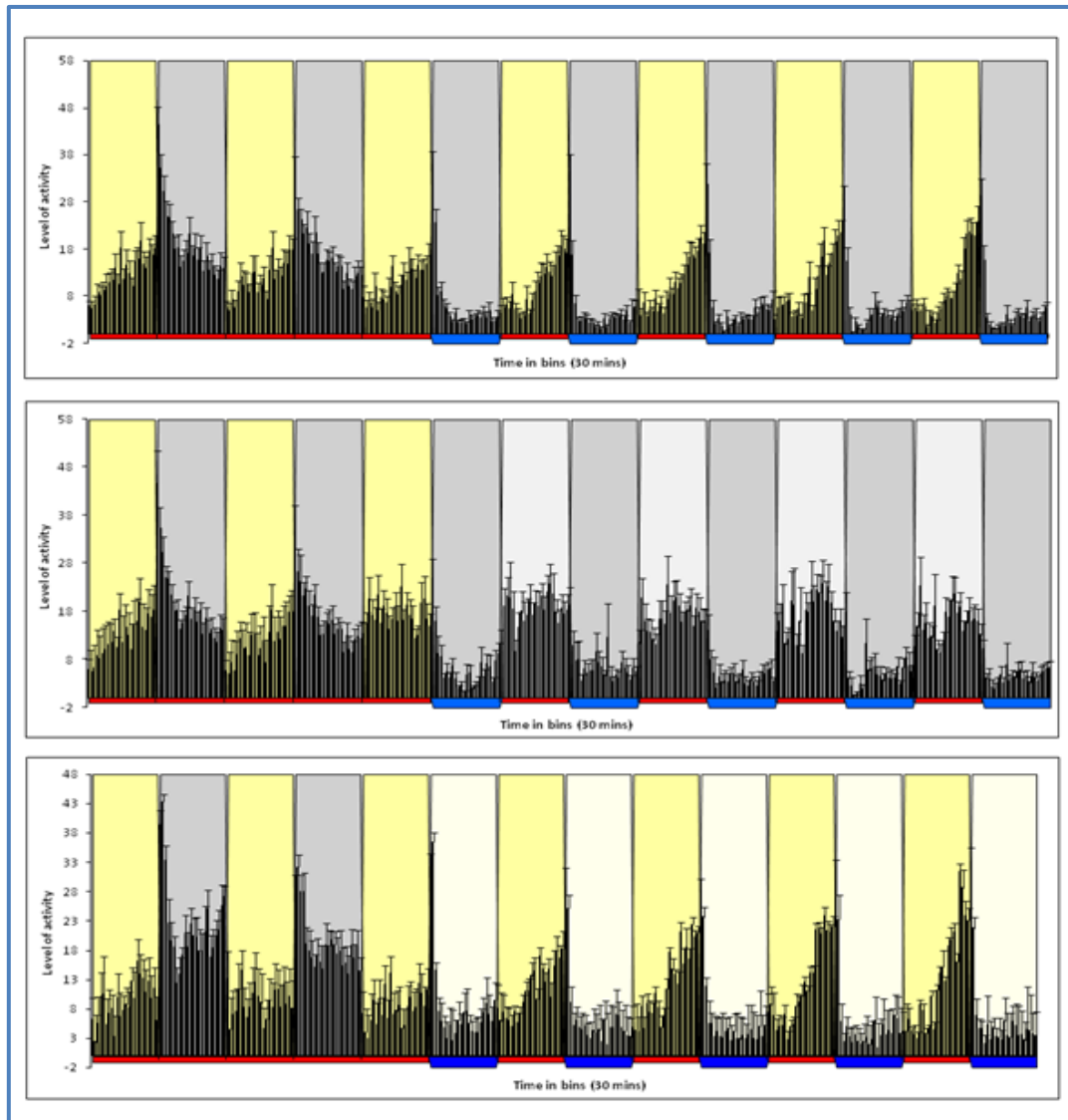


Figure 7.16: Averaged locomotor activity profiles of *glass^{60j}cry^b* flies in 25:18°C temperature cycles. Three different entrainment conditions are shown: LD 12:12 (top; N= 54), DD (middle; N= 46) and LL (bottom; N= 31). Flies were entrained for 2 days in LD 12:12 at constant 25°C before the experiment began. Red and blue bars indicate thermophase (25°C) and cryophase (18°C) respectively.

In the graphs above are shown the activity of *glass^{60j}cry^b* mutants in a temperature cycle where the thermophase (25°C) was applied during the day or during the subjective days (in DD and LL experiments). During the first two days of entrainment (at constant temperature) all flies presented the characteristic profile already described in LD at 25°C. This activity pattern was also maintained in

temperature cycles in LD and LL. The correspondence of light and warm temperature was able to evoke the anticipation event (i.e. progressive increasing of locomotor activity). This point was reinforced by the activity profile observed in DD: mutants reacted to the change in temperature by passively increasing immediately their activity in response to the temperature and decreasing it as the temperature decreased. This is called ‘masking’.

The same experiment was set up by inverting the temperature cycles during the 24 h: the thermophase was applied during the dark phase or the subjective night (in DD or LL) whereas the cryophase was set during the light phase or subjective day.

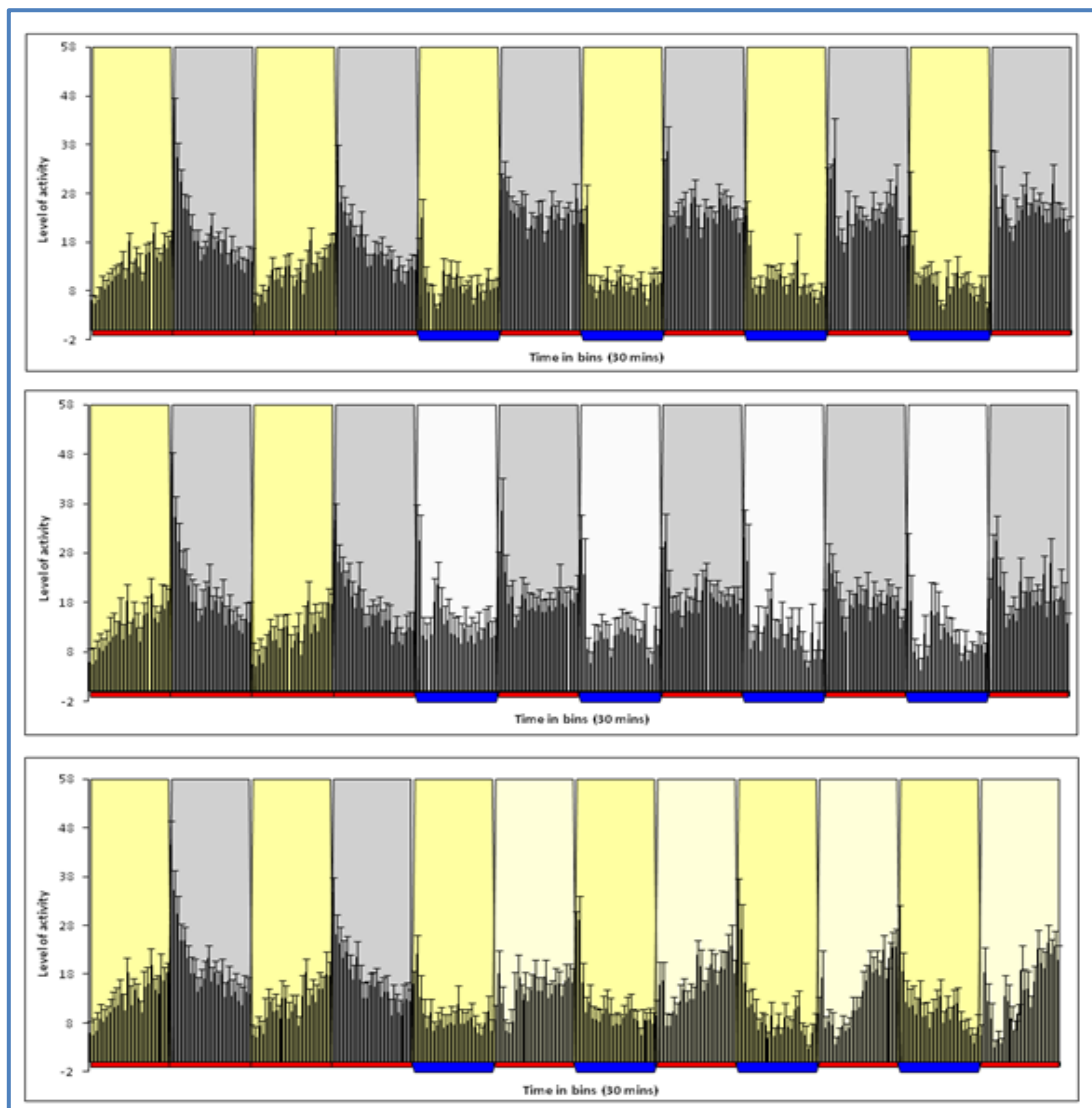


Figure 7.17: Averaged locomotor activity profiles of *glass^{60j}cry^b* flies in 18:25°C temperature cycles. Three different light/dark conditions are shown: LD 12:12 (top; N= 61), DD (middle; N= 31) and LL (bottom; N= 32). Flies were entrained for 2 days in LD 12:12 at 25°C before being subjected to the temperature cycle.

Flies were entrained for two days in LD at constant 25°C and then subjected to temperature variations and different LD conditions. In LD at 25°C, mutants were characterised by the expected locomotor activity. However, when the temperature cycles were applied, a masking effect emerged in LD and DD, where flies suddenly increased their activity as the temperature “stepped up”. Surprisingly, in LL, these mutants restored the anticipation effect during the thermophase at the second temperature cycle. This indicates again that the anticipation phenomenon coincides with the presence of light and high temperature. This conclusion is supported by the following experiment (Figure 7.18). Flies were subjected to temperature cycles (12 h at 25°C and 12 h at 18°C) but the photoperiods were placed out of step to the temperature alternation by 6 h. Thus, flies experienced “light off” transition in the middle of warm temperature and the “light on” event during the cryophase.

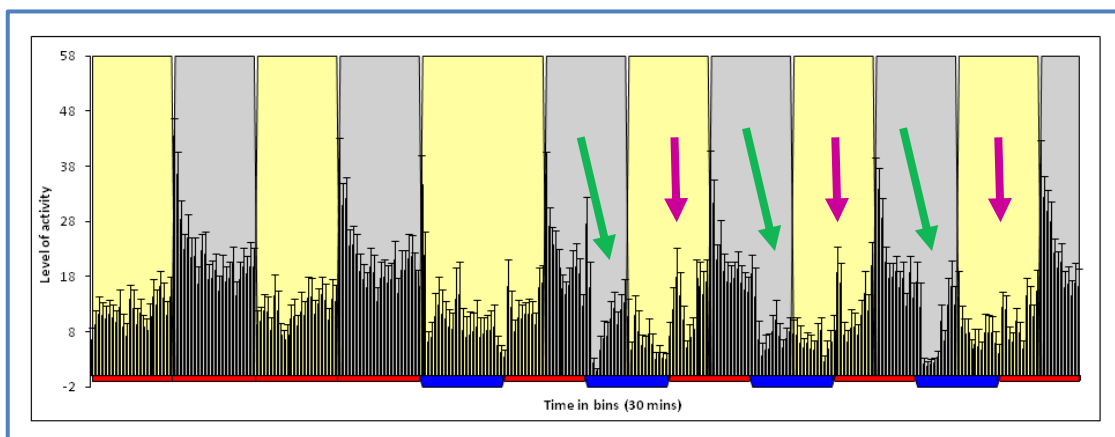


Figure 7.18: Averaged locomotor activity profiles of *glass^{60j}cry^b* flies in 18:25°C temperature cycles (N = 33). Flies were entrained for 2 days in LD 12:12 at 25°C before being subjected to temperature cycle. At the same time, the photoperiod was delayed of 6 h.

As described before, the presence of high temperature and light determined the anticipation of the evening activity component. This behaviour was not present in the first temperature cycle but became stable and robust from the second day onwards. The temperature drop caused a drastic decrease of locomotor activity during the dark phase. However, although the light off/on transition was in the middle of the cryophase, an anticipatory behaviour was observed (green arrow). This appeared from the first temperature cycle and remained stable for the entire duration of the experiment. Finally, a burst of activity (startle) was present at the cryophase/thermophase transition (violet arrow) but this component seemed to

dissipate during of experiment suggesting a masking effect of the sudden increase in temperature.

7.4. Discussion

D. melanogaster uses diverse light input structures and molecules to pass information to circadian cells which allow the fly to appropriately adapt locomotor activity to the existing conditions. In light-dark, the modulation of the morning surge depends on morning cells (MO, PDF⁺ neurons, Grima *et al.*, 2004) and the evening activity on the evening cells (EO, CRY⁺PDF⁻ neurons, Grima *et al.*, 2004). The visual system as well as the circadian photoreceptor CRY, feed in their signals *via* an elaborated pathway of neuronal interconnections (Cusumano *et al.*, 2009).

Flies lacking CRY, *norpA*-dependent photoreceptors (such as compound eyes) and *norpA-cry*-independent structures (such as Hofbauer-Buchner eyelets) were defined as being circadian blind (Helfrich-Förster *et al.*, 2001). This state is achieved by combining *cry^b* and *gl^{60j}* mutations which maintains individual rhythmicity but not light/dark synchronisation (Helfrich-Förster *et al.*, 2001). In order to verify this, behavioural activity was re-evaluated in an array of diverse LD regimes and temperatures. At low temperature, mutants do not show any morning peak and no anticipation of lights off, with a constant level of activity throughout the day and a fall in activity immediately after lights off. However at higher temperature, *glass^{60j}cry^b* mutants appear to be entrainable by LD cycles, with a lack of morning surge (explainable by the absence of compound eyes [Cusumano *et al.*, 2009; Rieger *et al.*, 2003]) and a clear rise of evening activity before the lights off transition. This increase of locomotor behaviour culminates with a peak centred at the light on/off transition (Figure 7.5). This observation may be a startle effect as it shows a high value compared to the average daytime activity (Mrosovsky, 1999).

Such pattern of behaviour was not only found in LD 12:12 but also in other LD conditions which were tested (Figure 7.13). Flies were subjected to long photoperiods (i.e. LD 18:6) or a new LD regime shifted by 6 h showing in both conditions, the anticipation of lights off (Figure 7.13). Moreover, exposure to DD or LL for three days did not influence or impair the ability of these mutants to entrain again to a following LD cycle (Figure 7.14 and 7.15). This entrained behaviour

observed in LD may be attributed to a possible temperature *Zeitgeber* generated by the light on/off transition. This possibility was evaluated and rejected by subjecting flies to temperature fluctuations in phase with the LD transition and *vice versa*, but keeping them in DD. The resulting behaviour was similar to flies maintained in constant DD, so the small temperature cycles associated with lights on/off do not entrain the double mutants (Wheeler *et al.*, 1993; Figure 7.11). The loss of entrainment is evident when mutants were released in DD. Indeed, *gl^{60j}cry^b* individuals started to free-run in DD but out-of-phase with each other, because the major proportion of flies show rhythmicity with a circadian period (close to 24 h) at the two temperatures (Figure 7.7). Also in LL at 25°C, mutants appeared to be rhythmic with an averaged activity profile similar to the one observed in LD and characterised by a drop of activity at the beginning of the subjective day and a constant increasing of activity during the light phase. This pattern culminates in a peak centred exactly at the subjective transition between light and dark (Figure 7.9). At low temperature, the locomotor activity profile of these flies was desynchronised, in LD, DD as well as LL (Figure 7.5, 7.7 and 7.9).

To verify the importance of temperature in the entrainment of these double mutants, they were tested in temperature cycles: subjecting flies to 12 h cycles of 18°-25°C. In addition to these conditions, the light/dark regimes were also varied, imposing LD cycles, DD or LL. Flies displayed an anticipation of the “lights off” transition only during the thermophase which coincided with the presence of light in 12:12 LD and LL (Figure 7.16 and 7.17). A masking effect was present when flies were subjected to the same temperature alternation but maintained in DD: they immediately increased their level of activity at 25°C or they reduced it if subjected to low temperature. This latter profile was observed when flies were exposed to the opposite temperature cycling in which the cryophase was set during the subjective day and the thermophase during the subjective night. In LD and DD, flies showed a pattern of activity driven by the temperature variation: they raised or diminished their activity at the time corresponding to the temperature change. Surprisingly, the anticipation of lights off was restored when mutants were subjected to LL. After one transition cycle, flies displayed a steady increase in their activity which ends at the transition between the thermo and cryophase (Figure 7.17, bottom panel). This

indicates that the synchronisation event in *glass^{60j}cry^b* mutants requires both light and warmer temperatures (such as 25°C).

Consequently, photoreceptor function appears to be restored at warmer temperatures. Since *glass^{60j}* impairs the formation of photoreceptor structure from the early stages of development (Moses *et al.*, 1989), it is unlikely that the mutation is temperature-sensitive. *cry^b*, is not a null mutation (Stanewsky *et al.*, 1998; Busza *et al.*, 2004; Dolezelova *et al.*, 2007) and CRY possesses a temperature function in the circadian core determining the basic rhythmicity when flies are subjected to diverse temperature wandering from 25°C (Dolezelova *et al.*, 2007; Kaushik *et al.*, 2007). Thus it is possible that increasing the temperature may generate structural modifications that can restore some CRY functions.

An alternative interpretation may be that an additional light input route exists, and its nature has not yet been characterised, particularly as an appreciable number of *norpA^{p41};;cry^b* flies are still capable of re-synchronising their locomotor activity to a shifted photic regime (Stanewsky *et al.*, 1998). Moreover, *norpA^{p41};cry⁰* individuals re-entrain to a new LD shift or to a longer and shorter photoperiod (Dolezelova *et al.*, 2007) suggesting a NORPA and CRY-independent pathway that generates the residual photoreceptive capabilities in these mutants.

The challenging question is to identify the putative photoreceptor molecule, its nature, where it is located and which are the circadian cells and structures involved in this residual entrainment. Evidences indicate that the dorsal part of *D. melanogaster* brain may be involved in the “extra” entrainment route. In fact, it has been shown that a small number of the heterogeneous DN1 group can mediate circadian rhythmicity in LL even in the absence of the LN_vs (Murad *et al.*, 2007). However, this cannot be the case for the mutants analysed here, because the mutation in *glass* leaves intact only 2 out of the normal 14-16 neurons in a wild-type fly (Veleri *et al.*, 2003). It is, then, possible that these two remaining DN1s escapers from the *glass* mutation (named anterior DN1s) retain some kind of photosensitivity mediated by a new photoreceptor which processes the light information and transfers it to the LN_vs (Shafer *et al.*, 2006). Alternatively, another set of neurons which could preserve some light entrainment pathway, may be the DN3s. These cells are located dorsally in each brain hemisphere in close contact with the head cuticle

(Nitabach and Taghert, 2008). Moreover, it has been shown that these cells express PER rhythmically and are able to regulate the evening locomotor activity component in LD (Veleri *et al.*, 2003). However, in DD this cell cluster is not sufficient to drive the behaviour in the absence of the LN_vs (Veleri *et al.*, 2003). Thus, given their CNS location, the circadian cycling of PER-expression (even in the *gl^{60j}cry^b* genetic background), and their morphological diversity (Shafer *et al.*, 2006), the DN3s represent candidate photoreceptor cells that might remain intact in *gl^{60j}cry^b*.

7.5. Conclusions

- *gl^{60j}cry^b* mutants synchronise to LD in the presence of moderate temperatures (i.e. 25°C) whereas they do not at low temperature (18 °C);
- Constant darkness desynchronises the activity of these mutants;
- Moderate temperature and light together restore the entrainment of *gl^{60j}cry^b* mutants.
- These mutants appear to retain some residual entrainment pathway that is not affected by the mutation in *glass* and *cry* genes.

Chapter 8. Orphan GPCRs

gl^{60j}cry^b mutants showed a residual ability to entrain to different LD regimes. The aim of this chapter is to define possible candidate genes that generate impaired locomotor behaviour in WT background and abolish completely the residual synchronisation in the circadian blind background.

8.1. Introduction

In the previous chapter, the locomotor activity profiles of *glass^{60j}cry^b* double mutants have been analysed and investigated. The analysis was focused on different LD regimes and temperatures. Results underlined the ability of this strain to entrain to light/dark cycles in contrast with previous published data affirming their circadian blindness (Helfrich-Förster *et al.*, 2001). The aim of this chapter is to discover a possible candidate for the residual synchronisation property of this line. The putative candidates may belong to the large and ancient family of the G-protein-coupled receptor (GPCR). They are integral cell membrane proteins that play a central role in signal transduction and are activated by an equally diverse array of ligands. A common feature between them is the seven hydrophobic α -helical domain structures, which are likely to span the membrane and linked by three extracellular loops that alternate with three intracellular loops.

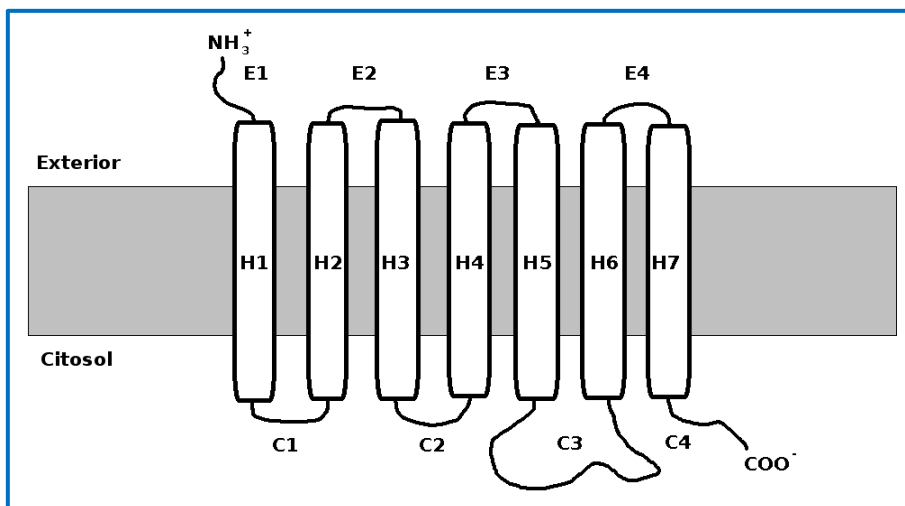


Figure 8.1: All GPCR receptors contain seven transmembrane α -helical regions. The loop between intracellular α -helices 5 and 6 is usually important for interactions with the coupled G protein. (Figure taken from Molecular Cell Biology, Lodish).

Furthermore, the extracellular NH₂ terminus is usually glycosylated whereas the cytoplasmic COOH terminus is generally phosphorylated. The signalling passage between the extracellular and the cytosolic environment is guaranteed by guanine nucleotide-binding regulatory proteins (G-protein). These cytosolic proteins switch between an “on” state (not bound to the receptor, GTP) to a “off” state (bound to the receptor, GDP). They are composed of three G_α, G_β and G_γ subunits which are closely associated with the intracellular face of the GPCRs. The GDP-bound G_α subunits bind tightly to the obligate heterodimer G_{βγ}. This association aids G_α localisation to the plasma membrane (Evanko *et al.*, 2001) and it is essential for functional coupling to GPCRs (Robillard *et al.*, 2000). The nucleotide-free G_α, then, binds GTP, which is present at significant excess over GDP in cells. The binding of GTP results in conformational changes within the three flexible regions of G_α, resulting in the dissociation of G_{βγ}. Both GTP-bound G_α and free G_{βγ} are capable of initiating signals by interacting with downstream effector proteins.

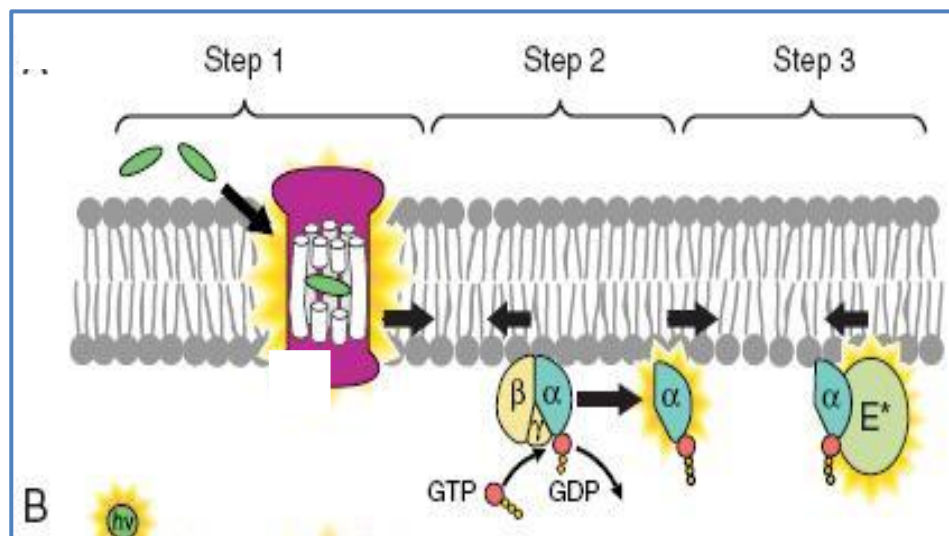


Figure 8.2: Signalling pathway: from ligands to the activation of an effector. (Figure taken from Molecular Cell Biology, Lodish).

The activated state of GTP-bound G_α is limited by its guanosine triphosphatase (GTPase) activity which causes the hydrolysis of GTP to GDP restoring the G_α subunit in the “off” state. Thus, this intrinsic enzymatic activity possessed by the latter subunits regulates the duration of signalling G_α GTP and free G_{βγ} subunits. Finally, the reassociation of G_{βγ} with G_α-GDP terminates all the effector interactions (Ford *et al.*, 1998).

Rhodopsins are retinal based photopigments where retinal serves as the chromophore (von Lintig *et al.*, 2001) and in general they belong to the GPCR superfamily. Once activated by absorption of light, a conversion event from rhodopsin to the active metarhodopsin state catalyses the activation of a heterotrimeric G protein (Hardie, 2001). Thus, it is possible that other genes and their relative products, especially if they are characterised by 7 transmembrane domains, may have a similar function to rhodopsins. Furthermore, the genome sequencing and gene annotation of *D. melanogaster* have predicted and documented a large number of putative new genes (Adams *et al.*, 2000). Amongst them, new GPCRs have been discovered, 12 of which are newly described and denoted as “orphan” receptor groups since they do not show a significant sequence homology to functionally characterised receptor (Brody and Cravchik, 2000). Moreover, most of these orphan GPCRs showed higher level of sequence identity to *C. elegans* and they may be possibly involved in developmental or physiological pathways in common between the two species (Brody and Cravchik, 2000).

In this chapter, some of these orphan receptors were analysed by taking advantage of the existence of transgenic flies that allow RNA interference. In particular, the attention was focused on those that in a “circadian blind” genetic background (i.e. *gl^{60j}cry^b*) lose partially or completely the residual entrainment displayed by the double mutants. Such flies should remain rhythmic, but be desynchronised with respect to each other.

8.2. Materials and methods

8.2.1. Fly Stocks

Flies generating downregulation of several GPCRs were ordered and obtained from VDRC stock center (Dietzl *et al.*, 2007). In the table below are listed all lines tested in addition to the locations of inserts and off-targets.

Gene	VRDC identification code	Name line	Location insertion	Off-target	Off-target gene
CG12290	1246	/	3	0	/
CG7497	9374	Line A	3	1	CG4360
	9375	Line B	3	1	CG4360
CG13995	42524	Line A	3	0	/
	42525	Line B	3	0	/
CG13579	9366	/	3	1	CG33221
CG16958	29644	/	2	4	CG6632 CG11491 CG9968 CG34226

Table 8.1: GPCR interference strains obtained form VDRC stock center.

8.2.2. Crosses

Flies carrying RNA interference constructs were crossed to *actinGAL4* driver (described in Materials and Methods; section 2.16) following the crossing scheme presented in Figure 8.3.

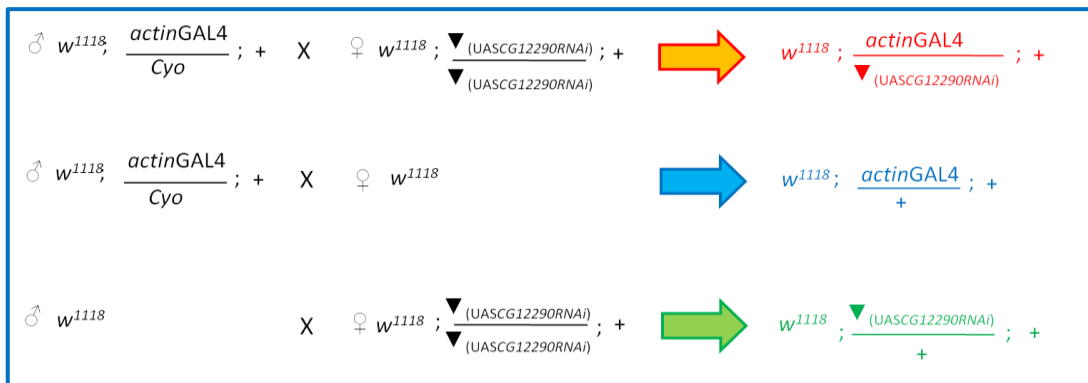


Figure 8.3: Scheme of crosses adopted to analyse the effects of the downregulation of GPCR genes. The first cross shown is to obtain interfered flies whereas the second and third crosses represent controls for the driver and the RNA interference construct, respectively.

In the case that the downregulation of a gene triggered by *actinGAL4* resulted in lethality, the *timGAL4* driver (Materials and Methods, section 2.16) was used. GPCRs were also tested in *gl^{60j}cry^b* genetic background. In Figure 3.1.1 (Appendix 3.1) is shown the crosses followed to obtain recombinants.

8.2.3. Locomotor activity

Locomotor activity assays were carried out as described in Materials and Methods (section 2.17 and 2.18). One to four day old male flies were placed in activity tubes and their locomotor patterns were monitored for 7 days at 25°C in LD (12:12 hrs), DD and LL after being entrained for 3 days in LD.

Differences in DD period were analysed using ANOVA and Newman-Keuls *post hoc* comparison (STATISTICA). In LL, possible relations between genotypes and rhythms were evaluated by contingency tables (<http://math.hws.edu/javamath/ryan/chisquare.html>).

8.3. Results

In this section, locomotor activity profiles obtained by the downregulation of some orphan GPCRs are described. Their behavioural patterns were examined in 3 diverse entrainment conditions: LD, DD and LL.

8.3.1. Behavioural analysis of flies downregulating *CG12290*

CG12290 is one of the GPCR studied in this chapter. This gene is located on the right arm of the third chromosome and no phenotypic data are yet available (Tweedie *et al.*, 2009; Flybase). RNAi knockdown was driven by *actinGAL4* driver in order to reduce the expression in all *Drosophila* tissues. As described in previous chapters, the locomotor activity of interfered flies was compared to two controls: one for the RNAi construct and the other for the driver. Their behaviour profiles were analysed for seven days at 25°C in different entrainment conditions: cycles of 12 hours of light and 12 hours of dark, constant darkness and light (Figure 8.4 and Appendix 3.2). For each experimental condition the locomotor activity periodicity was calculated and analysed.

In LD conditions, the locomotor activity of *CG12290* downregulated flies did not show any appreciable difference to both controls regarding morning and evening activities. In fact, these two components were both centred in the light off/on transition and *vice versa*, respectively.

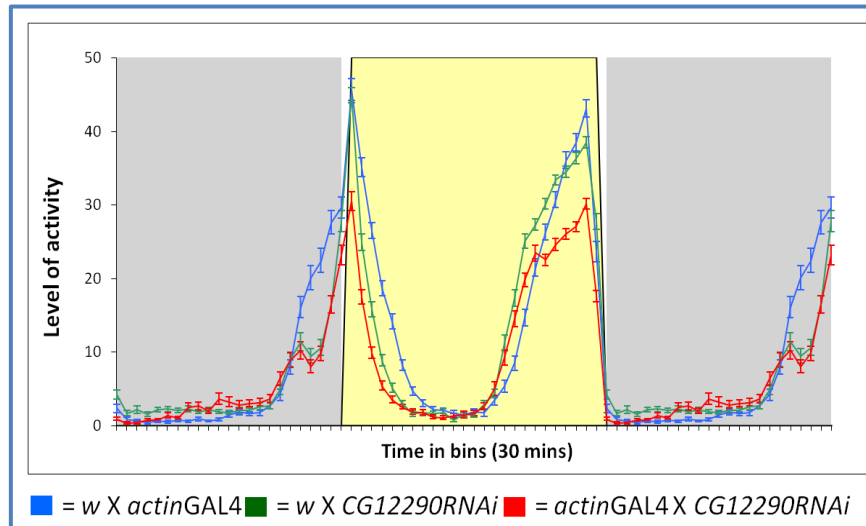


Figure 8.4: Averaged daily (\pm SEM) locomotor activity for *CG12290* RNAi and control flies at 25°C in LD. Yellow areas indicate photophase and the grey bar the scotophase.

The locomotor activity of these lines was tested in DD (Figure 8.5). The *CG12290* RNAi flies showed slightly longer periods than controls ($F_{2,89} = 50.83$ and $p \ll 0.001$). However the diversity in term of period values was very small and fell within circadian ranges, yet it was enough to accumulate over several days to cause a phase difference in the peak of locomotor activity.

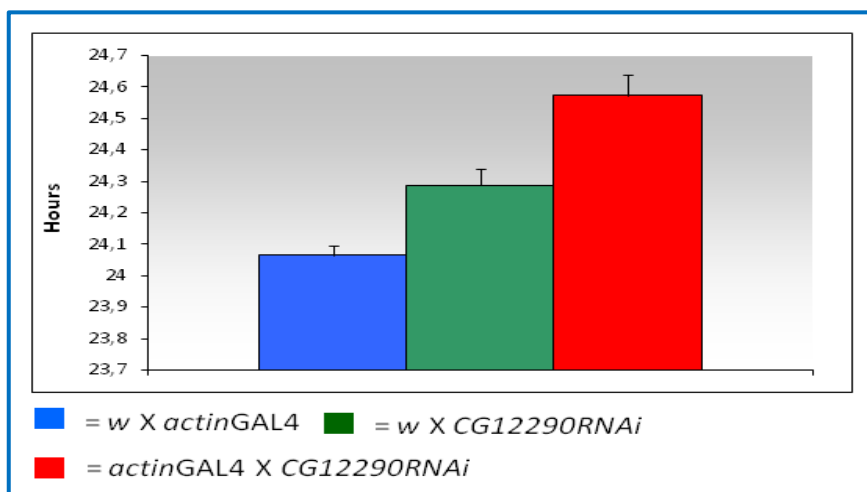


Figure 8.5: Average periods of *CG12290* RNAi flies and controls in DD at 25°C.

Finally, when the locomotor activity of these transgenic flies was tested in LL in order to determine a possible influence of this gene in the light input pathway, arrhythmic

periods were found (Figure 8.6). The *CG12290* RNAi lines showed the same level of rhythmicity, arrhythmicity and multiple rhythms of controls carrying an inactivated copy of the RNAi construct ($\chi^2 = 3.32$ d.f. = 4, $p = \text{n.s.}$).

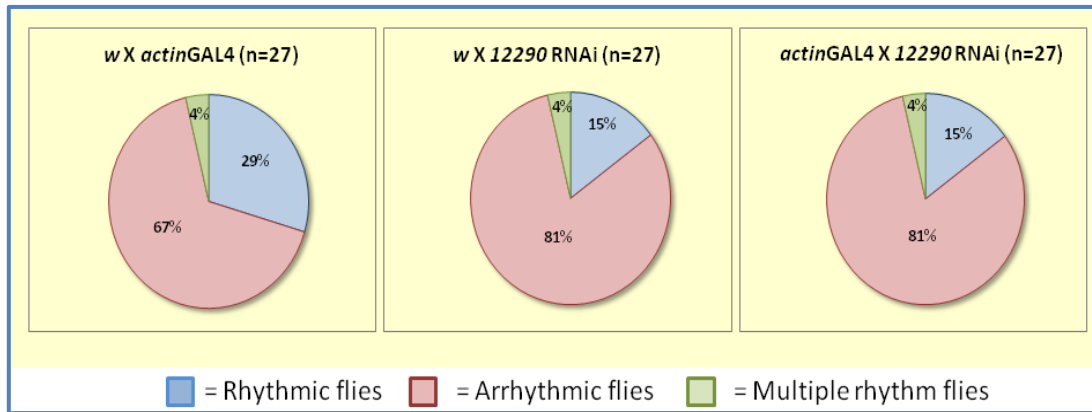


Figure 8.6: Rhythmicity of *CG12290* genotypes and *GAL4* control in LL.

8.3.2. Behavioural analysis of flies downregulating *CG7497*

The same approach described for *CG12290* was used to evaluate a possible importance in the entrainment pathway for *CG7497* gene. This orphan GPCR is located on 3L chromosome and no phenotypic data are available (Tweedie *et al.*, 2009; Flybase). The VDRC stock center generated two independent lines, which differ for the location of the RNA interference construct. These strains were analysed as before in LD, DD and LL. Initially, transgenic flies were crossed to *actinGAL4*, however, the ubiquitous knock-down of this gene resulted in lethality in both transgenics. Thus, the strategy adopted was to drive the downregulation in clock cells using the *timGAL4* driver which did not show any lethality.

The experimental *CG7497* RNAi flies did not show any impairment in their ability to synchronise to LD 12:12 with bimodal patterns of activity (Figure 8.7). Furthermore, the fact that these flies are able to entrain to light and dark cycles, was supported by their periodicities which were close to 24 h.

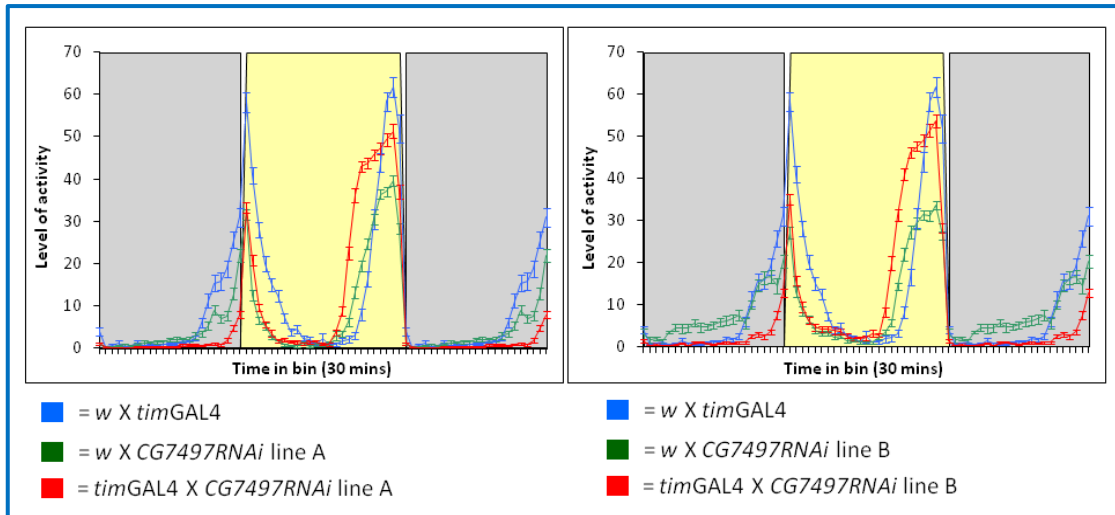


Figure 8.7: Daily locomotor activity of *CG7497* genotypes and *GAL4* control in LD at 25°C. Line A (left) and line B (right).

In DD, interfered strains were not significantly different from controls (Appendix 3.3).

In LL (Figure 8.8) RNAi flies showed a lower level of arrhythmicity compared to both controls ($\chi^2_{\text{line A}} = 26$, d.f. = 4, $p \ll 0.001$; $\chi^2_{\text{line B}} = 11.7$ d.f. = 4, $p \ll 0.05$), so silencing *CG7497* in circadian cells partially protects flies from the arrhythmic behaviour caused by constant light.

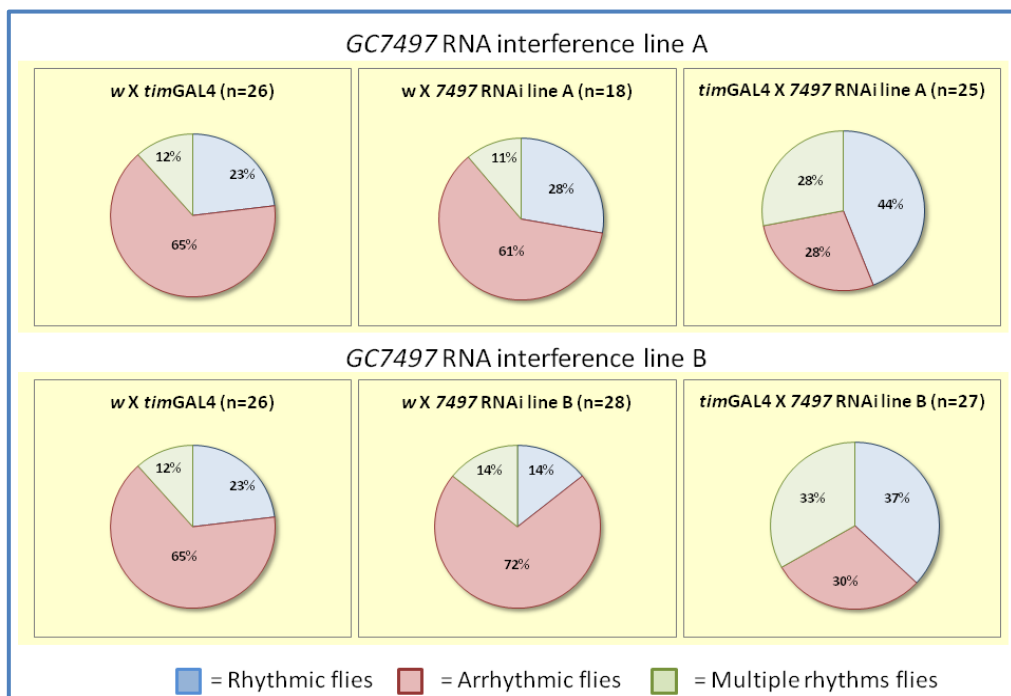


Figure 8.8: Rhythmicity of *timGAL4 CG7497* RNAi flies and controls in LL.

The effect of *CG7497* KD was also analysed in the *gl^{60j}cry^b* background. KD and controls flies were subjected to LD and LL regimes and their levels of rhythmicity were analysed. In LD, no significant differences in rhythmicity were observed ($\chi^2_{\text{line A}} = 2$, d.f. =4, $p = \text{n.s.}$; $\chi^2_{\text{line B}} = 5.59$, d.f. =4, $p = \text{n.s.}$), in contrast to LL ($\chi^2_{\text{line A}} = 15.1$, d.f. =4, $p \ll 0.05$; $\chi^2_{\text{line B}} = 15$, d.f. =4, $p \ll 0.05$). In LD, experimental as well as control flies displayed the *gl^{60j}cry^b* behavioural phenotype without losing their residual synchronisation (Figure 8.9). On the other hand, higher numbers of *CG7497* KD flies in LL (both lines) displayed arrhythmic behaviour compared to the controls (Figure 8.10) suggesting that *CG7497* is involved in the light input pathway.

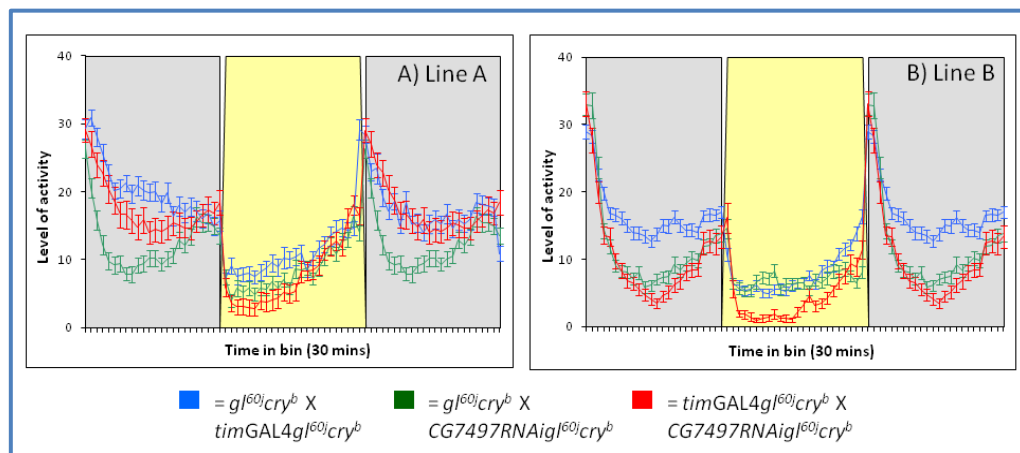


Figure 8.9: Average locomotor profile of *timGAL4 CG7497* RNAi *gl^{60j}cry^b* flies and controls in LD at 25°C.

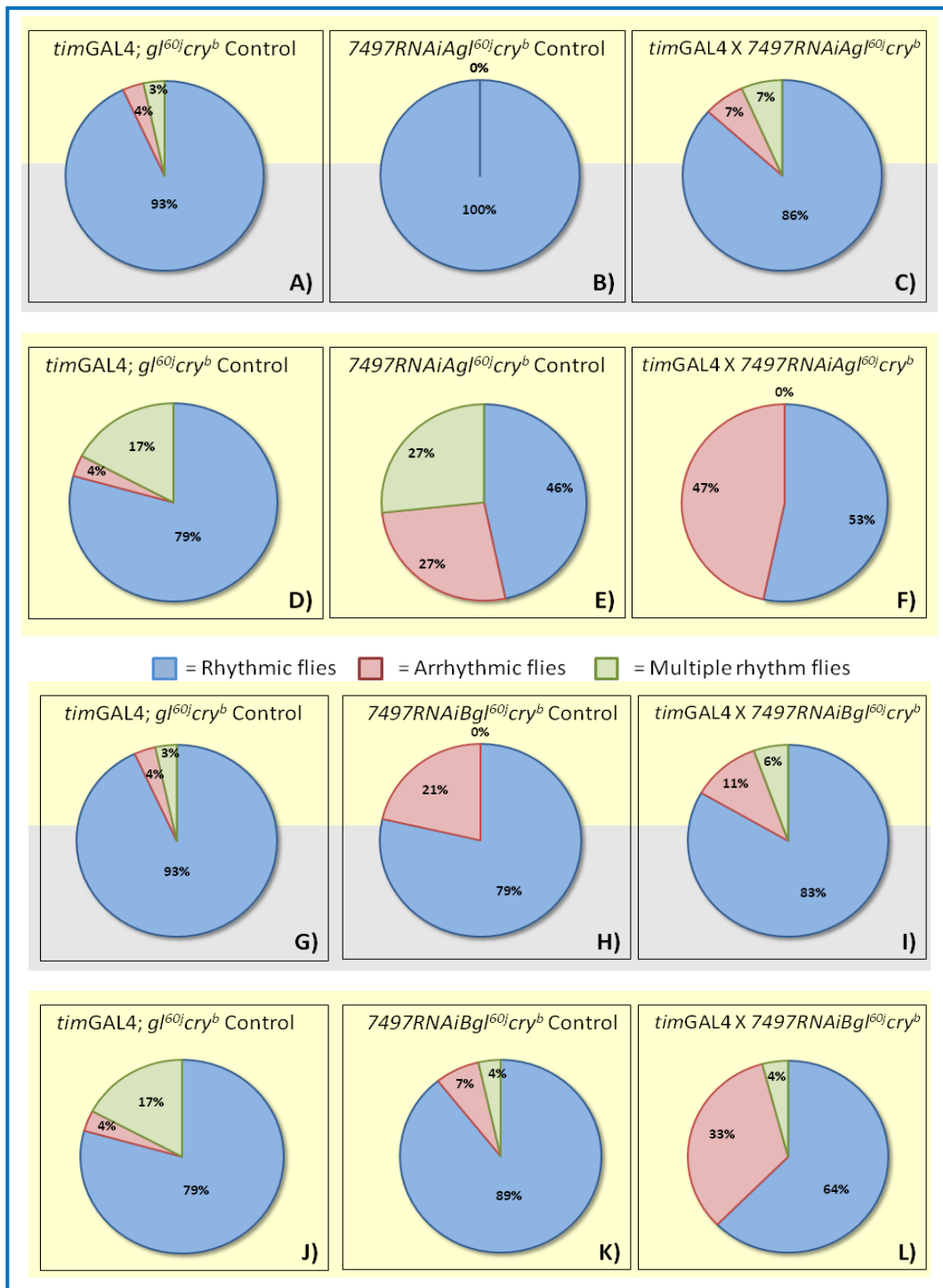


Figure 8.10: Levels of rhythmicity of flies downregulating *CG7497A* (C and F), *CG7497B* (I and L) and their controls in LD (A, B, C, G, H and I) and LL (D, E, F, J, K and L).

8.3.3. Behavioural analysis of flies downregulating *CG13995*

CG13995 (Tweedie *et al.*, 2009; Flybase), was downregulated using the *actinGAL4* driver. As in the case of *CG7497* above, two independent *CG13995* lines were available. The superimposed daily averaged locomotor activity patterns in LD

reveal no abnormalities (Figure 8.11). The periods in LD showed no significant differences from controls.

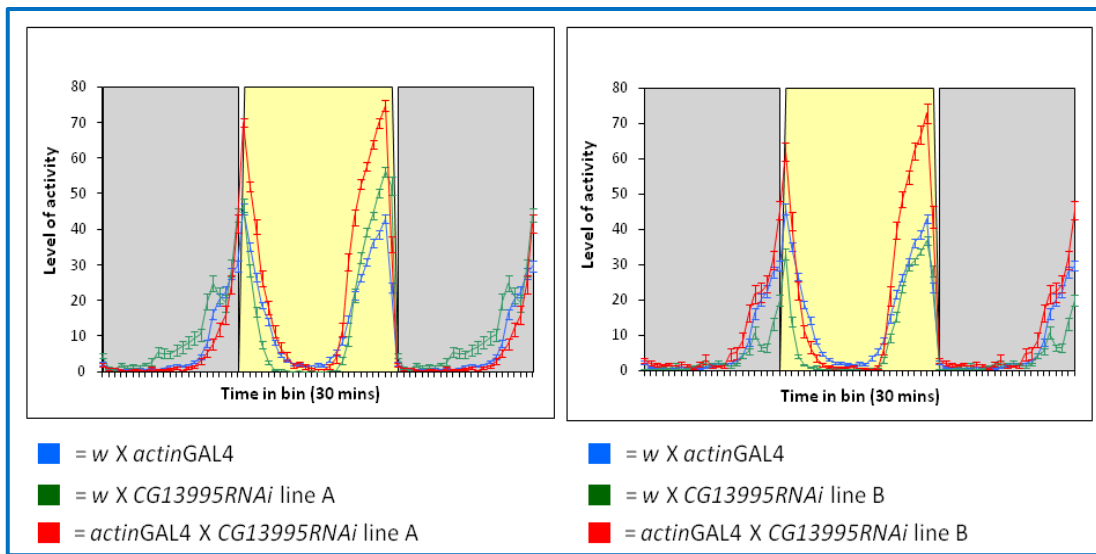


Figure 8.11: Averaged (\pm SEM) daily locomotor activity profile of *CG13995* RNAi lines and controls. Line A (left) and line B (right).

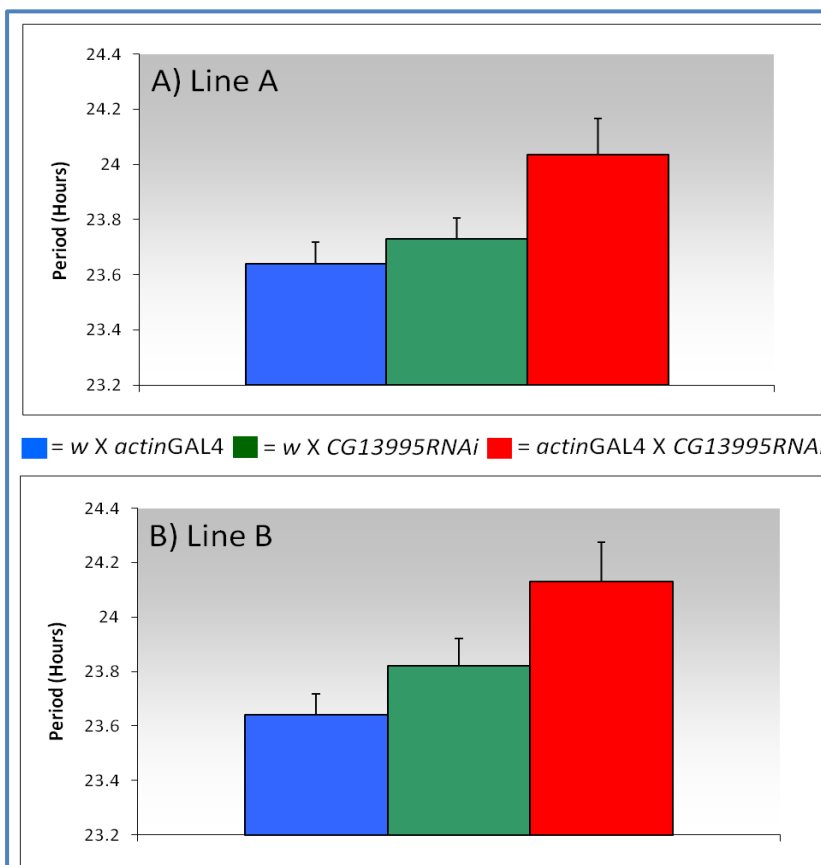


Figure 8.12: Periods in DD regime of *actinGAL4*; *CG13995* RNAi lines and controls.

Figure 8.12 shows that both lines showed longer free-running period than the controls in DD ($F_{2,53}$ line A = 4.36, $p < 0.05$; $F_{2,54}$ line B = 5.69, $p \ll 0.05$, Appendix 3.4).

In LL, no significant difference in their rhythmicity levels were observed ($\chi^2_{\text{Line A}} = 7.45$ d.f. =4, $p = \text{n.s.}$; $\chi^2_{\text{Line B}} = 4.53$ d.f. =4, $p = \text{n.s.}$), although line A RNAi showed completely arrhythmic behaviour (Figure 8.13).

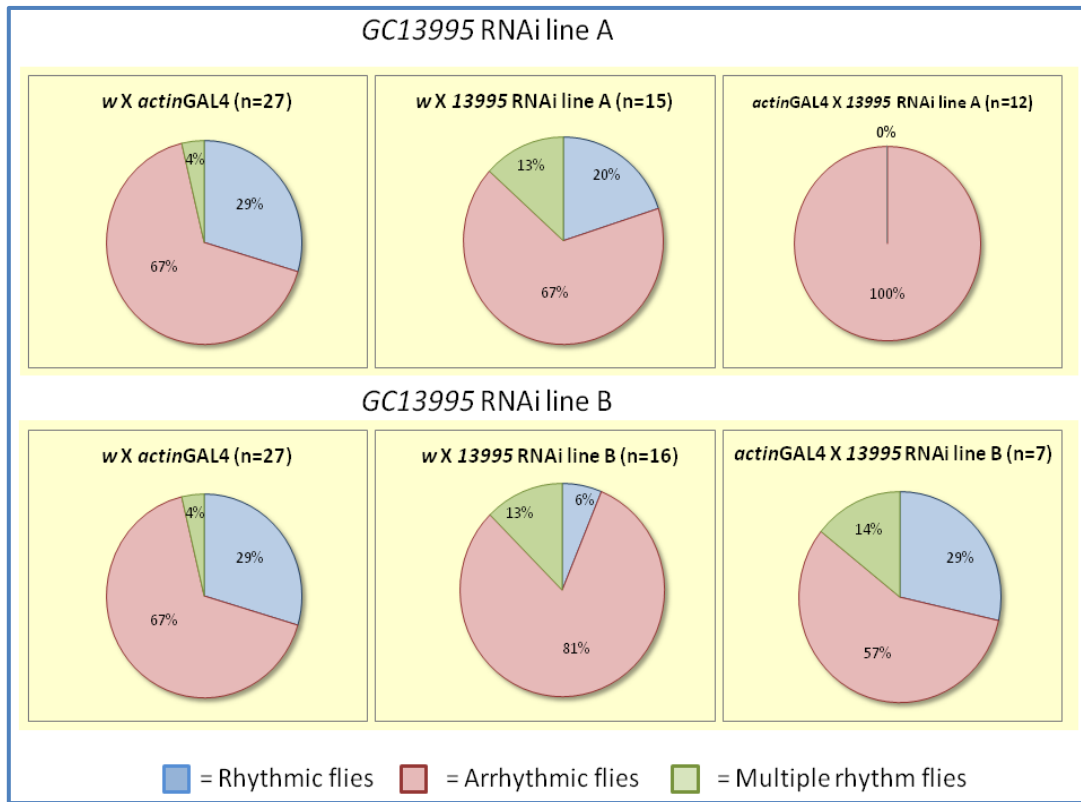


Figure 8.13: Levels of rhythmicity of flies downregulating *CG13995A* (top panel), *CG13995B* (bottom panel) and their controls in LL.

8.3.4. Behavioural analysis of flies downregulating *CG13579*

There are no annotations on *CG13579* function (chromosome 2L; Tweedie *et al.*, 2009; Flybase). RNAi flies entrained to the LD cycle with a 24 h period (Figure 8.14).

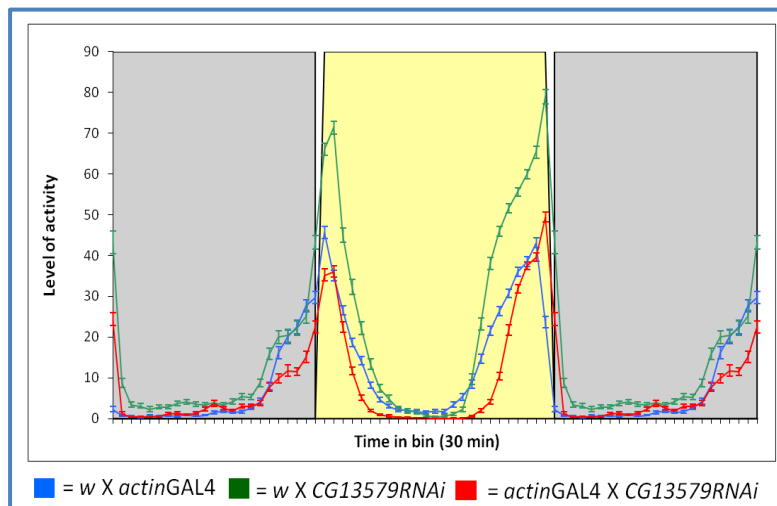


Figure 8.14: Averaged daily activity of *actinGAL4 CG13579* RNAi in LD.

Moreover, RNAi flies appeared to advance their morning offset and delay the evening onset giving a more prominent siesta. In DD, there were no significant differences between the free-running periods of the three genotypes (since KD flies displayed intermediate periods compared to controls, Appendix 3.5). In LL there was no significant difference between the experimental lines and controls (Figure 8.15). RNAi flies presented intermediate percentage in all the categories analysed ($\chi^2 = 5.30$ d.f.= 4, $p = n.s.$).

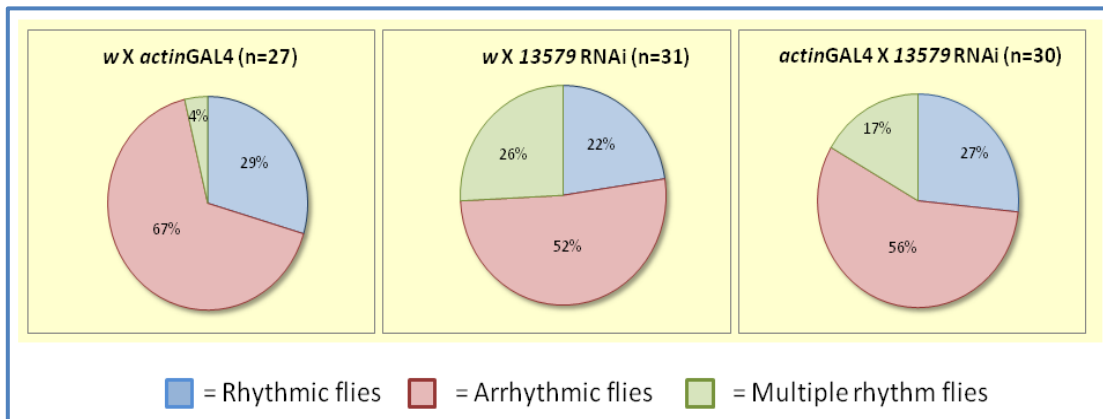


Figure 8.15: Rhythmicity in LL flies downregulating *CG13579*.

8.3.5. Behavioural analysis of flies downregulating *CG16958*

No phenotypic data have been published for *CG16958* (*X* chromosome; Tweedie *et al.*, 2009; Flybase).

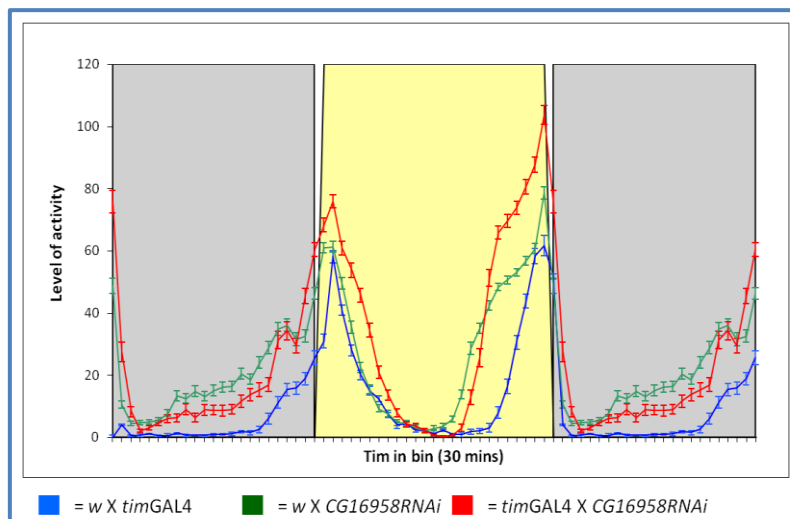


Figure 8.16: Averaged daily activity of *timGAL4 CG16958* RNAi flies.

Figure 8.16 shows that the downregulation of this GPCR did not modify the bimodal activity of these strains and the LD period. In DD, a significant reduction in period length was observed compared to controls ($F_{2,82} = 20.97$, $p < 0.001$; Figure 8.17, Appendix 3.6).

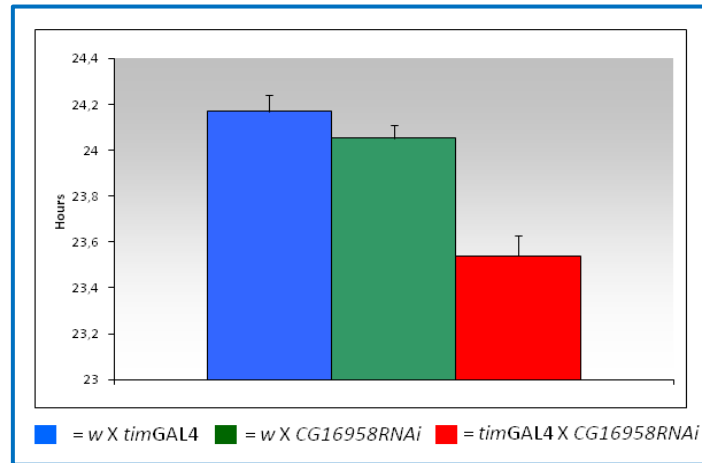


Figure 8.17: Average locomotor activity periods of *w; timGAL4 CG16958RNAi*; + flies and controls in DD at 25°C.

In LL, rhythmicity was affected by *CG16958* RNAi, with significantly more rhythmic flies than controls ($\chi^2 = 14.9$ d.f. = 4, $p < 0.05$; Figure 8.18).

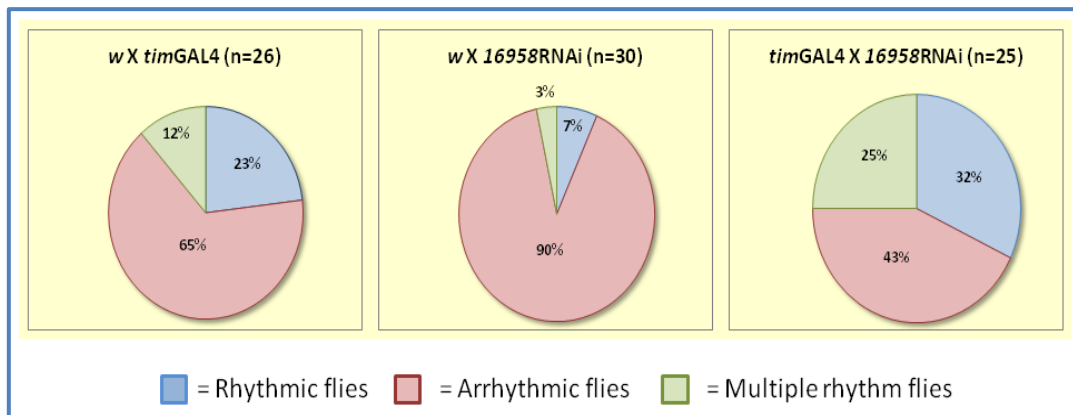


Figure 8.18: Percentage of flies displaying an arrhythmic or rhythmic period or multiple rhythms in LL.

In the *gl^{60j}cry^b* background, the RNAi flies did not display further synchronisation impairment compared to controls in LD (Figure 8.19).

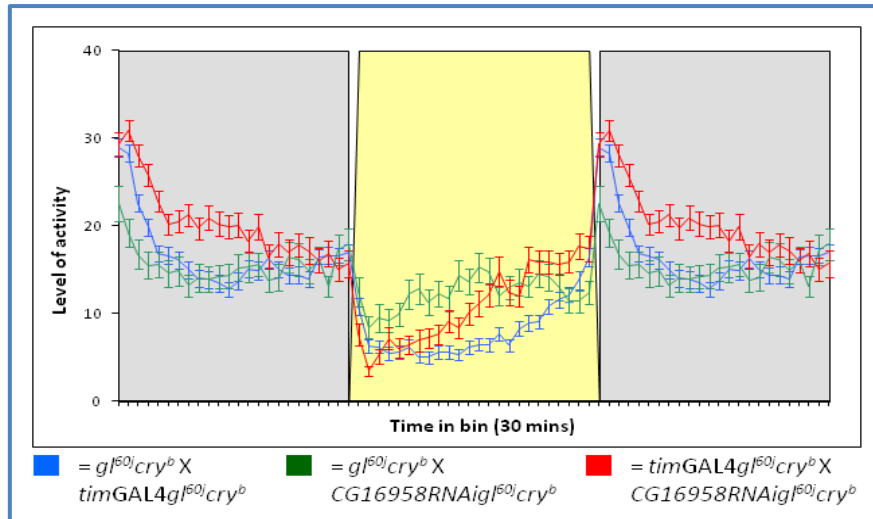


Figure 8.19: Averaged daily activity of *timGAL4 CG16958* RNAi flies in *gl^{60j} cry^b* background in LD.

In the *gl^{60j} cry^b* background and LL, the RNAi flies showed a significant reduction of rhythmicity ($\chi^2 = 9.43$ d.f. = 4, $p = 0.05$; Figure 8.20).

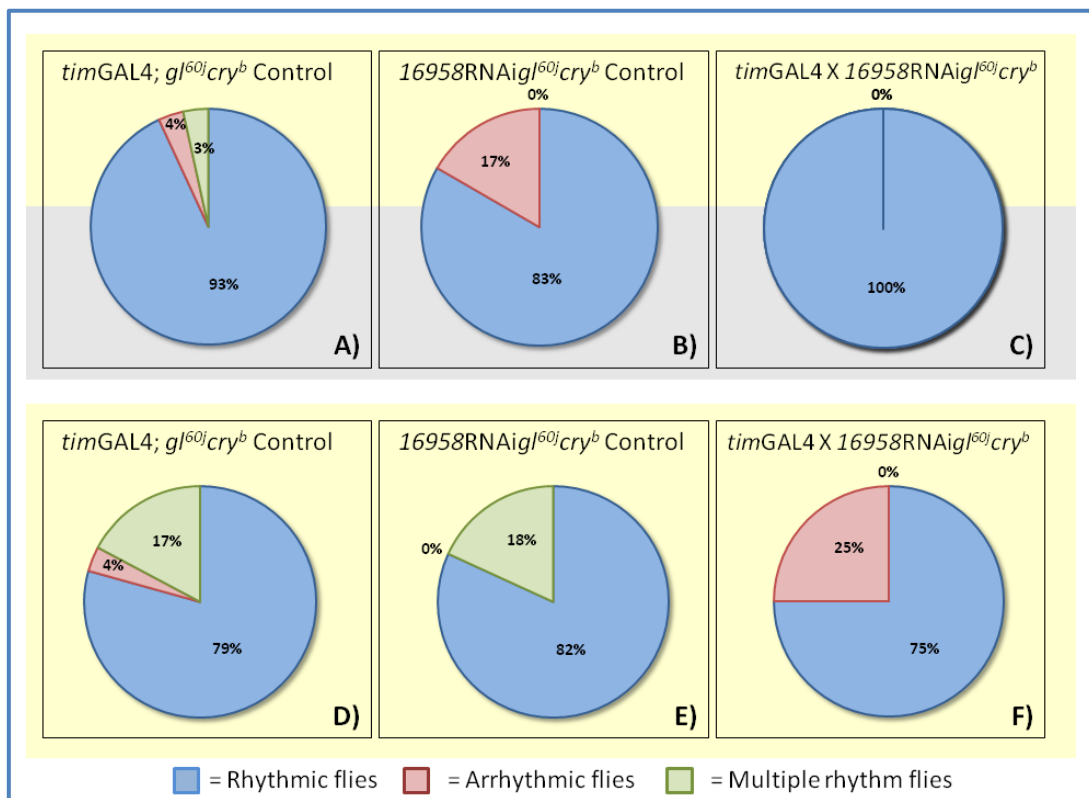


Figure 8.20: Rhythmicity of flies downregulating *CG16958* (C and F) and controls (A, B, D and E). Flies were analysed in LD (A, B and C) and in LL (D, E and F).

8.4. Discussion

This chapter was aimed at identifying any additional GPCRs that might contribute to the residual entrainment of *gl^{60j}cry^b* flies (Chapter 7). The recent *D. melanogaster* sequencing project predicted and revealed many new putative genes (Adams *et al.*, 2000) including 12 new GPCRs described as orphan receptors (Brody and Cravchik, 2000). Thus, it may be possible that one of these orphan GPCRs could be the extra photoreceptor with “rhodopsin function” which guarantees the entrainment in the “circadian double blind” mutants. To investigate this possibility, these orphan receptors have been silenced *via* RNAi in a ubiquitous or circadian manner (Dietzl *et al.*, 2007), monitoring their effect in diverse environmental conditions such as LD, constant darkness or light. The silencing of the GPCRs, either by *actin* or *tim* drivers, in a wild-type background did not impair the ability of flies to display a “classic” circadian behaviour when subjected to different regimes. All lines, in fact, were perfectly synchronised by light/dark cycles displaying a bimodal activity. In DD, it was found that downregulation of two GPCRs gave a long period (*CG12290* and *CG13995*, *via actinGAL4*; Figure 8.5 and 8.12, respectively) whereas one shortened it (*CG16958 via timGAL4*; Figure 8.17). However, these alterations were not so dramatic and limited to the circadian range (23-24 h). In LL, it was found that *CG7497* and *CG16958* KD reduced significantly the number of arrhythmic flies indicating that their downregulation is affecting normal light input into the clock and leading to blindness (Figure 8.8 and 8.18).

Thus, I focused my attention on these two lines (*CG7497* and *CG16958*) generating recombinant lines for the RNAi construct and *gl^{60j}cry^b* background. The intention of this screen was to characterise a putative photoreceptor which could be involved in the residual synchronisation observed in *glass^{60j}cry^b* flies in LD (Chapter 7). Thus, the expected phenotype generated by these flies would be characterised by a desynchronising locomotor rhythms, which would seem as a phase incoherence among rhythmic flies in daily LD plots. However, this was not achieved neither downregulation *via timGAL4 CG7497* or *CG16958* (Figure 8.9 and 8.19, respectively). Interfered flies presented a pattern of locomotor activity similar to controls and *gl^{60j}cry^b* mutants. Interestingly, when these silenced flies were exposed to LL, an

increase in the number of arrhythmic flies was observed suggesting a counterbalancing of the blindness (Figure 8.10 and 8.20). This indicates that somehow these two orphan receptors are involved in the light signalling pathway and responsible in part for the residual entrainment in the “circadian blind” mutants.

In the following Table 8.2, the major effects obtained by the orphan GPCRs KD are shown both in wild-type and *gl^{60j}cry^b* backgrounds.

GPCRs KD	Entrainment	Wild-type background	<i>gl^{60j}cry^b</i> background
<i>CG12290</i> (<i>actinGAL4</i>)	LD	Bimodal	
	DD	Long period	
	LL	/	
<i>CG7497</i> (<i>timGAL4</i>)	LD	Bimodal	<i>gl^{60j}cry^b</i> profile
	DD	/	
	LL	↓ Arrhythmic flies	↑ Arrhythmic flies
<i>CG13995</i> (<i>actinGAL4</i>)	LD	Bimodal	
	DD	Longer period	
	LL	/	
<i>CG13579</i> (<i>actinGAL4</i>)	LD	Bimodal	
	DD	/	
	LL	/	
<i>CG16958</i> (<i>timGAL4</i>)	LD	Bimodal	<i>gl^{60j}cry^b</i> profile
	DD	Short period	/
	LL	↓ Arrhythmic flies	↑ Arrhythmic flies

Table 8.2: Behavioural effects of GPCRs KD in WT and *gl^{60j}cry^b* genetic backgrounds.

A possible explanation for the free-running period alterations of KD flies may be a change in the cellular physiology. One candidate effector of these GPCRs may be intracellular cAMP and in last analysis the expression regulation of some output genes (e.g. Shafer *et al.*, 2008; Hyun *et al.*, 2005). cAMP is a second messenger that connects extracellular effector (i.e. hormone) to gene expression in diverse tissues (Sutherland, 1972). It has been shown that in mouse the absence of homologous counterpart G-protein VPAC₂, which is mainly expressed in the SCN and activated by VIP and PACAP, influences the cAMP level, the circadian gene expression of *mPer1*,

mPer2 and *mCry1* and behaviour (Harmar *et al.*, 2002). Alternatively, the release of intracellular Ca^{2+} may be the target of the receptor activation. For example, the concentration of this ion in LN_vs has been shown to cycle and regulated by GABA, a slow inhibitor neurotransmitter (Hamasaka *et al.*, 2005). Furthermore, Ca^{2+} has been shown to be a messenger which can modify the free-running period of flies (Harrisingh *et al.*, 2007).

Different hypothesis can be advanced regarding the behaviours observed in LL. The KD of the two orphan GPCRs gave opposite effects depending on the genetic background in which they were investigated. Thus, the fact that a significant number of experimental flies were rhythmic in LL in a wild-type background suggests that the receptors may preserve the interaction between CRY and TIM. In this scenario, CRY can partially escape from the light degradation interacting with TIM. On the other hand, in the “circadian blind” background, the same receptors are mitigating the effect of *cry^b* mutation determining an increase of arrhythmic flies. Alternatively, the effector of these two receptors may be a new molecule which can interact with CRY or TIM indirectly. Nevertheless, these results indicate that somehow these two orphan receptors are involved in the light signalling pathway (in opposite ways on the two backgrounds) and responsible in part for the residual entrainment in the “circadian blind” mutants at least in LL.

Interestingly, screening of the mRNA levels among the circadian pacemakers revealed the presence of *CG7497* as a highly expressed gene in TIM^+PDF^- cells (Nagoshi *et al.*, 2010; Supplementary Data). This cluster of cells includes the DN3s in which a residual light sensitivity has been previously proposed (Veleri *et al.*, 2003, Discussion Chapter 7). Thus, *CG7497* appears to be a new putative photoreceptor but a considerable effort is required in order to fully characterise its properties, mechanisms of action and downstream pathway in which this orphan GPCR is involved.

Finally, the existence of off-targets has to be taken into consideration. Although my results suggest GPCRs involvement, there is a possibility that off-targets silencing may contribute to the phenotypes. A Flybase search did not reveal associations between any of these genes and known circadian factors. However, in the case of

CG7497 and *CG16958*, it has been found that both off-targets represent uncharacterised proteins containing a zinc ion binding site, which may be important and regulate gene expression pathways. Importantly, this might also explain the lethality caused by *actinGAL4* and not by *timGAL4*, suggesting an involvement of these genes in development.

8.5. Conclusions

- In a wild-type genetic background:
 - The downregulation of *CG12290* and *CG13995* generate long period when triggered by *actinGAL4* whereas the circadian *CG16958* KD determine a short period in DD.
 - The *CG7497* and *CG16958* KD in TIM⁺ cells result in an increase of arrhythmic flies in LL.
- In *glass^{60j}cry^b* genetic background, the KD of *CG7497* and *CG16958*:
 - Do not impair the locomotor activity in LD. KD flies display a locomotor behaviour similar to *glass^{60j}cry^b* mutants.
 - Determine an increase in number of rhythmic flies in LL.

Chapter 9. Final discussion

The *D. melanogaster* circadian clock can be synchronised to the external environment by temperature and light, which are necessary and sufficient to entrain the self-sustained oscillator. In this thesis, both pathways have been investigated, focusing on the receptor-effector signalling cascade. For temperature, the implications of *norpA* effector have been studied, while for light, orphan GPCRs were examined.

9.1. Temperature entrainment: *norpA* and *plc21C*

norpA and *nocte* are the only genes reported to be involved in the fly's temperature synchronisation (Glaser and Stanewsky, 2005). *norpA* encodes a phospholipase C (PLC β) which has been shown to be mainly required in the visual system and therefore expressed in the photoreceptors (Hardie, 2001; Bloomquist *et al.*, 1988). However, this phospholipase is associated with the circadian mechanism *via* the thermosensitive *period* 3' UTR splicing (Collins *et al.*, 2004; Majercak *et al.*, 2004). High levels of *per* splicing are associated with colder environments, where evening activity is advanced into the afternoon, thereby reducing the 'siesta' seen in warmer conditions. NORPA, by an unknown mechanism, regulates the splicing event, as observed in *norpA*^{p41} nulls which show constitutively high levels of *per* splicing (Collins *et al.*, 2004). The locomotor phenotype displayed by these mutants is one with a reduced afternoon "siesta" due to an advance of the evening activity. All the available data regarding NORPA and the *per* splicing have been obtained with null mutants and by characterising *per* splice isoforms from fly heads.

To implicate specific clock neurons and tissues in this seasonal response, I initially investigated the localisation of NORPA. Two methods were used: *in situ* hybridisation and immunocytochemistry (ICC). It was not possible to localise NORPA distribution in the circadian pacemakers because of the inability of the antibody to penetrate the packed tissues of fly adult brains. I have found NORPA signal in the Bolwig Nerves and Organs when larval brains were prepared, as previously reported (Malpel *et al.*, 2002).

Additionally, when flies were entrained at low temperature (i.e. 18°C), NORPA was detected ventrally in one of the PDF⁺ LN_v cells and in proximity to the termini of the LN_vs dorsal projection. This dorsal location, in addition to two more dorsal cells, may putatively correspond to the position of the larval DN2s and DN1s, respectively. It has been reported that larval DN2s are necessary for temperature entrainment (Picot *et al.*, 2009) which together with other DNs, are temperature entrainable neurons in adult brains (Miyasako *et al.*, 2007). However, this observation needs to be verified in larval brains by co-labelling NORPA cells and dorsal circadian pacemakers, but also by analysing temperature effects on NORPA levels. The fact that NORPA may be highly expressed at low temperature suggests the possibility that the *per* splicing event needs to be finely controlled at this temperature. By *in situ* hybridisation, I detected *norpa* signal in larval and adult brains. Analysis on the circadian pacemaker clusters revealed that LNs and DNs express *norpa*.

These *in vivo* molecular data were also supported behaviourally when NORPA was downregulated by RNA interference. I used diverse sets of clock promoter-GAL4 drivers at “winter” and “summer” temperatures in LD 12:12. Generally, I found that different circadian cells are involved in the regulation of *D. melanogaster* behaviour *via* NORPA and ultimately by *per* splicing (Figure 9.1).

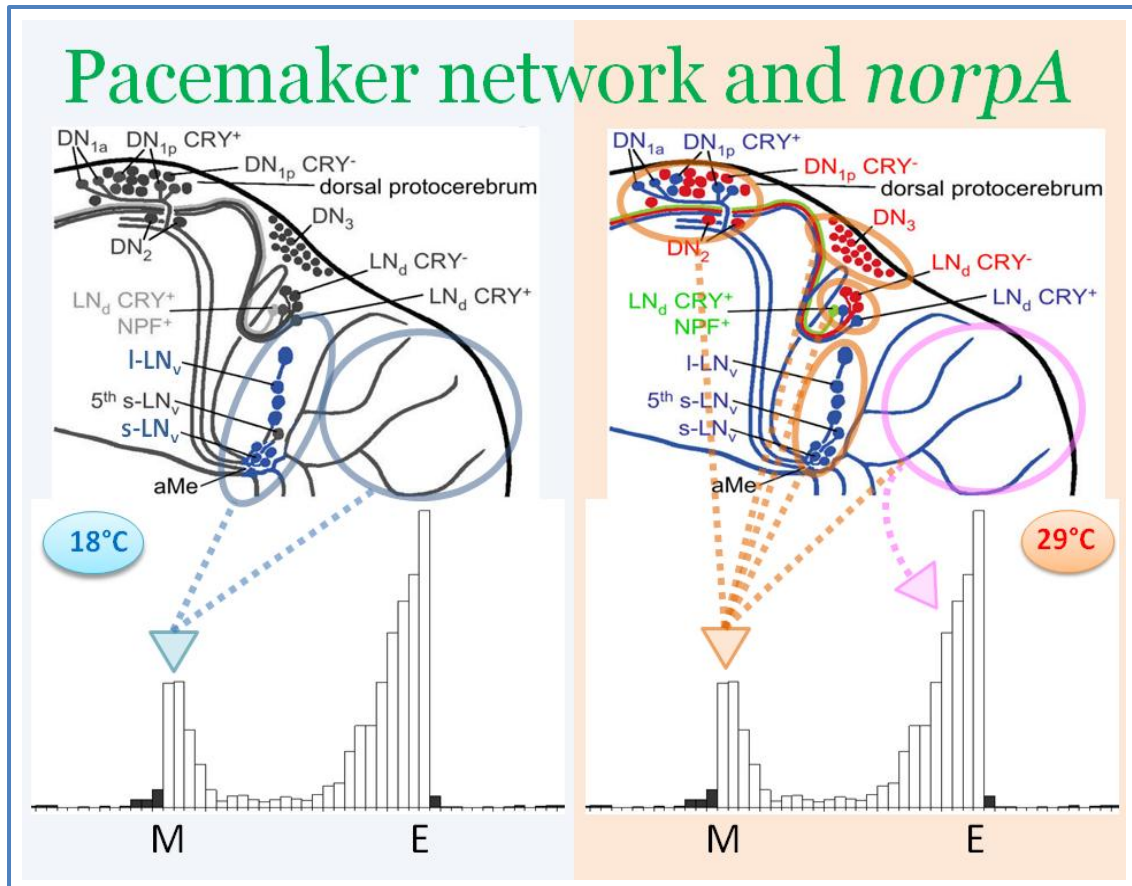


Figure 9.1: *norpA* effects on the circadian behaviour at low and high temperature (modified from Yoishii *et al.*, 2008). In the figure the involvement of different circadian neuron clusters are reported in relation to the locomotor components. Blue circles show structures influencing M behaviour at low temperature. At high temperature, orange and purple circles indicate brain neurons regulating the M and E locomotor components, respectively.

I have found that photoreceptor cells, where this phospholipase C is mainly expressed, set the upswing of the morning component at low temperature and the evening component at high temperature. The role of NORPA has been further dissected among clockwork neurons (i.e. LN_vs, CRY⁺ and DN cells). In general, I have found that the morning activity is the main component influenced by *norpA* downregulation. Morning cells (PDF⁺ s-LN_v and I-LN_v) act on the morning behaviour differently depending on the temperature: low thermal condition influence the upswing while hot temperature the offset. Other circadian drivers alter the offset of the morning component, generally advancing it, and suggest a role for the DNs *via* NORPA in the regulation of the morning component. This evidence agrees with the report that E cells (including LN_ds and DNs)

are able to set the morning behaviour in “summer” conditions (Stoleru *et al.*, 2007). However, it was not possible to rule out whether these behaviours are related exclusively to *per* splicing or some other processes. This was also due to the fact that the RNAi construct downregulates both *norpA* transcripts without discriminating between the two alternative splicing variants (Kim *et al.*, 1995). These *norpA* isoforms have diverse spatial and temporal patterns of expression. While one isoform is expressed exclusively in the retina, the other localises in different tissues including the brain (Kim *et al.*, 1995). Thus, it is reasonable to assume that this second variant may be involved in a different signalling pathway rather than phototransduction. The unanswered question is which signalling cascade can be controlled by this second *norpA* PLC β variant, although it has been shown that one isoform can rescue the phototransduction property of the other (Kim *et al.*, 2003) and the *per* splicing phenotype.

Diverse strategies can be adopted to verify: 1) if the *norpA* KD in PDF cells as well as in the other pacemakers act only *via per* splicing, and to 2) discriminate the level of expression of both *norpA* isoforms within circadian cells. For example, M cells can be selectively and physically separated from the remaining circadian population at different temperatures and subsequently used as a template for *per* or *norpA* variant PCRs (Nagoshi *et al.*, 2010). In the case, this hypothetical PCR might reveal changes in *per* splicing level and the relative ratios of the different *norpA* subtypes. Alternatively, *per* can be transgenically set in the “spliced” mode and the effect of *norpA* downregulation observed in the behaviour of these flies.

Given that both *norpA* isoforms may mediate seasonal behaviour, it may also be that paralogues or similar molecules to NORPA may also contribute to *per* splicing. PLC21C shares a 32% similarity and similar expression patterns with NORPA (Shortridge *et al.*, 1991), but I have found that *per* splicing was not altered when *plc21C* was downregulated in a ubiquitous manner. However, when this paralogous gene was knocked down in clock neurons, behavioural phenotypes emerged (Figure 9.2), suggesting independence from *per* splicing (at least in the eyes). As in the case of NORPA, the PLC21C KD in the photoreceptor and PDF⁺ cells influenced the onset of the

morning component at low temperature. In contrast, CRY^+ neurons (including 5th PDF⁻, LN_ds and some DNs) influenced the morning offset at warm temperatures. Furthermore, TIM^+ CRY^- PDF⁻ neurons (mostly DN2s, CRY^- DN1s and CRY^- DN3s) affect the evening locomotor phases at both temperatures *via plc21C*.

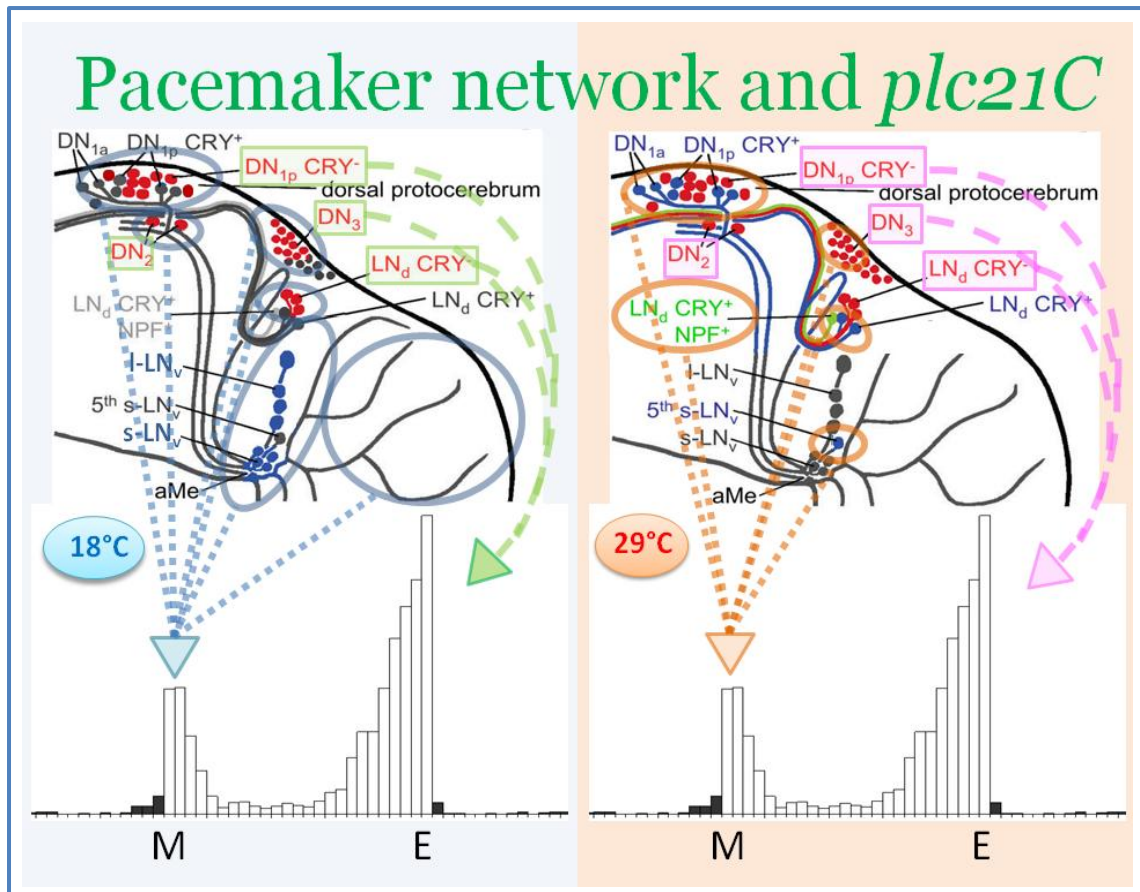


Figure 9.2: *plc21C* effects on the circadian behaviour (modified from Yoishii *et al.*, 2008). In the figure the involvement of different circadian neuron clusters are reported in relation to the locomotor components. Blue and orange circles show structures influencing the morning behaviour at low and high temperature, respectively. Green and purple circles indicate brain neurons regulating the evening locomotor components at 18 and 29°C, respectively.

As mentioned earlier, the *per* or *tim* splicing processes did not appear to be the targets of this phospholipase C, nor were clock genes affected significantly because no changes in free-running periods were observed. Therefore, *plc21C* opens new directions for exploring how this molecule can alter circadian entrainment.

I further examined the involvement of *norpA* in temperature synchronisation (Glaser and Stanewsky, 2005). The locomotor activity of *norpA* KD flies was monitored in temperature cycles in LL and under conditions where the thermal cycle was shifted. I did not find significant effects when *norpA* was knocked-down among circadian cells or in photoreceptors. Furthermore, no changes in behaviour were observed when *norpA* was silenced in the chordotonal organs which input circadian temperature information to the brain (Sehadova *et al.*, 2009). However, a role for CRY in temperature synchronisation emerged from these experiments. I have found that flies carrying *cry^b* or *cry⁰* mutations are unable to respond to temperature changes. Additionally, *glass^{60j}* mutants (Moses *et al.*, 1989) displayed impairment in their temperature responses. It appears that DN1s cells may be responsible since these have been shown to be temperature entrainable neurons (Miyasako *et al.*, 2007). It is plausible to assume that a temperature signalling may be mediated by the GLASS⁺CRY⁺ pDN1s since their absence (or the deletion of CRY) impairs thermal responses (Shafer *et al.*, 2006; Yoishii *et al.*, 2008).

9.2. Light signalling: *glass60jcryb* mutants and putative photoreceptor candidates

D. melanogaster uses different light-input pathways to synchronise locomotor activity to the LD regime. CRY, retinal and extraretinal photoreceptors are light routes that can synchronise the circadian clock. It has been reported that the absence of these determines “circadian blind” flies (Helfrich-Förster *et al.*, 2001). I evaluated again the activity profile of *gl^{60j}cry^b* in diverse LD regimes and temperatures. A clear evening activity peak which anticipates the light-off transition is observed in LD as well as in LL at warm temperature. Therefore, light and moderately warm temperatures seem to play an important role in the synchronization of this double mutant. This because synchronisation is lost or became poor when flies are released in DD, at 18°C or subjected to temperature cycles characterised by the cryophase coinciding with the light phase. Analysis of the locomotor profiles under different photoperiods further underline

the incomplete "blindness" of this genotype. This raises the possibility of a new *glass-cry* independent light input pathway.

Molecular analysis of circadian clock gene expression has indicated a possible location for such a residual light signalling cascade in the DN3s (Veleri *et al.*, 2003). I have tested a number of putative candidates by screening orphan GPCRs from the fly genome using RNAi. When *CG7497* and *CG16958* were silenced in the circadian neurons, flies were more preserved from LL arrhythmia in a wild-type background. Furthermore, when the KD was done in the "circadian blind" genetic background, experimental flies showed less rhythmicity than controls. Both experiments suggest that the two GPCRs are interacting with CRY signalling. In LL they are partially rescuing the CRY-TIM mediated effect of arrhythmia in LL, whereas on the *gl^{60j}cry^b* background, they are mitigating against the effects of *cry^b* increasing the arrhythmia. This suggests a new pathway into the circadian light signalling system. Interestingly, *CG7497* has been reported to be highly expressed among the TIM⁺PDF⁻ neurons (Nagoshi *et al.*, 2010). This population includes the GLASS⁻CRY⁺ and GLASS⁺CRY^{-/+} DN1s and DN3s. Thus, *CG7497* orphan receptor appears at present to be the best candidate for contributing to the residual entrainment in *gl^{60j}cry^b* flies. However, its expression patterns and downstream effectors have still to be investigated.

In summary, as with most PhDs, my work has answered a few questions but has opened up considerably more.

Appendix 1: NORPA overexpression

It has been reported that *norpA* can encode two different subtypes of protein. An alternative splicing event in a single exon in the mature *norpA* RNA, leads to the formation of two isoforms of proteins that differ by 14 amino acids (Kim *et al.*, 1995). Their expression patterns are different. Since *in situ* hybridization has shown that *norpA* subtype I RNA is expressed in retina, it is reasonable to conclude that this isoform is involved in the phototransduction pathway. On the other hand, since *norpA* subtype II RNA has been detected in a variety of tissues including brain but not in the retina, it is likely that this second isoform could be used in different signalling pathway other than phototransduction (Kim *et al.*, 1995). Different sets of primers were used in order to amplify and clone the two isoforms of *norpA* (Table 1.1).

Primer	DNA sequence	Isoform
Frstprt F	5' - ATACTCGAG <u>GCCGCCACC</u> ATGACCAAGAAGTACGAGTTCGATTGG - 3'	I and II
Frstprt R I subtype	5' - GCGTCAACCTGATGAAGCATTG - 3'	I
Frstprt R II subtype	5' - TGATGTGTCTGCGGAAACATTGG - 3'	II
Scndprt F I subtype	5' - AGCCAAGAGCTGGCAAAGAA - 3'	I
Scndprt F II subtype	5' - ACAGCCAAGATCTGGCTAGATGG - 3'	II
Scndprt R	5' - ATATTGCCACAACATGTCCTC - 3'	I and II
Trdprt F	5' - GCTCTGGCTGAAGGGCGAACT - 3'	I and II
Trdprt R	5' - GCAAGGAAAAACGGAATTTATGCCTCTAGAAATG - 3'	I and II

Table 1.1: Primer sequences used to amplify *norpA* isoforms. The abbreviation Frstprt, Scndprt and trdprt refer to the first, second and third parts of *norpA* since it was divided in three parts to avoid contaminations and increase the specificity of the products. Underlined nucleotides indicates restriction enzyme sites (XhoI in Frstprt F primer and XbaI in Trdprt R primer). Bold nucleotides refer to a Kozac sequence introduced by PCR in the sequence.

The cloning strategy to generate constructs for over-expressing *norpA* gene was based on PCR amplifications of cDNA extracted from adult flies. In order to minimise *in vitro* mutations introduced by amplification and generate different transgenes that

permit the expression of two alternative spliced isoforms, full *norpA* transcripts were divided and amplified in three fragments as shown in Figure 1.1.

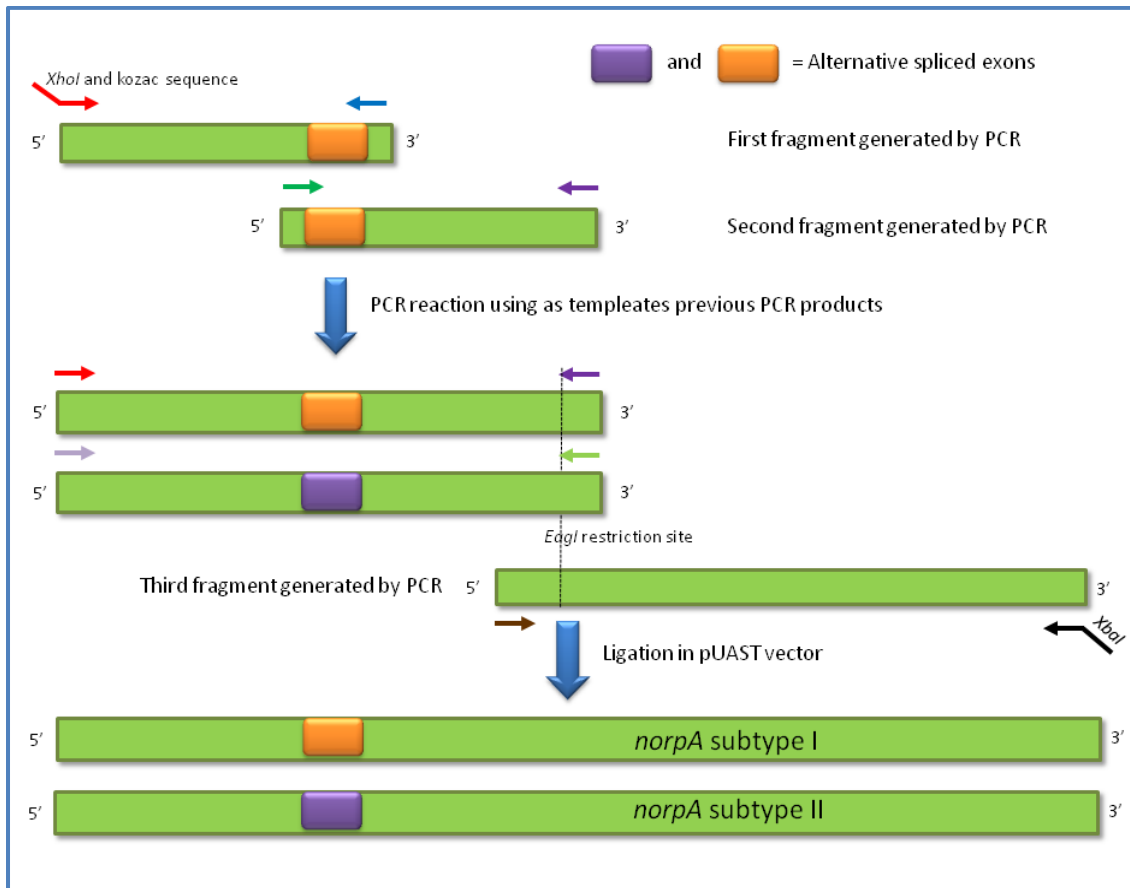


Figure 1.1: Cloning steps adopted to clone the two isoforms of *norpA*.

Because the alternative splicing event in *norpA* determines two types of mature RNAs that differ for a central portion (position 1039 to 1118 which is the orange fragment in Figure 1.1 [according to Bloomquist *et al.* 1988]), for each specific isoform, different PCR reactions were carried out in order to amplify two fragments overlapping for 60 nucleotides. Subsequently, these latter two fragments were combined together, taking advantage of this latter 60 nucleotides in common that allow the annealing of the two regions, and further ligated to a third part of *norpA* (similar in both isoforms). Once, the *norpA* full-length region was cloned in pUAST vector, it was send off to be microinjected by BestGene Inc. Ten independent lines for each isoform were obtained

and after being balanced, UAS transgenes were back-crossed into the *norpA^{p41}* genetic background.

The level of NORPA rescue was tested by western blots. Thus, *norpA^{p41}* *norpA*-expressing strains were crossed to *timGAL4* (*norpA^{p41}*; *timGAL4/+*; *UASnorpA/+*). In parallel, *norpA*-expressing lines were crossed to *w¹¹¹⁸* in order to generate *UAS-norpA* controls (*norpA^{p41}*; +; *UASnorpA/+*), and the driver line to *norpA^{p41}* mutants for generating driver controls (*norpA^{p41}*; *timGAL4/+*; +) (Figures 1.2 and 1.3).

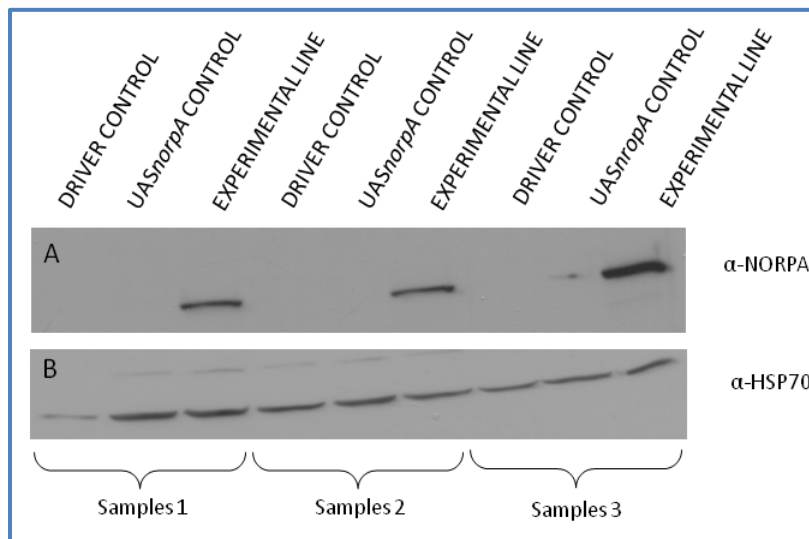


Figure 1.2: Western blot of NORPA (A) and HSP70 (B) in control (*norpA^{p41}*; +; + X *w*; *timGAL4*; + and *w*; +; + X *norpA^{p41}*; *UASnorpA*; +) and over-expressing *norpA* (*w*; *timGAL4*; + X *norpA^{p41}*; *UASnorpA*; +) flies entrained for three days at 25°C. Samples were loaded as triplicates from independent collections. The molecular marker is expressed in kDa. Films were exposed for one second.

The rescue of NORPA in *timeless* cells was efficient for both isoforms as shown in Figure 1.3. In fact, the level of NORPA in the expressing flies was significantly higher than both controls indicating high levels of over-expression ($F_{2,6} = 444.00$, $p \ll 0.001$ for the first isoform; $F_{2,6} = 5548.19$, $p \ll 0.001$ for the second isoform).

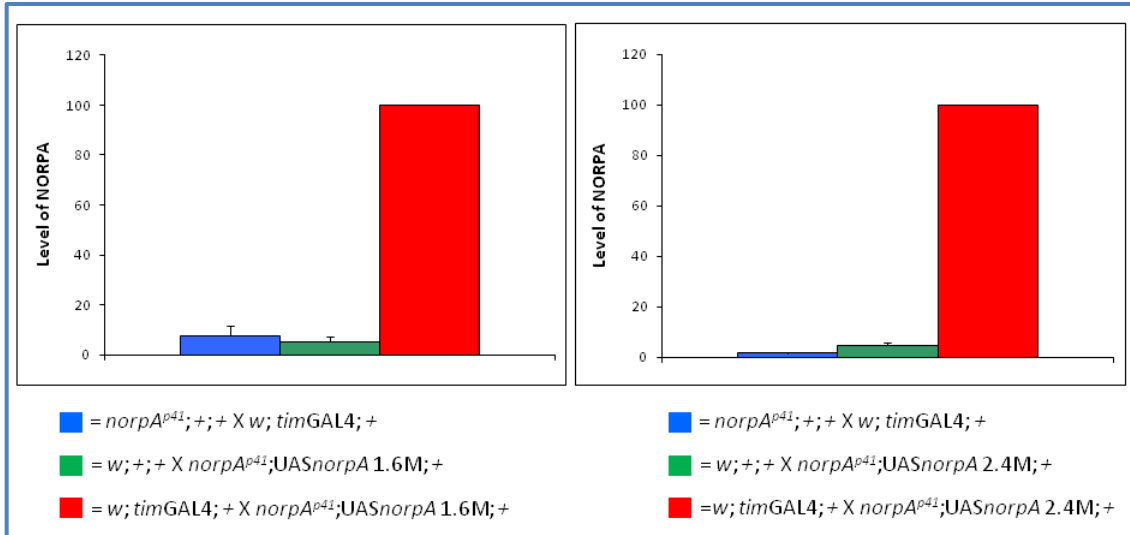


Figure 1.3: NORPA quantification in over-expressing *norpA^{p41}* flies. NORPA protein level was compared to driver and UAS-construct controls.

The locomotor profiles of these transgenic flies were monitored in LD 12:12 at 18 and 29°C. As shown in Figure 1.4 and 1.5, both isoforms rescue the *norpA* phenotype. Interestingly, the major effects were noticed at low temperature where the evening activity component resulted delayed compared to controls (arrows in the Figures).

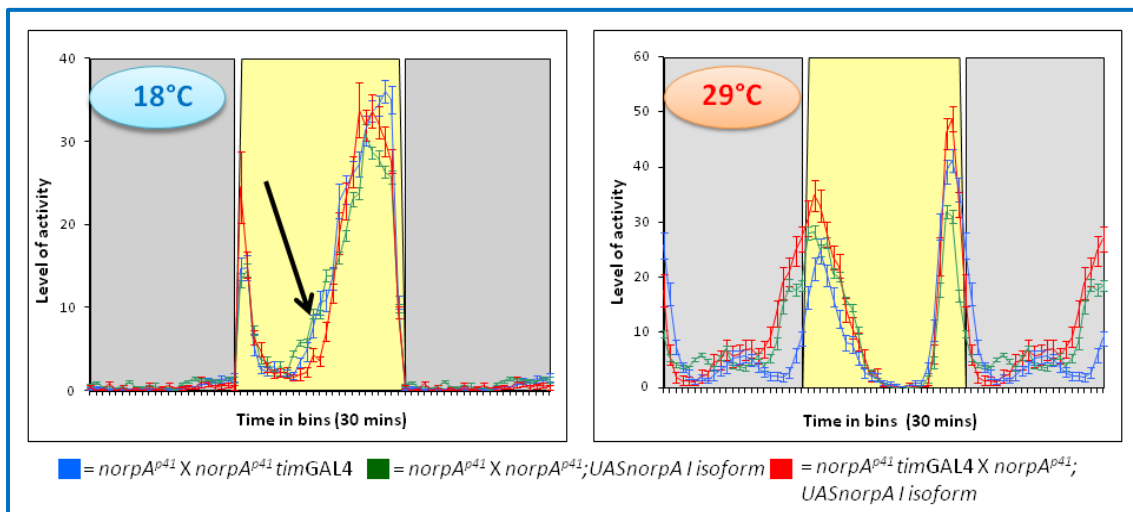


Figure 1.4: Averaged locomotor activity of flies expressing *norpA* I isoform in TIM cells and controls in LD at 18 and 29°C.

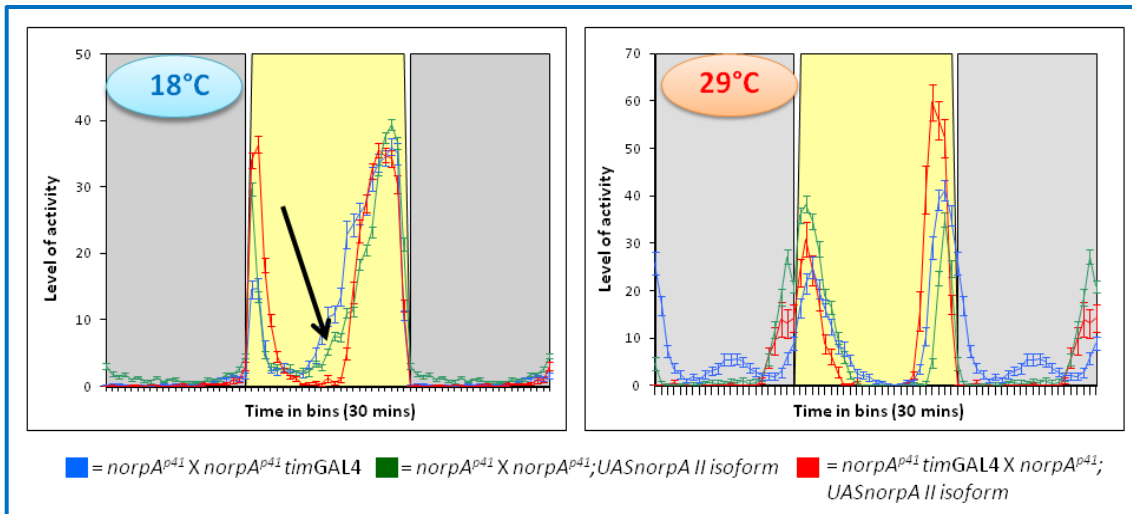


Figure 1.5: Averaged locomotor activity of flies expressing *norpA* II isoform in TIM cells and controls in LD at 18 and 29°C.

Appendix 2: Behaviour of *norpA* and *plc21C* knocked-down flies

2.1 *norpA* RNAi in LD 12:12

Analysis of Variance: NORPA level in *actinGAL4 X norpARNAi* at different temperatures

	df	MS	df	MS		
	Effect	Effect	Error	Error	F	p-level
Genotype	2	5747.896	18	208.9832	27.50411	3.36595E-06
Temperature	2	1704.021	18	208.9832	8.153864	0.003012485
Genotype & temperature	4	400.1701	18	208.9832	1.914843	0.151654243

Table 2.1.1: Analysis of variance of NORPA level in *actinGAL4 X norpARNAi* and controls entrained for 3 days at 12, 18 and 29°C.

Probabilities for Post Hoc Tests. Newman-Keuls test: NORPA level in *actinGAL4 X norpARNAi* flies at 12, 18 and 29°C

Interaction: Genotype X Temperature	{1}	{2}	{3}	{4}	{5}	{6}	{7}	{8}	{9}
	22.75 329	63.25 473	59.31 612	22.09 703	58.25 937	44.94 436	0.369 851	2.013 093	2.764 265
<i>w X actinGAL4</i> 12°C {1}		0.021 941	0.028 964	0.956 379	0.019 755	0.076 526	0.354 231	0.325 131	0.234 867
<i>w X actinGAL4</i> 18°C {2}	0.021 941		0.742 606	0.026 946	0.906 566	0.429 648	0.001 311	0.001 395	0.001 267
<i>w X actinGAL4</i> 29°C {3}	0.028 964	0.742 606		0.038 69	0.929 759	0.458 492	0.002 042	0.002 134	0.001 833
<i>w X norpARNAi</i> 12°C {4}	0.956 379	0.026 946	0.038 69		0.031 05	0.157 659	0.287 641	0.231 912	0.118 965
<i>w X norpARNAi</i> 18°C {5}	0.019 755	0.906 566	0.929 759	0.031 05		0.274 243	0.001 934	0.001 929	0.001 568
<i>w X norpARNAi</i> 29°C {6}	0.076 526	0.429 648	0.458 492	0.157 659	0.274 243		0.014 835	0.014 313	0.010 734
<i>actinGAL4 X norpARNAi</i> 12°C {7}	0.354 231	0.001 311	0.002 042	0.287 641	0.001 934	0.014 835		0.890 955	0.977 682
<i>actinGAL4 X norpARNAi</i> 18°C {8}	0.325 131	0.001 395	0.002 134	0.231 912	0.001 929	0.014 313	0.890 955		0.950 044
<i>actinGAL4 X norpARNAi</i> 29°C {9}	0.234 867	0.001 267	0.001 833	0.118 965	0.001 568	0.010 734	0.977 682	0.950 044	

Table 2.1.2: Newman Keuls *post hoc* comparisons for NORPA down-regulation level in *actinGAL4 X norpARNAi* flies and their relative controls at 12, 18 and 29°C.

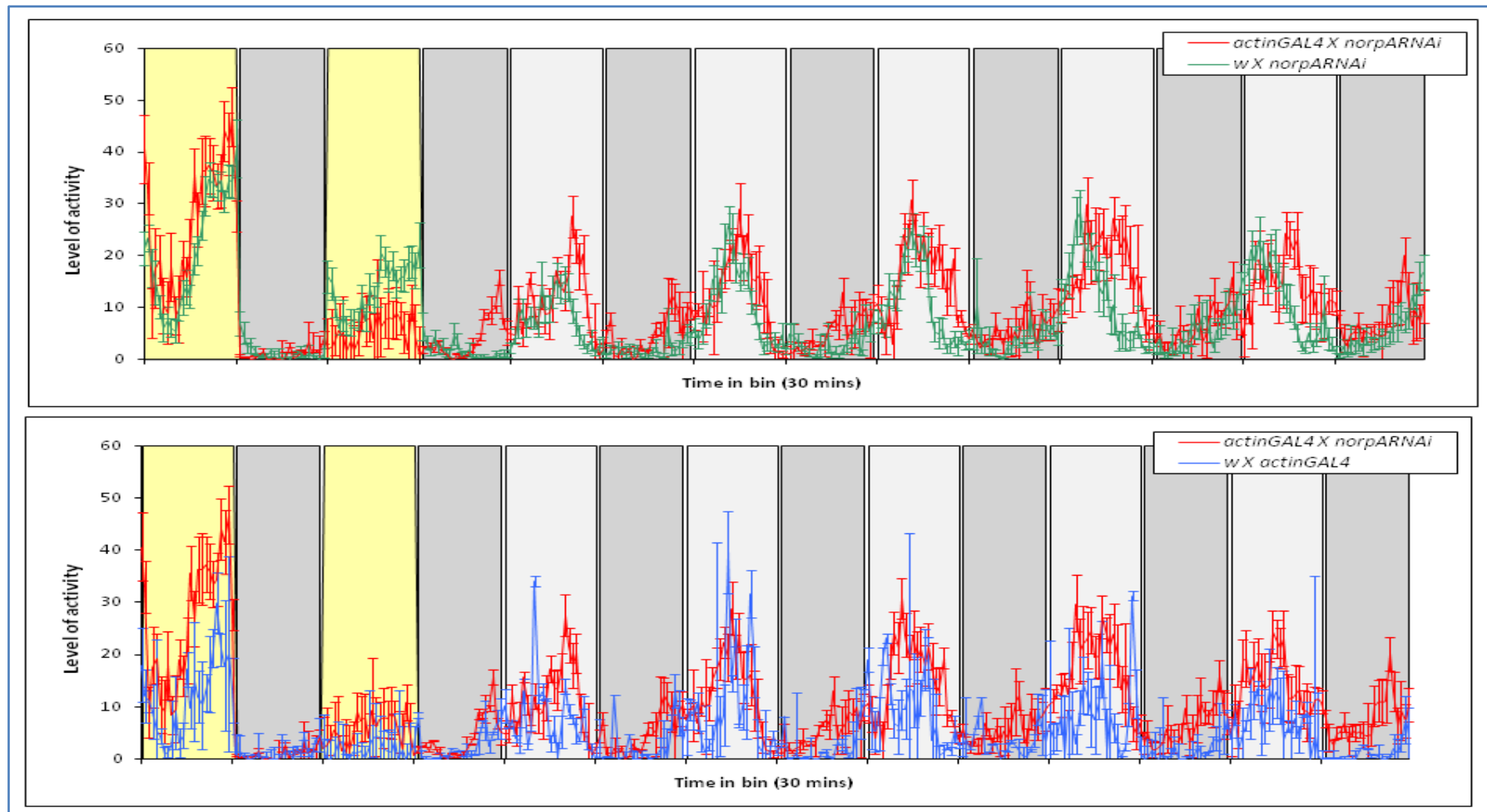


Figure 2.1.1: Comparison of *norpA* interfered averaged locomotor activity (\pm SEM) to RNA interference construct (upper graph) and driver (lower graph) controls at 18°C in DD regime. Yellow area indicates light on, dark grey represents subjective night and light grey the subjective day.

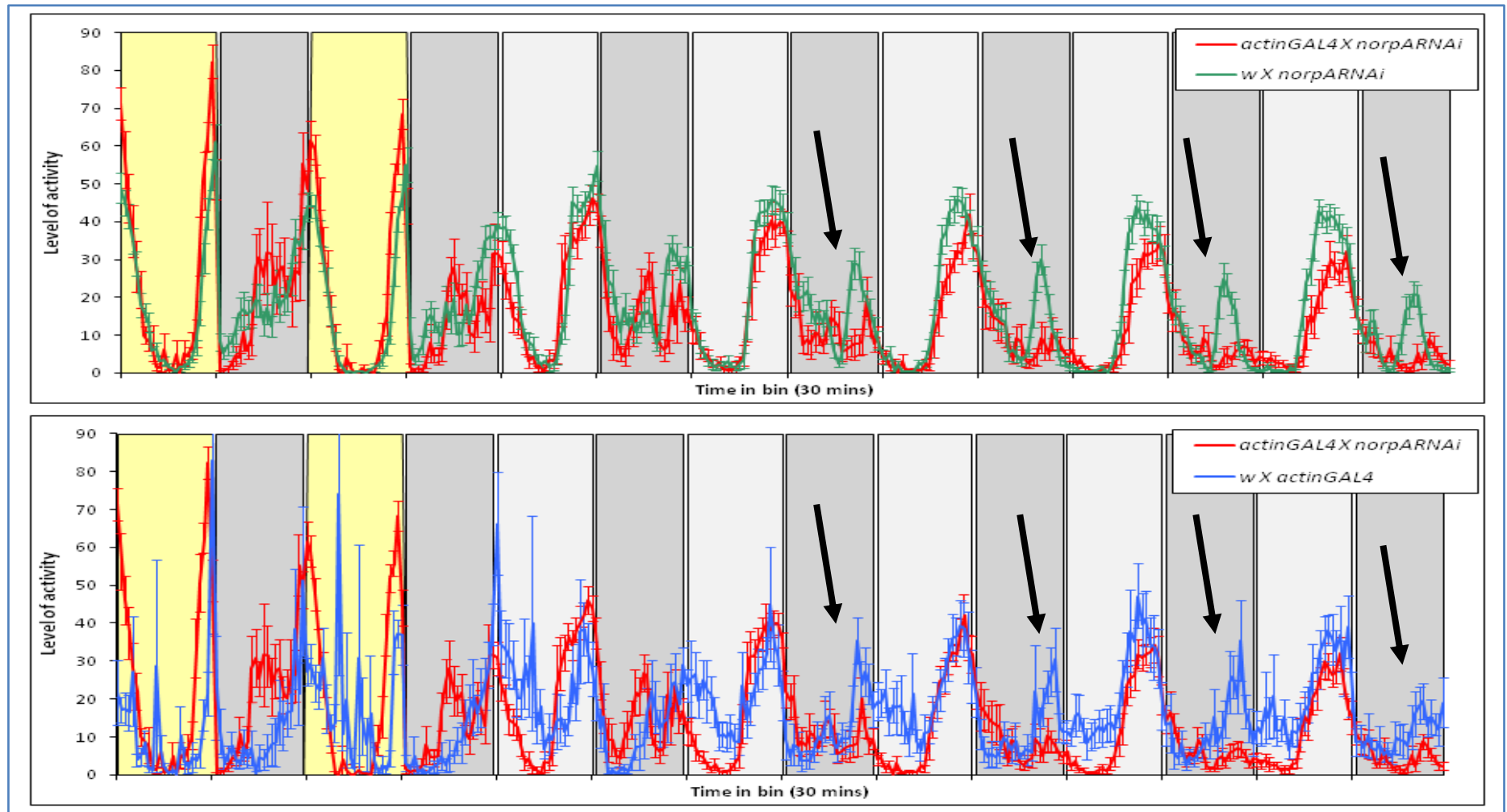


Figure 2.1.2: Comparison of *norpA* interfered averaged locomotor activity (\pm SEM) to RNA interference construct line (upper graph) and driver (lower graph) controls at 29°C in DD regime. Yellow area indicates light on, dark grey represents subjective night and light grey the subjective day.

Analysis of variance: Period of *timGAL4 X norpARNAi* in DD at 18 and 29°C

	df	MS	df	MS		
	Effect	Effect	Error	Error	F	p-level
Genotype	2	9.125209	132	0.710845	12.83713	8.04761E-06
Temperature	1	5.41359	132	0.710845	7.615712	0.006609057
Genotype X Temperature	2	2.072383	132	0.710845	2.91538	0.057681106

Table 2.1.3: Analysis of period activity variance of *timGAL4 X norpARNAi* and controls in DD at 18 and 29°C.

Newman-Keuls test: Period of *timGAL4 X norpARNAi* in DD at 18 and 29°C

	{1}	{2}	{3}	{4}	{5}	{6}
	24.17333	23.93000	23.27900	23.13300	24.33889	23.43057
<i>timGAL4 X norpARNAi</i> 18°C {1}		0.37010	0.00546	0.00121	0.54199	0.01713
<i>timGAL4 X norpARNAi</i> 29°C {2}	0.37010		0.04353	0.01752	0.28799	0.06583
w X <i>norpARNAi</i> 18°C {3}	0.00546	0.04353		0.59073	0.00091	0.57664
w X <i>norpARNAi</i> 18°C {4}	0.00121	0.01752	0.59073		0.00015	0.51648
w X <i>timGAL4</i> 18°C {5}	0.54199	0.28799	0.00091	0.00015		0.00457
w X <i>timGAL4</i> 29°C {6}	0.01713	0.06583	0.57664	0.51648	0.00457	

Table 2.1.4: Newman Keuls *post hoc* comparisons of *timGAL4 X norpARNAi* and control periods in DD at 18 and 29°C.

Analysis of variance: Period of *pdfGAL4 X norpARNAi* in DD at 18 and 29°C

	df	MS	df	MS		
	Effect	Effect	Error	Error	F	p-level
Genotype	2	2.2626064	154	0.4188822	5.4015346	0.0054047
Temperature	1	2.5729241	154	0.4188822	6.1423578	0.014277
Genotype X Temperature	2	0.1622896	154	0.4188822	0.3874349	0.6794555

Table 2.1.5: Analysis of period activity variance of *pdfGAL4 X norpARNAi* and controls in DD at 18 and 29°C.

Newman-Keuls test: Period of *pdfGAL4 X norpARNAi* in DD at 18 and 29°C

	{1}	{2}	{3}	{4}	{5}	{6}
	23.82750	23.49533	23.61439	23.28107	23.27900	23.13300
<i>pdfGAL4 X norpARNAi</i> 18°C {1}		0.18424	0.25961	0.02010	0.03048	0.00327
<i>pdfGAL4 X norpARNAi</i> 29°C {2}	0.18424		0.52883	0.25704	0.48673	0.22092
w X <i>pdfGAL4</i> 18°C {3}	0.25961	0.52883		0.18210	0.28580	0.08065
w X <i>pdfGAL4</i> 29°C {4}	0.02010	0.25704	0.18210		0.99126	0.71333
w X <i>norpARNAi</i> 18°C {5}	0.03048	0.48673	0.28580	0.99126		0.43993
w X <i>norpARNAi</i> 29°C {6}	0.00327	0.22092	0.08065	0.71333	0.43993	

Table 2.1.6: Newman Keuls *post hoc* comparisons of *pdfGAL4 X norpARNAi* and control periods in DD at 18 and 29°C.

Analysis of variance: Period of *cryGAL4 X norpARNAi* in DD at 18 and 29°C

	df	MS	df	MS		
	Effect	Effect	Error	Error	F	p-level
Genotypes	2	6.713469982	161	0.546288431	12.28924084	1.07897E-05
Temperatures	1	4.048698902	161	0.546288431	7.411284924	0.007196003
Genotypes X Temperatures	2	1.428061604	161	0.546288431	2.614116669	0.076339178

Table 2.1.7: Analysis of period activity variance of *cryGAL4 X norpARNAi* and controls in DD at 18 and 29°C.

Newman-Keuls test: Period of *cryGAL4 X norpARNAi* in DD at 18 and 29°C

	{1}	{2}	{3}	{4}	{5}	{6}
	23.92069	23.82667	23.97062	23.24937	23.27900	23.13300
w X <i>cryGAL4</i> 18°C {1}		0.64465	0.80652	0.00548	0.00470	0.00107
w X <i>cryGAL4</i> 29°C {2}	0.64465		0.75986	0.01286	0.00724	0.00374
<i>cryGAL4 X norpARNAi</i> L {3}	0.80652	0.75986		0.00372	0.00387	0.00058
<i>cryGAL4 X norpARNAi</i> H {4}	0.00548	0.01286	0.00372		0.88447	0.56811
w X <i>norpARNAi</i> 18°C {5}	0.00470	0.00724	0.00387	0.88447		0.75392
w X <i>norpARNAi</i> 29°C {5}	0.00107	0.00374	0.00058	0.56811	0.75392	

Table 2.1.8: Newman Keuls *post hoc* comparisons of *cryGAL4 X norpARNAi* and control periods in DD at 18 and 29°C.

2.2. *fra* KD in PDF cells

In the figure below (2.2.1), the averaged locomotor profile of flies downregulating *fra* in the M cells is shown.

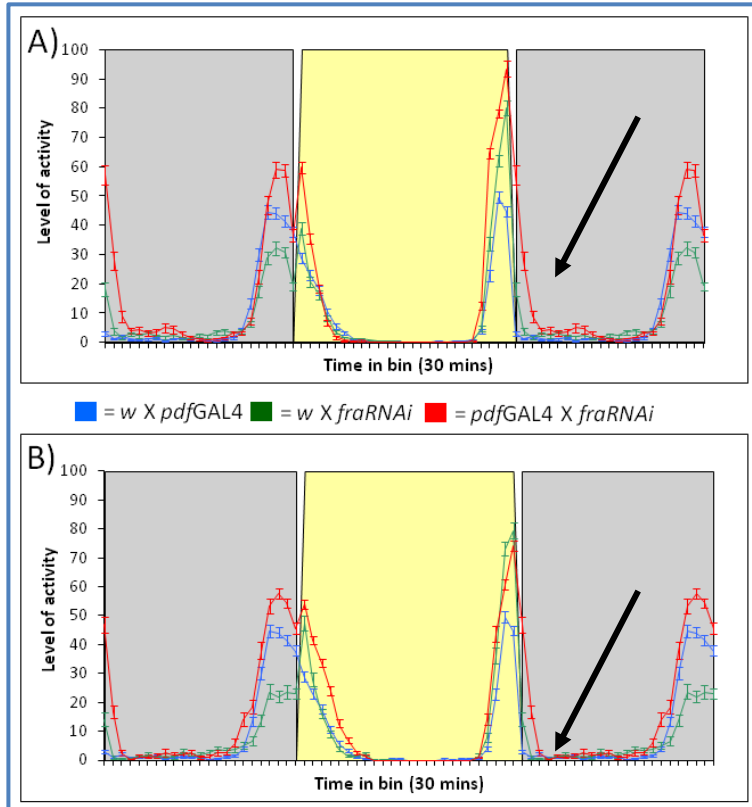


Figure 2.2.1: Averaged activity profiles of transgenic flies (A) 29909 and (B) 29910 downregulating *fra* via *pdfGAL4* and controls in LD at 29°C.

Both *fra* KD lines were characterised by a bimodal behaviour in LD at high temperature. All the locomotor activity components were not affected, apart for the E offset which appears delayed compared to controls (arrows in the Figure).

2.3. Temperature synchronisation of the *Drosophila* circadian clock

Summary of all Effects Breda protocol Canton-S and *norpA*^{p41}

	df Effect	MS Effect	df Error	MS Error	F	p-level
Genotype	1	5.786087	312	3.342055321	1.731295943	0.189211458
Day	11	20.81172	312	3.342055321	6.227221489	2.78532E-09
Genotype X Day	11	21.53861	312	3.342055321	6.444718838	1.18308E-09

Table 2.3.1: Summary of significant effect for Canton-S and *norpA*^{p41} mutant under “Breda” protocol.

Summary of all Effects Stanewsky protocol Canton-S and <i>norpA</i> ^{p41}						
	df	MS	df	MS		
	Effect	Effect	Error	Error	F	p-level
Genotype	1	8367.036133	631	832.9507	10.04506	0.001601471
Day	11	4774.791992	631	832.9507	5.732382	7.40494E-09
Genotype X Day	11	4537.154297	631	832.9507	5.447086	2.52963E-08

Table 2.3.2: Summary of significant effect for Canton-S and *norpA*^{p41} mutant under "Stanewsky" protocol.

Summary of all Effects; "Breda" protocol						
	df	MS	df	MS		
	Effect	Effect	Error	Error	F	p-level
Genotype	3	8.134433746	612	2.030992	4.005153	0.007702444
Day	11	45.87483978	612	2.030992	22.5874	0
Genotype X Day	33	7.349529266	612	2.030992	3.618689	1.69839E-10

Table 2.3.3: Summary of significant effect for Canton-S, *gl*^{60j}, *cry*^b and *cry*^{out} mutants under "Breda" protocol.

Summary of all Effects; "Stanewsky" protocol						
	df	MS	df	MS		
	Effect	Effect	Error	Error	F	p-level
Genotype	3	3103.664	679	774.0675	4.009552	0.007619358
Day	11	1326.661	679	774.0675	1.713883	0.066337533
Genotype X Day	33	1649.963	679	774.0675	2.131549	0.000282143

Table 2.3.4: Summary of significant effect for Canton-S, *gl*^{60j}, *cry*^b and *cry*^{out} mutants under "Stanewsky" protocol.

Summary of all Effects; "Breda" protocol						
	df	MS	df	MS		
	Effect	Effect	Error	Error	F	p-level
Genotype	3	2.654359341	612	2.368413925	1.120732903	0.339960635
Day	11	39.37675858	612	2.368413925	16.62579346	7.71615E-29
Genotype X Day	33	9.296819687	612	2.368413925	3.925335884	7.04713E-12

Table 2.3.5: Summary of significant effect for Canton-S, *norpA*^{p41}, *cry*^b and *norpA*^{p41};;*cry*^b mutants under "Breda" protocol.

Summary of all Effects; "Stanewsky" protocol						
	df	MS	df	MS		
	Effect	Effect	Error	Error	F	p-level
Genotype	3	3501.83	919	572.0289917	6.121769905	0.000401112
Day	11	1666.358	919	572.0289917	2.913065672	0.000867393
Genotype X Day	33	1861.491	919	572.0289917	3.254190445	3.6573E-09

Table 2.3.6: Summary of significant effect for Canton-S, *norpA*^{p41}, *cry*^b and *norpA*^{p41};;*cry*^b mutants under "Stanewsky" protocol.

Summary of all Effects under Breda protocol: *FGAL4 X norpARNAi*

	df	MS	df	MS		
	Effect	Effect	Error	Error	F	p-level
Genotype	2	245.7795	492	76.23374	3.224025	0.040637
Day	5	305.4965	492	76.23374	4.007366	0.001423
Genotype X Day	10	231.1736	492	76.23374	3.032432	0.000972

Table 2.3.7: Summary of significant effect for *FGAL4 X norpARNAi* flies and control under “Breda” protocol.

Summary of all Effects under Stanewsky protocol: *FGAL4 X norpARNAi*

	df	MS	df	MS		
	Effect	Effect	Error	Error	F	p-level
Genotype	2	7.377497	462	0.483992	15.24301	3.88423E-07
Day	5	20.27237	462	0.483992	41.88573	0
Genotype X Day	10	1.855787	462	0.483992	3.834333	5.3284E-05

Table 2.3.8: Summary of significant effect for *FGAL4 X norpARNAi* flies and control under “Stanewsky” protocol.

2.4. *plc21C* RNAi in LD 12:12

Summary of all Effects: *plc21C* level in CS, *w* and *norpA^{p41}* at 18 and 29°C

	df	MS	df	MS		
	Effect	Effect	Error	Error	F	p-level
Genotype	2	0.054387	270	0.008186	6.644102	0.001524972
Time	8	0.008321	270	0.008186	1.016541	0.423686981
Temperature	1	0.009434	270	0.008186	1.152489	0.283987224
Genotype X Time	16	0.011878	270	0.008186	1.451087	0.117988624
Genotype X Temperature	2	0.227263	270	0.008186	27.76327	1.08378E-11
Time X Temperature	8	0.005922	270	0.008186	0.723501	0.670722961
Genotype X Time X Temperature	16	0.011261	270	0.008186	1.375707	0.153073296

Table 2.4.1: ANOVA of *plc21C* level in Canton-S, *w¹¹¹⁸* and *norpA^{p41}* flies.

Probabilities for Post Hoc Tests. Newman-Keuls test: Genotype and Temperature Interaction

	{1}	{2}	{3}	{4}	{5}	{6}
	.1354567	.252017	.169628	.132721	.183762	.136485
Canton-S l {1}		1.7166E-05	0.1216040	0.87516683	0.0283291	0.952905
Canton-S h {2}	1.7166E-05		2.75373E-05	2.01464E-05	9.578E-05	7.689E-06
w1118 l {3}	0.12160408	2.7537E-05		0.14679426	0.4169625	0.0569805
w1118 h {4}	0.87516683	2.0146E-05	0.14679426		0.0278956	0.9745767
norpAp41 l {5}	0.02832919	9.5784E-05	0.41696250	0.027895629		0.0181971
norpAp41 h {6}	0.95290535	7.68E-06	0.05698049	0.974576652	0.0181970	

Table 2.4.2: Newman Keuls *post hoc* comparisons of *plc21C* level in Canton-S, *w¹¹¹⁸* and *norpA^{p41}* flies. l indicates 18°C whereas h 29°C.

Summary of all Effects: *actinGAL4 X plc21CRNAi* line A for the interference region

	df	MS	df	MS		
	Effect	Effect	Error	Error	F	p-level
Line	2	1054.8	12	441.96	2.38663	0.134085
Time course	1	387.1	12	441.96	0.87588	0.367785
Line X Time course	2	2114.1	12	441.96	4.78345	0.029673

Table 2.4.3: ANOVA of *plc21C* downregulation level in *actinGAL4 X plc21CRNAi* line A strain at 18°C. Line corresponds to the interference or control lines whereas time course refers at the two time points in which flies were collected.

Probabilities for Post Hoc Tests. Newman-Keuls test: INTERFERENCE REGION

INTERACTION: Line x Time course	{1}	{2}	{3}	{4}	{5}	{6}
	25.8360	68.3567	71.0397	39.5996	21.0030	37.7470
GAL4 control ZT0 {1}		0.1148	0.1255	0.7091	0.7832	0.5011
GAL4 control ZT12 {2}	0.1148		0.8785	0.1199	0.1024	0.2166
UAS control ZT0 {3}	0.1255	0.8785		0.2013	0.1040	0.2633
UAS control ZT12 {4}	0.7091	0.1199	0.2013		0.7058	0.9160
interference line ZT 0 {5}	0.7832	0.1024	0.1040	0.7058		0.6055
interference line ZT 12 {6}	0.5011	0.2166	0.2633	0.9160	0.6055	

Table 2.4.4: Newman Keuls *post hoc* comparisons of *plc21C* downregulation level in *actinGAL4 X plc21CRNAi* line A flies and controls at 18°C.

Summary of all Effects: *actinGAL4 X plc21CRNAi* line B for the interference region

1-Line. 2-Time course	df	MS	df	MS		
	Effect	Effect	Error	Error	F	p-level
Line	2.0000	1464.3480	12.0000	280.1171	5.2276	0.0233
Time course	1.0000	6486.2900	12.0000	280.1171	23.1556	0.0004
Line X Time course	2.0000	77.6240	12.0000	280.1171	0.2771	0.7627

Table 2.4.5: ANOVA of *plc21C* downregulation level of *actinGAL4 X plc21CRNAi* line B strain at 18°C.

Probabilities for Post Hoc Tests. Newman-Keuls test: INTERFERENCE REGION

INTERACTION: Line X Time course	{1}	{2}	{3}	{4}	{5}	{6}
	25.8360	68.3568	34.4792	76.1831	10.2755	39.9481
GAL4 control ZT0 {1}		0.0392	0.5391	0.0215	0.2772	0.5715
GAL4 control ZT12 {2}	0.0392		0.0696	0.5776	0.0082	0.0599
UAS control ZT0 {3}	0.5391	0.0696		0.0434	0.2206	0.6962
UAS control ZT12 {4}	0.0215	0.5776	0.0434		0.0044	0.0516
interference line ZT 0 {5}	0.2772	0.0082	0.2206	0.0044		0.1866
interference line ZT 12 {6}	0.5715	0.0599	0.6962	0.0516	0.1866	

Table 2.4.6: Newman Keuls *post hoc* comparisons of *plc21C* downregulation level in *actinGAL4 X plc21CRNAi* line B flies and controls at 18°C.

Summary of all Effects: *actinGAL4 X plc21CRNAi* line A for the external region

1-Line. 2-Time course	df	MS	df	MS		
	Effect	Effect	Error	Error	F	p-level
Line	2.0000	1229.7950	12.0000	549.0826	2.2397	0.1491
Time course	1.0000	177.4259	12.0000	549.0826	0.3231	0.5802
Line X Time course	2.0000	955.5039	12.0000	549.0826	1.7402	0.2170

Table 2.4.7: ANOVA of *plc21C* downregulation level of *actinGAL4 X plc21CRNAi* line A strain at 18°C. The silencing was evaluated in an external region to the interference.

Summary of all Effects: *actinGAL4 X plc21CRNAi* line B for the external region

1-LINE. 2-TIME	df	MS	df	MS		
	Effect	Effect	Error	Error	F	p-level
Line	2.0000	2082.9741	12.0000	234.8243	8.8704	0.0043
Time course	1.0000	4179.8311	12.0000	234.8243	17.7998	0.0012
Line X Time course	2.0000	66.5996	12.0000	234.8243	0.2836	0.7580

Table 2.4.8: ANOVA of *plc21C* downregulation level of *actinGAL4 X plc21CRNAi* line B strain at 18°C. The silencing was evaluated in an external region to the interference.

Probabilities for Post Hoc Tests. Newman-Keuls test: EXTERNAL REGION

INTERACTION: Line X Time course	{1}	{2}	{3}	{4}	{5}	{6}
	41.5321	65.1053	43.5528	80.4233	10.7730	41.7606
GAL4 control ZT0 {1}		0.2849	0.9858	0.0573	0.0303	0.9858
GAL4 control ZT12 {2}	0.2849		0.1108	0.2445	0.0070	0.1910
UAS control ZT0 {3}	0.9858	0.1108		0.0306	0.0907	0.8886
UAS control ZT12 {4}	0.0573	0.2445	0.0306		0.0014	0.0406
interference line ZT 0 {5}	0.0303	0.0070	0.0907	0.0014		0.0699
interference line ZT 12 {6}	0.9858	0.1910	0.8886	0.0406	0.0699	

Table 2.4.9: Newman Keuls *post hoc* comparisons of *plc21C* downregulation level in *actinGAL4 X plc21CRNAi* line B flies and controls at 18°C.

Summary of all Effects: *actinGAL4 X plc21CRNAi* line A for the interference region

1-Line. 2-Time course	df	MS	df	MS		
	Effect	Effect	Error	Error	F	p-level
Line	2	1787.131	12	417.5691	4.279846	0.039536
Time course	1	224.5728	12	417.5691	0.53781	0.477425
Line X Time Course	2	1111.715	12	417.5691	2.662349	0.110432

Table 2.4.10: ANOVA of *plc21C* downregulation level in *actinGAL4 X plc21CRNAi* line A strain at 29°C. Line corresponds to the interference or control lines whereas time course refers at the two time points in which flies were collected.

Summary of all Effects: *actinGAL4 X plc21CRNAi* line B for interference region

1-Line. 2-Time course	df	MS	df	MS		
	Effect	Effect	Error	Error	F	p-level
Line	2	3047.3	12	149.4306	20.39274	0.00138
Time course	1	2899.005	12	149.4306	19.40034	0.000858
Line X Time course	2	1125.276	12	149.4306	7.530424	0.007604

Table 2.4.11: ANOVA of *plc21C* downregulation level in *actinGAL4 X plc21CRNAi* line B strain at 29°C. Line corresponds to the interference or control lines whereas time course refers at the two time points in which flies were collected.

Probabilities for Post Hoc Tests. Newman-Keuls test: INTERFERENCE REGION

INTERACTION: Line X Time course	{1}	{2}	{3}	{4}	{5}	{6}
	60.9746	26.1385	74.3693	27.5781	6.02199	11.5047
GAL4 control ZT0 {1}		0.01162	0.20456	0.00598	0.00116	0.00178
GAL4 control ZT12 {2}	0.01162		0.00215	0.88784	0.15089	0.16846
UAS control ZT0 {3}	0.20456	0.00215		0.00154	0.000331	0.000433
UAS control ZT12 {4}	0.00598	0.88784	0.00154		0.189911	0.279061
interference line ZT 0 {5}	0.00116	0.15089	0.00033	0.18991		0.593015
interference line ZT 12 {6}	0.00178	0.16846	0.00043	0.27906	0.593015	

Table 2.4.12: Newman Keuls *post hoc* comparisons of *plc21C* downregulation level in *actinGAL4 X plc21CRNAi* line B flies and controls at 29°C.

Summary of all Effects: *actinGAL4 X plc21CRNAi* line A for the external region

1-Line. 2-Time course	df	MS	df	MS		
	Effect	Effect	Error	Error	F	p-level
Line	2	1592.212	12	483.8805	3.290507	0.072556
Time course	1	1620.925	12	483.8805	3.349845	0.092147
Line X Time course	2	2166.213	12	483.8805	4.476753	0.035282

Table 2.4.13: ANOVA of *plc21C* downregulation level of *actinGAL4 X plc21CRNAi* line A strain at 29°C. The silencing was evaluated in an external region to the interference.

Probabilities for Post Hoc Tests. Newman-Keuls test: EXTERNAL REGION

INTERACTION: Line X Time course	{1}	{2}	{3}	{4}	{5}	{6}
	86.5088	26.4814	48.4679	63.4450	33.9577	22.0708
GAL4 control ZT0 {1}		0.039	0.128	0.223	0.054	0.034
GAL4 control ZT12 {2}	0.039		0.462	0.222	0.685	0.810
UAS control ZT0 {3}	0.128	0.462		0.421	0.435	0.484
UAS control ZT12 {4}	0.223	0.222	0.421		0.267	0.209
interference line ZT 0 {5}	0.054	0.685	0.435	0.267		0.789
interference line ZT 12 {6}	0.034	0.810	0.484	0.209	0.789	

Table 2.4.14: Newman Keuls *post hoc* comparisons of *plc21C* downregulation level in *actinGAL4 X plc21CRNAi* line A flies and controls at 29°C.

Summary of all Effects: *actinGAL4 X plc21CRNAi* line B for the external region

1-Line. 2-Time course	df	MS	df	MS		
	Effect	Effect	Error	Error	F	p-level
Line	2	3846.053	12	74.09711	51.90557	1.23761E-06
Time course	1	6189.389	12	74.09711	83.53078	9.38264E-07
Line X Time course	2	1352.608	12	74.09711	18.25453	0.000229166

Table 2.4.15: ANOVA of *plc21C* downregulation level of *actinGAL4 X plc21CRNAi* line B strain at 29°C. The silencing was evaluated in an external region to the interference.

Probabilities for Post Hoc Tests. Newman-Keuls test: EXTERNAL REGION

INTERACTION: Line X Time course	{1}	{2}	{3}	{4}	{5}	{6}
	86.509	26.481	86.181	38.047	17.273	14.174
GAL4 control ZT0 {1}		0.00020	0.96367	0.00023	0.00015	0.00016
GAL4 control ZT12 {2}	0.00020		0.00019	0.12593	0.21477	0.22731
UAS control ZT0 {3}	0.96367	0.00019		0.00018	0.00020	0.00015
UAS control ZT12 {4}	0.00023	0.12593	0.00018		0.03011	0.02383
interference line ZT 0 {5}	0.00015	0.21477	0.00020	0.03011		0.66726
interference line ZT 12 {6}	0.00016	0.22731	0.00015	0.02383	0.66726	

Table 2.4.16: Newman Keuls *post hoc* comparisons of *plc21C* downregulation level in *actinGAL4 X plc21CRNAi* line B flies and controls at 29°C.

Summary of all Effects: *per* mRNA level in *actinGAL4 X plc21C RNAi* flies at 18°C

	df	MS	df	MS		
	Effect	Effect	Error	Error	F	p-level
Line	1	0.060292	24	0.111102	0.542671	0.468468
Genotype	2	0.001577	24	0.111102	0.014192	0.985916
ZT	1	3.556707	24	0.111102	32.01299	7.94E-06
Line X Genotype	2	0.016063	24	0.111102	0.144582	0.866132
Line X ZT	1	0.239618	24	0.111102	2.156739	0.154932
Genotype X ZT	2	0.321118	24	0.111102	2.890303	0.075047
Line X Genotype X ZT	2	0.084994	24	0.111102	0.765007	0.476346

Table 2.4.17: Analysis of Variance of *per* mRNA level in *actinGAL4 X plc21CRNAi* lines and controls at ZT 0 and 12 at 18°C.

Summary of all Effects: *per* mRNA level in *actinGAL4 X plc21C RNAi* flies at 29°C

	df	MS	df	MS		
	Effect	Effect	Error	Error	F	p-level
Line (A or B)	1	0.005536	24	0.066334	0.083461	0.775142
Genotype	2	0.055566	24	0.066334	0.837665	0.444982
ZT	1	0.291846	24	0.066334	4.399616	0.046659
Line X Genotype	2	0.002019	24	0.066334	0.030437	0.970059
Line X ZT	1	0.010459	24	0.066334	0.157664	0.694826
Genotype X ZT	2	0.111224	24	0.066334	1.676715	0.208158
Line X Genotype X ZT	2	0.034449	24	0.066334	0.519317	0.601461

Table 2.4.18: Analysis of Variance of *per* mRNA level in *actinGAL4 X plc21CRNAi* lines and controls at ZT 0 and 12 at 29°C.

Summary of all Effects: Unspliced and spliced *per* level in *actinGAL4 X plc21C* RNAi flies at 18°C

	df	MS	df	MS		
	Effect	Effect	Error	Error	F	p-level
Line	1	0.005226	24	0.007522	0.694733	0.412778
Genotype	2	0.018538	24	0.007522	2.464468	0.106303
ZT	1	0.029941	24	0.007522	3.980385	0.057507
Line X Genotype	2	0.002477	24	0.007522	0.329247	0.722664
Line X ZT	1	0.010388	24	0.007522	1.381043	0.251451
Genotype X ZT	2	0.003468	24	0.007522	0.46098	0.636134
Line X Genotype X ZT	2	0.002663	24	0.007522	0.354034	0.705456

Table 2.4.19: Analysis of Variance of unspliced and spliced *per* level in *actinGAL4 X plc21CRNAi* lines and controls at ZT 0 and 12 at18°C.

Summary of all Effects: Unspliced and spliced *per* level in *actinGAL4 X plc21C* RNAi flies at 29°C

	df	MS	df	MS		
	Effect	Effect	Error	Error	F	p-level
Line (A or B)	1	0.000156	24	0.005805	0.026851	0.871211
Genotype	2	0.005783	24	0.005805	0.996186	0.384047
ZT	1	0.056029	24	0.005805	9.65126	0.00481
Line X Genotype	2	0.000485	24	0.005805	0.083553	0.920108
Line X ZT	1	0.001584	24	0.005805	0.27284	0.606222
Genotype X ZT	2	0.005519	24	0.005805	0.950727	0.400539
Line X Genotype X ZT	2	0.005364	24	0.005805	0.923988	0.410598

Table 2.4.20: Analysis of Variance of unspliced and spliced *per* level in *actinGAL4 X plc21CRNAi* lines and controls at ZT 0 and 12 at29°C.

Summary of all Effects: Total *tim* level in *actinGAL4 X plc21C* RNAi flies at 18°C

	df	MS	df	MS		
	Effect	Effect	Error	Error	F	p-level
Line (A or B)	1	0.020747	24	0.521439	0.039787	0.843577743
Genotype	2	0.130145	24	0.521439	0.249589	0.781118095
ZT	1	52.27401	24	0.521439	100.2496	4.79729E-10
Line X Genotype	2	0.078983	24	0.521439	0.15147	0.8602584
Line X ZT	1	1.564114	24	0.521439	2.999613	0.096120149
Genotype X ZT	2	2.578036	24	0.521439	4.944084	0.015920544
Line X Genotype X ZT	2	0.491052	24	0.521439	0.941726	0.403895199

Table 2.4.21: Analysis of Variance of *tim* mRNA level in *actinGAL4 X plc21CRNAi* lines and controls at ZT 0 and 12 at18°C.

Summary of all Effects: Unspliced and spliced *tim* level in *actinGAL4 X plc21C* RNAi flies at 18°C

	df	MS	df	MS		
	Effect	Effect	Error	Error	F	p-level
Line (A or B)	1	0.064515	24	0.003486	18.50468	0.000245235
Genotype	2	0.019507	24	0.003486	5.595204	0.010126125
ZT	1	0.011097	24	0.003486	3.182874	0.087063886
Line X Genotype	2	0.022508	24	0.003486	6.456002	0.005708518
Line X ZT	1	0.011955	24	0.003486	3.428953	0.076404735
Genotype X ZT	2	0.083774	24	0.003486	24.02895	1.86361E-06
Line X Genotype X ZT	2	0.003752	24	0.003486	1.076125	0.356801152

Table 2.4.22: Analysis of Variance of unspliced and spliced *tim* level in *actinGAL4 X plc21C* RNAi lines and controls at ZT 0 and 12 at 18°C.

Appendix 3: GPCRs

3.1. GPCRs in *glass^{60j}cry^b* genetic background

Some of the transgenic lines analysed in this chapter carried the RNAi construct on the third chromosome. In order to test their locomotor activity in the *gl^{60j}cry^b* mutant background, recombination was required (Figure 3.6.1).

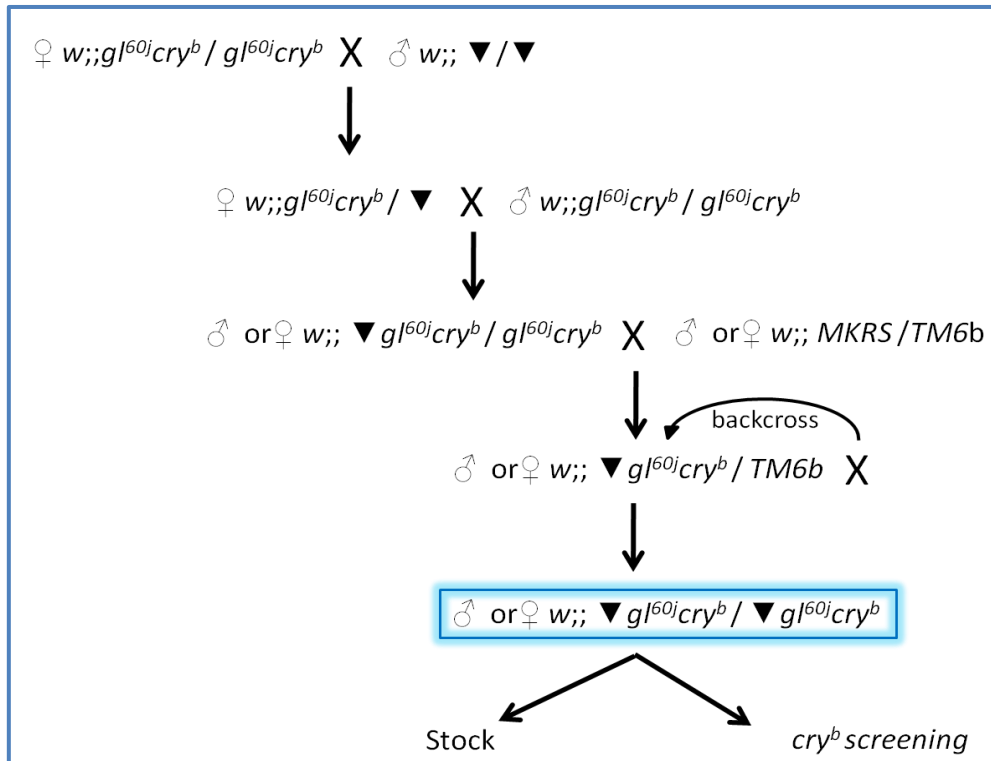


Figure 3.1.1: Scheme of crosses adopted to move GPCR construct in *glass^{60j}cry^b* background.

The recombination efficiency was tested by:

- *glass^{60j}* phenotype (section 7.2.1, Figure 7.2 B and C)
- red eyes due the presence of the RNAi construct (section 7.2.1, Figure 7.2 C)
- testing the presence of *cry^b* mutation by PCR and restriction reaction (section 7.2.1, Figure 7.3 and 7.4)

3.2. CG12290

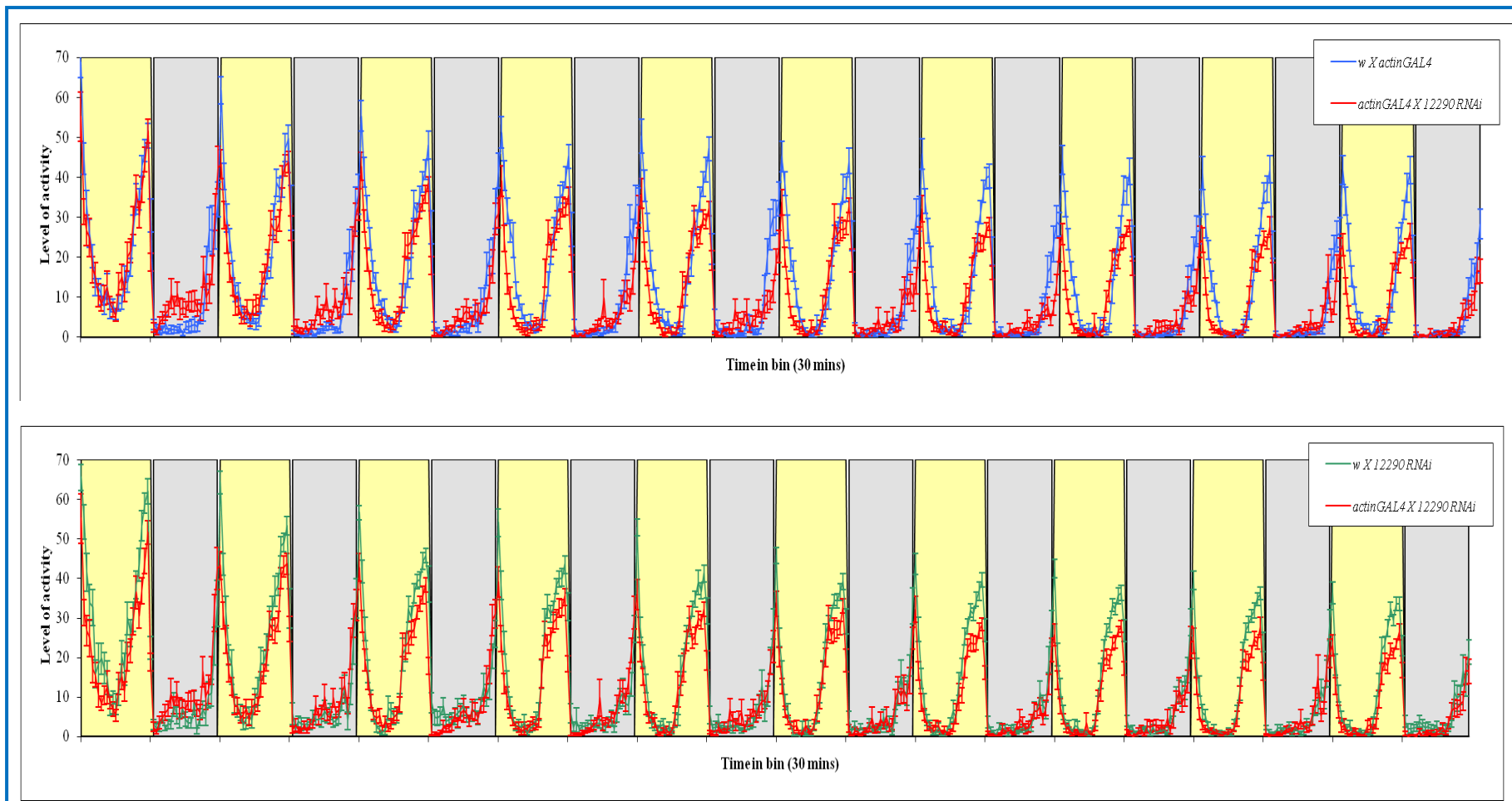


Figure 3.2.1: Comparison of averaged locomotor activity profiles of *actinGAL4* driving RNA interference of *CG12290* and controls in light/dark regime at 25°C. The full experiment is shown: the first three days were for the entrainment and the following seven were the experimental ones. The interfered flies (red line) were compared to the driver (blue line) and the RNAi (green line) controls, respectively. Yellow bars indicate light and grey bars dark. Bars indicate SEM.

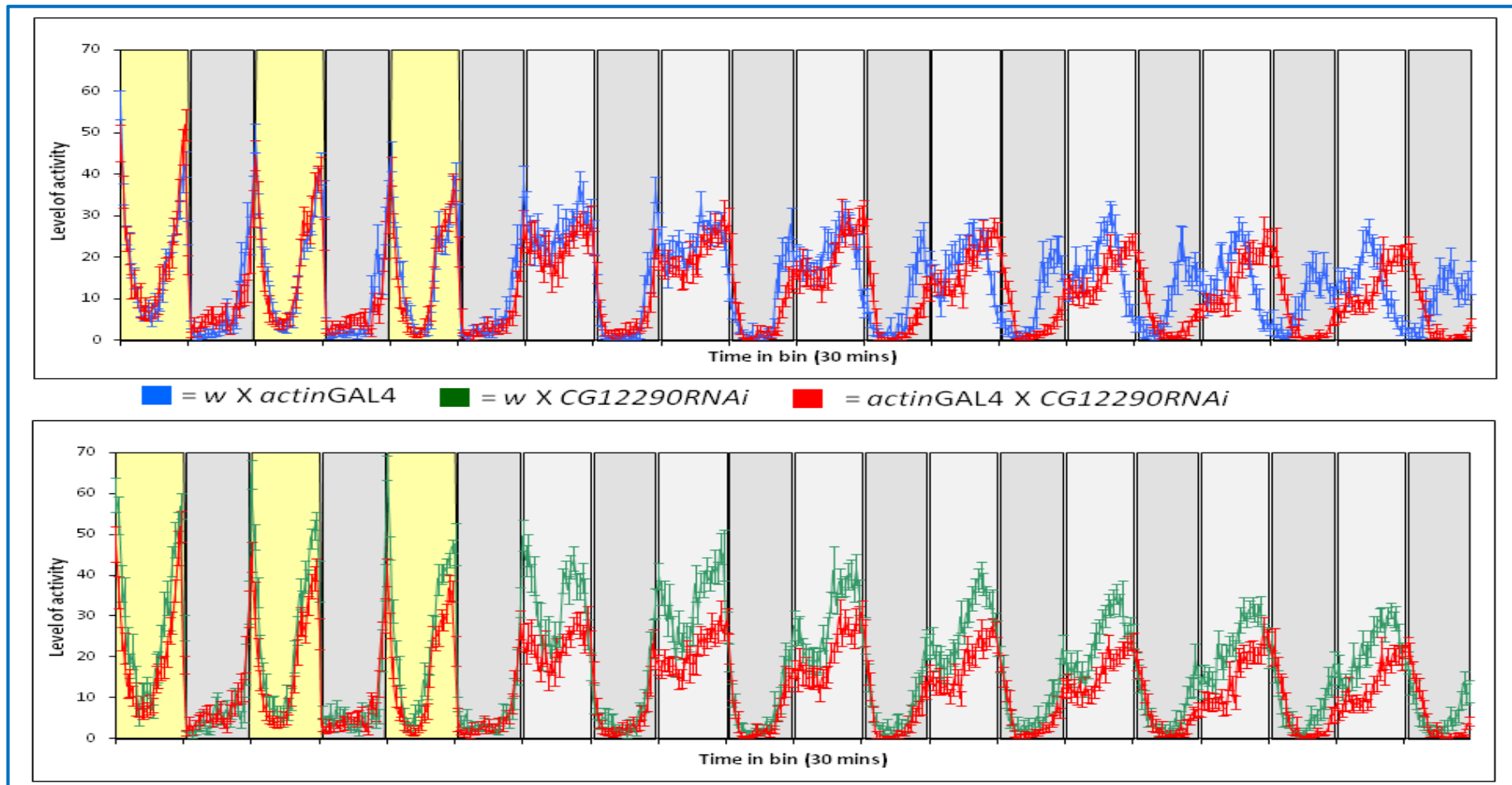


Figure 3.2.2: Comparison of averaged locomotor activity patterns of *actinGAL4* driving RNA interference of *CG12290* and controls in DD at 25°C. The first three entrainment days were followed by seven in DD. The interfered flies (red line) are compared to the driver (blue line) and RNAi (green line) controls. Yellow bars indicate light, light grey subjective day and dark grey bars subjective night.

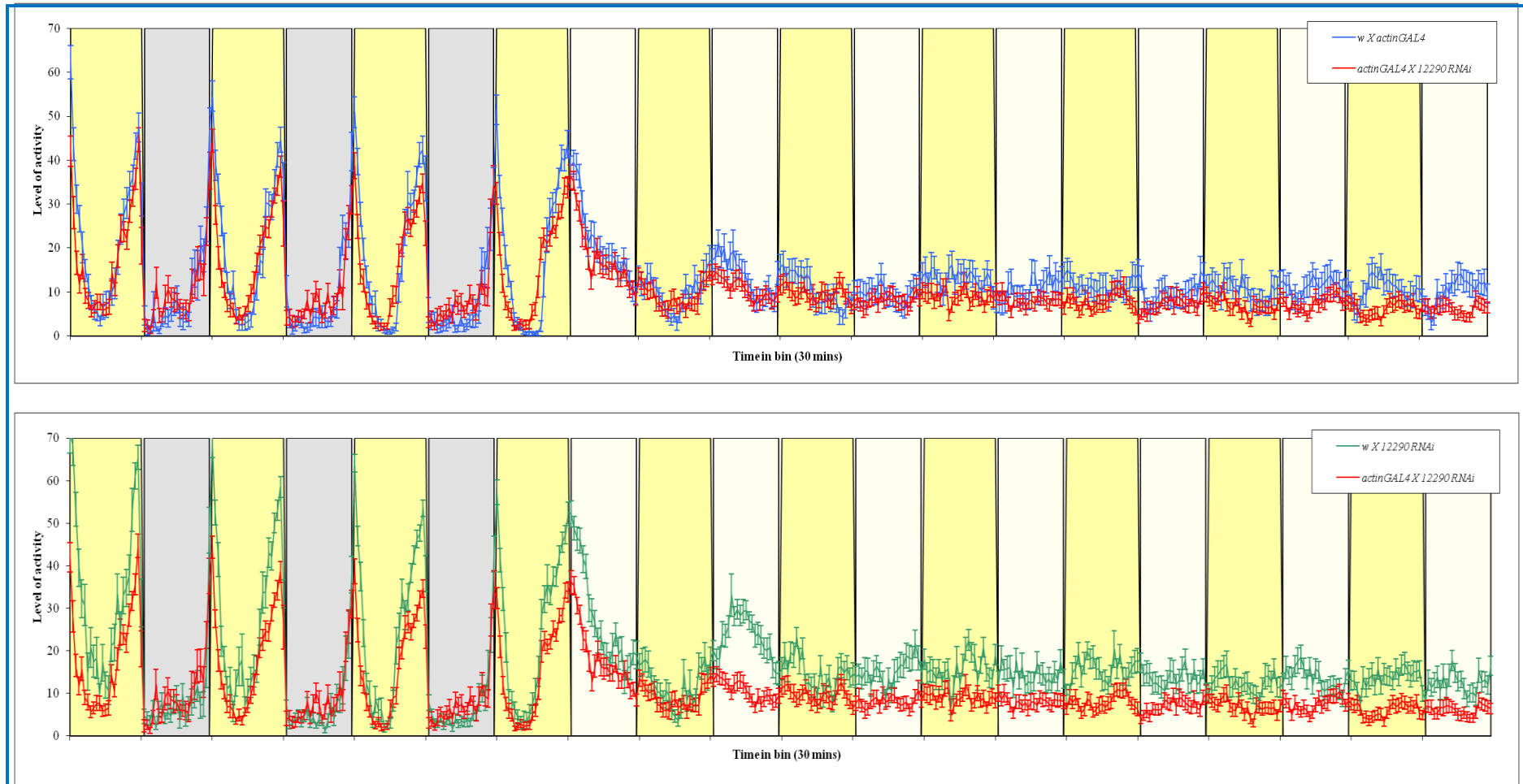


Figure 3.2.3: Comparison of the locomotor activity profiles of *actinGAL4* driving RNA interference of *CG12290* and controls constant light at 25°C. The first three entrainment days were followed by seven in LL conditions. The interfered flies (red line) were compared to the driver control (blue line) and RNAi (green line) controls, respectively. Yellow bars indicated light, grey bars night and light yellow the subjective night.

3.3. CG7497

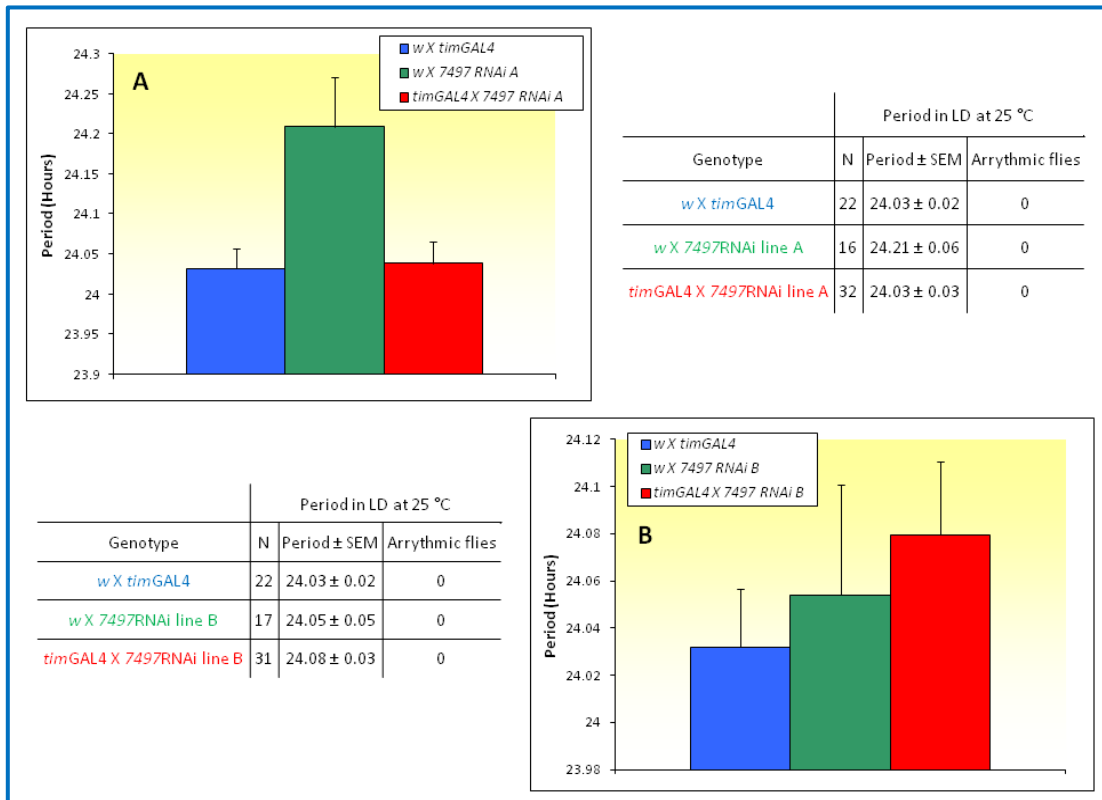
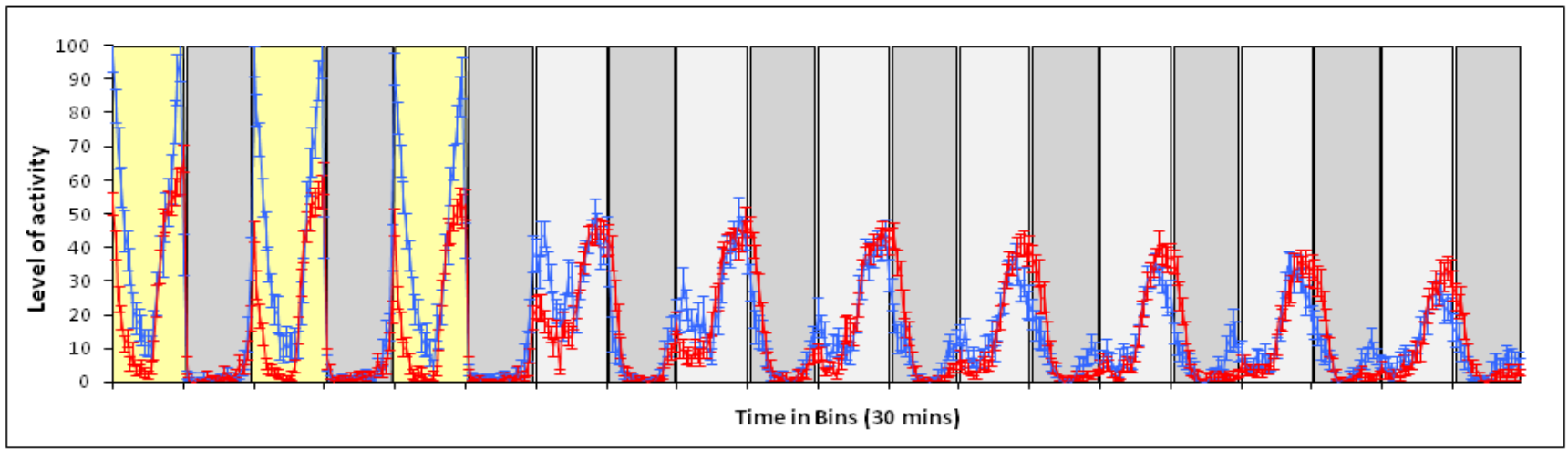
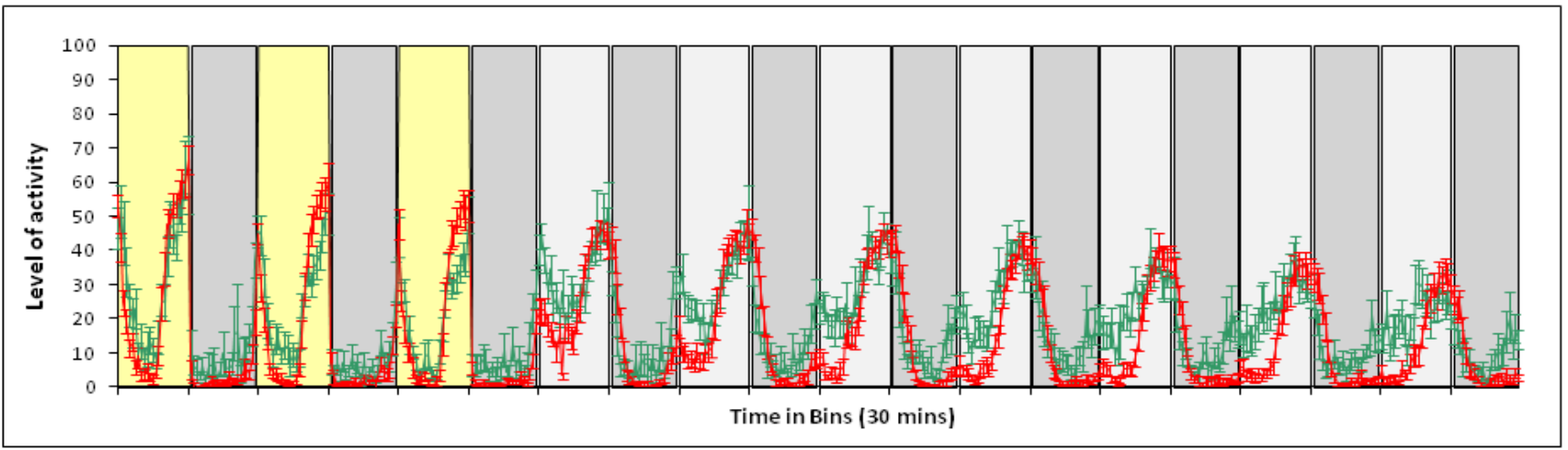


Figure 3.3.1: Averaged periods of flies downregulating *CG7497* gene (line A in graph A whereas line B in graph B) and their controls in LD cycles at 25°C. Bars indicate SEM.



■ = *w* X *timGAL4*
 ■ = *w* X *CG7497RNAi* line A
 ■ = *timGAL4* X *CG7497RNAi* line A



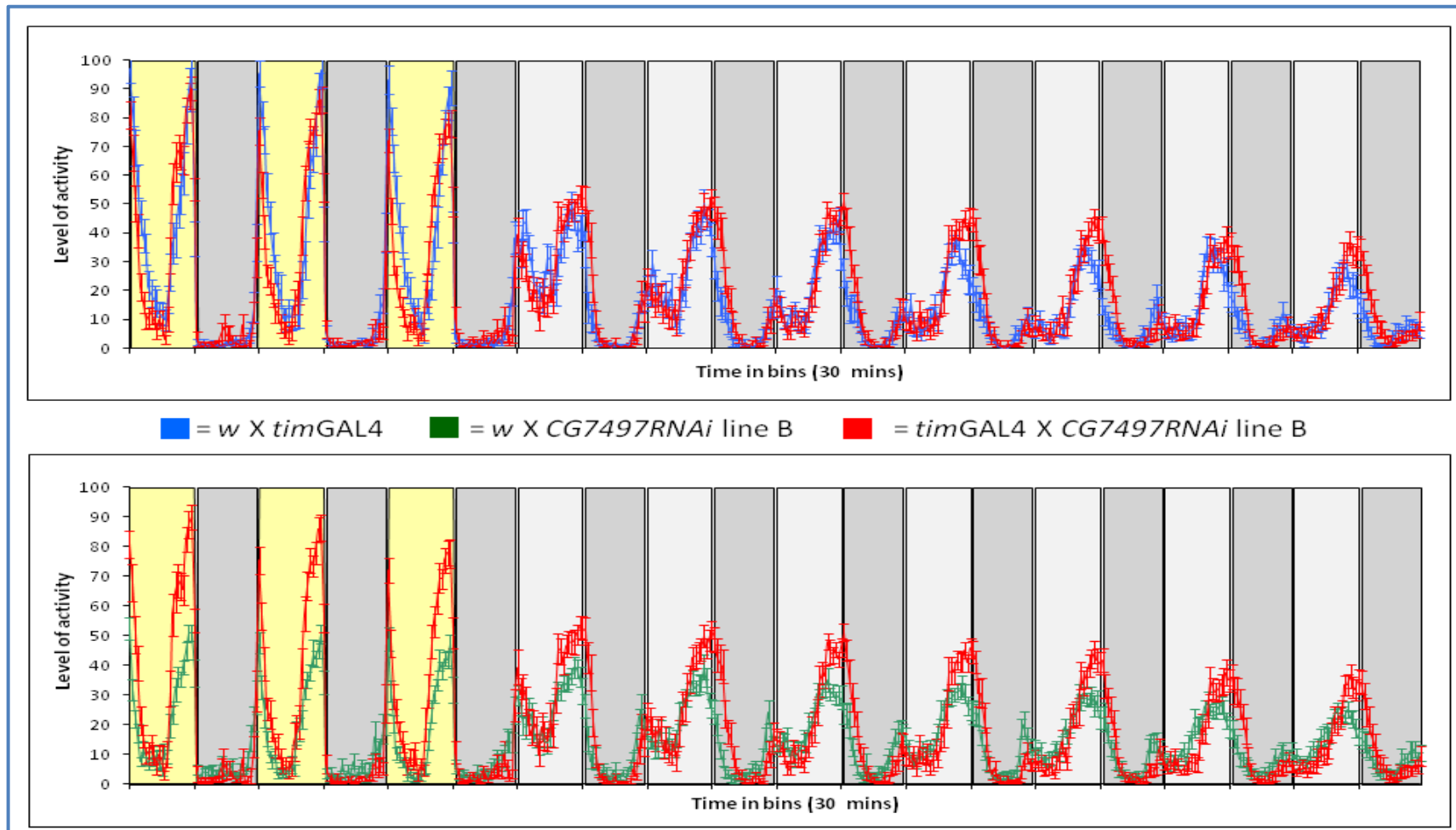
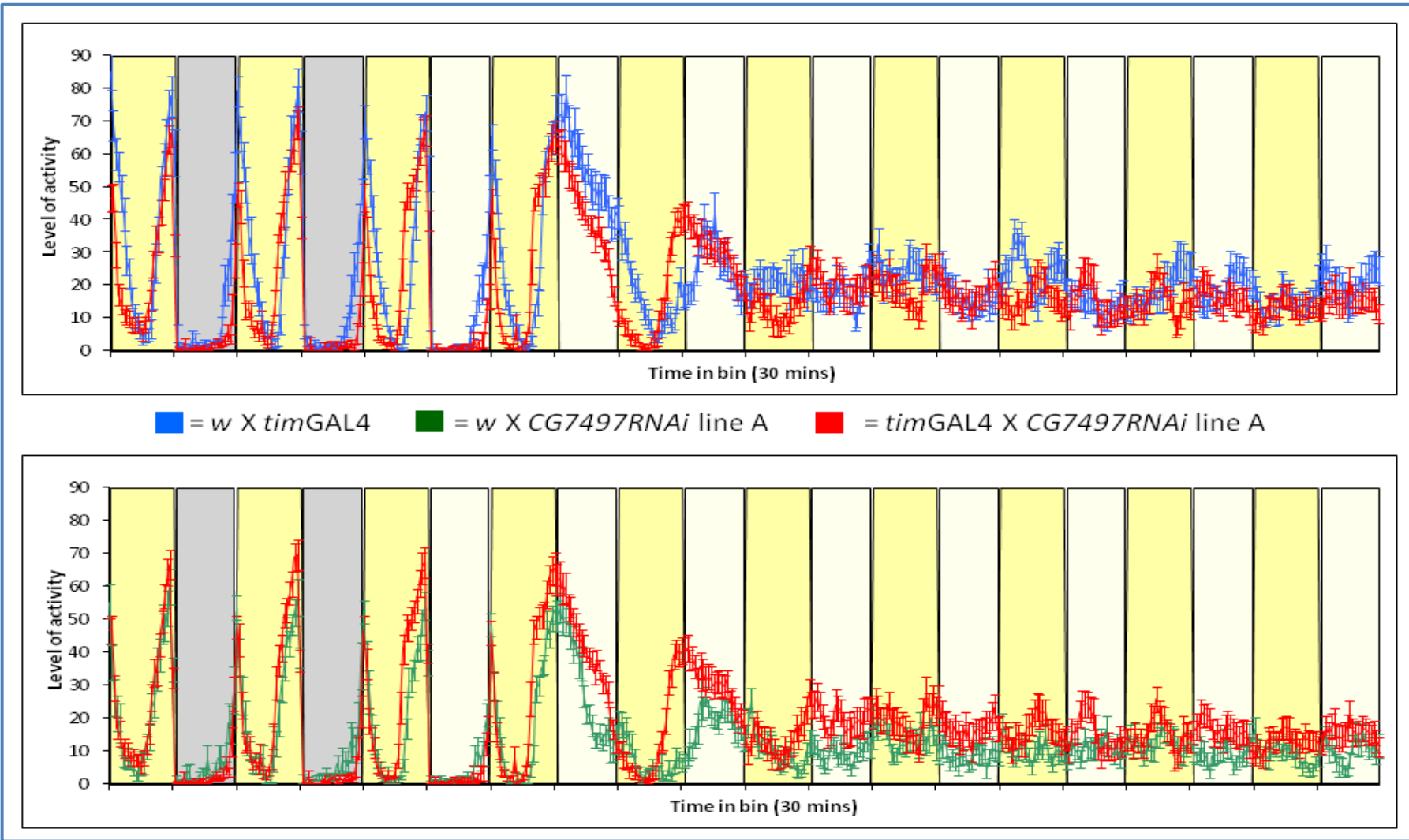


Figure 3.3.2: Comparison of average locomotor activity profiles of *timGAL4* driving RNA interference of *CG7497* and controls in constant darkness at 25°C. In previous page the locomotor activity profile of line A is shown whereas in this page locomotor behaviour of line B is presented.



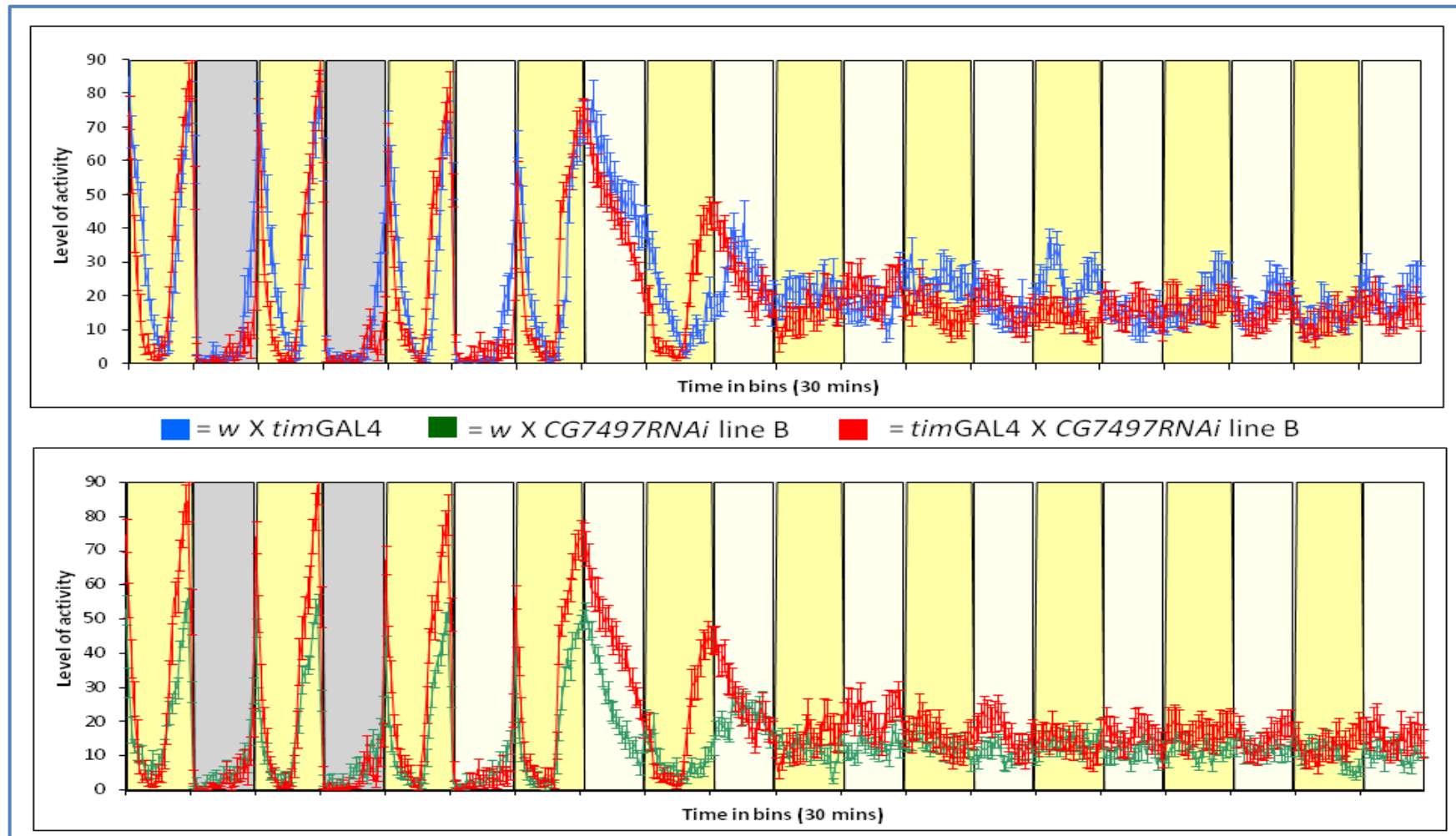


Figure 3.3.3: Comparison of averaged locomotor activity profiles of *timGAL4* driving RNA interference of *CG7497* A (previous page) and B (this page) and controls in LL at 25°C.

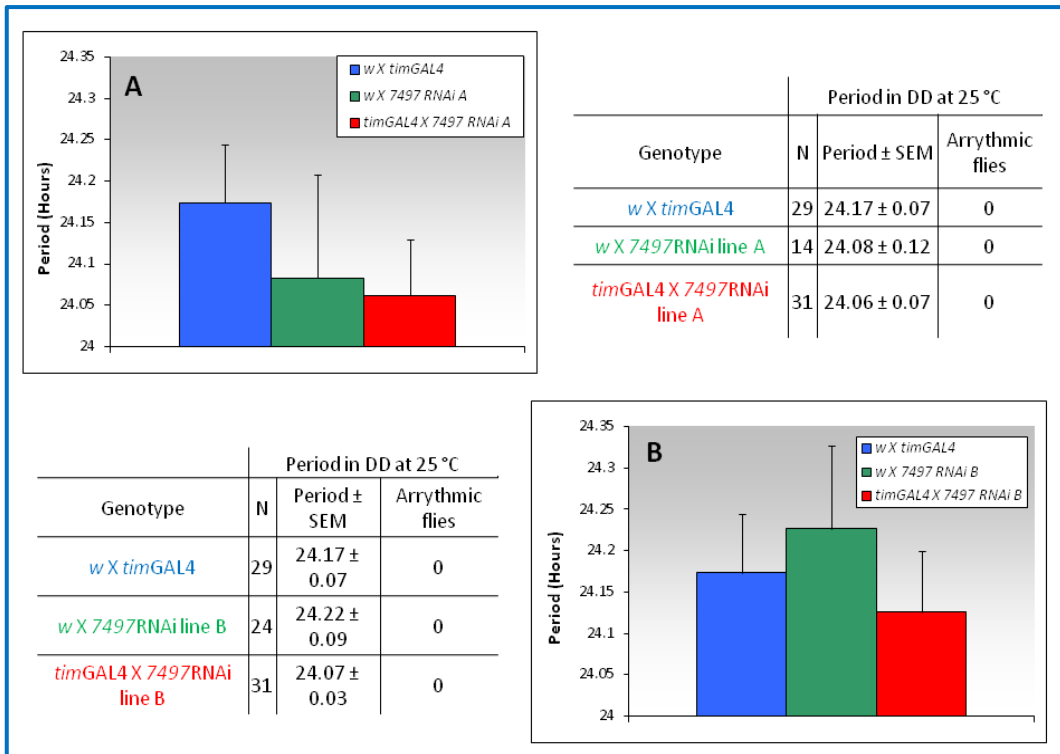


Figure 3.3.4: Averaged free-running periods of CG7497 downregulating flies (A shows line A and B shows line B) and controls in DD at 25°C. Bars indicate SEM.

3.4. CG13995

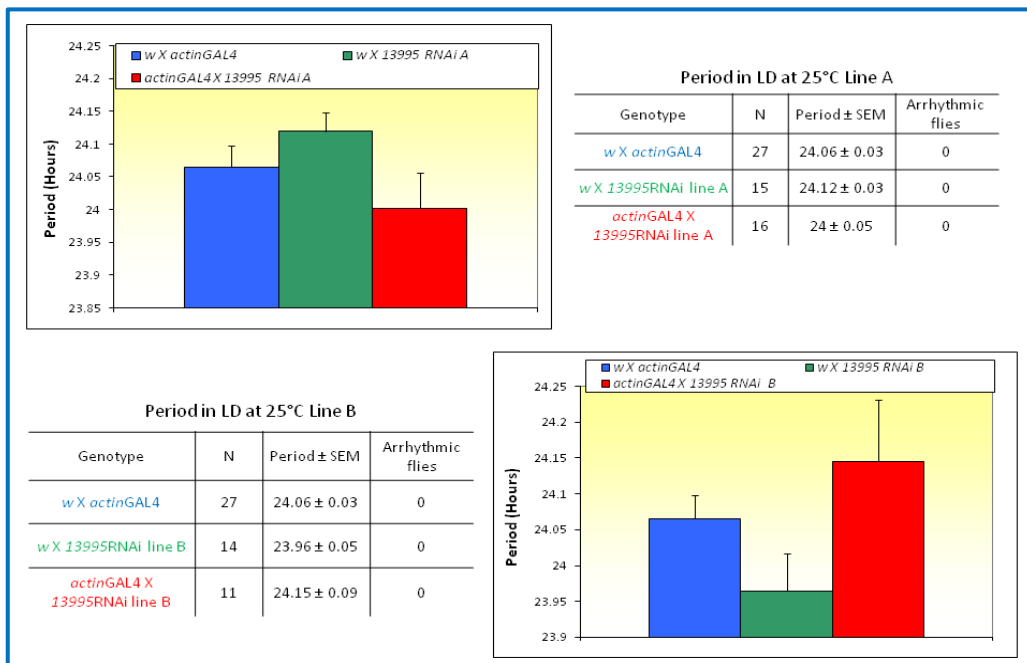
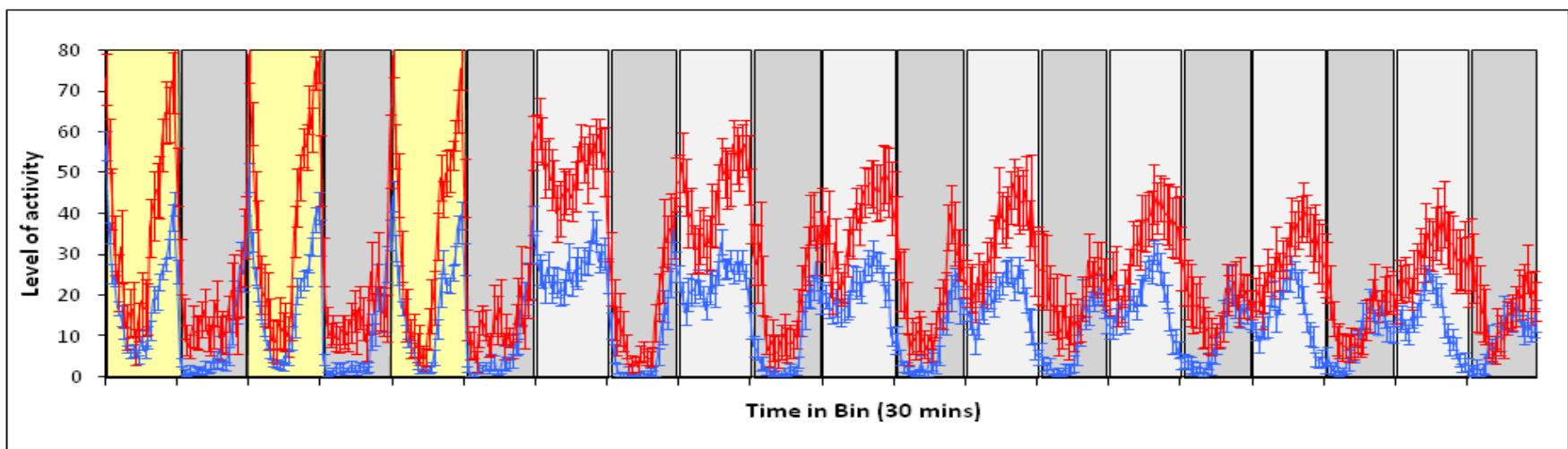
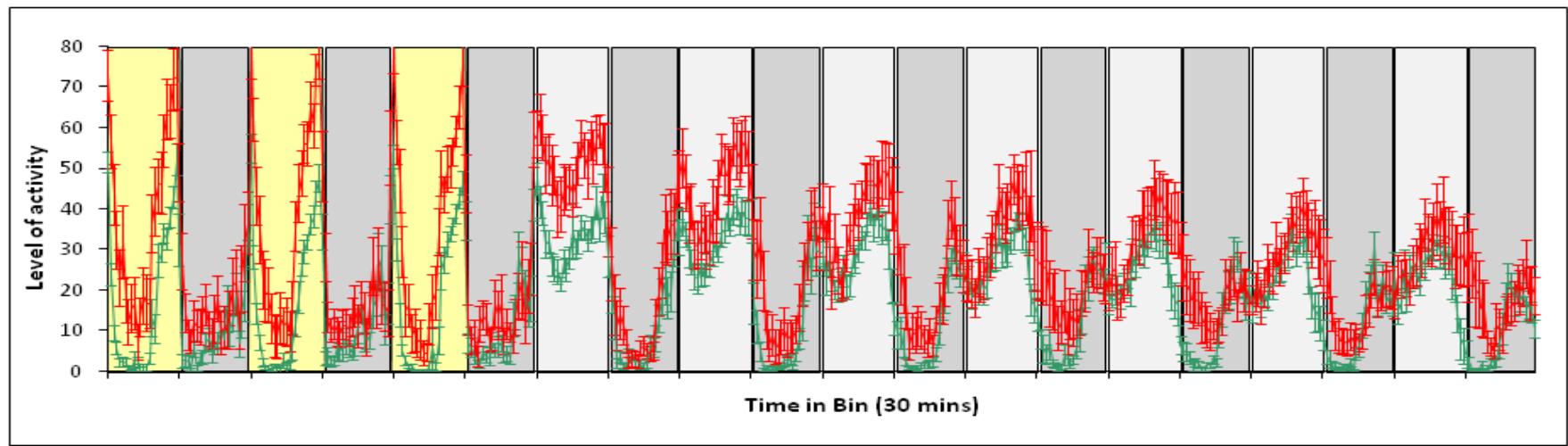


Figure 3.4.1: Averaged period in LD of flies downregulating CG13995. On the left the period of line A and on the right the one obtained from line B. Bars indicate SEM.



■ = *w X actinGAL4*
 ■ = *w X CG13995RNAi line A*
 ■ = *actinGAL4 X CG13995RNAi line A*



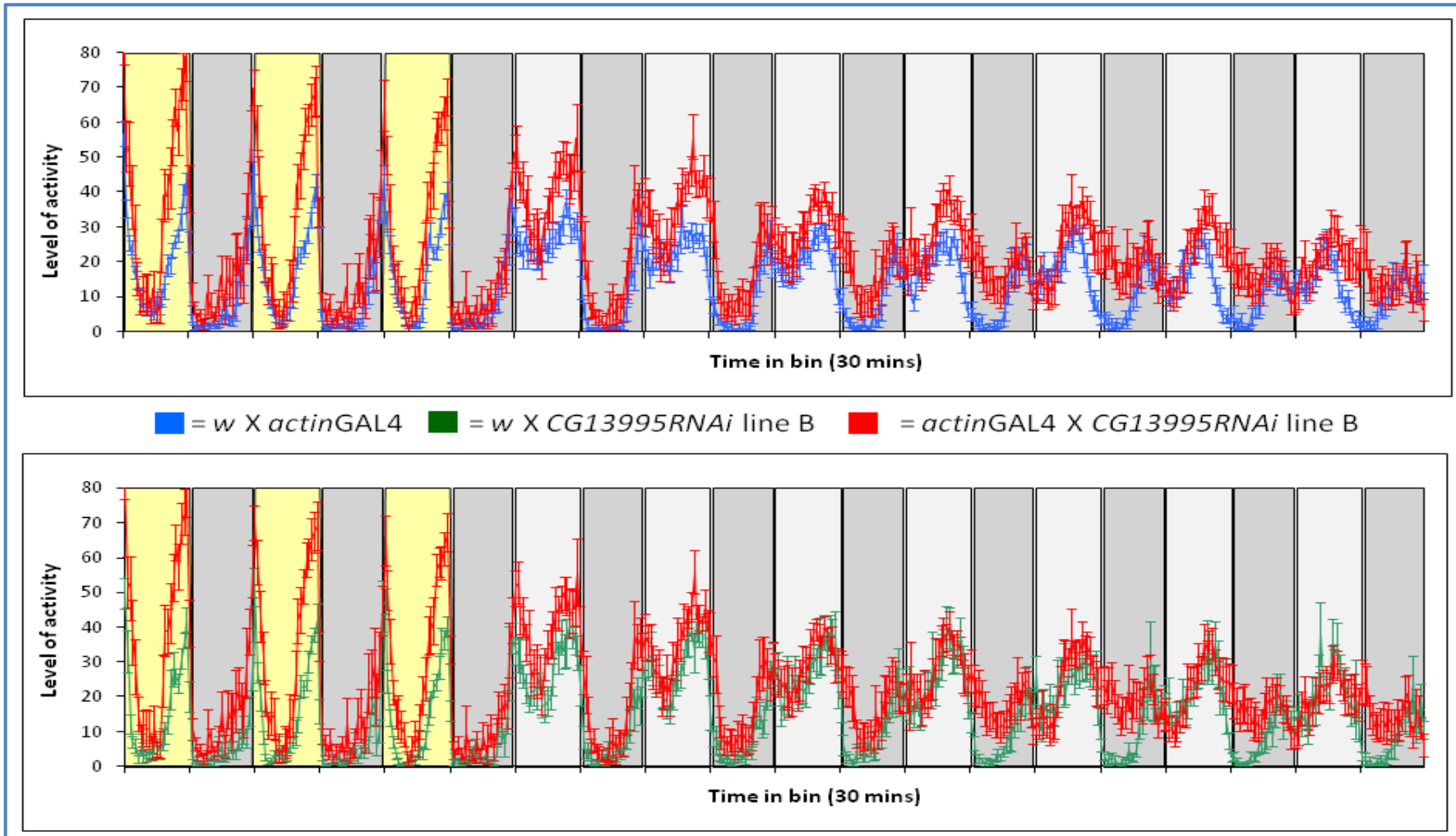
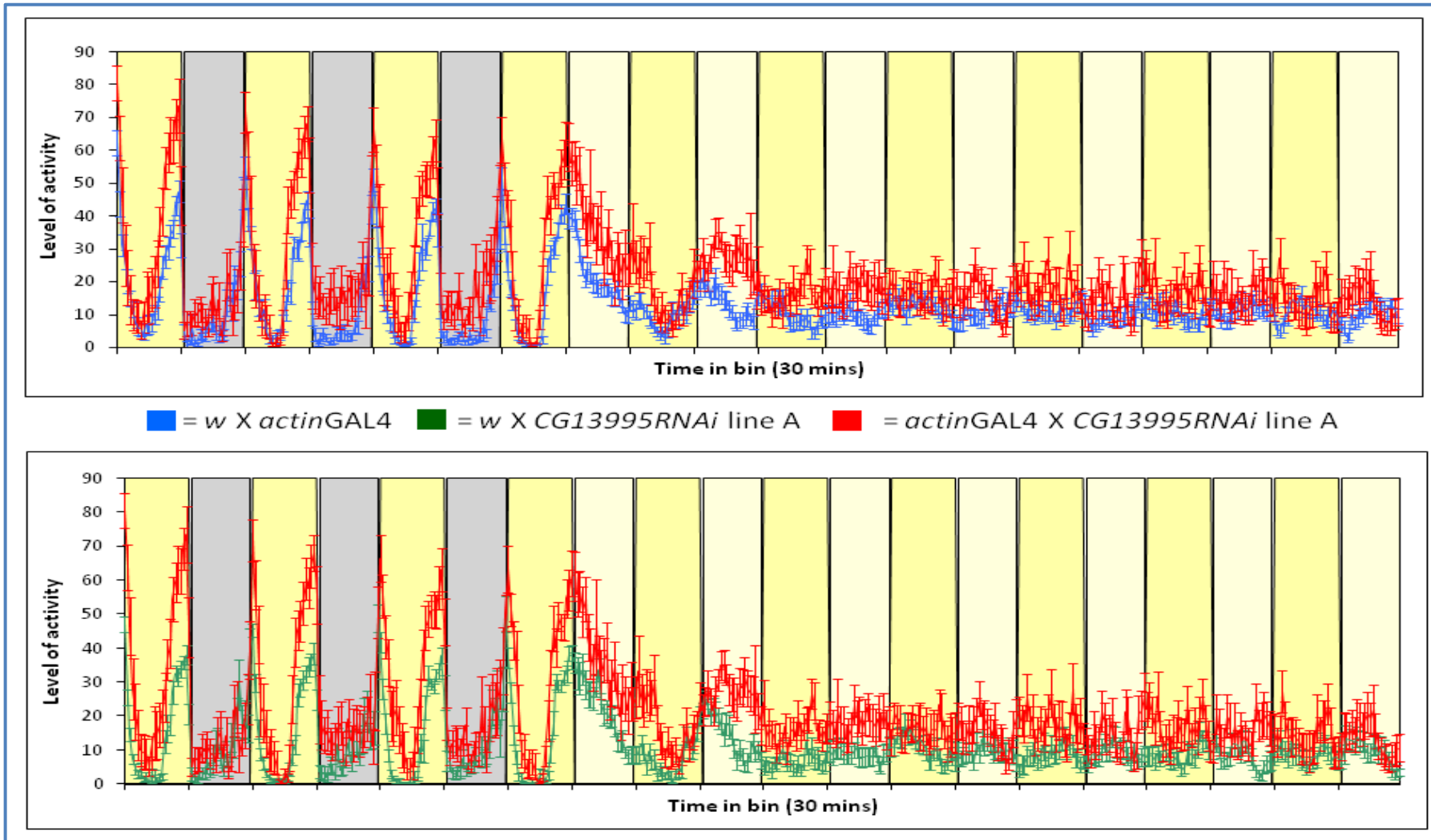


Figure 3.4.2: Comparison of averaged locomotor activity profiles of *actinGAL4* driving RNA interference of *CG13995* and controls in DD at 25°C. In previous page the locomotor activity profile of line A is shown and in this page line B is presented.



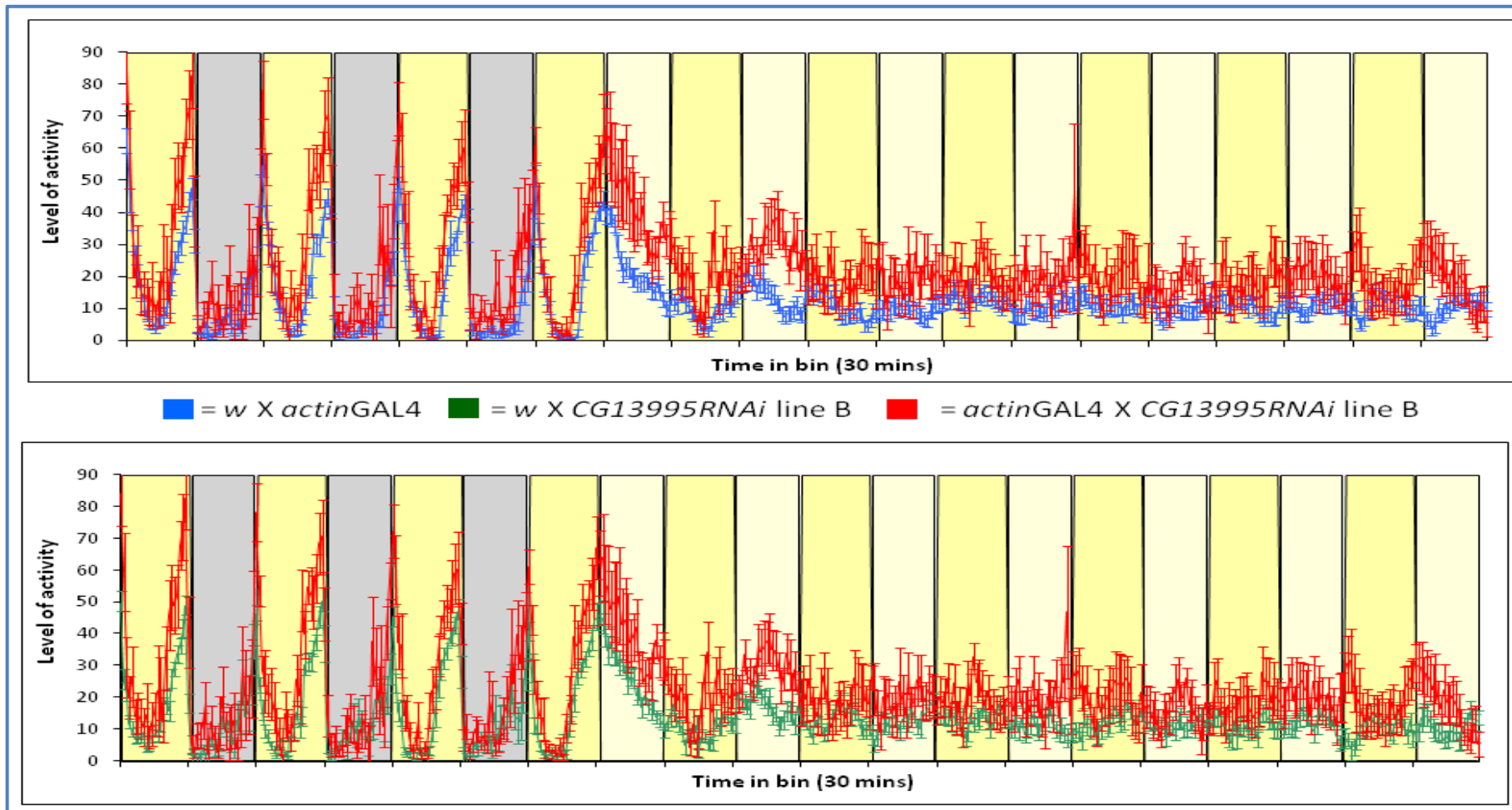


Figure 3.4.3: Comparison of averaged locomotor activity profiles of *actinGAL4* driving RNA interference of *CG13995* A (previous page) and B (this page) and controls in LL at 25°C.

3.5. *CG13579*

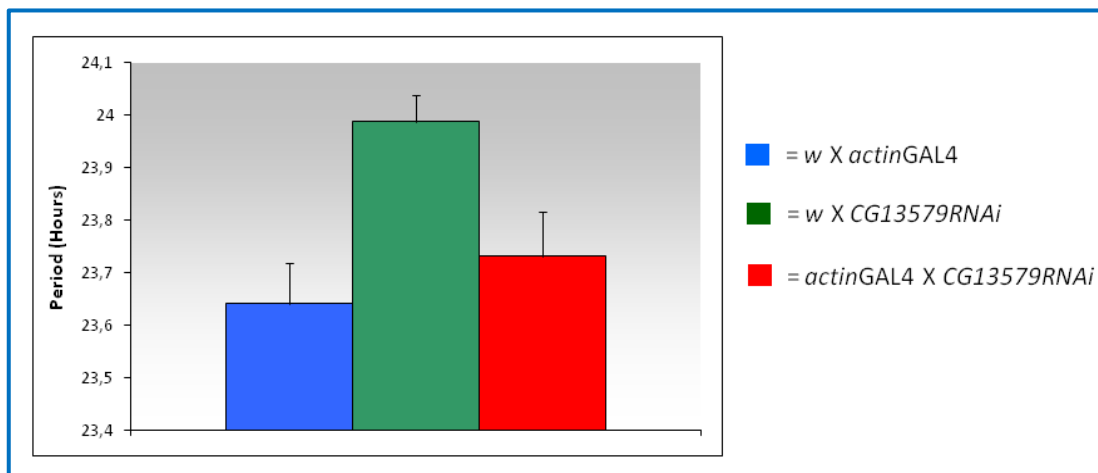


Figure 3.5.1: Averaged locomotor activity periods of *w*; *actinGAL4*; *CG13579RNAi* flies and controls in DD at 25°C.

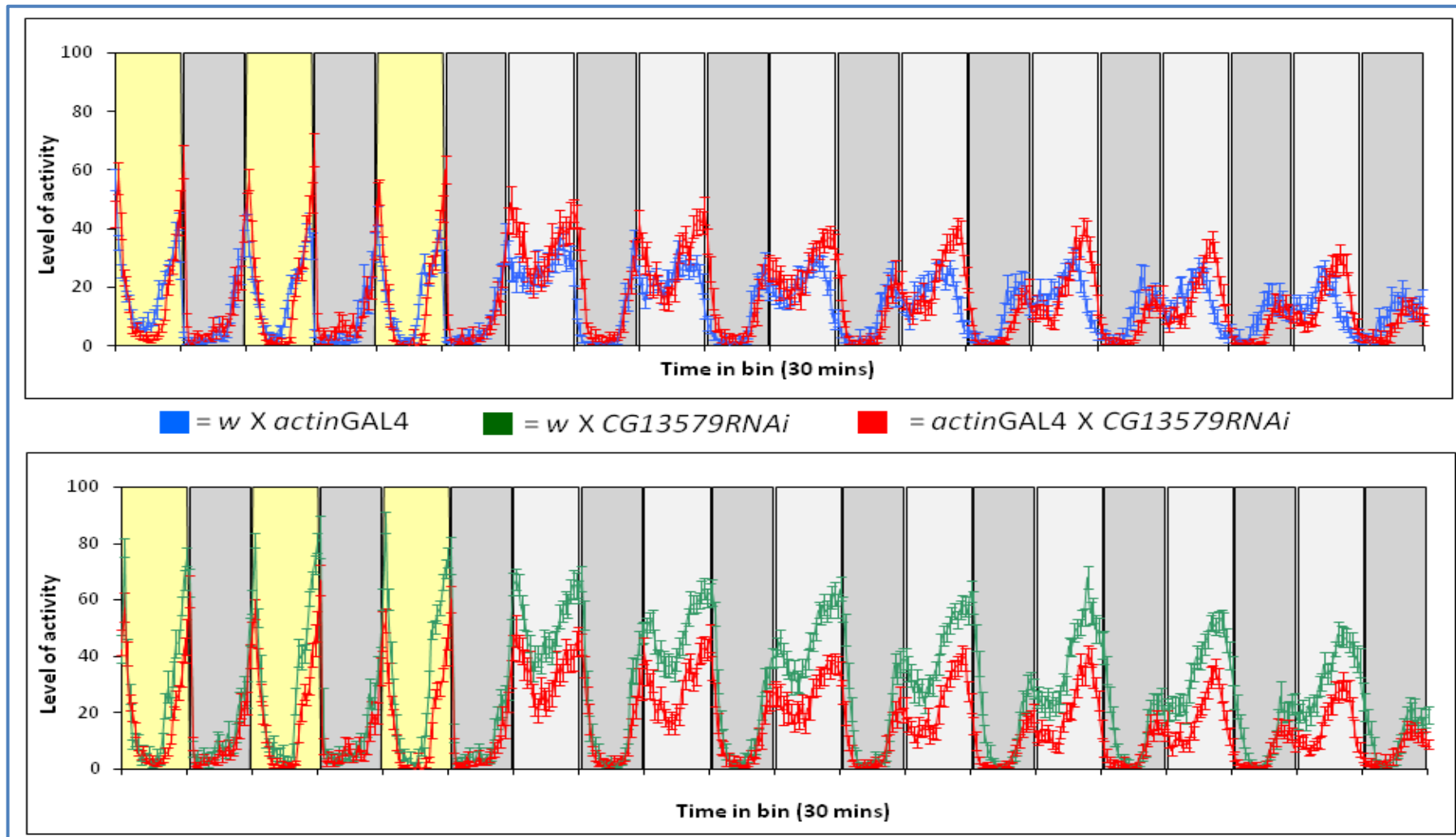


Figure 3.5.2: Comparison of averaged locomotor activity profiles of *actinGAL4* driving RNA interference of *CG13579* and controls in DD at 25°C.

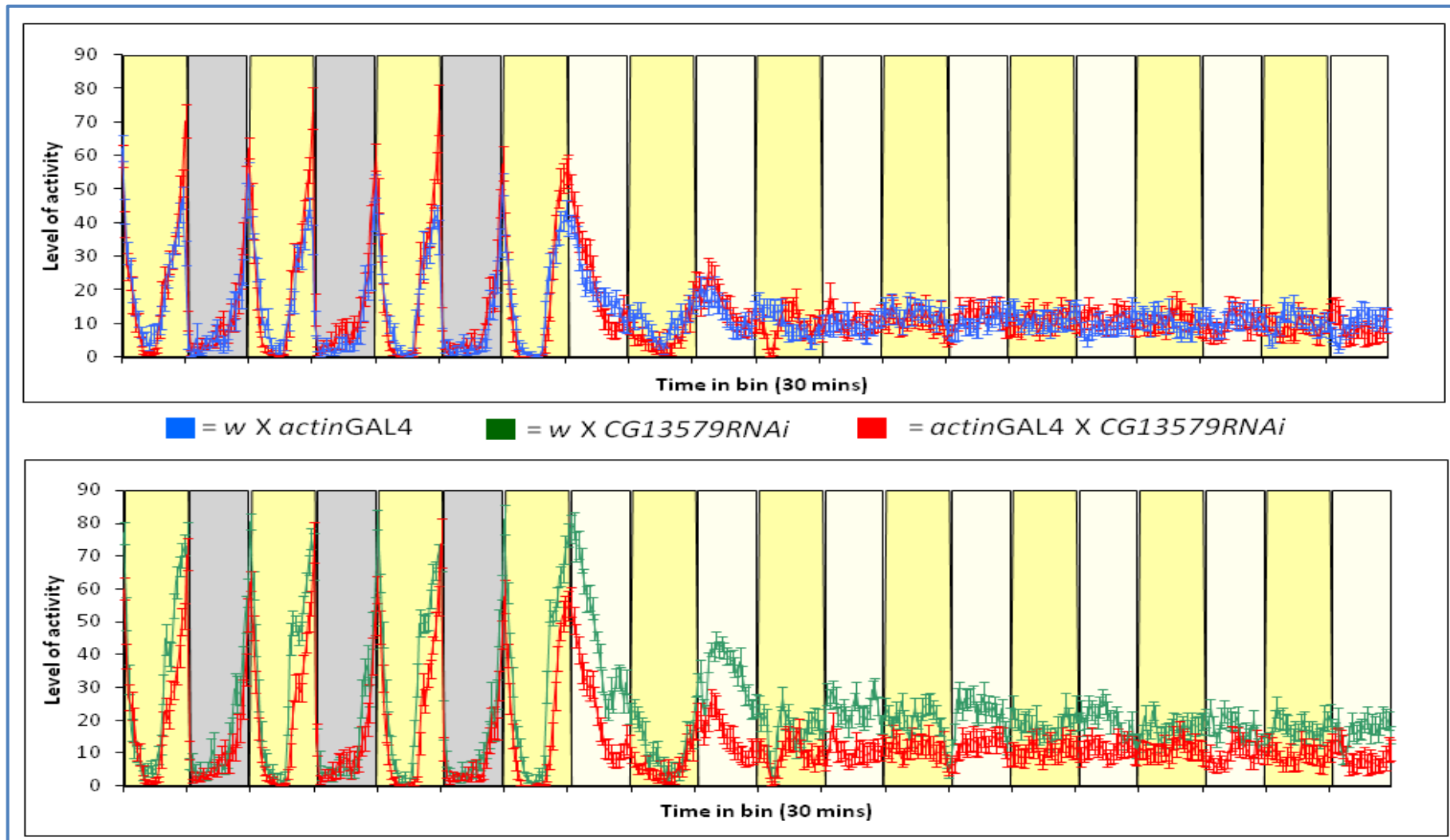


Figure 3.5.3: Comparison of averaged locomotor activity profiles of *actinGAL4* driving RNA interference of *CG13579* and controls in LL at 25°C.

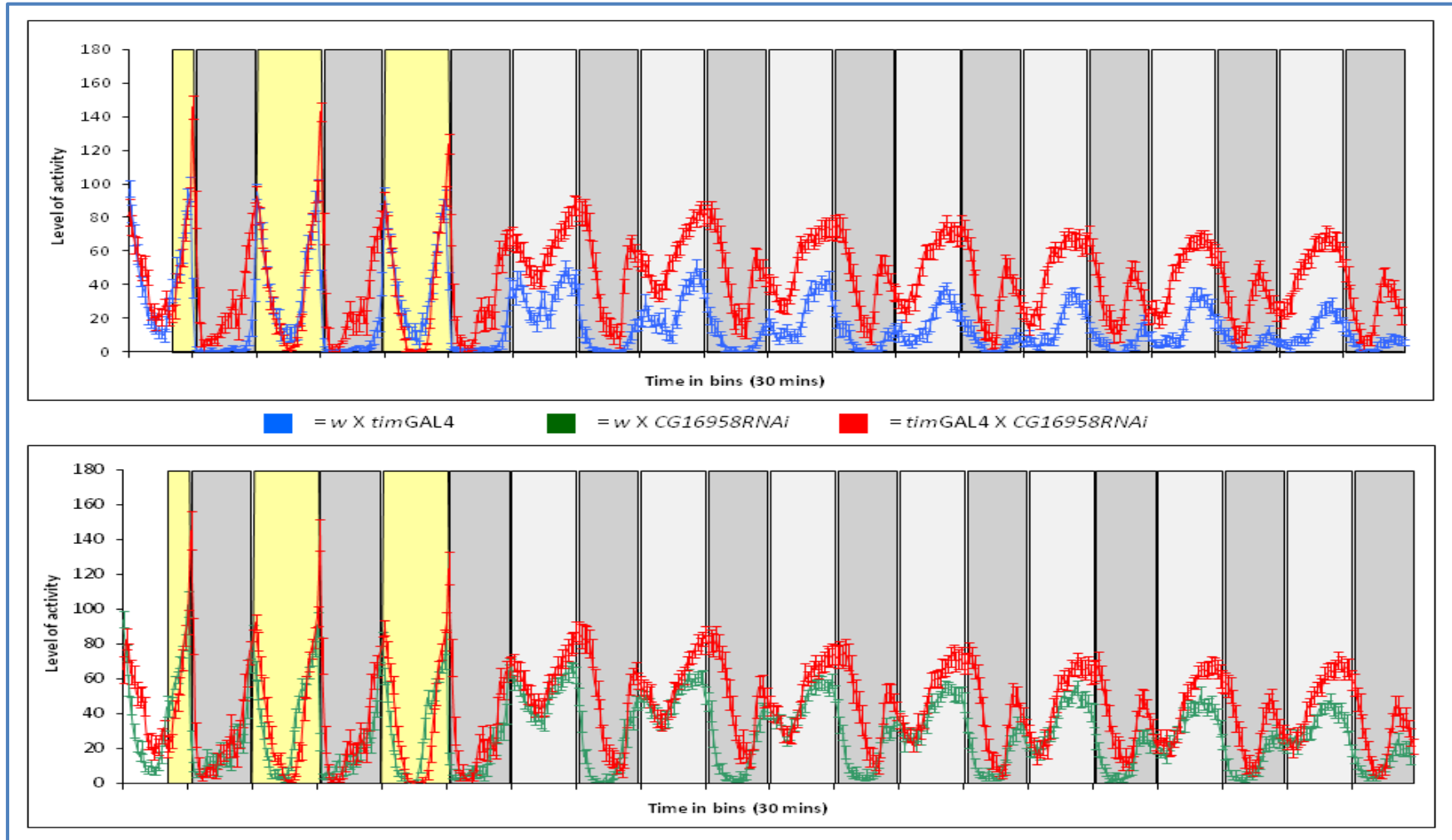


Figure 3.6.1: Comparison of averaged locomotor activity profiles of *timGAL4* driving RNA interference of *CG16958* and controls in DD at 25°C.

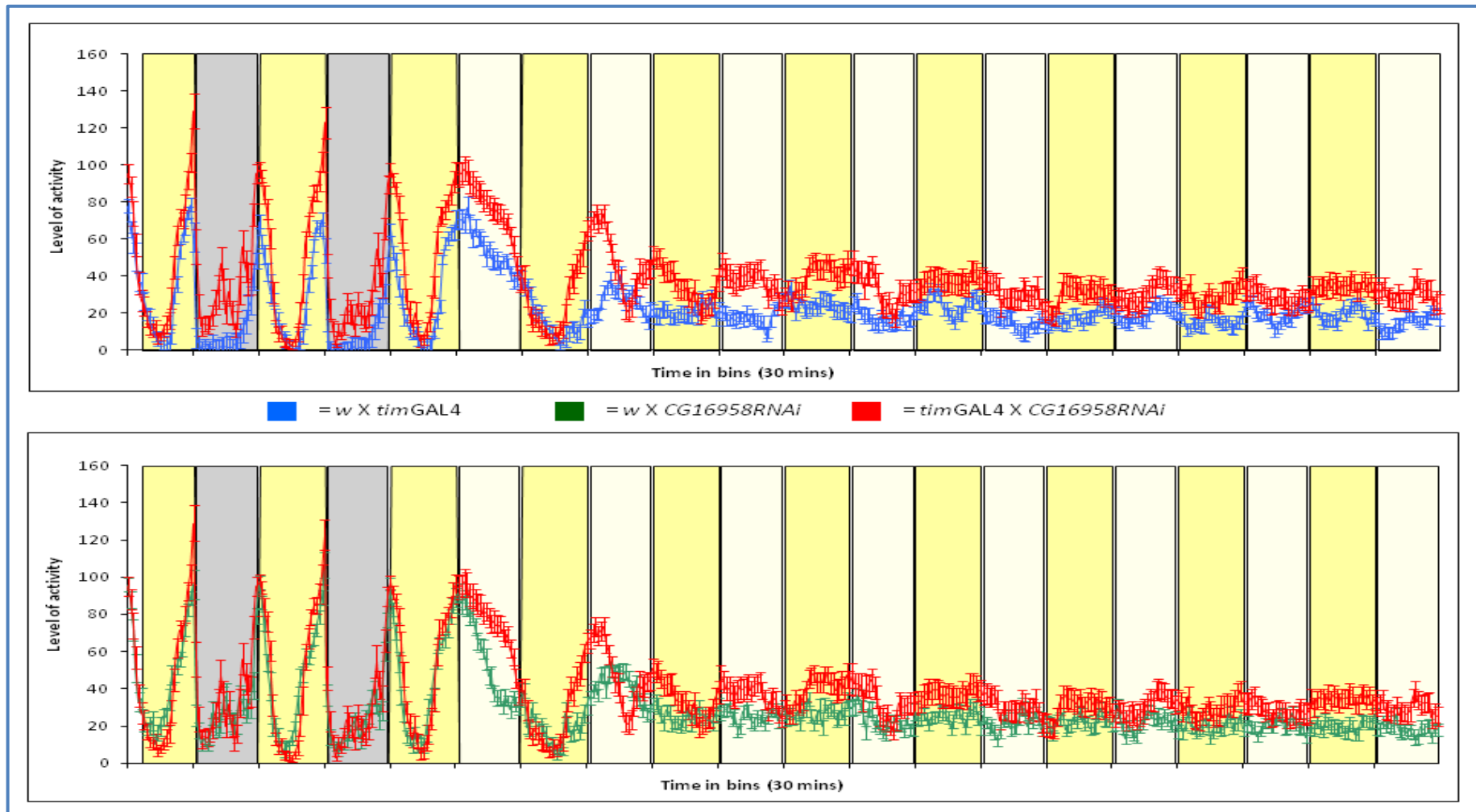


Figure 3.6.2: Comparison of averaged locomotor activity profiles of *tim*GAL4 driving RNA interference of *CG16958* and controls in DD at 25°C. The first three entrainment days were followed by seven cycles in LL.

References

Adams MD, Celniker SE, Holt RA, Evans CA, Gocayne JD, Amanatides PG, Scherer SE, Li PW, Hoskins RA, Galle RF, George RA, Lewis SE, Richards S, Ashburner M, Henderson SN, Sutton GG, Wortman JR, Yandell MD, Zhang Q, Chen LX, Brandon RC, Rogers YH, Blazej RG, Champe M, Pfeiffer BD, Wan KH, Doyle C, Baxter EG, Helt G, Nelson CR, Gabor GL, Abril JF, Agbayani A, An HJ, Andrews-Pfannkoch C, Baldwin D, Ballew RM, Basu A, Baxendale J, Bayraktaroglu L, Beasley EM, Beeson KY, Benos PV, Berman BP, Bhandari D, Bolshakov S, Borkova D, Botchan MR, Bouck J, Brokstein P, Brottier P, Burtis KC, Busam DA, Butler H, Cadieu E, Center A, Chandra I, Cherry JM, Cawley S, Dahlke C, Davenport LB, Davies P, de Pablos B, Delcher A, Deng Z, Mays AD, Dew I, Dietz SM, Dodson K, Doup LE, Downes M, Dugan-Rocha S, Dunkov BC, Dunn P, Durbin KJ, Evangelista CC, Ferraz C, Ferriera S, Fleischmann W, Fosler C, Gabrielian AE, Garg NS, Gelbart WM, Glasser K, Glodek A, Gong F, Gorrell JH, Gu Z, Guan P, Harris M, Harris NL, Harvey D, Heiman TJ, Hernandez JR, Houck J, Hostin D, Houston KA, Howland TJ, Wei MH, Ibegwam C, Jalali M, Kalush F, Karpen GH, Ke Z, Kennison JA, Ketchum KA, Kimmel BE, Kodira CD, Kraft C, Kravitz S, Kulp D, Lai Z, Lasko P, Lei Y, Levitsky AA, Li J, Li Z, Liang Y, Lin X, Liu X, Mattei B, McIntosh TC, McLeod MP, McPherson D, Merkulov G, Milshina NV, Mobarry C, Morris J, Moshrefi A, Mount SM, Moy M, Murphy B, Murphy L, Muzny DM, Nelson DL, Nelson DR, Nelson KA, Nixon K, Nusskern DR, Pacleb JM, Palazzolo M, Pittman GS, Pan S, Pollard J, Puri V, Reese MG, Reinert K, Remington K, Saunders RD, Scheeler F, Shen H, Shue BC, Sidén-Kiamos I, Simpson M, Skupski MP, Smith T, Spier E, Spradling AC, Stapleton M, Strong R, Sun E, Svirskas R, Tector C, Turner R, Venter E, Wang AH, Wang X, Wang ZY, Wassarman DA, Weinstock GM, Weissenbach J, Williams SM, WoodageT, Worley KC, Wu D, Yang S, Yao QA, Ye J, Yeh RF, Zaveri JS, Zhan M, Zhang G, Zhao Q, Zheng L, Zheng XH, Zhong FN, Zhong W, Zhou X, Zhu S, Zhu X, Smith HO, Gibbs RA, Myers EW, Rubin GM and Venter JC. The genome sequence of *Drosophila melanogaster*. Science. 2000; 287 (5461): 2185-95.

Ahmad M and Cashmore AR. HY4 gene of *A. thaliana* encodes a protein with characteristics of a blue-light photoreceptor. Nature. 1993; 366 (6451): 162-6.

Allada R, White NE, So WV, Hall JC and Rosbash M. A mutant *Drosophila* homolog of mammalian *Clock* disrupts circadian rhythms and transcription of *period* and *timeless*. Cell. 1998; 93 (5): 791-804.

Alt S, Ringo J, Talyn B, Bray W and Dowse H. The *period* gene controls courtship song cycles in *Drosophila melanogaster*. Anim Behav. 1998; 56(1): 87-97.

Ashburner M. *Drosophila* genetics. Love-song and circadian rhythm. Nature. 1987; 326 (6115): 741.

Ashmore LJ and Sehgal A. A fly's eye view of circadian entrainment. J. Biol. Rhythms. 2003; 18 (3): 206-16. Review.

Bachleitner W, Kempinger L, Wülbeck C, Rieger D and Helfrich-Förster C. Moonlight shifts the endogenous clock of *Drosophila melanogaster*. Proc Natl Acad Sci U S A. 2007; 104(9): 3538-43.

Bae K, Lee C, Hardin PE and Edery I. dCLOCK is present in limiting amounts and likely mediates daily interactions between the dCLOCK-CYC transcription factor and the PER-TIM complex. J Neurosci. 2000; 20 (5): 1746-53.

Bae K, Lee C, Sidote D, Chuang KY and Edery I. Circadian regulation of a *Drosophila* homolog of the mammalian *Clock* gene: PER and TIM function as positive regulators. Mol Cell Biol. 1998; 18 (10): 6142-51.

Baylies MK, Bargiello TA, Jackson FR and Young MW. Changes in abundance or structure of the *per* gene product can alter periodicity of the *Drosophila* clock. Nature. 1987; 326 (6111): 390-2.

Beaver LM, Gvakharia BO, Vollintine TS, Hege DM, Stanewsky R and Giebultowicz JM. Loss of circadian clock function decreases reproductive fitness in males of *Drosophila melanogaster*. Proc Natl Acad Sci U S A. 2002; 99 (4): 2134-9.

Bell-Pedersen D, Cassone VM, Earnest DJ, Golden SS, Hardin PE, Thomas TL and Zoran MJ. Circadian rhythms from multiple oscillators: lessons from diverse organisms. Nat Rev Genet. 2005; 6 (7): 544-56. Review.

Blanchardon E, Grima B, Klarsfeld A, Chélot E, Hardin PE, Prémat T and Rouyer F. Defining the role of *Drosophila* lateral neurons in the control of circadian rhythms in motor activity and eclosion by targeted genetic ablation and PERIOD protein overexpression. Eur J Neurosci. 2001; 13 (5): 871-88.

Blau J and Young MW. Cycling *vriille* expression is required for a functional *Drosophila* clock. Cell. 1999; 99 (6): 661-71.

Bloomquist BT, Shortridge RD, Schneuwly S, Perdew M, Montell C, Steller H, Rubin G and Pak WL. Isolation of a putative phospholipase C gene of *Drosophila*, *norpA*, and its role in phototransduction. Cell. 1988; 54 (5): 723-33.

Boothroyd CE, Wijnen H, Naef F, Saez L and Young MW. Integration of light and temperature in the regulation of circadian gene expression in *Drosophila*. PLoS Genet. 2007; 3 (4): e54.

Brand AH and Perrimon N. Targeted gene expression as a means of altering cell fates and generating dominant phenotypes. Development. 1993; 118: 401-15.

Brody T and Cravchik A. *Drosophila melanogaster* G protein-coupled receptors. J Cell Biol. 2000; 150 (2): F83-8. Review.

Busza A, Emery-Le M, Rosbash M and Emery P. Roles of the two *Drosophila* CRYPTOCHROME structural domains in circadian photoreception. *Science*. 2004; 304 (5676): 1503-6.

Busza A, Murad A and Emery P. Interactions between circadian neurons control temperature synchronization of *Drosophila* behavior. *J Neurosci*. 2007; 27 (40): 10722-33.

Ceriani MF, Darlington TK, Staknis D, Más P, Petti AA, Weitz CJ and Kay SA. Light-dependent sequestration of TIMELESS by CRYPTOCHROME. *Science*. 1999; 285 (5427): 553-6.

Ceriani MF, Hogenesch JB, Yanovsky M, Panda S, Straume M and Kay SA. Genome-wide expression analysis in *Drosophila* reveals genes controlling circadian behavior. *J Neurosci*. 2002; 22 (21): 9305-19.

Chang DC and Reppert SM. A novel C-terminal domain of *Drosophila* PERIOD inhibits dCLOCK:CYCLE-mediated transcription. *Curr Biol*. 2003; 13 (9): 758-62.

Cheng Y and Hardin PE. *Drosophila* photoreceptors contain an autonomous circadian oscillator that can function without *period* mRNA cycling. *J Neurosci*. 1998; 18 (2): 741-50.

Cheng Y, Gvakharia B and Hardin PE. Two alternatively spliced transcripts from the *Drosophila period* gene rescue rhythms having different molecular and behavioral characteristics. *Mol Cell Biol*. 1998; 18 (11): 6505-14.

Cheyette BN, Green PJ, Martin K, Garren H, Hartenstein V and Zipursky SL. The *Drosophila sine oculis* locus encodes a homeodomain-containing protein required for the development of the entire visual system. *Neuron*. 1994; 12 (5): 977-96.

Citri Y, Colot HV, Jacquier AC, Yu Q, Hall JC, Baltimore D and Rosbash M. A family of unusually spliced biologically active transcripts encoded by a *Drosophila* clock gene. *Nature*. 1987; 326 (6108): 42-7.

Claridge-Chang A, Wijnen H, Naef F, Boothroyd C, Rajewsky N and Young MW. Circadian regulation of gene expression systems in the *Drosophila* head. *Neuron*. 2001; 32 (4): 657-71.

Collins BH, Rosato E and Kyriacou CP. Seasonal behavior in *Drosophila melanogaster* requires the photoreceptors, the circadian clock, and phospholipase C. *Proc Natl Acad Sci U S A*. 2004; 101 (7): 1945-50.

Costa R and Kyriacou CP. Functional and evolutionary implications of natural variation in clock genes. *Curr Opin Neurobiol*. 1998; 8(5): 659-64. Review.

Cusumano P, Klarsfeld A, Chélot E, Picot M, Richier B and Rouyer F. PDF-modulated visual inputs and *cryptochrome* define diurnal behaviour in *Drosophila*. *Nat Neurosci*. 2009; 12 (11): 1431-7.

Cyran SA, Buchsbaum AM, Reddy KL, Lin MC, Glossop NR, Hardin PE, Young MW, Storti RV and Blau J. *vriille*, *Pdp1*, and *dClock* form a second feedback loop in the *Drosophila* circadian clock. *Cell*. 2003; 112 (3): 329-41.

Damiola F, Le Minh N, Preitner N, Kornmann B, Fleury-Olela F and Schibler U. Restricted feeding uncouples circadian oscillators in peripheral tissues from the central pacemaker in the suprachiasmatic nucleus. *Genes Dev*. 2000; 14 (23): 2950-61.

Darlington TK, Wager-Smith K, Ceriani MF, Staknis D, Gekakis N, Steeves TD, Weitz CJ, Takahashi JS and Kay SA. Closing the circadian loop: CLOCK-induced transcription of its own inhibitors *per* and *tim*. *Science*. 1998; 280 (5369): 1599-603.

Dietzl G, Chen D, Schnorrer F, Su KC, Barinova Y, Fellner M, Gasser B, Kinsey K, Oppel S, Scheiblauer S, Couto A, Marra V, Keleman K and Dickson BJ. A genome-wide transgenic RNAi library for conditional gene inactivation in *Drosophila*. *Nature*. 2007; 448 (7150): 151-6.

Dissel S, Codd V, Fedic R, Garner KJ, Costa R, Kyriacou CP and Rosato E. A constitutively active *cryptochrome* in *Drosophila melanogaster*. *Nat Neurosci*. 2004; 7 (8): 834-40.

Dolezelova E, Dolezel D and Hall JC. Rhythm defects caused by newly engineered null mutations in *Drosophila's cryptochrome* gene. *Genetics*. 2007; 177 (1): 329-45.

Duffy JB. GAL4 system in *Drosophila*: a fly geneticist's swiss army knife. *Genesis* 2002; 34 (1-2): 1-15.

Ederly I, Zwiebel LJ, Dembinska ME and Rosbash M. Temporal phosphorylation of the *Drosophila period* protein. *Proc Natl Acad Sci U S A*. 1994; 91 (6): 2260-4.

Emery P, So WV, Kaneko M, Hall JC and Rosbash M. CRY, a *Drosophila* clock and light-regulated *cryptochrome*, is a major contributor to circadian rhythm resetting and photosensitivity. *Cell*. 1998; 95 (5): 669-79.

Emery P, Stanewsky R, Helfrich-Förster C, Emery-Le M, Hall JC and Rosbash M. *Drosophila* CRY is a deep brain circadian photoreceptor. *Neuron*. 2000; 26 (2): 493-504.

Evanko DS, Thiyagarajan MM, Siderovski DP and Wedegaertner PB. G β isoforms selectively rescue plasma membrane localization and palmitoylation of mutant G α s and G α q. *J Biol Chem*. 2001; 276 (26): 23945-53.

Ewer J, Frisch B, Hamblen-Coyle MJ, Rosbash M and Hall JC. Expression of the *period* clock gene within different cell types in the brain of *Drosophila* adults and mosaic analysis of these cells' influence on circadian behavioral rhythms. *J Neurosci*. 1992; 12 (9): 3321-49.

Fire A, Xu S, Montgomery MK, Kostas SA, Driver SE and Mello CC. Potent and specific genetic interference by double-stranded RNA in *Caenorhabditis elegans*. *Nature*. 1998; 391 (6669): 806-11.

Ford CE, Skiba NP, Bae H, Daaka Y, Reuveny E, Shekter LR, Rosal R, Weng G, Yang CS, Iyengar R, Miller RJ, Jan LY, Lefkowitz RJ and Hamm HE. Molecular basis for interactions of G protein β subunits with effectors. *Science*. 1998; 280 (5367): 1271-4.

Freeman M. Reiterative use of the EGF receptor triggers differentiation of all cell types in the *Drosophila* eye. *Cell*. 1996; 87 (4): 651-60.

Fujii S, Krishnan P, Hardin P and Amrein H. Nocturnal male sex drive in *Drosophila*. *Curr Biol*. 2007; 17 (3): 244-51.

Fuller PM, Lu J and Saper CB. Differential rescue of light- and food-entrainable circadian rhythms. *Science*. 2008; 320 (5879): 1074-7.

Giebultowicz JM and Hege DM. Circadian clock in Malpighian tubules. *Nature*. 1997; 386 (6626): 664.

Giebultowicz JM. Peripheral clocks and their role in circadian timing: insights from insects. *Philos Trans R Soc Lond B Biol Sci*. 2001; 356 (1415): 1791-9. Review.

Glaser FT and Stanewsky R. Temperature synchronization of the *Drosophila* circadian clock. *Curr Biol*. 2005; 15 (15): 1352-63.

Gloor GB, Preston CR, Johnson-Schlitz DM, Nassif NA, Phillis RW, Benz WK, Robertson HM and Engels WR. Type I repressors of P element mobility. *Genetics*. 1993; 135 (1): 81-95.

Glossop NR, Houl JH, Zheng H, Ng FS, Dudek SM and Hardin PE. VRILLE feeds back to control circadian transcription of *Clock* in the *Drosophila* circadian oscillator. *Neuron*. 2003; 37 (2): 249-61.

Grima B, Chélot E, Xia R and Rouyer F. Morning and evening peaks of activity rely on different clock neurons of the *Drosophila* brain. *Nature*. 2004; 431(7010): 869-73.

Hall JC. Circadian pacemakers blowing hot and cold - but they're clocks, not thermometers. *Cell*. 1997; 90 (1): 9-12.

Hall JC. Tripping along the trail to the molecular mechanisms of biological clocks. *Trends Neurosci.* 1995; 18 (5): 230-40.

Hamasaka Y, Wegener C and Nässel DR. GABA modulates *Drosophila* circadian clock neurons via GABAB receptors and decreases in calcium. *J Neurobiol.* 2005; 65 (3): 225-40.

Hara R, Wan K, Wakamatsu H, Aida R, Moriya T, Akiyama M and Shibata S. Restricted feeding entrains liver clock without participation of the suprachiasmatic nucleus. *Genes Cells.* 2001; 6 (3): 269-78.

Hardie RC and Raghu P. Visual transduction in *Drosophila*. *Nature.* 2001; 413 (6852): 186-93. Review.

Hardie RC. Phototransduction in *Drosophila melanogaster*. *J Exp Biol.* 2001; 204 (Pt 20): 3403-9. Review.

Hardin PE, Hall JC and Rosbash M. Feedback of the *Drosophila period* gene product on circadian cycling of its messenger RNA levels. *Nature.* 1990; 343 (6258): 536-40.

Hardin PE. Analysis of *period* mRNA cycling in *Drosophila* head and body tissues indicates that body oscillators behave differently from head oscillators. *Mol Cell Biol.* 1994; 14 (11): 7211-8.

Harmar AJ, Marston HM, Shen S, Spratt C, West KM, Sheward WJ, Morrison CF, Dorin JR, Piggins HD, Reubi JC, Kelly JS, Maywood ES and Hastings MH. The VPAC (2) receptor is essential for circadian function in the mouse suprachiasmatic nuclei. *Cell.* 2002; 109 (4): 497-508.

Harrisingh MC, Wu Y, Lnenicka GA and Nitabach MN. Intracellular Ca²⁺ regulates free-running circadian clock oscillation *in vivo*. *J Neurosci.* 2007; 27 (46): 12489-99.

Hassan J, Busto M, Iyengar B and Campos AR. Behavioral characterization and genetic analysis of the *Drosophila melanogaster* larval response to light as revealed by a novel individual assay. *Behav Genet.* 2000; 30 (1): 59-69.

Hege DM, Stanewsky R, Hall JC and Giebultowicz JM. Rhythmic expression of a PER-reporter in the Malpighian tubules of decapitated *Drosophila*: evidence for a brain-independent circadian clock. *J Biol Rhythms.* 1997; 12 (4): 300-8.

Helfrich-Förster C, Edwards T, Yasuyama K, Wisotzki B, Schneuwly S, Stanewsky R, Meinertzhagen IA and Hofbauer A. The extraretinal eyelet of *Drosophila*: development, ultrastructure, and putative circadian function. *J Neurosci.* 2002; 22 (21): 9255-66.

Helfrich-Förster C, Winter C, Hofbauer A, Hall JC and Stanewsky R. The circadian clock of fruit flies is blind after elimination of all known photoreceptors. *Neuron*. 2001; 30 (1): 249-61.

Helfrich-Förster C, Wulf J and de Belle JS. Mushroom body influence on locomotor activity and circadian rhythms in *Drosophila melanogaster*. *J Neurogenet*. 2002; 16 (2): 73-109.

Helfrich-Förster C. The circadian system of *Drosophila melanogaster* and its light input pathways. *Zoology (Jena)*. 2002; 105 (4): 297-312.

Helfrich-Förster C. The locomotor activity rhythm of *Drosophila melanogaster* is controlled by a dual oscillator system. *J. Insect Physiol*. 2001; 47: 877-887.

Helfrich-Förster C. The neuroarchitecture of the circadian clock in the brain of *Drosophila melanogaster*. *Microsc Res Tech*. 2003; 62 (2): 94-102.

Helfrich-Förster C. The *period* clock gene is expressed in central nervous system neurons which also produce a neuropeptide that reveals the projections of circadian pacemaker cells within the brain of *Drosophila melanogaster*. *Proc Natl Acad Sci U S A*. 1995; 17: 92(2): 612-6.

Hiramoto M, Hiromi Y, Giniger E and Hotta Y. The *Drosophila* Netrin receptor *Frazzled* guides axons by controlling Netrin distribution. *Nature*. 2000; 406 (6798): 886-9.

Hogenesch JB, Gu YZ, Jain S and Bradfield CA. The basic-helix-loop-helix-PAS orphan MOP3 forms transcriptionally active complexes with circadian and hypoxia factors. *Proc Natl Acad Sci U S A*. 1998; 95 (10): 5474-9.

Honma S and Honma K. The biological clock: Ca²⁺ links the pendulum to the hands. *Trends Neurosci*. 2003; 26 (12): 650-3. Review.

Howlader G and Sharma VK. Circadian regulation of egg-laying behavior in fruit flies *Drosophila melanogaster*. *J Insect Physiol*. 2006; 52 (8): 779-85. Review.

Huang ZJ, Edery I and Rosbash M. PAS is a dimerization domain common to *Drosophila period* and several transcription factors. *Nature*. 1993; 364 (6434): 259-62.

Hyun S, Lee Y, Hong ST, Bang S, Paik D, Kang J, Shin J, Lee J, Jeon K, Hwang S, Bae E and Kim J. *Drosophila* GPCR *Han* is a receptor for the circadian clock neuropeptide PDF. *Neuron*. 2005; 48 (2): 267-78.

Ivanchenko M, Stanewsky R and Giebultowicz JM. Circadian photoreception in *Drosophila*: functions of *cryptochrome* in peripheral and central clocks. *J Biol Rhythms*. 2001; 16 (3): 205-15.

Johnson RF, Moore RY and Morin LP. Loss of entrainment and anatomical plasticity after lesions of the hamster retinohypothalamic tract. *Brain Res.* 1988; 460 (2): 297-313.

Kain P, Chakraborty TS, Sundaram S, Siddiqi O, Rodrigues V and Hasan G. Reduced odor responses from antennal neurons of *G(q)alpha*, *phospholipase Cbeta*, and *rdgA* mutants in *Drosophila* support a role for a phospholipid intermediate in insect olfactory transduction. *J Neurosci.* 2008; 28 (18): 4745-55.

Kalidas S and Smith DP. Novel genomic cDNA hybrids produce effective RNA interference in adult *Drosophila*. *Neuron.* 2002 17; 33 (2): 177-84.

Kaneko M and Hall JC. Neuroanatomy of cells expressing clock genes in *Drosophila*, transgenic manipulation of the *period* and *timeless* genes to mark the perikarya of circadian pacemaker neurons and their projections. *J. Comp. Neurol.* 2000; 422, 66-94.

Kaneko M, Helfrich-Forster C and Hall JC. Spatial and temporal expression of the *period* and *timeless* genes in the developing nervous system of *Drosophila*, newly identified pacemaker candidates and novel features of clock gene product cycling. *J. Neurosci.* 1997; 6745–6760.

Karsisiotis Y and Breda C. Seasonal *per* splicing in *norpa* downregulating strains. 2009; undergraduate report.

Kaushik R, Nawathean P, Busza A, Murad A, Emery P and Rosbash M. PER-TIM interactions with the photoreceptor *cryptochrome* mediate circadian temperature responses in *Drosophila*. *PLoS Biol.* 2007; 5 (6): e146.

Kernan MJ. Mechanotransduction and auditory transduction in *Drosophila*. *Pflugers Arch.* 2007; 454 (5): 703-20. Review.

Kim J, Chung YD, Park DY, Choi S, Shin DW, Soh H, Lee HW, Son W, Yim J, Park CS, Kernan MJ and Kim C. A TRPV family ion channel required for hearing in *Drosophila*. *Nature.* 2003; 424 (6944): 81-4.

Kim S, Chen DM, Zavarella K, Fournier CF, Stark WS and Shortridge RD. Substitution of a non-retinal phospholipase C in *Drosophila* phototransduction. *Insect Mol Biol.* 2003; 12 (2): 147-53.

Kim S, McKay RR, Miller K and Shortridge RD. Multiple subtypes of phospholipase C are encoded by the *norpa* gene of *Drosophila melanogaster*. *J Biol Chem.* 1995; 270 (24): 14376-82.

King DP, Zhao Y, Sangoram AM, Wilsbacher LD, Tanaka M, Antoch MP, Steeves TD, Vitaterna MH, Kornhauser JM, Lowrey PL, Turek FW and Takahashi JS. Positional cloning of the mouse circadian *clock* gene. *Cell.* 1997; 89 (4): 641-53.

Klarsfeld A, Malpel S, Michard-Vanhée C, Picot M, Chélot E and Rouyer F. Novel features of *cryptochrome*-mediated photoreception in the brain circadian clock of *Drosophila*. *J Neurosci*. 2004; 24 (6): 1468-77.

Kloss B, Price JL, Saez L, Blau J, Rothenfluh A, Wesley CS and Young MW. The *Drosophila* clock gene *double-time* encodes a protein closely related to human *casein kinase I epsilon*. *Cell*. 1998; 94 (1): 97-107.

Koh K, Zheng X and Sehgal A. JETLAG resets the *Drosophila* circadian clock by promoting light-induced degradation of TIMELESS. *Science*. 2006; 312 (5781):1809-12.

Konopka RJ and Benzer S. Clock mutants of *Drosophila melanogaster*. *Proc Natl Acad Sci U S A*. 1971; 2112-6.

Kornmann B, Schaad O, Bujard H, Takahashi JS and Schibler U. System-driven and oscillator-dependent circadian transcription in mice with a conditionally active liver clock. *PLoS Biol*. 2007; 5 (2): e34.

Krishnan B, Dryer SE and Hardin PE. Circadian rhythms in olfactory responses of *Drosophila melanogaster*. *Nature*. 1999 22;400 (6742): 375-8.

Krishnan B, Levine JD, Lynch MK, Dowse HB, Funes P, Hall JC, Hardin PE and Dryer SE. A new role for *cryptochrome* in a *Drosophila* circadian oscillator. *Nature*. 2001; 411 (6835): 313-7.

Kume K, Zylka MJ, Sriram S, Shearman LP, Weaver DR, Jin X, Maywood ES, Hastings MH and Reppert SM. mCRY1 and mCRY2 are essential components of the negative limb of the circadian clock feedback loop. *Cell*. 1999; 98 (2): 193-205.

Kyriacou CP and Hall JC. Circadian rhythm mutations in *Drosophila melanogaster* affect short-term fluctuations in the male's courtship song. *Proc Natl Acad Sci U S A*. 1980; 77 (11): 6729-33.

Lee C, Bae K and Edery I. PER and TIM inhibit the DNA binding activity of a *Drosophila* CLOCK-CYC/dBMAL1 heterodimer without disrupting formation of the heterodimer: a basis for circadian transcription. *Mol Cell Biol*. 1999; 19 (8): 5316-25.

Lee C, Etchegaray JP, Cagampang FR, Loudon AS and Reppert SM. Posttranslational mechanisms regulate the mammalian circadian clock. *Cell*. 2001; 107 (7): 855-67.

Lee C, Weaver DR and Reppert SM. Direct association between mouse PERIOD and CKIepsilon is critical for a functioning circadian clock. *Mol Cell Biol*. 2004; 24 (2): 584-94.

Lee T and Luo L. Mosaic analysis with a repressible cell marker (MARCM) for *Drosophila* neural development. *Trends Neurosci*. 2001; 24 (5): 251-4.

Levine JD, Funes P, Dowse HB and Hall JC. Resetting the circadian clock by social experience in *Drosophila melanogaster*. *Science*. 2002; 298 (5600): 2010-2.

Levine JD. Sharing time on the fly. *Curr Opin Cell Biol*. 2004; 16 (2): 210-6. Review.

Lim C, Lee J, Koo E and Choe J. Targeted inhibition of *Pdp1epsilon* abolishes the circadian behavior of *Drosophila melanogaster*. *Biochem Biophys Res Commun*. 2007; 364 (2): 294-300.

Lin C. Blue light receptors and signal transduction. *Plant Cell*. 2002; 14 Suppl: S207-25. Review.

Lin FJ, Song W, Meyer-Bernstein E, Naidoo N and Sehgal A. Photic signaling by *cryptochrome* in the *Drosophila* circadian system. *Mol Cell Biol*. 2001; 21 (21): 7287-94.

Lin Y, Han M, Shimada B, Wang L, Gibler TM, Amarakone A, Awad TA, Stormo GD, Van Gelder RN and Taghert PH. Influence of the *period*-dependent circadian clock on diurnal, circadian, and aperiodic gene expression in *Drosophila melanogaster*. *Proc Natl Acad Sci U S A*. 2002; 99 (14): 9562-7.

Lin Y, Stormo GD and Taghert PH. The neuropeptide pigment-dispersing factor coordinates pacemaker interactions in the *Drosophila* circadian system. *J Neurosci*. 2004; 24 (36): 7951-7.

Liu X, Lorenz L, Yu QN, Hall JC and Rosbash M. Spatial and temporal expression of the *period* gene in *Drosophila melanogaster*. *Genes Dev*. 1988; 2 (2): 228-38.

Luo L, Liao YJ, Jan LY and Jan YN. Distinct morphogenetic functions of similar small GTPases: *Drosophila Drac1* is involved in axonal outgrowth and myoblast fusion. *Genes Dev*. 1994; 8 (15): 1787-802.

Ma J and Ptashne M. The carboxy-terminal 30 amino acids of GAL4 are recognized by GAL80. *Cell*. 1987; 50 (1): 137-42.

Majercak J, Chen WF and Edery I. Splicing of the *period* gene 3'-terminal intron is regulated by light, circadian clock factors, and phospholipase C. *Mol Cell Biol*. 2004; 24 (8): 3359-72.

Majercak J, Sidote D, Hardin PE and Edery I. How a circadian clock adapts to seasonal decreases in temperature and day length. *Neuron*. 1999; 24 (1): 219-30.

Malpel S, Klarsfeld A and Rouyer F. Larval optic nerve and adult extra-retinal photoreceptors sequentially associate with clock neurons during *Drosophila* brain development. *Development*. 2002; 129 (6): 1443-53.

Maniatis T and Reed R. An extensive network of coupling among gene expression machines. *Nature*. 2002; 416 (6880): 499-506. Review.

Martin JR, Ernst R and Heisenberg M. Mushroom bodies suppress locomotor activity in *Drosophila melanogaster*. *Learn Mem*. 1998; 5(1-2): 179-91.

Martinek S, Inonog S, Manoukian AS and Young MW. A role for the segment polarity gene *shaggy*/GSK-3 in the *Drosophila* circadian clock. *Cell*. 2001; 105 (6): 769-79.

McDonald MJ and Rosbash M. Microarray analysis and organization of circadian gene expression in *Drosophila*. *Cell*. 2001; 107 (5): 567-78.

McNeil GP, Zhang X, Genova G and Jackson FR. A molecular rhythm mediating circadian clock output in *Drosophila*. *Neuron*. 1998; 20 (2): 297-303.

Meinertzhagen IA and Pyza E. Daily rhythms in cells of the fly's optic lobe: taking time out from the circadian clock. *Trends Neurosci*. 1996; 19 (7): 285-91.

Mistlberger RE. Circadian food-anticipatory activity: formal models and physiological mechanisms. *Neurosci Biobehav Rev*. 1994; 18 (2): 171-95.

Miyasako Y, Umezaki Y and Tomioka K. Separate sets of cerebral clock neurons are responsible for light and temperature entrainment of *Drosophila* circadian locomotor rhythms. *J Biol Rhythms*. 2007; 22 (2): 115-26.

Montell C. Visual transduction in *Drosophila*. *Annu Rev Cell Dev Biol*. 1999; 15: 231-68. Review.

Moses K, Ellis MC and Rubin GM. The *glass* gene encodes a zinc-finger protein required by *Drosophila* photoreceptor cells. *Nature*. 1989; 340 (6234): 531-6.

Mrosovsky N. Masking: history, definitions, and measurement. *Chronobiol Int*. 1999; 16 (4): 415-29. Review.

Murad A, Emery-Le M and Emery P. A subset of dorsal neurons modulates circadian behavior and light responses in *Drosophila*. *Neuron*. 2007; 53 (5): 689-701.

Myers MP, Wager-Smith K, Wesley CS, Young MW and Sehgal A. Positional cloning and sequence analysis of the *Drosophila* clock gene, *timeless*. *Science*. 1995; 270 (5237): 805-8.

Nagoshi E, Sugino K, Kula E, Okazaki E, Tachibana T, Nelson S and Rosbash M. Dissecting differential gene expression within the circadian neuronal circuit of *Drosophila*. *Nat Neurosci*. 2010; 13 (1): 60-8.

Newby LM and Jackson FR. A new biological rhythm mutant of *Drosophila melanogaster* that identifies a gene with an essential embryonic function. *Genetics*. 1993; 135 (4): 1077-90.

Nitabach MN and Taghert PH. Organization of the *Drosophila* circadian control circuit. *Curr Biol*. 2008; 18 (2): R84-93

O'Connell PO and Rosbash M. Sequence, structure, and codon preference of the *Drosophila ribosomal protein 49* gene. *Nucleic Acids Res*. 1984; 12 (13): 5495-513.

Park JH and Hall JC. Isolation and chronobiological analysis of a neuropeptide pigment-dispersing factor gene in *Drosophila melanogaster*. *J Biol Rhythms*. 1998; 13 (3): 219-28.

Park JH, Helfrich-Förster C, Lee G, Liu L, Rosbash M and Hall JC. Differential regulation of circadian pacemaker output by separate clock genes in *Drosophila*. *Proc Natl Acad Sci U S A*. 2000; 97 (7): 3608-13.

Pearn MT, Randall LL, Shortridge RD, Burg MG and Pak WL. Molecular, biochemical, and electrophysiological characterization of *Drosophila norpA* mutants. *J Biol Chem*. 1996; 271 (9): 4937-45.

Peschel N, Chen KF, Szabo G and Stanewsky R. Light-dependent interactions between the *Drosophila* circadian clock factors *cryptochrome*, *jetlag*, and *timeless*. *Curr Biol*. 2009; 19 (3): 241-7.

Petersen G, Hall JC and Rosbash M. The *period* gene of *Drosophila* carries species-specific behavioral instructions. *EMBO J*. 1988; 7 (12): 3939-47.

Piccin A, Salameh A, Benna C, Sandrelli F, Mazzotta G, Zordan M, Rosato E, Kyriacou CP and Costa R. Efficient and heritable functional knock-out of an adult phenotype in *Drosophila* using a GAL4-driven hairpin RNA incorporating a heterologous spacer. *Nucleic Acids Res*. 2001; 29 (12): E55-5.

Picot M, Cusumano P, Klarsfeld A, Ueda R and Rouyer F. Light activates output from evening neurons and inhibits output from morning neurons in the *Drosophila* circadian clock. *PLoS Biol*. 2007; 5 (11): e315.

Picot M, Klarsfeld A, Chélot E, Malpel S and Rouyer F. A role for blind DN2 clock neurons in temperature entrainment of the *Drosophila* larval brain. *J Neurosci*. 2009; 29 (26): 8312-20.

Pittendrigh CS and Daan S. A functional analysis of circadian pacemakers in nocturnal rodents. V. pacemaker structure: a clock for all seasons. *J. Comp. Physiol [A]*. 1976; 106: 333-355.

Pittendrigh CS. Circadian systems. I. the driving oscillation and its assay in *Drosophila pseudoobscura*. Proc Natl Acad Sci U S A. 1967; 58: 1762-7.

Plautz JD, Kaneko M, Hall JC and Kay SA. Independent photoreceptive circadian clocks throughout *Drosophila*. Science. 1997; 278 (5343): 1632-5.

Pregueiro AM, Price-Lloyd N, Bell-Pedersen D, Heintzen C, Loros JJ and Dunlap JC. Assignment of an essential role for the *Neurospora frequency* gene in circadian entrainment to temperature cycles. Proc Natl Acad Sci U S A. 2005; 102 (6): 2210-5.

Preitner N, Damiola F, Lopez-Molina L, Zakany J, Duboule D, Albrecht U and Schibler U. The orphan nuclear receptor REV-ERB α controls circadian transcription within the positive limb of the mammalian circadian oscillator. Cell. 2002; 110 (2): 251-60.

Price JL, Blau J, Rothenfluh A, Abodeely M, Kloss B and Young MW. *double-time* is a novel *Drosophila* clock gene that regulates PERIOD protein accumulation. Cell. 1998; 94 (1): 83-95.

Price JL, Dembinska ME, Young MW and Rosbash M. Suppression of PERIOD protein abundance and circadian cycling by the *Drosophila* clock mutation *timeless*. EMBO J. 1995; 14 (16): 4044-9.

Qiu J and Hardin PE. Developmental state and the circadian clock interact to influence the timing of eclosion in *Drosophila melanogaster*. J Biol Rhythms. 1996; 11 (1): 75-86.

Ralph MR, Foster RG, Davis FC and Menaker M. Transplanted suprachiasmatic nucleus determines circadian *period*. Science. 1990; 247 (4945): 975-8.

Recht LD, Lew RA and Schwartz WJ. Baseball teams beaten by jet lag. Nature. 1995; 377 (6550): 583.

Renn SC, Park JH, Rosbash M, Hall JC and Taghert PH. A pdf neuropeptide gene mutation and ablation of PDF neurons each cause severe abnormalities of behavioral circadian rhythms in *Drosophila*. Cell. 1999; 99 (7): 791-802.

Reppert SM and Weaver DR. Comparing clockworks: mouse versus fly. J Biol Rhythms. 2000; 15 (5): 357-64. Review.

Reppert SM and Weaver DR. Coordination of circadian timing in mammals. Nature. 2002 Aug 29;418 (6901): 935-41. Review.

Rhee SG, Suh PG, Ryu SH and Lee SY. Studies of inositol phospholipid-specific phospholipase C. Science. 1989; 244 (4904): 546-50. Review.

Rieger D, Stanewsky R and Helfrich-Förster C. Cryptochrome, compound eyes, Hofbauer-Buchner eyelets, and ocelli play different roles in the entrainment and

masking pathway of the locomotor activity rhythm in the fruit fly *Drosophila melanogaster*. *J Biol Rhythms*. 2003; 18 (5):377-91.

Robillard L, Ethier N, Lachance M and Hébert TE. Gβγ subunit combinations differentially modulate receptor and effector coupling *in vivo*. *Cell Signal*. 2000; 12 (9-10): 673-82.

Rosato E and Kyriacou CP. Analysis of locomotor activity rhythms in *Drosophila*. *Nat Protoc*. 2006; 1 (2): 559-68.

Rosato E, Codd V, Mazzotta G, Piccin A, Zordan M, Costa R and Kyriacou CP. Light-dependent interaction between *Drosophila* CRY and the clock protein PER mediated by the carboxy terminus of CRY. *Curr Biol*. 2001; 11 (12): 909-17.

Rosato E, Trevisan A, Sandrelli F, Zordan M, Kyriacou CP and Costa R. Conceptual translation of *timeless* reveals alternative initiating methionines in *Drosophila*. *Nucleic Acids Res*. 1997; 25 (3): 455-8.

Rutila JE, Suri V, Le M, So WV, Rosbash M and Hall JC. CYCLE is a second bHLH-PAS clock protein essential for circadian rhythmicity and transcription of *Drosophila period* and *timeless*. *Cell*. 1998; 93 (5): 805-14.

Saez L and Young MW. Regulation of nuclear entry of the *Drosophila* clock proteins *period* and *timeless*. *Neuron*. 1996; 17 (5): 911-20.

Sancar A. Structure and function of DNA photolyase and *cryptochrome* blue-light photoreceptors. *Chem Rev*. 2003; 103 (6): 2203-37. Review.

Sandrelli F, Tauber E, Pegoraro M, Mazzotta G, Cisotto P, Landskron J, Stanewsky R, Piccin A, Rosato E, Zordan M, Costa R and Kyriacou CP. A molecular basis for natural selection at the *timeless* locus in *Drosophila melanogaster*. *Science*. 2007; 316 (5833): 1898-900.

Sarov-Blat L, So WV, Liu L and Rosbash M. The *Drosophila takeout* gene is a novel molecular link between circadian rhythms and feeding behavior. *Cell*. 2000; 101 (6): 647-56.

Sathyanarayanan S, Zheng X, Xiao R and Sehgal A. Posttranslational regulation of *Drosophila* PERIOD protein by protein *phosphatase 2A*. *Cell*. 2004; 116 (4): 603-15.

Saunders DS. The circadian basis of ovarian diapause regulation in *Drosophila melanogaster*: is the *period* gene causally involved in photoperiodic time measurement? *J Biol Rhythms*. 1990; 5 (4): 315-31.

Sawyer LA, Hennessy JM, Peixoto AA, Rosato E, Parkinson H, Costa R and Kyriacou CP. Natural variation in a *Drosophila* clock gene and temperature compensation. *Science*. 1997 19; 278 (5346): 2117-20.

Sehadova H, Glaser FT, Gentile C, Simoni A, Giesecke A, Albert JT and Stanewsky R. Temperature entrainment of *Drosophila*'s circadian clock involves the gene *nocte* and signaling from peripheral sensory tissues to the brain. *Neuron*. 2009; 64 (2): 251-66.

Sehgal A, Price JL, Man B and Young MW. Loss of circadian behavioral rhythms and *per* RNA oscillations in the *Drosophila* mutant *timeless*. *Science*. 1994; 263 (5153): 1603-6.

Sehgal A, Rothenfluh-Hilfiker A, Hunter-Ensor M, Chen Y, Myers MP and Young MW. Rhythmic expression of *timeless*: a basis for promoting circadian cycles in *period* gene autoregulation. *Science*. 1995; 270 (5237): 808-10.

Shafer OT, Helfrich-Förster C, Renn SC and Taghert PH. Reevaluation of *Drosophila melanogaster*'s neuronal circadian pacemakers reveals new neuronal classes. *J Comp Neurol*. 2006; 498 (2): 180-93.

Shafer OT, Kim DJ, Dunbar-Yaffe R, Nikolaev VO, Lohse MJ and Taghert PH. Widespread receptivity to neuropeptide PDF throughout the neuronal circadian clock network of *Drosophila* revealed by real-time cyclic AMP imaging. *Neuron*. 2008; 58 (2): 223-37.

Shafer OT, Rosbash M and Truman JW. Sequential nuclear accumulation of the clock proteins *period* and *timeless* in the pacemaker neurons of *Drosophila melanogaster*. *J Neurosci*. 2002; 22 (14): 5946-54.

Sharp PA. RNAi and double-strand RNA. *Genes Dev*. 1999; 13 (2): 139-41. Review.

Shaw PJ, Cirelli C, Greenspan RJ and Tononi G. Correlates of sleep and waking in *Drosophila melanogaster*. *Science*. 2000; 287 (5459): 1834-7.

Shearman LP, Sriram S, Weaver DR, Maywood ES, Chaves I, Zheng B, Kume K, Lee CC, van der Horst GT, Hastings MH and Reppert SM. Interacting molecular loops in the mammalian circadian clock. *Science*. 2000; 288 (5468): 1013-9.

Sheeba V, Fogle KJ, Kaneko M, Rashid S, Chou YT, Sharma VK and Holmes TC. Large ventral lateral neurons modulate arousal and sleep in *Drosophila*. *Curr Biol*. 2008; 18 (20): 1537-45.

Shim HS, Kim H, Lee J, Son GH, Cho S, Oh TH, Kang SH, Seen DS, Lee KH and Kim K. Rapid activation of CLOCK by Ca²⁺-dependent protein kinase C mediates resetting of the mammalian circadian clock. *EMBO Rep*. 2007; 8 (4): 366-71.

Shirasu N, Shimohigashi Y, Tominaga Y and Shimohigashi M. Molecular cogs of the insect circadian clock. *Zool Sci*. 2003; 20 (8): 947-55. Review.

Shortridge RD and McKay RR. Invertebrate phosphatidylinositol-specific phospholipases C and their role in cell signaling. *Invert Neurosci.* 1995; 1 (3): 199-206. Review.

Shortridge RD, Yoon J, Lending CR, Bloomquist BT, Perdew MH and Pak WL. A *Drosophila* phospholipase C gene that is expressed in the central nervous system. *J Biol Chem.* 1991; 266 (19): 12474-80.

Siddiqi O. Neurogenetics of olfaction in *Drosophila melanogaster*. *Trends Genet.* 1987; 137:142.

Sidote D, Majercak J, Parikh V and Edery I. Differential effects of light and heat on the *Drosophila* circadian clock proteins PER and TIM. *Mol Cell Biol.* 1998; 18 (4): 2004-13.

Soller M and White K. ELAV. *Curr Biol.* 2004; 14 (2): R53.

Stanewsky R, Frisch B, Brandes C, Hamblen-Coyle MJ, Rosbash M and Hall JC. Temporal and spatial expression patterns of transgenes containing increasing amounts of the *Drosophila* clock gene *period* and a lacZ reporter: mapping elements of the PER protein involved in circadian cycling. *J Neurosci.* 1997; 17 (2): 676-96.

Stanewsky R, Kaneko M, Emery P, Beretta B, Wager-Smith K, Kay SA, Rosbash M and Hall JC. The *cry^b* mutation identifies *cryptochrome* as a circadian photoreceptor in *Drosophila*. *Cell.* 1998; 95 (5): 681-92.

Stanislawska J and Olszewski WL. RNA interference-significance and applications. *Arch Immunol Ther Exp (Warsz).* 2005; 53 (1): 39-46. Review.

Stoleru D, Nawathean P, Fernández MP, Menet JS, Ceriani MF and Rosbash M. The *Drosophila* circadian network is a seasonal timer. *Cell.* 2007; 129 (1): 207-19.

Stoleru D, Peng Y, Agosto J and Rosbash M. Coupled oscillators control morning and evening locomotor behaviour of *Drosophila*. *Nature.* 2004; 431 (7010): 862-8.

Stoleru D, Peng Y, Nawathean P and Rosbash M. A resetting signal between *Drosophila* pacemakers synchronizes morning and evening activity. *Nature.* 2005; 438 (7065): 238-42.

Suh J and Jackson FR. *Drosophila ebony* activity is required in glia for the circadian regulation of locomotor activity. *Neuron.* 2007; 55 (3): 435-47.

Suh PG, Park JJ, Manzoli L, Cocco L, Peak JC, Katan M, Fukami K, Kataoka T, Yun S and Ryu SH. Multiple roles of phosphoinositide-specific phospholipase C isozymes. *BMB Rep.* 2008; 41 (6): 415-34. Review.

Sutherland EW. Studies on the mechanism of hormone action. *Science*. 1972; 177 (47): 401-8.

Suzuki E and Hirose K. Immunocytochemical studies on light-induced changes in phosphatidylinositol 4,5-bisphosphate immunoreactivity in the visual system of normal and *norpA* mutant of *Drosophila*. *Neurosci Res*. 1992; 13 (2): 155-60.

Tauber E, Roe H, Costa R, Hennessy JM and Kyriacou CP. Temporal mating isolation driven by a behavioral gene in *Drosophila*. *Curr Biol*. 2003; 13 (2): 140-5.

Tauber E, Zordan M, Sandrelli F, Pegoraro M, Osterwalder N, Breda C, Daga A, Selmin A, Monger K, Benna C, Rosato E, Kyriacou CP and Costa R. Natural selection favors a newly derived *timeless* allele in *Drosophila melanogaster*. *Science*. 2007; 316 (5833): 1895-8.

Technau GM. Fiber number in the mushroom bodies of adult *Drosophila melanogaster* depends on age, sex and experience. *J Neurogenet*. 1984; 1 (2): 113-26.

Tijsterman M and Plasterk RH. Dicers at RISC; the mechanism of RNAi. *Cell*. 2004; 117 (1): 1-3. Review.

Turek FW. Circadian neural rhythms in mammals. *Annu Rev Physiol*. 1985; 47: 49-64. Review.

Tweedie S, Ashburner M, Falls K, Leyland P, McQuilton P, Marygold S, Millburn G, Osumi-Sutherland D, Schroeder A, Seal R, Zhang H and The FlyBase Consortium. FlyBase: enhancing *Drosophila* Gene Ontology annotations. *Nucleic Acids Research* (2009) 37: D555-D559; doi:10.1093/nar/gkn788.

Udo R, Hamada T, Horikawa K, Iwahana E, Miyakawa K, Otsuka K and Shibata S. The role of *Clock* in the plasticity of circadian entrainment. *Biochem Biophys Res Commun*. 2004; 318 (4): 893-8.

Ueda HR, Matsumoto A, Kawamura M, Iino M, Tanimura T and Hashimoto S. Genome-wide transcriptional orchestration of circadian rhythms in *Drosophila*. *J Biol Chem*. 2002; 277 (16): 14048-52.

van der Horst GT, Muijtjens M, Kobayashi K, Takano R, Kanno S, Takao M, de Wit J, Verkerk A, Eker AP, van Leenen D, Buijs R, Bootsma D, Hoeijmakers JH and Yasui A. Mammalian *Cry1* and *Cry2* are essential for maintenance of circadian rhythms. *Nature*. 1999; 398 (6728): 627-30.

Veleri S, Brandes C, Helfrich-Förster C, Hall JC and Stanewsky R. A self-sustaining, light-entrainable circadian oscillator in the *Drosophila* brain. *Curr Biol*. 2003; 13 (20): 1758-67.

Venken KJ and Bellen HJ. Emerging technologies for gene manipulation in *Drosophila melanogaster*. Nat Rev Genet. 2005; 167-78.

Vitaterna MH, King DP, Chang AM, Kornhauser JM, Lowrey PL, McDonald JD, Dove WF, Pinto LH, Turek FW and Takahashi JS. Mutagenesis and mapping of a mouse gene, *Clock*, essential for circadian behavior. Science. 1994; 264 (5159): 719-25.

von Lintig J, Dreher A, Kiefer C, Wernet MF and Vogt K. Analysis of the blind *Drosophila* mutant *ninaB* identifies the gene encoding the key enzyme for vitamin A formation *in vivo*. Proc Natl Acad Sci U S A. 2001; 98 (3): 1130-5.

Vosshall LB, Price JL, Sehgal A, Saez L and Young MW. Block in nuclear localization of *period* protein by a second clock mutation, *timeless*. Science. 1994; 263 (5153): 1606-9.

Wheeler DA, Hamblen-Coyle MJ, Dushay MS and Hall JC. Behavior in light-dark cycles of *Drosophila* mutants that are arrhythmic, blind, or both. J Biol Rhythms. 1993 Spring; 8 (1): 67-94.

Wheeler DA, Kyriacou CP, Greenacre ML, Yu Q, Rutila JE, Rosbash M and Hall JC. Molecular transfer of a species-specific behavior from *Drosophila simulans* to *Drosophila melanogaster*. Science. 1991; 251 (4997): 1082-5.

Woelfle MA, Ouyang Y, Phanvijhitsiri K and Johnson CH. The adaptive value of circadian clocks: an experimental assessment in cyanobacteria. Curr. Biol. 2004; 14 (16): 1481-6.

Wülbeck C and Helfrich-Förster C. RNA *in situ* hybridizations on *Drosophila* whole mounts. Methods Mol Biol. 2007; 362: 495-511.

Xu K, Zheng X and Sehgal A. Regulation of feeding and metabolism by neuronal and peripheral clocks in *Drosophila*. Cell Metab. 2008; 8 (4): 289-300.

Yoshii T, Heshiki Y, Ibuki-Ishibashi T, Matsumoto A, Tanimura T and Tomioka K. Temperature cycles drive *Drosophila* circadian oscillation in constant light that otherwise induces behavioural arrhythmicity. Eur J Neurosci. 2005; 22 (5): 1176-84.

Yoshii T, Sakamoto M and Tomioka K. A temperature-dependent timing mechanism is involved in the circadian system that drives locomotor rhythms in the fruit fly *Drosophila melanogaster*. Zoolog Sci. 2002; 19 (8): 841-50.

Yoshii T, Todo T, Wülbeck C, Stanewsky R and Helfrich-Förster C. *Cryptochrome* is present in the compound eyes and a subset of *Drosophila*'s clock neurons. J Comp Neurol. 2008; 508 (6): 952-66.

Zars T. Two thermosensors in *Drosophila* have different behavioral functions. J Comp Physiol [A]. 2001; 187 (3): 235-42.

Zehring WA, Wheeler DA, Reddy P, Konopka RJ, Kyriacou CP, Rosbash M and Hall JC. P-element transformation with *period* locus DNA restores rhythmicity to mutant, arrhythmic *Drosophila melanogaster*. *Cell*. 1984; 39: 369-76.

Zeng H, Qian Z, Myers MP and Rosbash M. A light-entrainment mechanism for the *Drosophila* circadian clock. *Nature*. 1996; 380 (6570): 129-35.

Zerr DM, Hall JC, Rosbash M and Siwicki KK. Circadian fluctuations of *period* protein immunoreactivity in the CNS and the visual system of *Drosophila*. *J Neurosci*. 1990; 10 (8): 2749-62.

Zheng B, Albrecht U, Kaasik K, Sage M, Lu W, Vaishnav S, Li Q, Sun ZS, Eichele G, Bradley A and Lee CC. Nonredundant roles of the *mPer1* and *mPer2* genes in the mammalian circadian clock. *Cell*. 2001; 105 (5): 683-94.

Zhu L, McKay RR and Shortridge RD. Tissue-specific expression of phospholipase C encoded by the *norpA* gene of *Drosophila melanogaster*. *J Biol Chem*. 1993; 268 (21): 15994-6001.